WADD TECHNICAL REPORT 60-767

Study of Physiochemical Properties of Selected Military Fuels

E. FINDL
H. BRANDE
H. EDWARDS

THOMPSON PRODUCTS INC.
INGLEWOOD LABORATORY

DECEMBER 1960

WRIGHT AIR DEVELOPMENT DIVISION

NOTICES

When Government drawings, specifications, or other data are used for any purpose other than in connection with a definitely related Government procurement operation, the United States Government thereby incurs no responsibility nor any obligation whatsoever; and the fact that the Government may have formulated, furnished, or in any way supplied the said drawings, specifications, or other data, is not to be regarded by implication or otherwise as in any manner licensing the holder or any other person or corporation, or conveying any rights or permission to manufacture, use, or sell any patented invention that may in any way be related thereto.

☆

Qualified requesters may obtain copies of this report from the Armed Services Technical Information Agency, (ASTIA), Arlington Hall Station, Arlington 12, Virginia.

☆

This report has been released to the Office of Technical Services, U. S. Department of Commerce, Washington 25, D. C., for sale to the general public.

☆

Copies of WADD Technical Reports and Technical Notes should not be returned to the Wright Air Development Division unless return is required by security considerations, contractual obligations, or notice on a specific document.

WADD TECHNICAL REPORT 60-767

Study of Physiochemical Properties of Selected Military Fuels

E. Findl

H. Brande

H. Edwards

Thompson Products Inc.
Inglewood Laboratory

December 1960

Materials Central
Contract No. AF 33(616)-3729
Project No. 3048

Wright Air Development Division
Air Research and Development Command
United States Air Force
Wright-Patterson Air Force Base, Ohio

FOREWORD

This report was prepared by the Inglewood Laboratory, Aircraft System Division of Thompson Products, Inc. under USAF Contract No. 33(616)-3729. The contract was initiated under Project No. 3048, "Aviation Fuels", Task No. 30178, "Effect of Fuel Properties on Fuel Systems". It was administered under the direction of the Propulsion Laboratory and Materials Central, Directorate of Advanced Systems Technology, Wright Air Development Division, with C. R. Hudson, J. H. Johnson and Lt. T. L. Gossage acting as project engineers.

This report covers the work performed during the period February 1955 to December 1958.

L. A. Schlagel was the project manager for Thompson Products, Inc. and E. Findl, H. Brande and H. Edwards conducted the experimental work at the Inglewood Laboratory, Inglewood, California.

ABSTRACT

The purpose of the program was to determine certain physical and thermodynamic properties of four selected aircraft fuels. These fuels were MIL-F-5624C Grade JP-4, a MIL-F-25558 Grade RJ-1*, MIL-F-25656 Grade JP-6-H, and Decalin, a commercial hydrocarbon mixture of the cis and trans isomers of decahydronapthalene.

Specific properties evaluated were:

1. Equilibrium solubility of air, nitrogen and ethane in the JP-4 and RJ-1 fuels.

2. Effect of dissolved air, nitrogen, and ethane on the viscosity of the JP-4 and RJ-1 fuels.

3. Effect of dissolved ethane on density of the JP-4 and RJ-1 fuels.

4. Effect of pressure level, agitation rate, and rate of pressure change on the evolution rate of air and ethane from the JP-4 and RJ-1 fuels.

5. Thermodynamic properties of each of the four test fuels including specific heats, enthalpy, and entropy.

6. Vaporization characteristics of each of the test fuels including vapor pressure, equilibrium vaporization curves, minimum reflux curves, variation of vapor molecular weight during minimum reflux distillations, and variation of density during minimum reflux distillations.

7. Variation of liquid density as a function of temperature.

8. Literature survey correlation compilation for the determination of physical and thermodynamic properties of petroleum fuels.

*Formerly designated as Shell UMF, Grade C.

PUBLICATION REVIEW

This report has been reviewed and is approved.

FOR THE COMMANDER:

M. P. Dunnam

M. P. DUNNAM
Chief, Fuel & Lubricant Branch
Applications Laboratory
Materials Central

TABLE OF CONTENTS

TABLE OF CONTENTS (Cont'd)

LIST OF ILLUSTRATIONS

LIST OF ILLUSTRATIONS (Cont'd)

LIST OF ILLUSTRATIONS (Cont'd)

LIST OF ILLUSTRATIONS (Cont'd)

LIST OF ILLUSTRATIONS (Cont'd)

LIST OF ILLUSTRATIONS (Cont'd)

GENERAL INTRODUCTION

This report is presented in five Parts:

PART I - EQUILIBRIUM SOLUBILITY.

The equilibrium solubility of air, nitrogen and ethane and their effect on viscosity were determined for an RJ-1 fuel. In addition, the equilibrium solubility of ethane and its effect on viscosity in a JP-4 fuel were determined. Part I includes generalized correlations for extension of the data to other fuels of the same type. Studies of the equilibrium solubility of air, nitrogen and carbon dioxide in JP-4 are also reported. These studies performed at the West Coast Laboratory prior to this program were reported to the Coordinating Research Council at an earlier date.

PART II - EVOLUTION RATE STUDIES.

This second Part is concerned with non-equilibrium evolution rate studies on JP-4 and RJ-1 fuels. The studies were accomplished through the use of a simulated aircraft fuel tank. Rate of pressure change, agitation rate and pressure level are the variables evaluated. It became increasingly evident during this phase of the program that the phenomena of evolution is extremely complex. While the study results reported are informative, it has not yet been possible to correlate the data and evolve a definite statement regarding non-equilibrium evolution. The test program has shown however, that certain variables are probable controllable variables.

PART III - VAPORIZATION CYCLE AND THE THERMODYNAMIC PROPERTIES OF JP-4, RJ-1 AND JP-6-H.

Certain thermodynamic and physical properties of each of the test fuels are described in Part III. Emphasis was placed on the construction of entropy-temperature charts. The use of these charts for the study and evaluation of petroleum fractions of the JP and RJ variety is discussed.

PART IV - VAPORIZATION CYCLE AND THERMODYNAMIC PROPERTIES OF DECALIN.

Certain thermodynamic and physical properties of Decalin are described in Part IV.

Manuscript released by authors September 1960 for disbribution as a Technical Report.

PART V - GENERALIZED THERMODYNAMIC AND PHYSICAL PROPERTIES OF PETROLEUM TYPE FUELS.

Part V is a compilation of various physiochemical correlations taken from available literature. Considerable effort went into the evaluation of a great variety of this type information reported in technical journals. The charts presented in Part V are believed the most accurate and suitable correlations published to date.

This Final Technical Report is treated in five Parts. A general Table of Contents, and List of Illustrations appears at the beginning of the report. A list of Symbols for each part appears at the end of that part; reference follow each part. An individual set of calculations and an Appendix are also included where applicable.

The overall research program, as initially proposed, was designed to provide information for various aspects of the SM64 Navaho Program. Numerous changes were made and modifications incorporated during the life of the program.

PART I EQUILIBRIUM SOLUBILITY

INTRODUCTION

An engineering report, Ing. Er. No. 183, was published by Thompson Products West Coast Laboratory on August 19, 1955. This report was concerned with gas solubilities in selected military fuels. The studies were performed under an Air Force contract. After the publication of this report, interest in a new fuel, RJ-1*, and a pressurizing gas, ethane, arose. An investigation of gas solubilities in these two military turbine fuels and the effect on viscosity then was conducted. The research results of this investigation, conducted under contract No. AF 33(616)3729, are presented herein.

OBJECTIVE

The investigation was made for the following purposes:

1) The determination of equilibrium solubility of ethane in a JP-4 fuel at temperatures to 500°F and at pressures to 400 psia,

2) The determination of equilibrium solubility of nitrogen, air, and ethane in RJ-1 fuel at temperatures to 500°F and at pressures to 400 psia, and

3) The determination of viscosities of both JP-4 and RJ-1 fuels as functions of temperature and dissolved gas concentrations.

SUMMARY

The test results indicate that the solubility of nitrogen and air, in the RJ-1 fuel, increases with rising temperature. The solubility of ethane, in both the JP-4 and RJ-1 fuels, decreases with increasing temperature. The solubility of ethane was lower in the RJ-1 fuels than in the JP-4 fuels.

* Former designation, Shell UMF, Grade C.

Apparent irregularities in air solubility at 300°F and 400°F, were observed in both fuels. These irregularities are believed to be caused by oxygen-consuming chemical-reactions such as gum formation. Similar irregularities were reported previously. See Reference 1.

METHOD AND PROCEDURE

TEST APPARATUS

Figure 1 is a schematic of the Test Apparatus designed and built by the West Coast Laboratory of Thompson Products, Inc. This unit was used to determine liquid viscosity, gas solubility and fuel expansion. The test cell is further illustrated in Figure 2.

In general, the methods and procedures described in Reference 1 were followed. Certain small changes in procedure and test instrumentation were incorporated to improve accuracy.

The test sample was contained in the inner, true-bore glass tube of the cell as shown in Figure 3. This tube also contained a glass ball which was 0.0083 inch smaller in diameter than the tube. Installed adjacent to the tube in the cell was a steel scale which indicated the total fuel volume at test conditions, with an accuracy of ±0.3 per cent.

Encasing the inner cell was an outer glass tube. The heating fluid was circulated through the annular space between the two tubes. The fluid was a high-flash-point, water-white, mineral oil to which a flash inibitor had been added.

The ends of both tubes of the test cell were plugged with invar metal end-caps housing "O" ring seals. Two "O" rings were required for each end of the inner glass tube. A suitable compound for use in contact with both the heating oil and the fuel could not be found. Silicone Compound No. SE-360* "O" rings were used in contact with the heat exchange oil. Silicone Compound No. 7180* "O" rings were used at the point of contact with the fuel.

* Plastic & Rubber Products, Inc. - Identification Numbers

The end caps were supported and spaced by a steel sleeve. The sleeve was mounted on pivots so that the cell could be rocked for agitation of the fuel and rapid dissolution of the solute. A spirit level was mounted on the sleeve so that the angle of the tube was held constant within ± 30 seconds for viscosity measurement.

Thermocouples were installed in each end of the test assembly to measure temperatures of the heating oil, the liquid fuel sample, and the vapor. Temperatures were indicated on a potentiometer with an accuracy of ±1°F. A transducer was used to measure the pressure in the test cell. This transducer was calibrated within ±1 psi. To reduce volume external to the test cell, the transducer cavity was filled with mercury. The external volume was less than 0.020 cubic inch. A schematic diagram of the test installation is shown in Figure 1.

Flexible metal hose was used to carry heating oil to the test cell in order to allow for oscillation of the assembly during test. The heating oil reservoir contained thermostatically controlled, immersion-type electrical heaters. Also installed in the reservoir was a water coil which was used for cooling. For the high temperature run, additional electrical bayonet-type heaters were installed in-line.

The gas to be dissolved was contained in steel bottles. These reservoirs were charged with pressurizing gas to approximately 700 psig. They were immersed in an oil bath. The oil bath was maintained at a constant temperature of 150°F ±1°. A Bourdon tube-type pressure guage, accurate to ±1 psi, and a differential pressure transducer calibrated to ±1psi were used to measure the pressure in the steel bottles. One reservoir was used as a reference in order to utilize a differential-pressure transducer with a 0 to 200 psi range. To increase the accuracy of the test results, this transducer was preferred to a conventional transducer or pressure guage having a 0 to 700 psi range.

Connections to the test cell were made by flexible capillary tubing.

The cell, shown in Figure 4, was used to measure the gas-free vapor-pressure of the fuel. The reflux column was cooled by a dry ice and acetone bath. The cell could be sealed from the reflux column. A hot oil bath was provided for temperature control of the cell assembly as shown. Cell pressure was measured with the calibrated transducer described above. Temperatures were measured by means of a thermocouple (and potentiometer).

TEST PROCEDURE

Each test fuel was subjected to the following physical and chemical inspections in accordance with the applicable military specification.

Distillation	- per VV-L-791, Method 1001.7
Gravity	- per VV-L-791, Method 401.3
Reid Vapor Pressure	- per VV-L-791, Method 1201.4

Initial oxygen and nitrogen contents of the fuels were determined by a special laboratory apparatus which is shown in Figure 5. The fuels were degassed by means of mercury pumps and the gases were stored in separate burettes. After complete evolution of the gases, Orsat analyses were made on the total gas sample collected.

Solutes of high purity were used in the investigation. Analyses of each solute are presented in Table I.

The volume of the test cell and the gas reservoir were determined independently by reduction of pressure in each cell to one-half atmosphere. The volume of gas removed was measured. Inasmuch as the cells and the gas reservoirs were maintained at a constant temperature, the volume of gas removed was a direct measurement of the cell volume.

The volume increase of the test cell due to thermal expansion at 500°F was found to be less than 0.3 per cent. This change in volume did not significantly affect the calculations.

The viscosity calibrations were reported previously. See Reference 1.

Solubility and viscosity measurements were made in the test cell by use of the following procedure:

> Before each run the test cell and ball were cleaned with a sulfuric acid-potassium dichromate, glass-cleaning solution. When required, the end caps were cleaned with hydrochloric acid. All parts were thoroughly rinsed with water and acetone and dried before assembly.

The outer glass tube, and the inner glass tube containing the glass ball, were assembled inside the metal spacer with one of two end caps. At a known temperature a measured volume of the fuel to be tested was placed in the cell. The quantity was adjusted so that the vapor-liquid ratio at the run temperature would be approximately 0.15. The second end cap then was fastened in place. The cell was placed on a test stand under a vapor hood. The capillary gas line, the heating fluid lines, and the thermocouple leads were then connected. The fuel temperature and liquid level in the cell were recorded. The liquid level was indicated by a metal scale inside the cell, read with the cell in a vertical position.

The heating-oil circulating-pump and the heaters were then turned on and the cell oscillated to agitate the fuel. Run temperatures were reached in 10 to 50 minutes.

As soon as the cell was stabilized at the run temperature another liquid level reading was taken and the cell pressure and temperature were recorded. The cell was then positioned at an angle of approximately 15° above horizontal for the viscosity determination; this angle was constant within ± 30 seconds for all measurements.

After this measurement the cell was again set into oscillation. A quantity of gas was metered through the capillary-line valve into the cell. The flow-rate was adjusted so that the cell pressure never exceeded the chosen pressure point by more than 5 psi. Agitation was continued for 10 minutes after the cell pressure had stabilized. The liquid level, roll time, cell pressure, and the pressure drop in the gas reservoir were recorded.

Additional gas was introduced into the cell and the above process repeated until data, at a minimum of four pressure-levels, were recorded. The highest pressure-level investigated was 415 psia. This procedure was repeated at various fuel temperatures to 500°F.

The data obtained from the above procedure were reduced in the following manner.

1. Roll time was converted to absolute viscosity by use of a calibration curve.

2. The calculations used in the reduction of the solubility data are described in the solubility calculations.

SOLUBILITY CALCULATIONS

The solubility calculations were based on Dalton's law of partial pressures: Each constituent contributes to the total pressure a partial pressure equal to the pressure it would exert if it alone were present at the given temperature in the volume occupied by the mixture. Reference 3. From the meager quantity of mixture data available in the literature, Dalton's law appears to be quite satisfactory for mixtures at pressures below 50 atmospheres.

Dalton's law can be expressed mathematically as follows:

$$P_t = \sum p_i = p_1 + p_2 + p_3 \text{ ---------- } + p_z \qquad (1)$$

$$p_i \; V_i = p_i \; \frac{V_t}{y_i} \qquad (2)$$

$$p_i = y_i \; P_t \left(\frac{p_i \; V_i}{P_t \; V_t} \right) \qquad (3)$$

By definition $Z = \frac{PV}{RT}$ or similarly $Z_i = \frac{p_i \; V_i}{RT}$

and $Z_t = \frac{P_t \; V_t}{RT}$

$$p_i = y_i \; P_t \left(\frac{Z_i}{Z_t} \right) \qquad (4)$$

A simplified block diagram, as shown below, will be used to illustrate the relationships derived from Dalton's law. These relationships were used to determine the solubilities of the three solutes (air, nitrogen and ethane) in the two solvents, RJ-1 and JP-4.

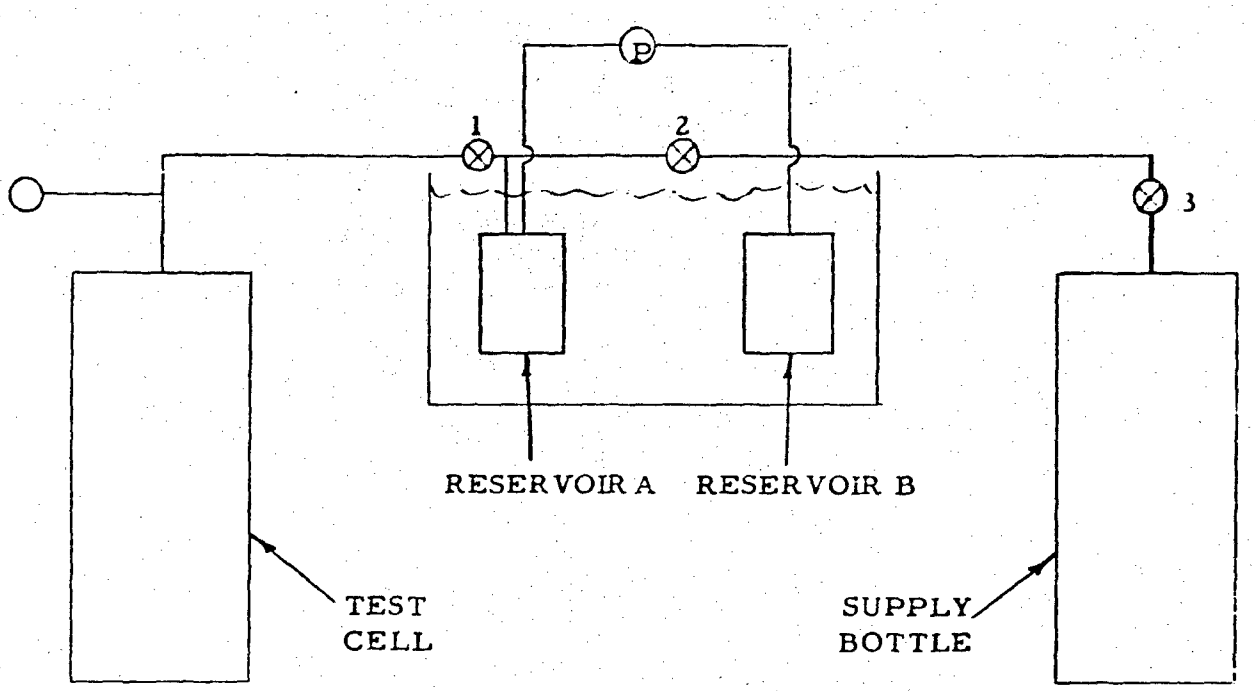

It is evident that once Valves 2 and 3 have been closed, all gas leaving Reservoir A must enter the test cell. Reservoir B was used only to provide a constant reference pressure.

The quantity of gas entering the cell can be expressed in terms of the compressibility form of the equation of state.

$$\Delta n_r = \frac{\Delta P_i \; V_i}{Z_r \; RT_r} = \Delta n_c \qquad (5)$$

In order to determine the quantity of pressurizing gas that has been dissolved, all that is necessary is to determine the quantity of gas that remains in the ullage. The difference between the quantity of pressurizing gas which enters the cell and that which remains in the ullage, is the quantity added to the solution.

$$n_d = \Delta n_r - n_{v,x} \qquad (6)$$

To evaluate $n_{vx,}$ Dalton's law is utilized.

The equation

$$P_{t,c} = p_x + p_a + p_F \qquad (7)$$

which states that the total cell pressure is due to the combined partial pressures of the pressurizing gas, the residual-air partial pressure, and the fuel-vapor pressure. The fuel-vapor pressure and air-partial pressure was assumed to be a function of temperature alone.

$$p_x = P_{t,c} - (p_a + p_F) \qquad (8)$$

The calculation of p_x can be made when the cell pressure prior to the addition of the pressurizing gas is known.

The quantity of pressurizing gas in the ullage can be determined utilizing p_x.

$$n_v = \frac{p_x V_v}{Z_x R T_v} \tag{9}$$

combining equations (5), (6) and (9),

$$n_d = \frac{P_i V_i}{Z_v R T_i} - \frac{p_x V_v}{Z_x R T_v} \tag{10}$$

The Ostwald coefficient is used to put Equation (10) into a more useful form. The Ostwald coefficient is defined as the volume of solute, measured at the temperature and pressure at which it is dissolved, per unit volume of solvent.

$$O_x = \frac{V_x}{V_L} \tag{11}$$

$$V_d = \frac{n_d Z_x R T_v}{p_x} \tag{12}$$

$$O_x = \frac{n_d Z_x R T_v}{p_x V_L} \tag{13}$$

Another useful form to express the quantity of Equation (1) is to state the volume dissolved, per unit weight of solvent, measured at standard conditions.

$$V^\circ = \frac{n_d Z_x RT^\circ}{P^\circ} \tag{14}$$

$$W = \rho V_L \tag{15}$$

$$\frac{V^\circ}{W} = \frac{n_d Z_x RT^\circ}{P^\circ V_L} \tag{16}$$

When air and nitrogen are used as pressurizing agents, certain minor modifications of the foregoing equations are required. Dissolved air has been arbitrarily defined as the combination of nitrogen and oxygen dissolved in the solvent, not necessarily in the same ratio as found in the atmosphere. This definition is necessary due to the somewhat greater solubility of oxygen, as compared to nitrogen, in hydrocarbon fuels.

When air is used as the pressurizing agent, Equation (8) simplifies to

$$p_x = p_a = P_{t\,c} - P_F \tag{17}$$

Since air is already dissolved in the solvent, Equation (6) must be modified to include the gas initially dissolved. The total gas in the cell at any time is defined by

$$n_t = n_v + n_d \tag{18}$$

At initial conditions prior to pressurization from the reservoir this becomes

$$n_{t\,\text{initial}} = n_y + n_i \tag{19}$$

After gas has been added from the reservoir the total air in the cell is the sum of that initially there plus that added from the reservoir:

$$n_t = n_{t\ \text{initial}} + \Delta n_r = n_y + n_i + \Delta n_r \qquad (20)$$

Combining Equation (18) and Equation (20)

$$n_d = n_t - n_v = n_y + n_i + \Delta n_r - n_v \qquad (21)$$

When nitrogen is used as the pressurizing agent a different correction to Equation (8) is required. This is due to the fact that the air initially in the cell ullage consists of approximately 21% oxygen and 79% nitrogen. Thus for nitrogen calculations, Equation (8) becomes

$$p_n = P_{t\,c} - (P_F + 0.21\ p_a) \qquad (22)$$

To summarize, the relationships used for air, nitrogen and ethane solubilities are as follows:

Air

$$O_a = \left[\left(\frac{P_{r1}}{Z_{r1}} - \frac{P_{r2}}{Z_{r2}}\right)\left(\frac{V_r}{T_r}\right) + \frac{14.7\ V_{v,\ n\ \text{initial}}}{T_{v\ \text{initial}}} + \frac{14.7\ V^{\circ}_{l,a}}{T^{\circ}} - \frac{(P_{t,\ c} - P_F)\ V_v}{Z_a\ T_v}\right] \frac{Z_a\ T_v}{(P_{t,c} - P_F)\ V_L} \qquad (23)$$

$$\frac{V^\circ}{W} = \frac{O_a\ T^\circ\ (P_{t,c} - p_F)}{T_v\ P^\circ} \tag{24}$$

Nitrogen

$$O_N = \left[\left(\frac{P_{r1}}{Z_1} \frac{P_{r2}}{Z_2} \right) \left(\frac{V_r}{T_r} \right) + \frac{14.7\ V_{v,n\ initial}}{T_{v\ initial}} + \frac{14.7\ V^\circ_{l,N}}{T^\circ} - \right.$$

$$\left. \frac{\left[P_{t,c} - (p_f + 0.21\ p_a) \right] V_v}{Z_N\ T_v} \right] \frac{Z_N\ T_v}{\left[P_{t,c} - (p_f + 0.21\ p_a) \right] V_L} \tag{25}$$

$$\frac{V^\circ}{W} = \frac{O_N\ T^\circ\ \left[P_{t,c} - (p_f + 0.21\ p_a) \right]}{T_v\ P^\circ \rho} \tag{26}$$

Ethane

$$O_e = \left[\left(\frac{P_{r1}}{Z_{r1}} - \frac{P_{r2}}{Z_{r2}} \right) \left(\frac{V_r}{T_r} \right) - \right.$$

$$\left. \frac{\left[P_{t\,c} - (p_F + p_a) \right]\ V_v}{Z_e\ T_v} \right] \frac{Z_e\ T_v}{\left[P_{t\,c} - (p_F - p_a) \right]\ V_L} \tag{27}$$

$$\frac{V^\circ}{W} = \frac{O_e \, T^\circ \left[P_{t\,c} - (p_F + p_a) \right]}{T_v \, \rho \, P^\circ} \qquad (28)$$

The compressibility factors of air and nitrogen are nearly unity in the range investigated and were neglected to simplify the calculation.

Ethane compressibility factors were computed from data in References 2, 3, 4, and 5. The information contained in these References was cross-plotted and converted to a form of the virial equation of state, i.e., $Z = 1 + B(T)\,P + C(T)P^2 + D(T)P^3$. Figure 6 shows the results of the virial equation, plotted at the test temperatures. Figures 7 through 9 show the values of the second, third and fourth virial coefficients used.

DISCUSSION

The test results demonstrate the general trend indicated in Reference 1, i.e., solubility decreases with increasing molecular weight of solvent fuel.

As anticipated, ethane is extremely soluble in the test fuels. Solubility of this solute, as determined by the Ostwald Coefficient, is pressure dependent. This is due to the large deviation of the ethane compressibility factor from unity and the radical change in liquid density caused by this solute. The deviation can best be expressed mathematically.

$$O_x = \frac{V_d}{V_L} = \frac{n_d Z_x R T_v}{p_x} \frac{\rho_L}{W_L} = \frac{R T_v}{W_L} \left(\frac{Z_x \rho_L n_d}{p_x} \right) \quad (1)$$

Differentiation of Equation (1) with respect to p_x at constant temperature results in

$$\left(\frac{\partial O_x}{\partial p_x} \right)_T = f \left[\left(\frac{\partial Z_x}{\partial p_x} \right)_T, \left(\frac{\partial \rho_L}{\partial x} \right)_T, \left(\frac{\partial n_d}{\partial p_x} \right)_T \right] \quad (2)$$

Ideally,

$\left(\frac{\partial n_d}{\partial p_x}\right)_T$ = a constant, $\left(\frac{\partial Z_x}{\partial p_x}\right)_T$ $\left(\frac{\partial \rho_L}{\partial p_x}\right)_T$ = 0 and thus

the change of Ostwald Coefficient with pressure is zero. In the case of the ethane-Fuel A (JP-4) and the ethane - Fuel B (RJ-1) systems,

$\left(\frac{\partial Z_x}{\partial p_x}\right)_T$ and $\left(\frac{\partial \rho_L}{\partial p_x}\right)_T$ do not equal zero. Therefore, the

Ostwald Coefficient can increase or decrease with pressure. The slope, i.e., $\left(\frac{\partial O_x}{\partial p_x}\right)_T$, is dependent upon the relationship between ρ_L, Z_z and p_x. Both Fuel A and Fuel B show deviations from ideality. See Figures 12 and 15. In the low temperature region (100°F to 200°F),

$\left(\frac{\partial O_x}{\partial p_x}\right)_T$ is negative. At the high temperatures, (300°F to 500°F)

$\left(\frac{\partial O_x}{\partial p_x}\right)_T$ is positive, indicating that in the 200°F to 300°F range

$\left(\frac{\partial O_x}{\partial p_x}\right)_T$ = 0: That is, a point is reached where the system behaves ideally.

Air and nitrogen behave ideally in both JP-4 and RJ-1 fuels, which could be predicted since $\left(\frac{\partial Z_x}{\partial p_x}\right)_T$ and $\left(\frac{\partial \rho_L}{\partial p_x}\right)_T$ are both nearly equal to zero. In the 200° F to 400°F range the apparent solubility of air increases somewhat rapidly. This is due to a visible chemical reaction (presumably oxidation) which causes formation of deposits. A

true solution effect is not achieved. The 400°F runs on nitrogen do not follow the $\frac{\Delta O_x}{\Delta T}$ trend shown by the runs performed at other temperatures. An explanation for this behavior has not been deduced.

The solubility of various pressurizing gases present in the test fuels were compared and are illustrated in Figures 10 and 11. Specific information on carbon dioxide, air and nitrogen in JP-4 fuels was obtained from Reference 1. The data has been extrapolated to the critical temperature, since by definition, the Ostwald Coefficient must equal 1.0 at the critical temperature of the solvent.

There does not seem to be any theoretical reason for the apparent reversal of solubility of ethane, in Fuel B, with increasing temperature. See Figure 11. Due to the method used in the evaluation of solubilities, the ethane data at the higher temperatures is believed to be accurate only to ±10%. * This deviation is a result of the comparatively large changes in compressibility factor resulting from changes in temperature and pressure. With this deviation, it is possible that the Ostwald Coefficient does not fall below 1.0 and a solubility reversal does not occur.

* The compressibility data is believed to be accurate to 0.5%, temperature instrumentation to ±1.0% and pressure instrumentation accurate to ±1.0%. However, a 1% temperature deviation could mean a change of as much as 1.5°F in the reservoirs. This change could increase the compressibility factor deviation. In the calculations, any error in compressibility factor is multiplied due to the mathematical methods employed. Thus, from relatively small instrumentation errors, large errors in results are possible.

Air and nitrogen have compressibilities nearly equal to unity and are relatively insensitive to compressibility difficulties. The data for these gases should approach an accuracy of ± 2%.

The solubility data obtained in terms of the Ostwald Coefficient are shown in Figures 12 through 15. Figures 16 through 19 show solubility, in terms of weight of solute dissolved per weight of solvent, as a function of pressure.

The effect of dissolved gases on the viscosity of the test solvents is shown in Figures 20 through 23. The ability of ethane to lower viscosity is much more pronounced at lower-liquid temperatures.

Figures 24 and 25 show the effect of dissolved ethane on the density of the two test fuels, JP-4 and RJ-1.

REFERENCES

1. Schlagel, L. A., Findl, E., and Edwards, H. An Investigation of the Solubility of Three Gases in Selected Military Fuels at High Temperatures and Pressures and the Effect of Temperature and Gas Solubility on Fuel Viscosity. Ing. Er. 183. Thompson Products, Inc., Inglewood Laboratory, Inglewood, Calif. August 19, 1955.

2. Sage, G. H. and Lacey, W. N. Thermodynamic Properties of the Lighter Paraffin Hydrocarbons and Nitrogen. American Petroleum Institute, New York, N. Y. 1950.

3. Paul, M. A. Principles of Chemical Thermodynamics. 1st Edition. McGraw Hill Book Company, New York, N. Y. 1951.

4. Sage, B. H. and Lacey, W. N. Volumetric and Phase Behavior of Hydrocarbons. Gulf Publishing Company, Houston, Texas. 1939.

5. Rossini, F. D. Thermodynamics and Physics of Matter. Princeton University Press, Princeton, N. J. 1955.

SYMBOLS

B, C, D,	=	Constants
n	=	Moles of pressurizing gas
O	=	Ostwald coefficient
P	=	Pressure
p	=	Partial pressure
R	=	Gas constant
T	=	Temperature
V	=	Volume
W	=	Weight
Z	=	Compressibility factor
Δ	=	Change
ρ	=	Solvent density at charge

SUBSCRIPTS AND SUPERSCRIPTS

a	=	Air
c	=	Cell
d	=	Solute dissolved
e	=	Ethane
f	=	Fuel
i	=	Solute initially dissolved in solvent
L	=	Liquid solvent
N	=	Nitrogen
r	=	Reservoir
t	=	Total
v	=	Cell ullage or vapor space
x	=	Pressurizing gas
y	=	Solute initially in vapor space
z	=	Last constituent
o	=	Standard conditions
1, 2, 3	=	Constituents 1, 2, 3, etc.

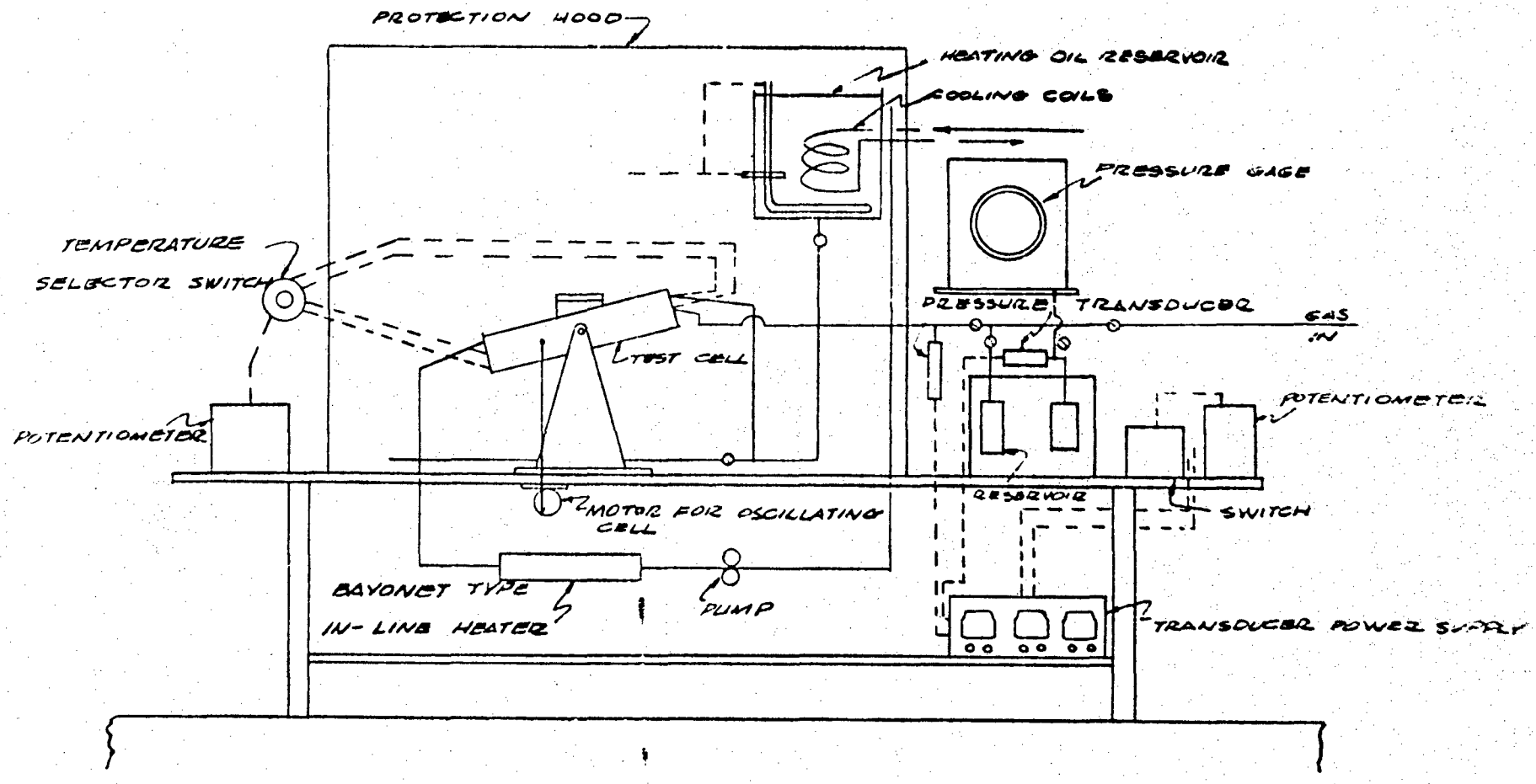

Figure No. 1 - Schematic of Test Apparatus

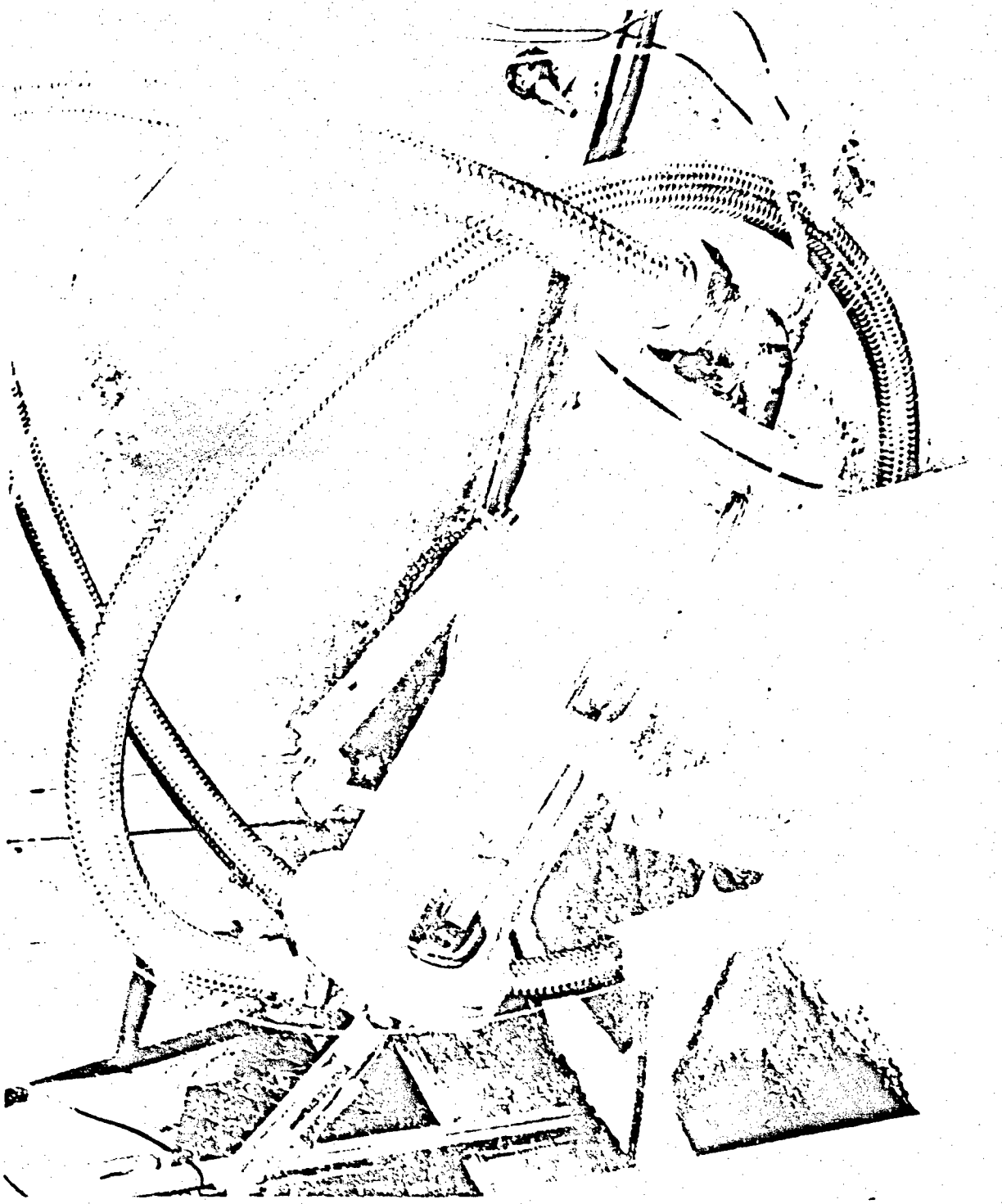

Figure No. 2 - Photograph of Test Cell Assembly

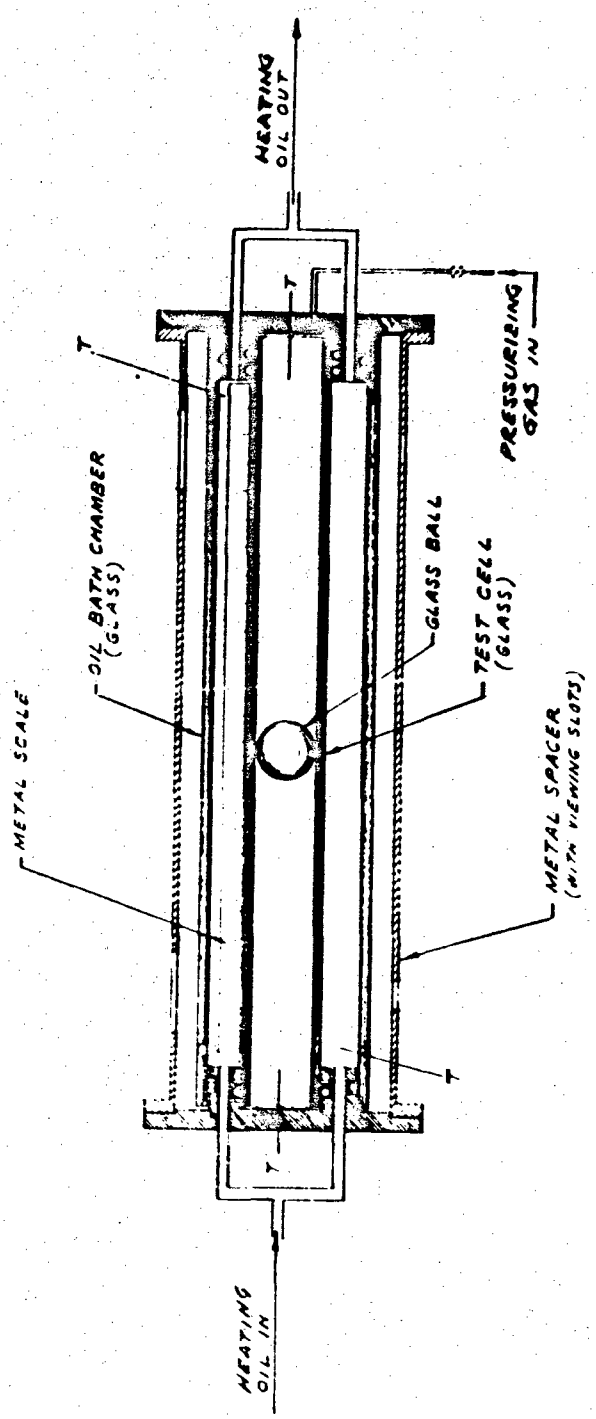

Figure No. 3 - Schematic of Test Cell

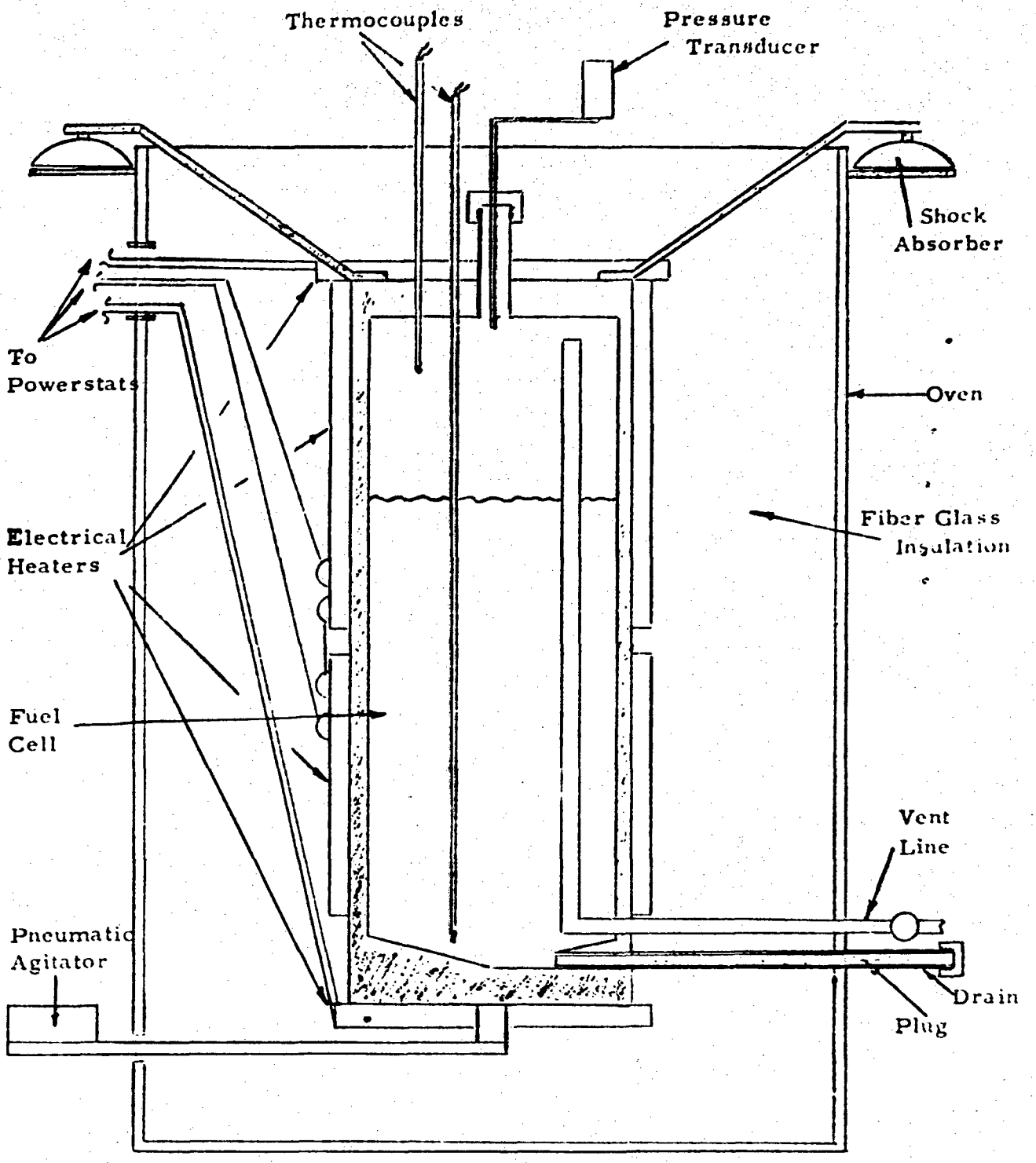

Figure No. 4 - Schematic of the Vapor Pressure Measurement Device

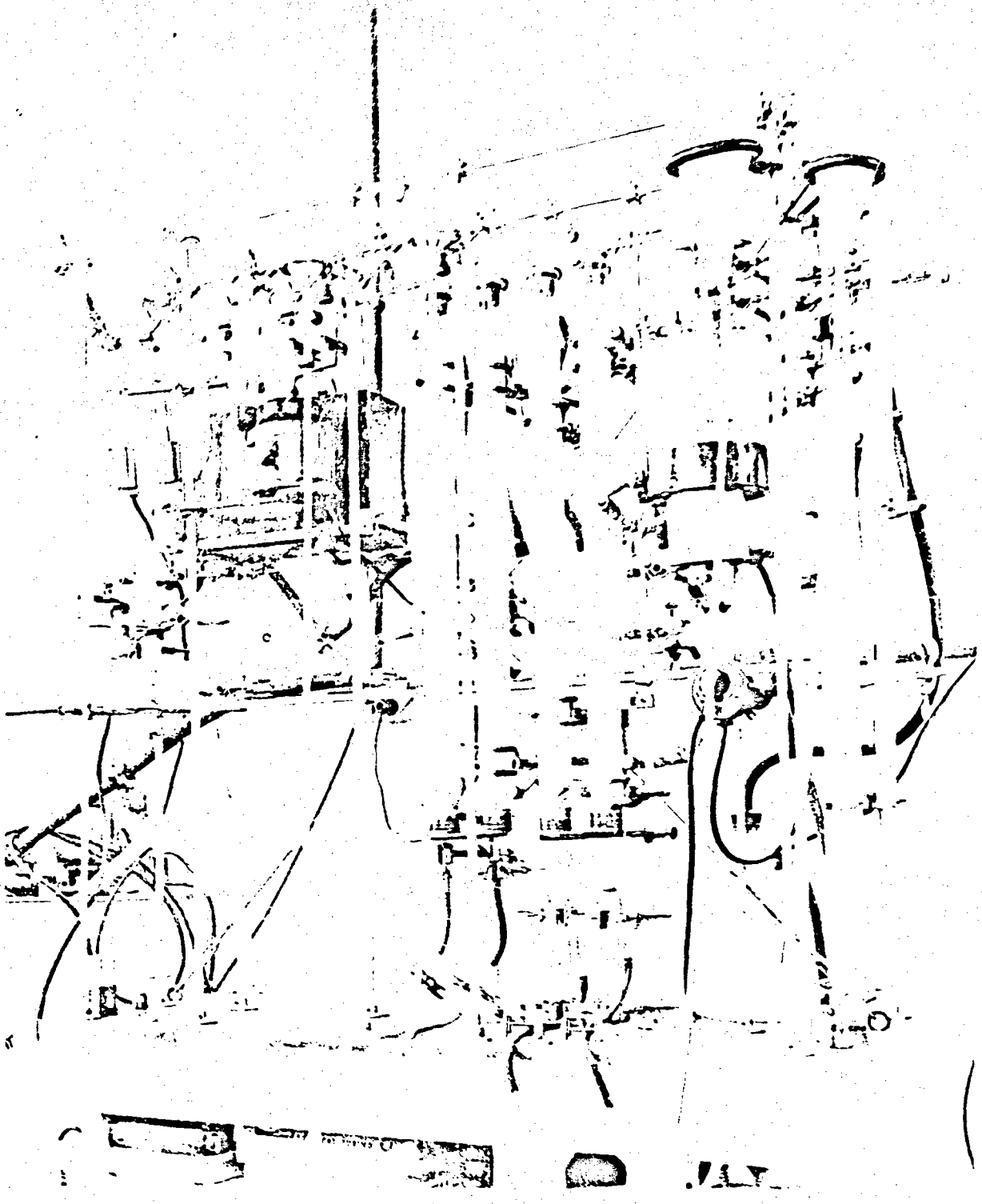

Figure No. 5 - Photograph of Laboratory Apparatus Used to Determine Oxygen and Nitrogen Content of Fuels.

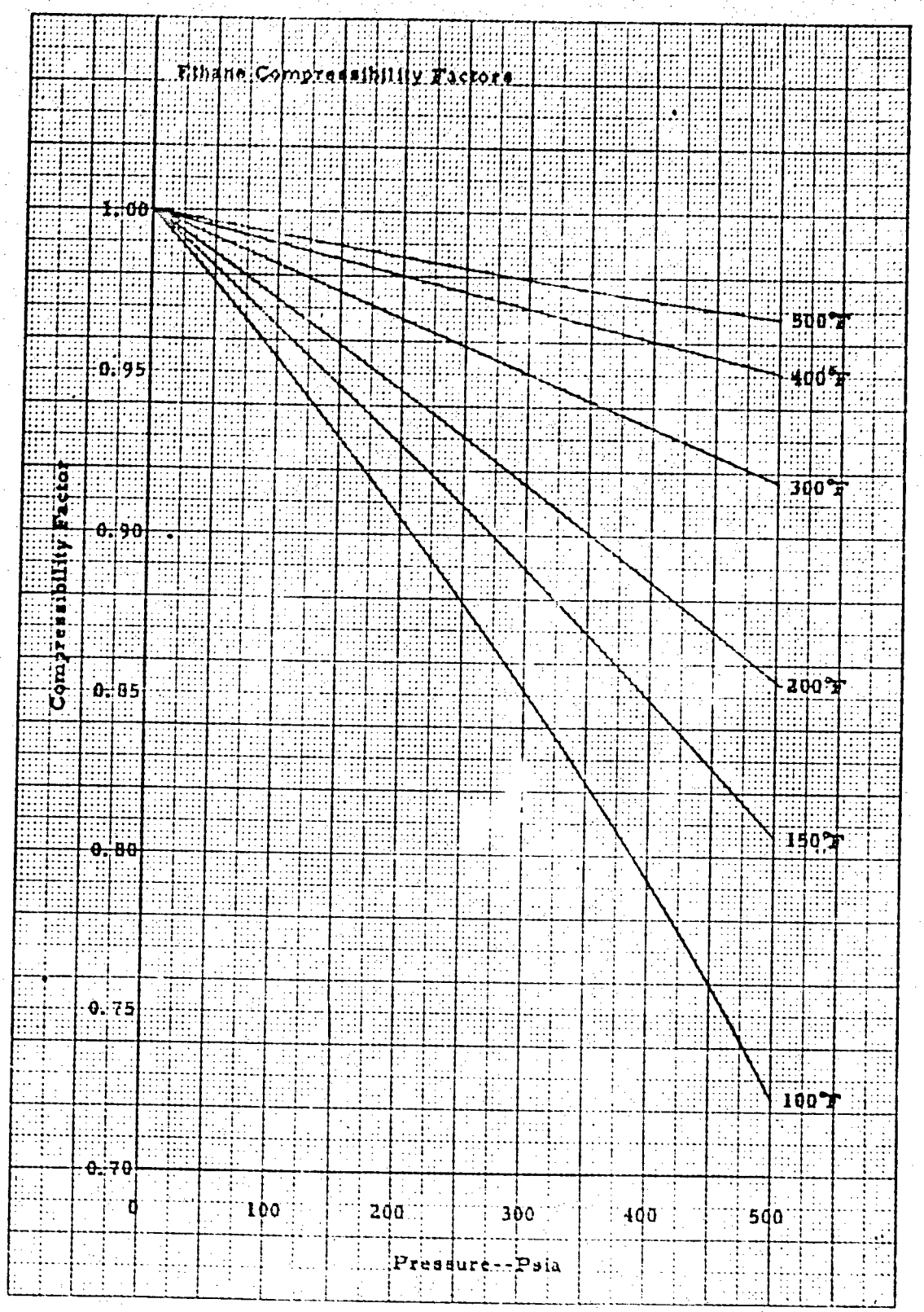

Figure No. 6 Ethane Compressibility Factors

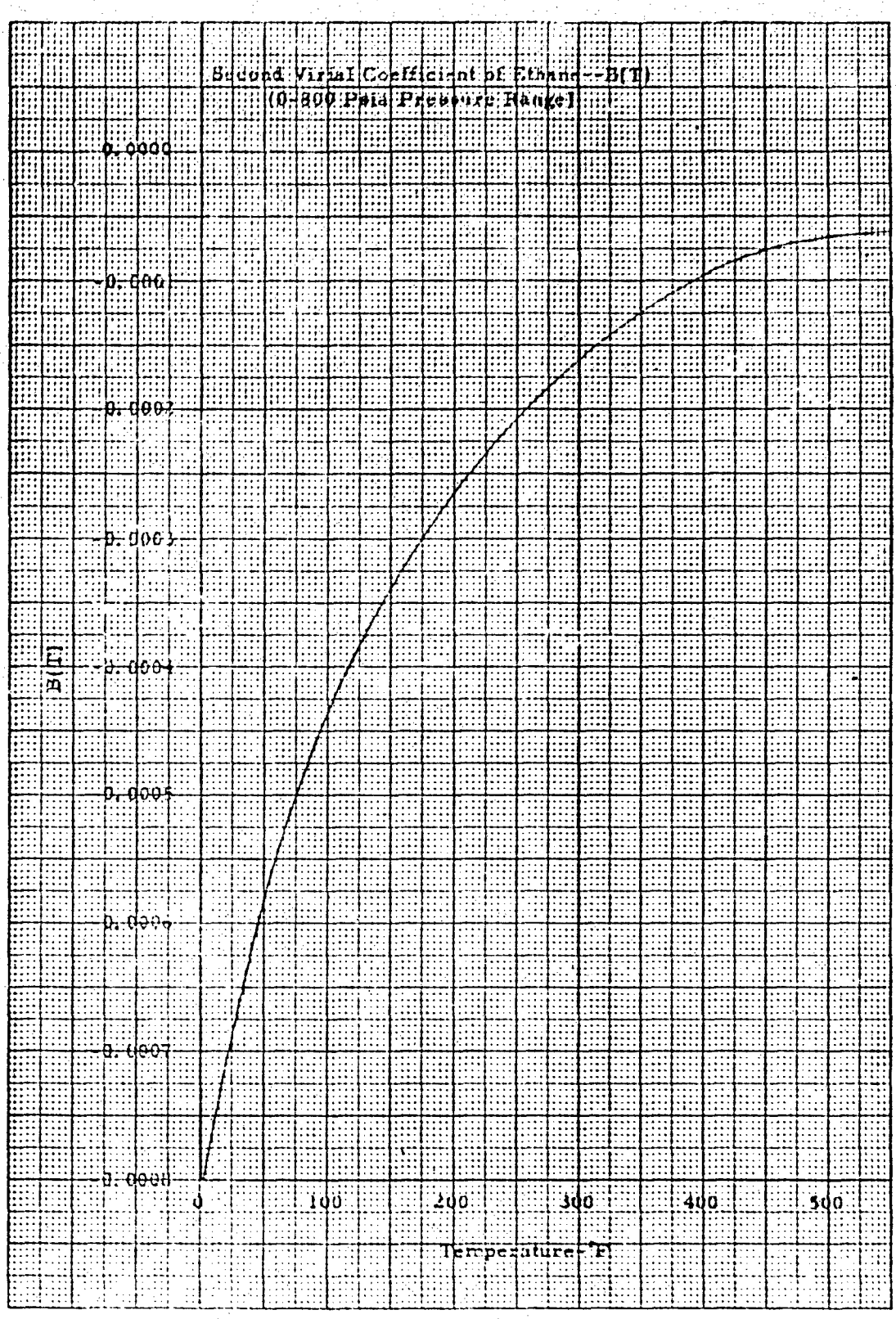

Figure No. 7 - Second Virial Coefficient of Ethane

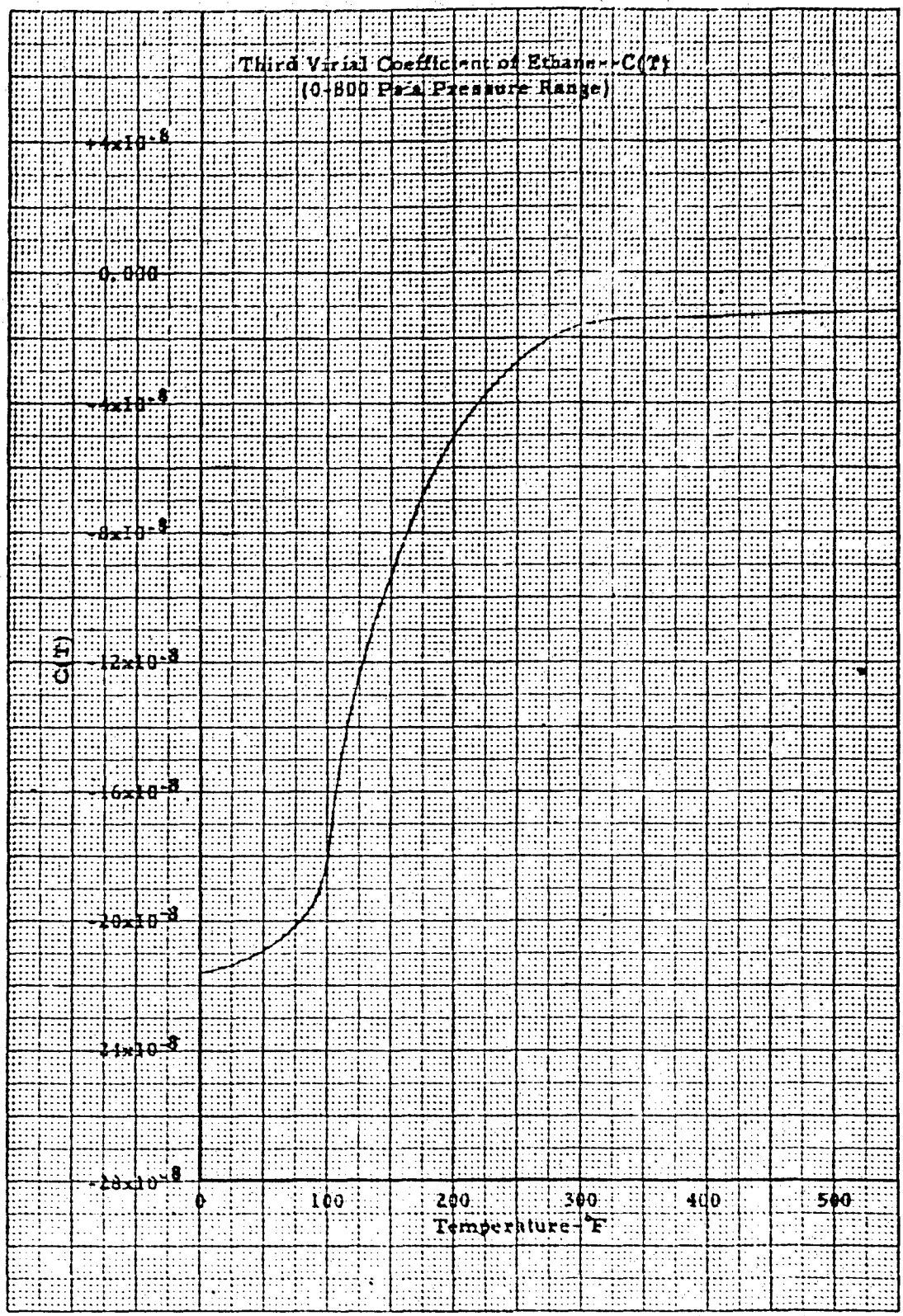

Figure No. 8 - Third Virial Coefficient of Ethane

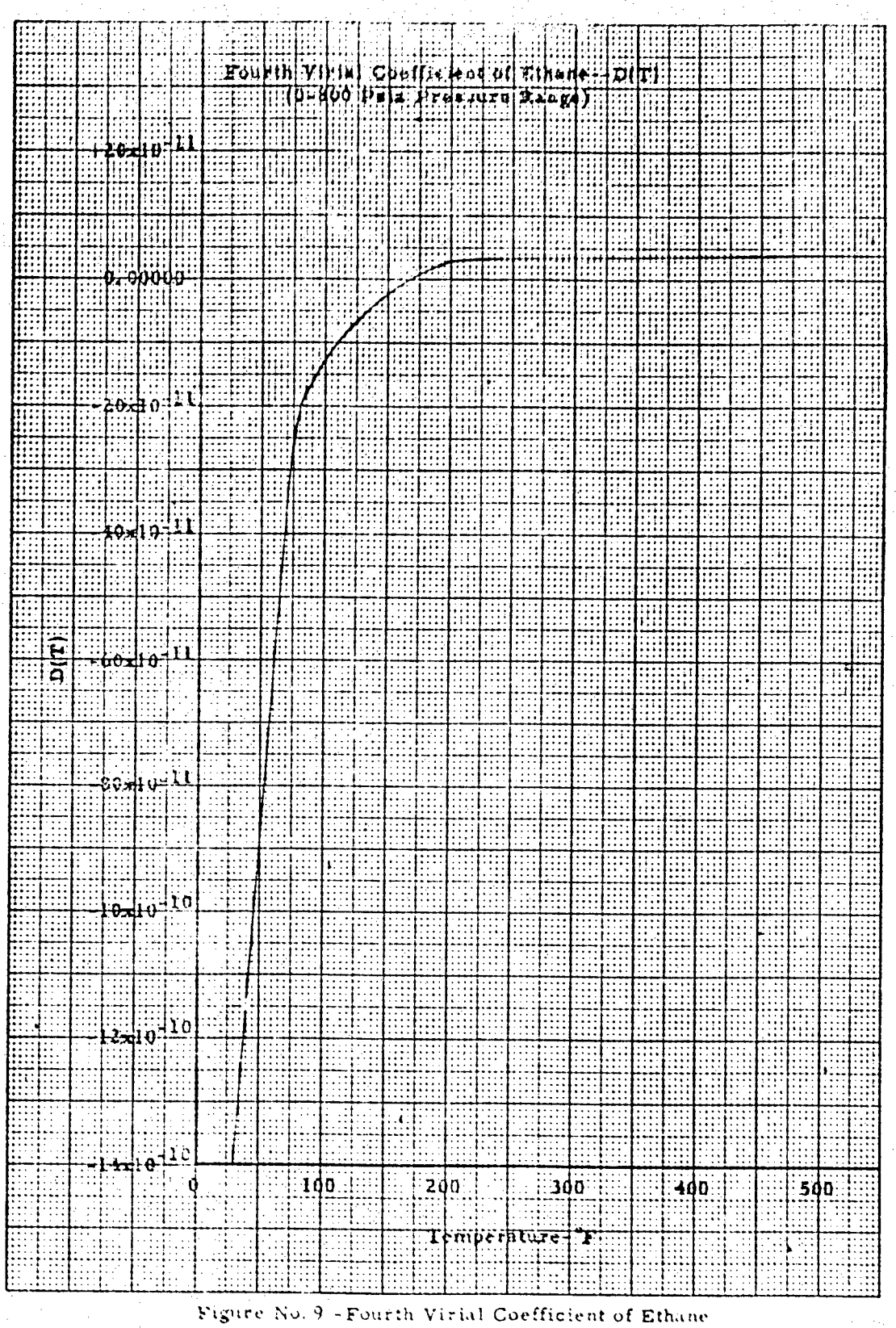

Figure No. 9 - Fourth Virial Coefficient of Ethane

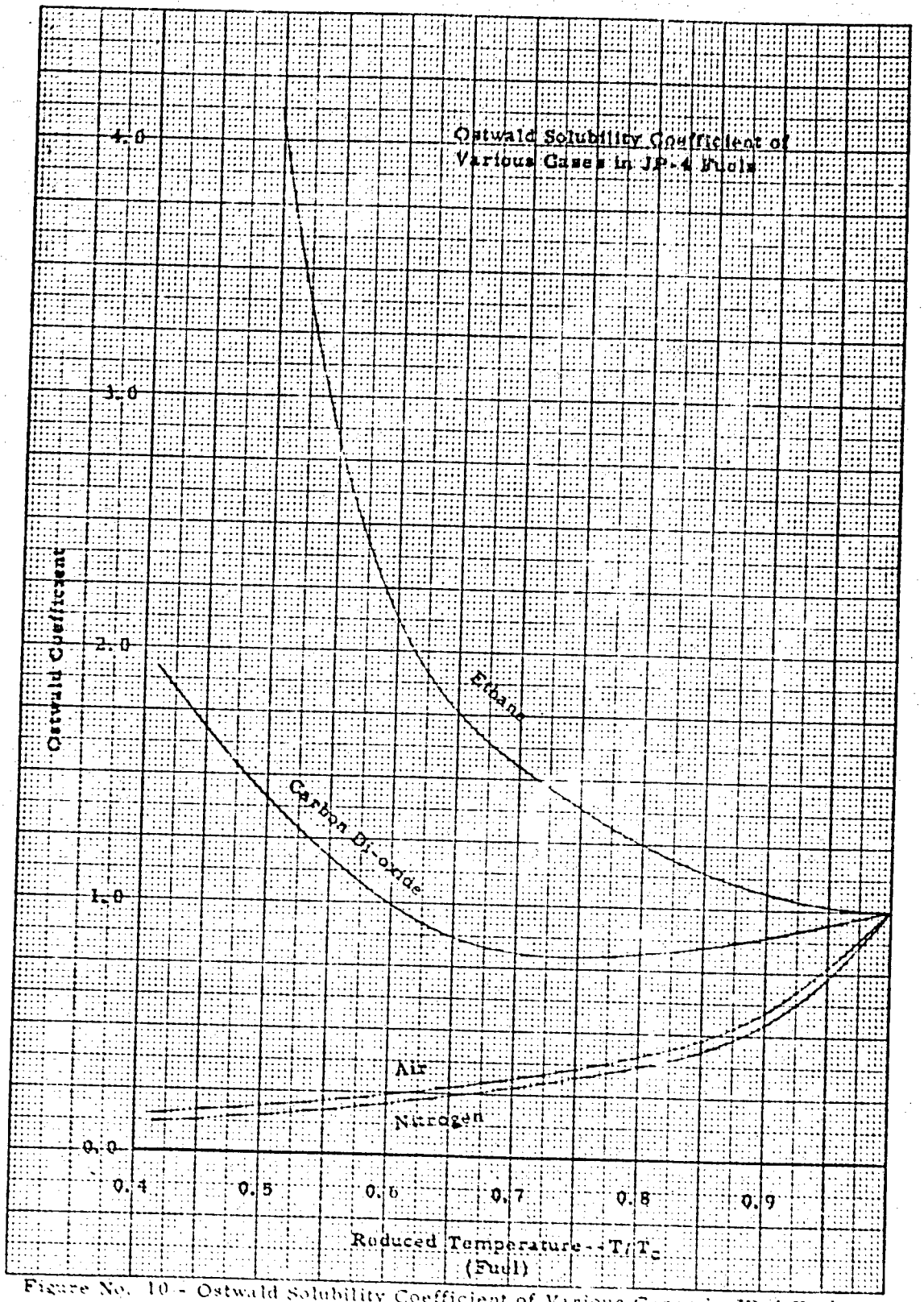

Figure No. 10 - Ostwald Solubility Coefficient of Various Gases in JP-4 Fuels.

AD TR 60-767

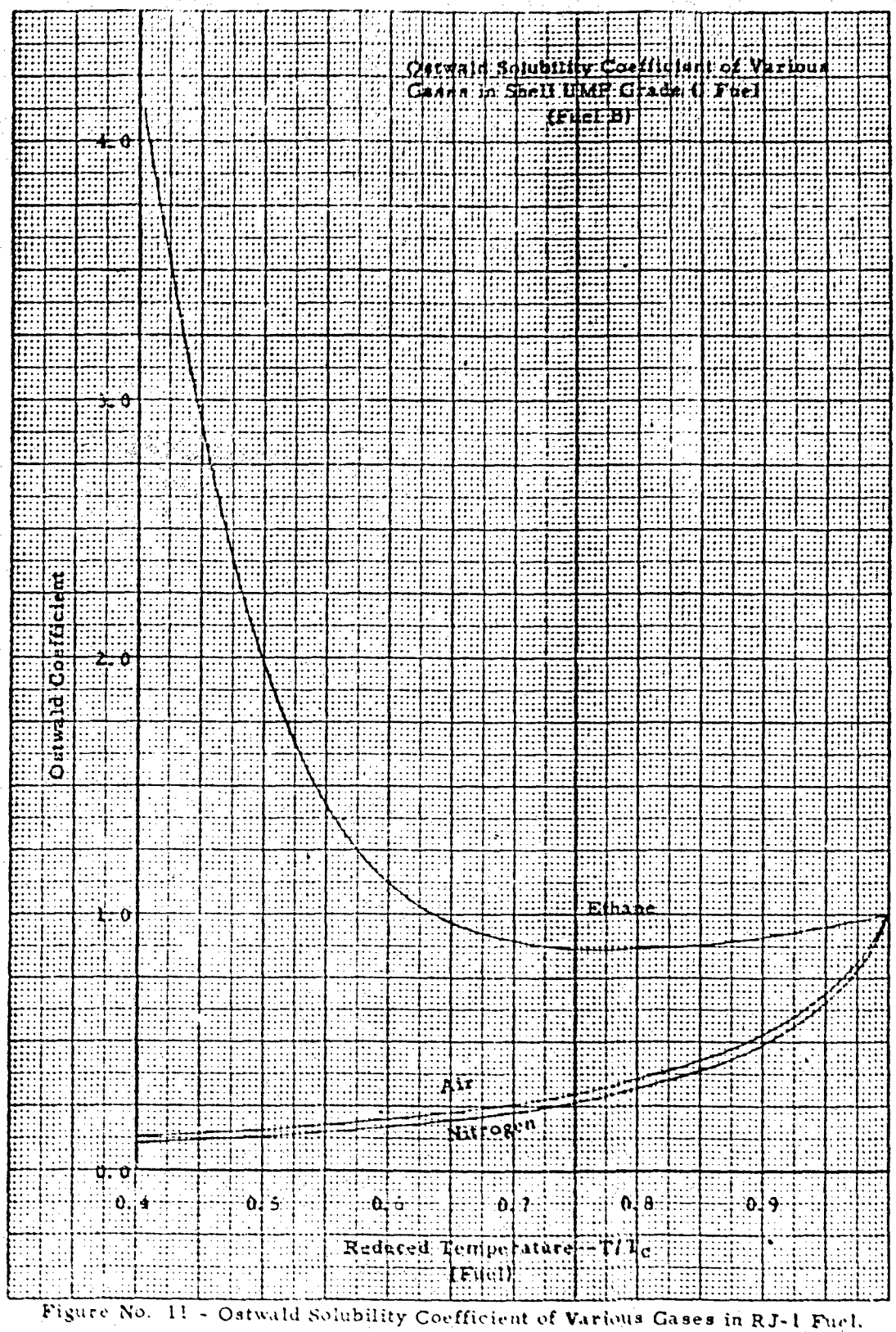

Figure No. 11 - Ostwald Solubility Coefficient of Various Gases in RJ-1 Fuel.

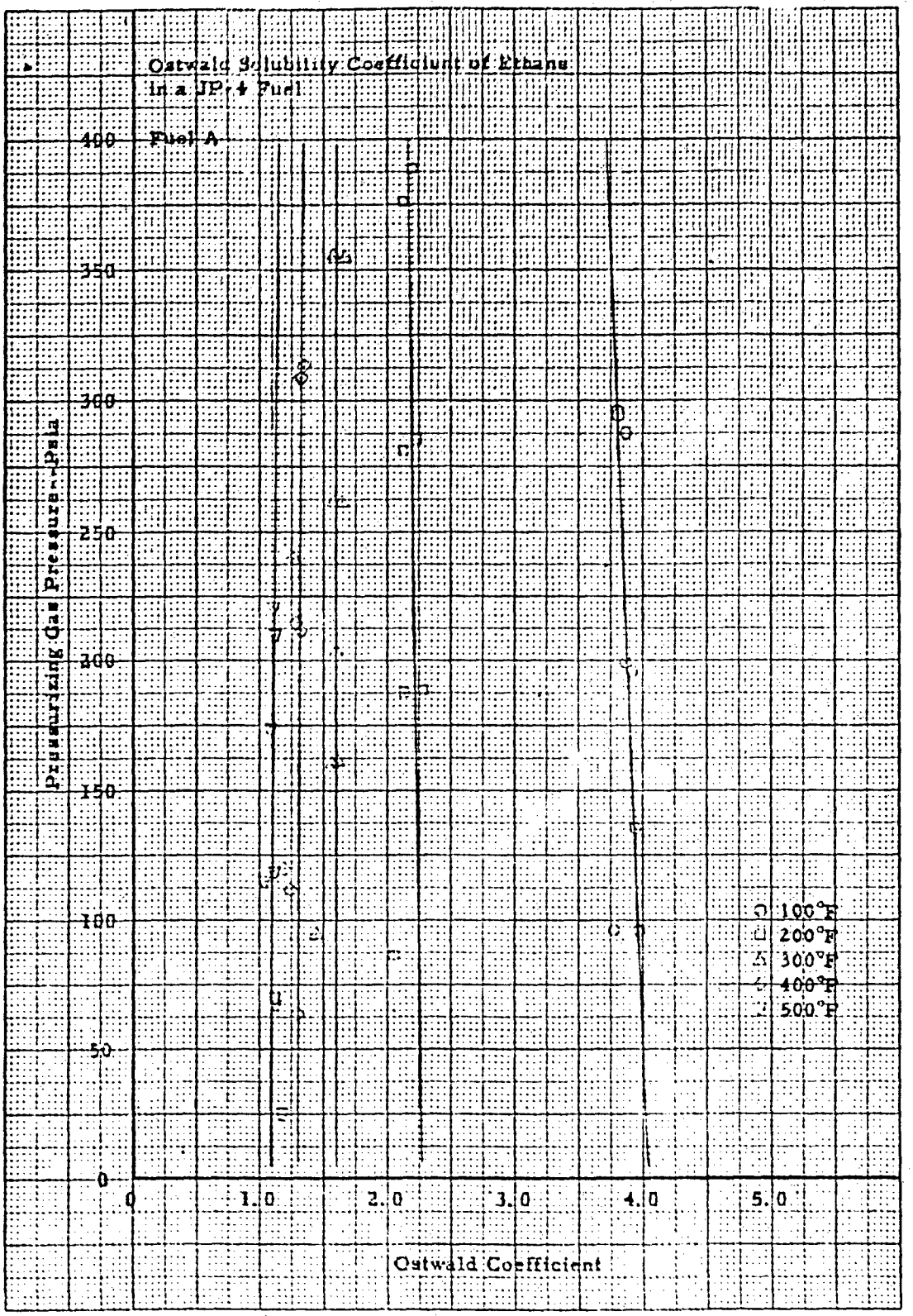

Figure No. 12 - Ostwald Solubility Coefficient of Ethane in a JP-4 Fuel

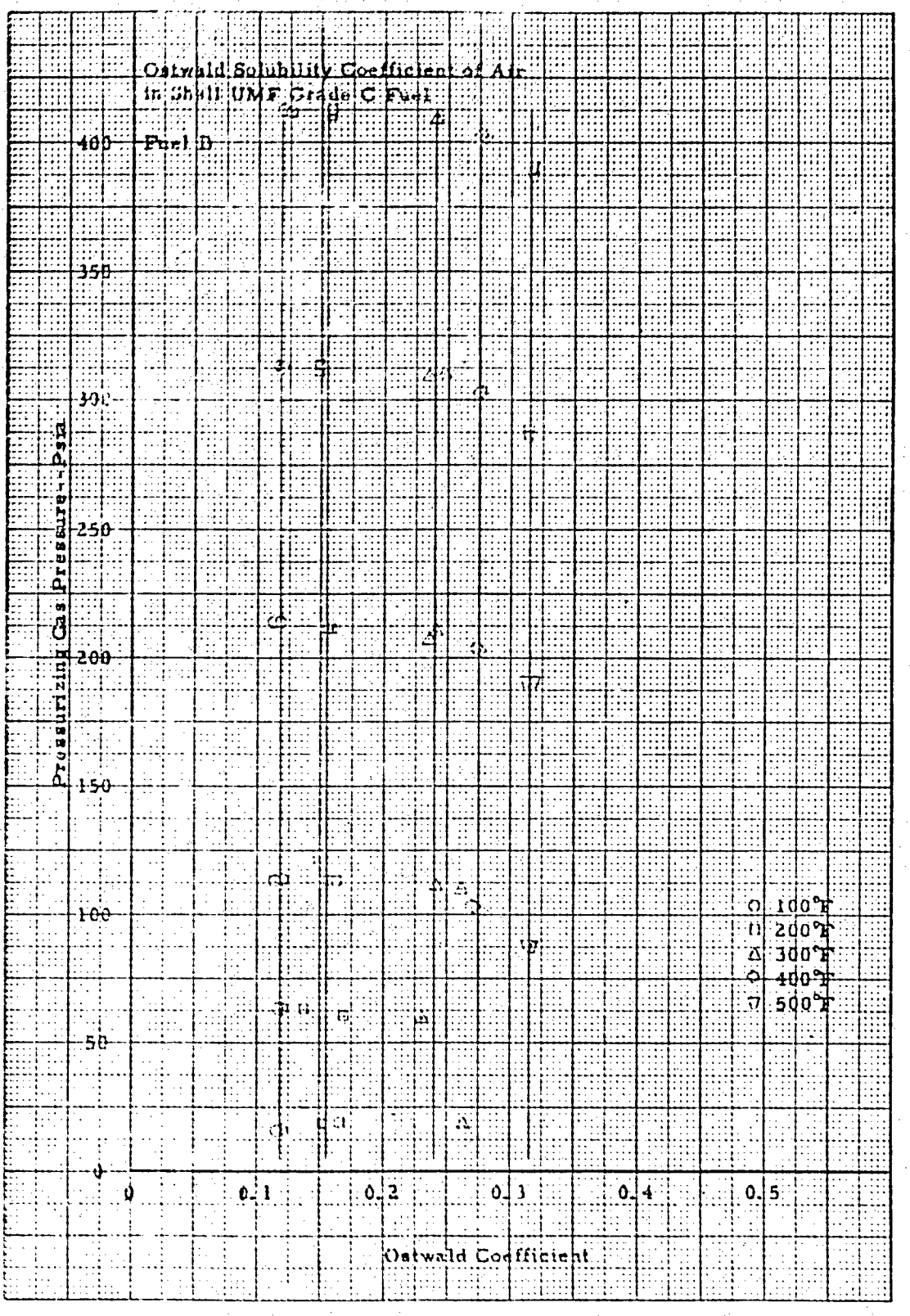

Figure No. 13 - Ostwald Solubility Coefficient of Air in RJ-1 Fuel.

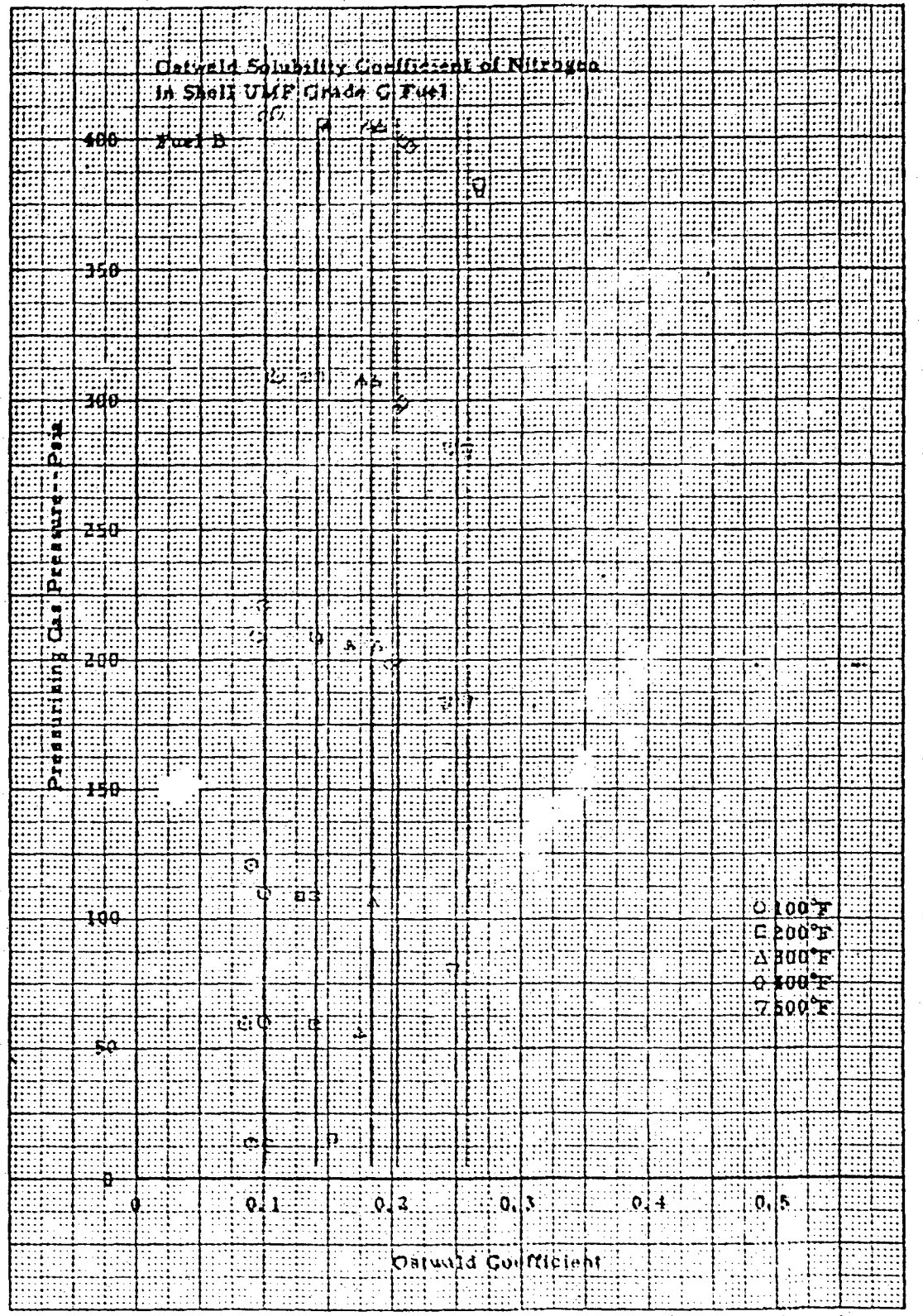

Figure No. 14 - Ostwald Solubility Coefficient of Nitrogen in RJ-1 Fuel.

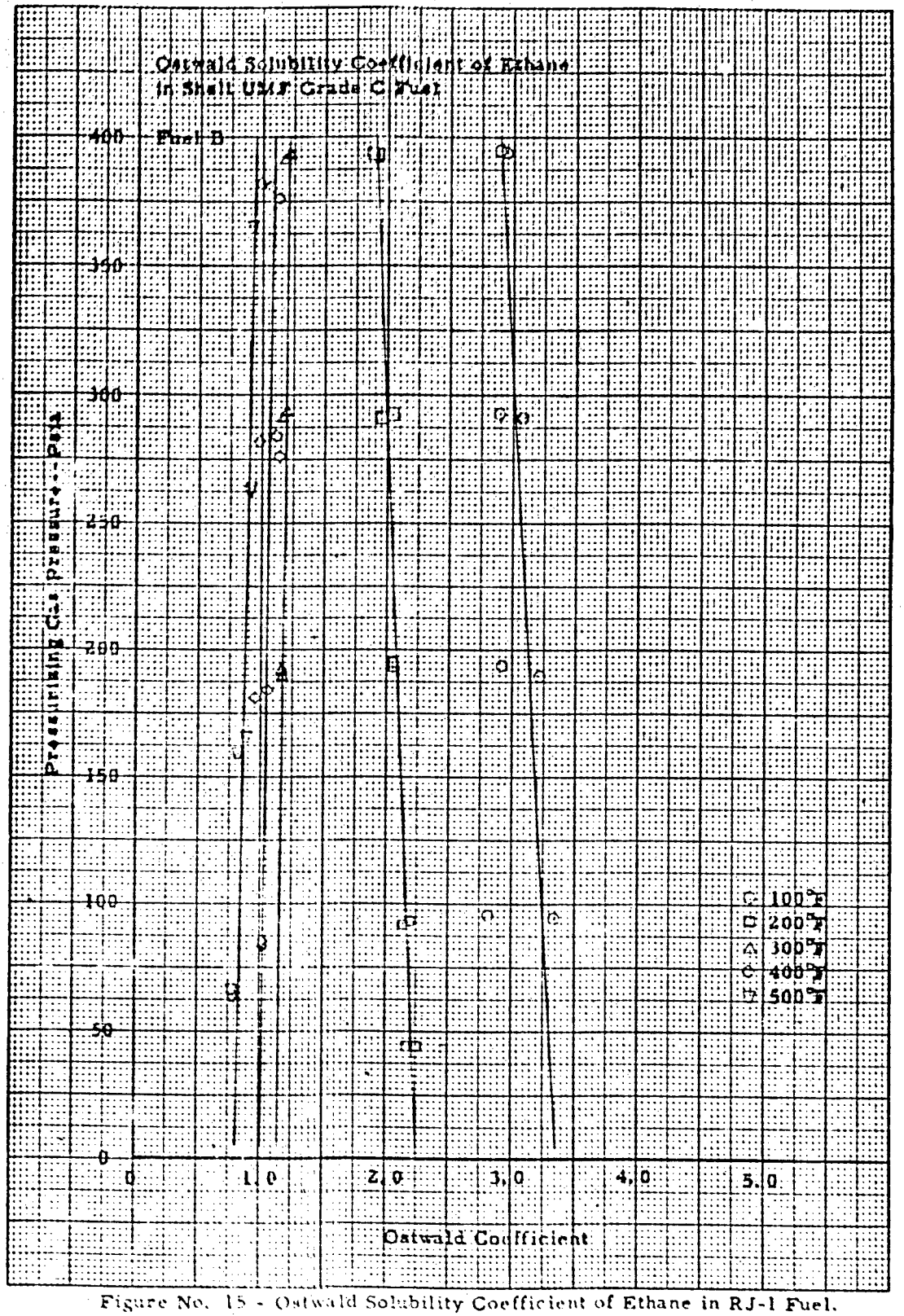

Figure No. 15 - Ostwald Solubility Coefficient of Ethane in RJ-1 Fuel.

Figure No. 16 - Solubility of Ethane in Fuel A - JP-4.

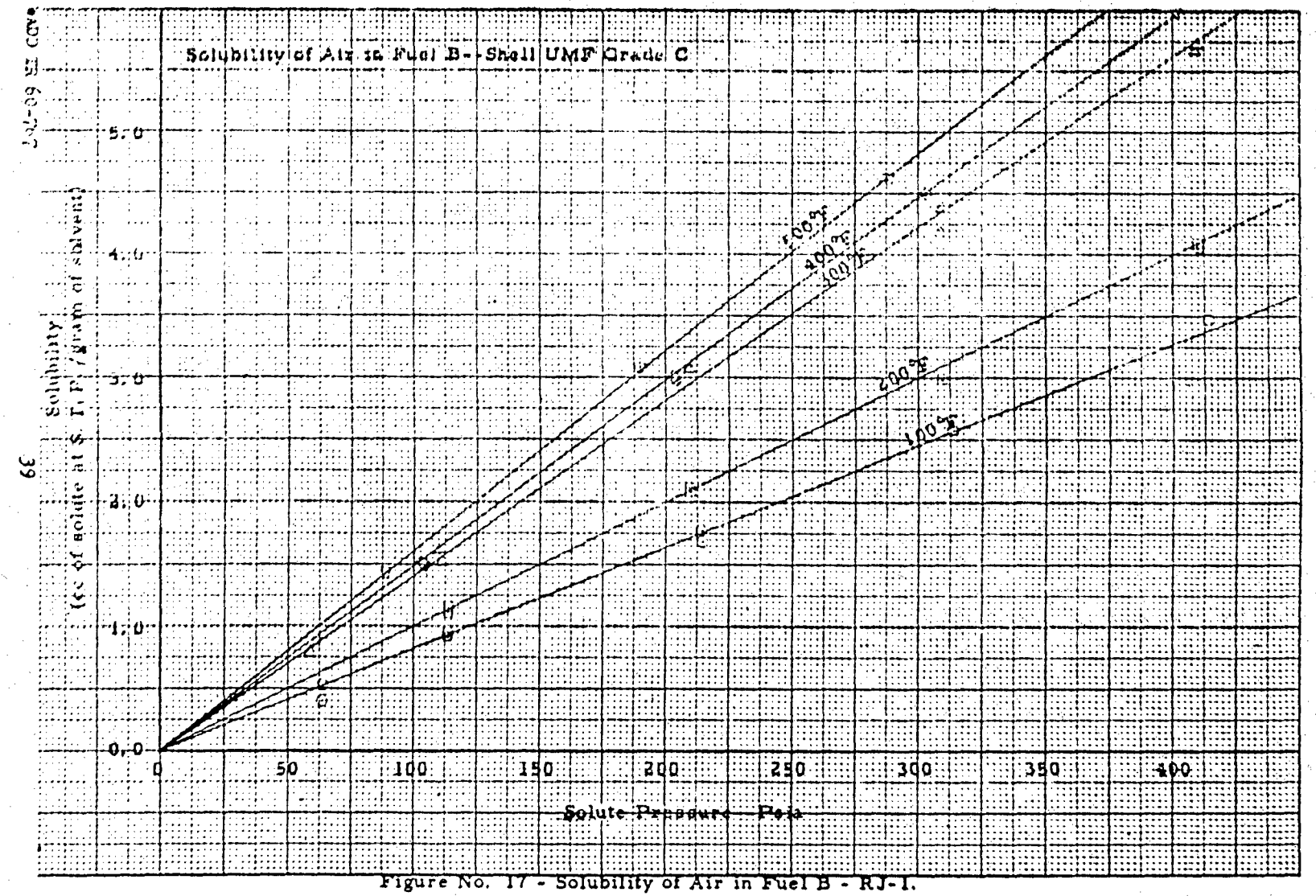

Figure No. 17 - Solubility of Air in Fuel B - RJ-1.

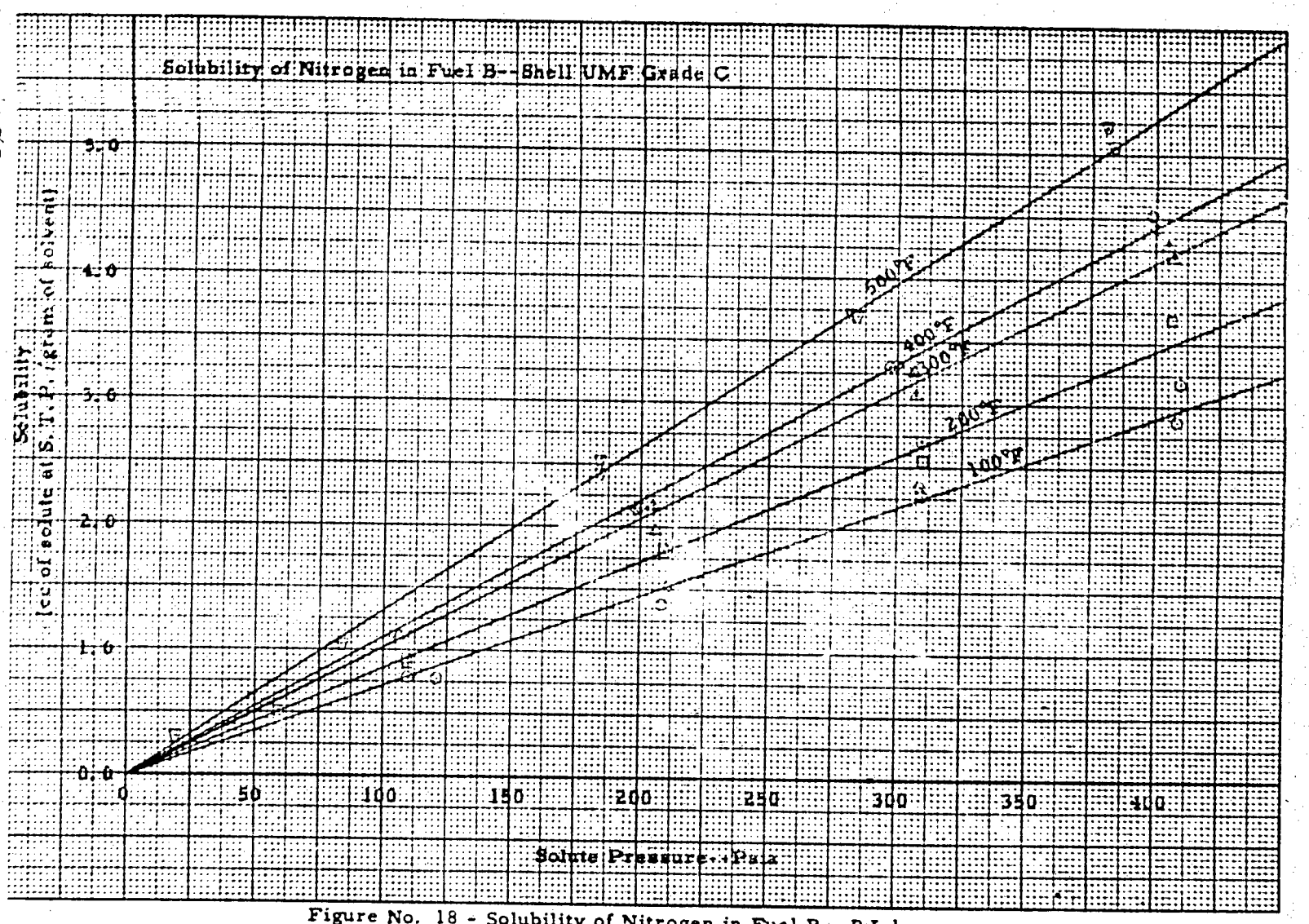

Figure No. 18 - Solubility of Nitrogen in Fuel B - RJ-1

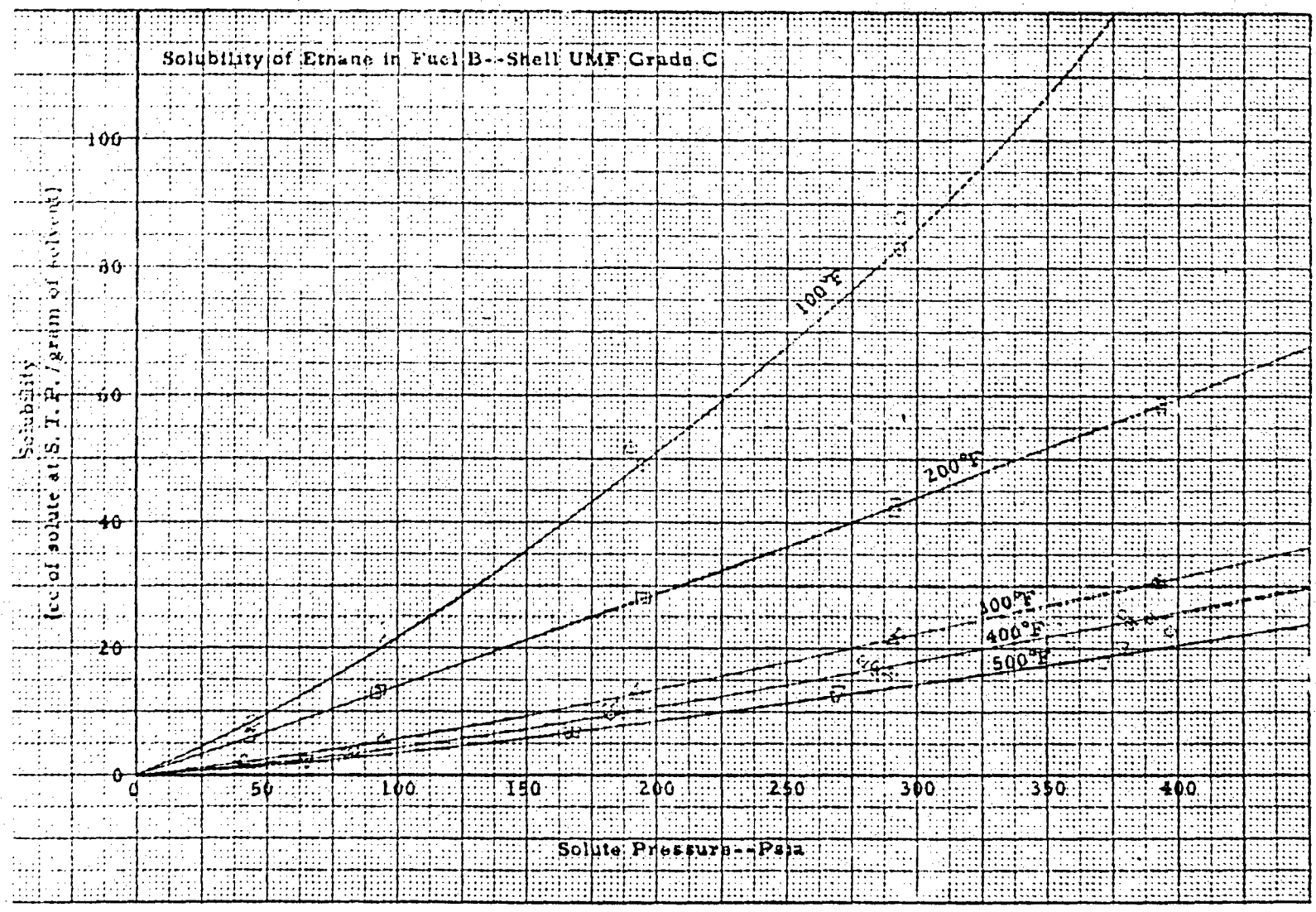

Figure No. 19 - Solubility of Ethane in Fuel B - RJ-1.

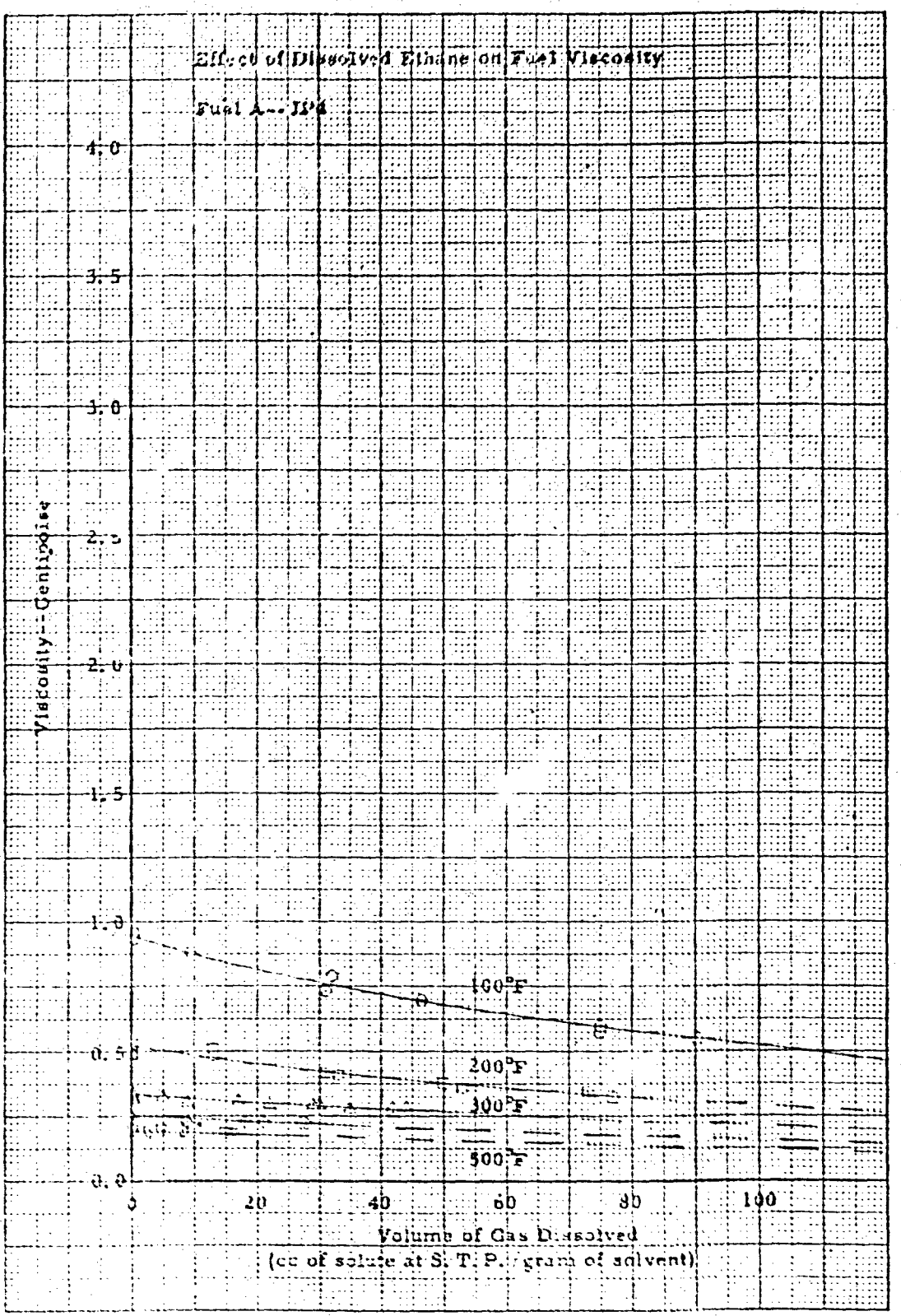

Figure No. 20 - Effect of Dissolved Ethane on Fuel Viscosity, Fuel A - JP - 4.

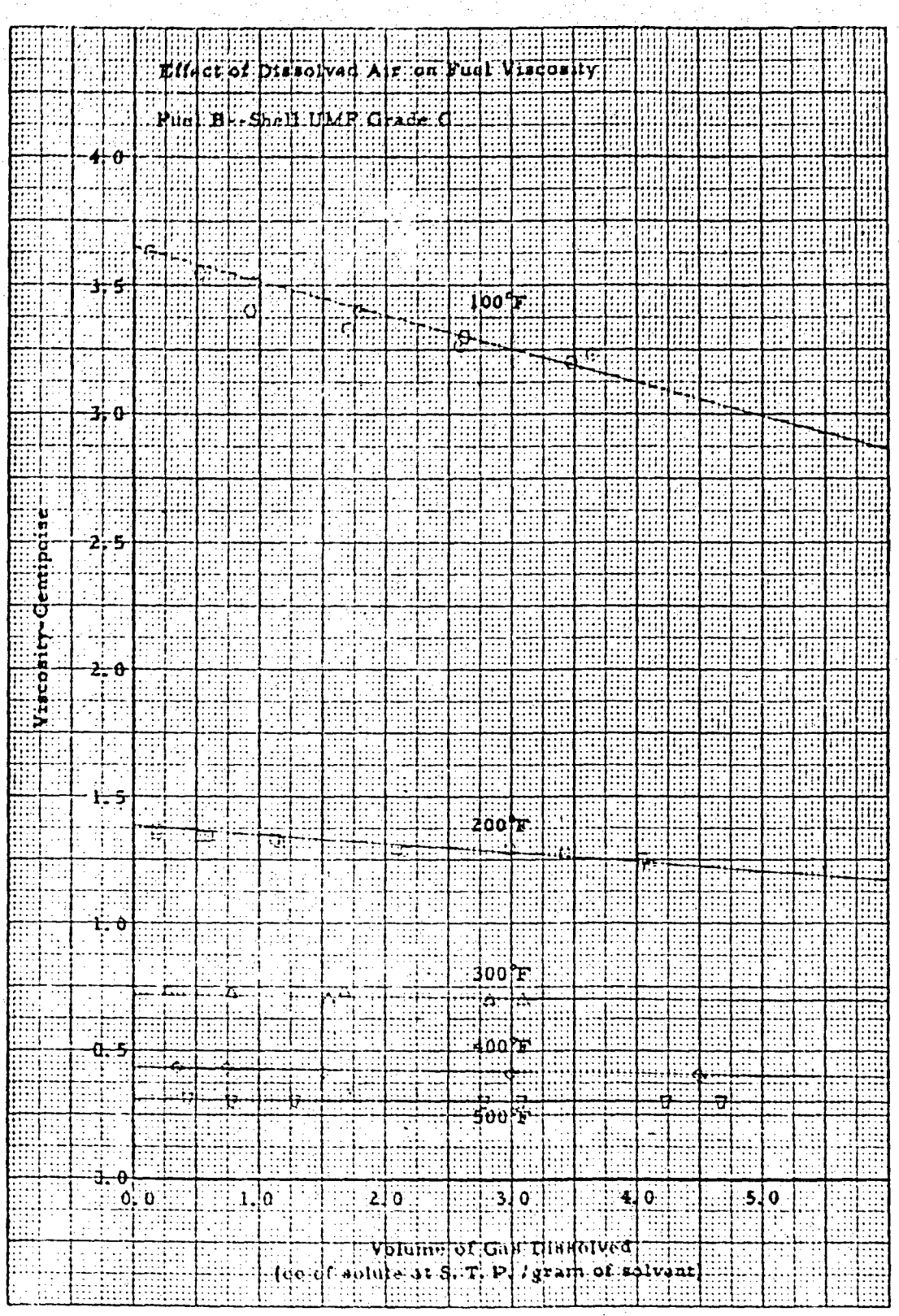

Figure No. 21 - Effect of Dissolved Air on Fuel Viscosity, Fuel B - RJ - 1.

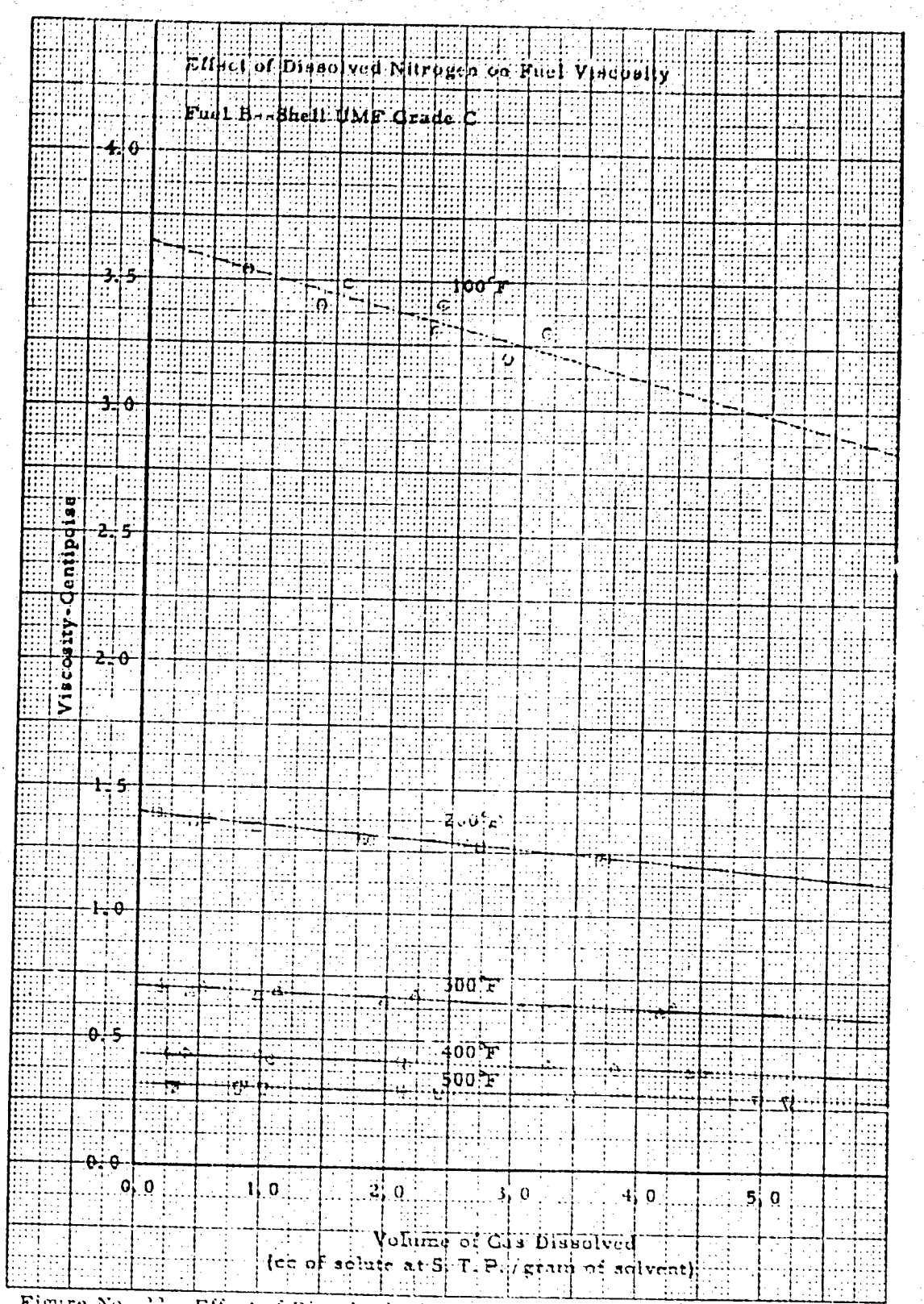

Figure No. 22 - Effect of Dissolved Nitrogen on Fuel Viscosity, Fuel B - RJ - 1.

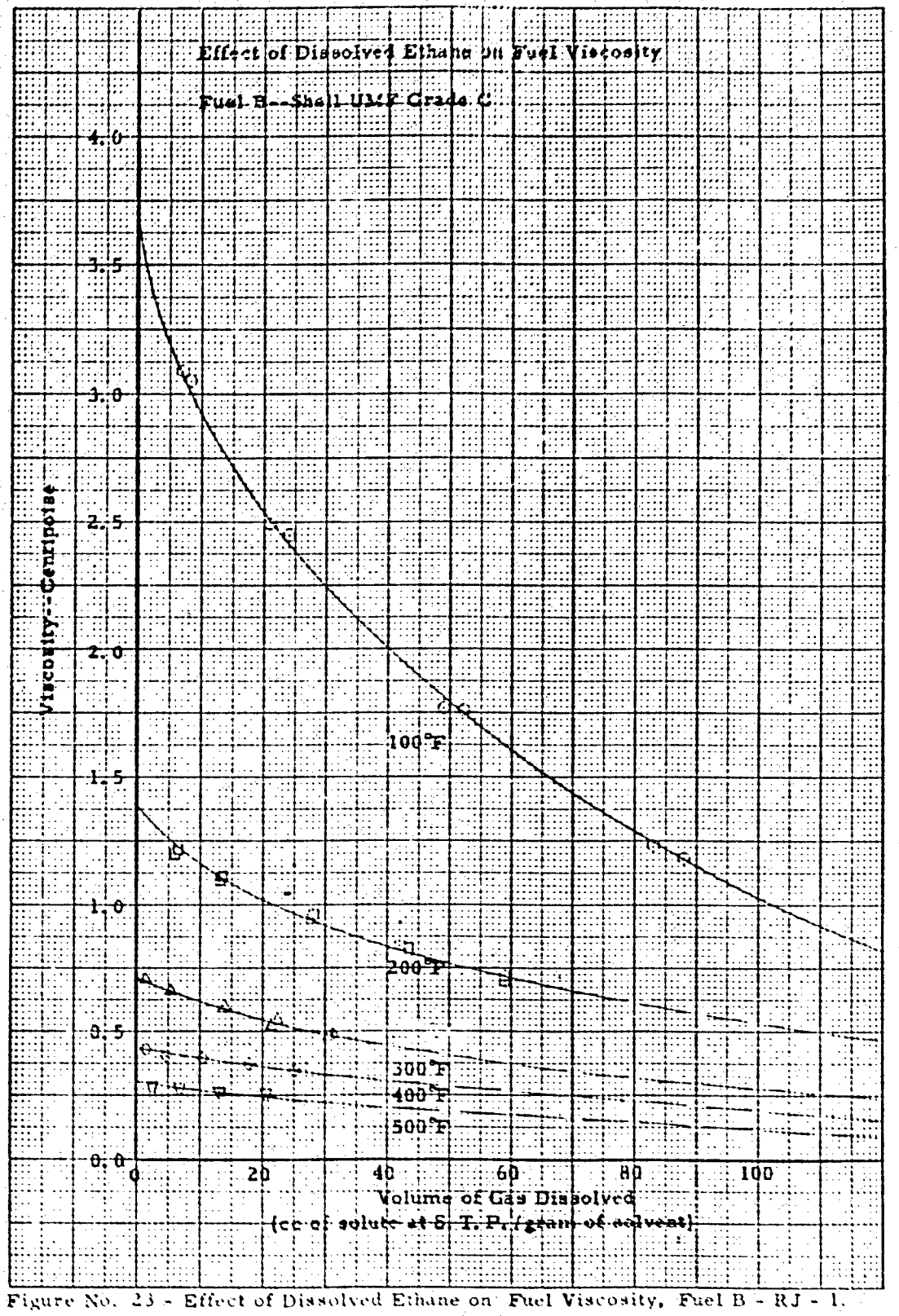

Figure No. 23 - Effect of Dissolved Ethane on Fuel Viscosity, Fuel B - RJ - 1.

Figure No. 24 - Effect of Dissolved Ethane on Density, Fuel A - JP - 4.

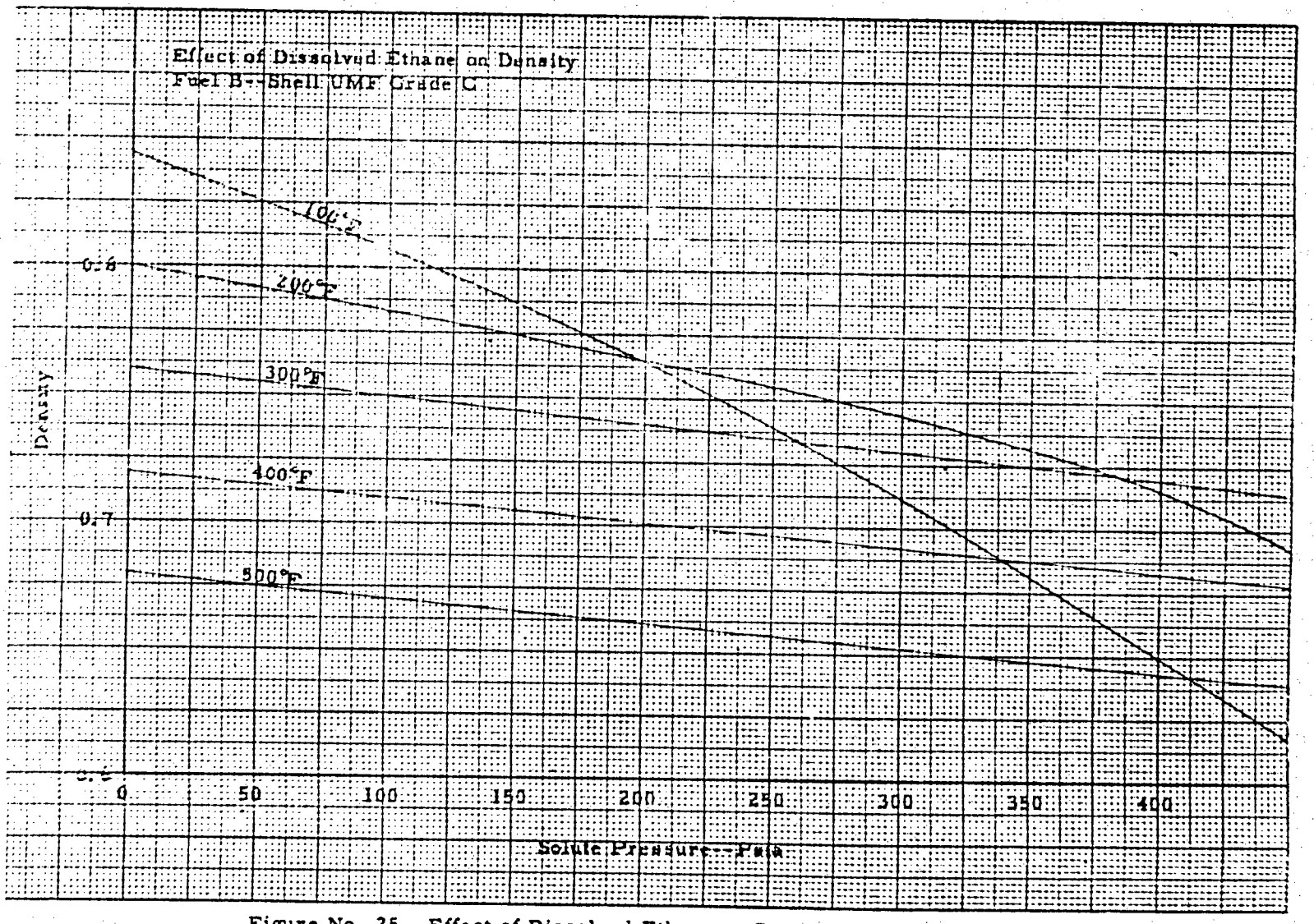

Figure No. 25 - Effect of Dissolved Ethane on Density, Fuel B - RJ - 1.

TABLE I

SOLUTE ANALYSES	
1. AIR	
H_2O	0.0 % by volume
CO_2	0.0
Illuminants	0.0
O_2	21.08
CO	0.0
Hydrocarbons	0.0
N_2	78.92
2. NITROGEN	
Purity (minimum)	99.7 0%
3. ETHANE	
Research Grade	99.9%

PART II EVOLUTION RATE STUDIES

INTRODUCTION

This Part is one of a series of interim reports, each of which is offered in partial fulfillment of Research Program AF 33(616)3729. This program was initiated in June, 1956. The results reported herein cover Phase 4 of the Research Program. Phase 4 represents a study of the evolution rates of three pressurizing gases from two selected, military fuels. The two fuels are: Fuel A, (JP-4) and Fuel B (RJ-1).

OBJECTIVE

The purpose of Phase 4 of the Research Program was to determine the effect of fuel type, plus pressure-change and agitation rates, on the evolution rate of three pressurizing gases. Test conditions simulated, as closely as practical, conditions occurring in present aircraft and missiles. Conditions anticipated in future aircraft and missiles were also simulated and tests performed in this environment.

SUMMARY

Experimental data were obtained for the evolution rates of four systems:

Air - JP-4	Air - RJ-1
Ethane - JP-4	Nitrogen - RJ-1

These tests determined that the evolution rate of ethane is considerably higher than that of air. Further, agitation level has a pronounced effect on evolution rate. The effect of pressure level on evolution rate was not observable in the air-fuel systems, but was conspicuous in the ethane-fuel system.

Comparison between the test data and the work of Schweitzer and Szebehely * showed little correlation. This is believed due, at least in part, to different experimental approaches and control of variables.

TEST EQUIPMENT AND PROCEDURE

The equipment of this phase of the program was designed to simulate an aircraft fuel tank. Certain environmental test conditions were then imposed upon this tank. The conditions approximated those occurring in high performance missiles and aircraft.

Initially, it was intended to schedule a programmed flight plan through take-off and cruise, monitoring both evolution rate and tank ullage composition. One of the environmental conditions to be imposed on the tank during the cruise portion of this simulated flight was heat. Skin temperatures to 1000°F and pressures to 200 psia were to be investigated. The tank ullage composition was to be monitored using a rapid-scan mass spectrometer. Due to time and monetary considerations, this portion of the program was deleted.

The test tank, however, was constructed to meet the initial, severe environmental conditions. The tank is contained in a stainless-steel oven where radiant heaters (stainless-steel-sheath) supply the thermal energy. A special steel test chamber was built to house the entire unit. See Figures 26 through 29 for additional detail.

A considerable effort went into the development of a suitable means of providing agitation. There appears to be no set standard of agitation, nor is there any approved test method for simulating aircraft agitation. Initially it was proposed to develop a stirrer-type agitator that did not employ seals. Tank leakage could not be tolerated because of the

* Schweitzer, P. H. and Szebehely, V. G. Gas Evolution in Liquids and Cavitation. Journal of Applied Physics. Volume 21. December, 1950. pp 1218 - 1224.

radiant heaters, even though provisions for inerting the oven space were provided.

The agitator that was developed was a propeller type. See Figure 30. The propeller was driven by an eccentric shaft and pinion device enclosed in a bellows. The entire construction was of stainless steel. Trouble developed however, when the bellows failed repeatedly after a short period of operation.

A second type of agitator was then developed. This agitator consisted of a rocker mechanism which tilted the oven and tank about its center of gravity. See Schematic shown in Figure 25. The amplitude of deflection, measured at the end of the oven, is $\frac{1}{2}$ inch. The agitation rate is varied by changing rocking frequency, by using different pulley ratios, while using a constant speed, one-half HP motor. Four agitation frequencies were arbitrarily chosen: 350 CPM, 240 CPM, 150 CPM and zero CPM. This method of agitation proved feasible and was used to obtain the data presented in this Supplement.

A 35 liter aircraft-oxygen-bottle was used as the vapor reservoir. The bottle was connected to the tank with a flexible tubing line to damp the tank vibrations. A sump container was inserted between the reservoir and the tank to prevent any liquid entrainment losses from entering the reservoir.

Tank and reservoir pressures were recorded using pressure transducers and a light beam oscillograph. Tank and reservoir pressures were monitored visually by means of pressure guages. Temperatures were measured using iron-constantan thermocouples and galvanometer read-out instruments. All temperature measurements were recorded manually.

The test-procedure steps follow:

1. Flush tank with fuel to remove possible contamination.

2. Fill tank with fuel to prescribed level.

3. Evacuate reservoir.

4. Record initial conditions.

5. Pressurize tank to desired level. Agitate with rocker to speed dissolution of pressurizing gas.

6. Measure and record the tank liquid and vapor temperatures, plus the reservoir temperature, after equilibrium is reached in tank.

7. Set tank agitation rate by pulley adjustment.

8. Turn on recording instrumentation.

9. Vent into reservoir to drop tank pressure. Rate of pressure drop is manually controlled for a linear decline.

10. Close vent valve when desired final pressure is reached.

11. Turn off recording instrumentation and note temperatures.

12. Repeat steps 6 through 11, over the desired pressure range, after equilibrium is reached in the tank.

Static equilibrium was evaluated by noting pressure changes. Initially, if a pressure change was not noted within a 10-minute period, tank equilibrium was assumed. This time period proved to be insufficient and the procedure was modified to allow a minimum of $\frac{1}{2}$-hour for the system to come to equilibrium after a test run. Where air and nitrogen were the pressurizing gases, a $\frac{1}{2}$-hour period was satisfactory. Ethane required much longer periods of time, ranging from one to six hours. This time period was dependent to a large degree on the previous rate of pressure change. If the pressure change rate had been rapid, a longer period of time would have been required for the ethane fuel system to achieve equilibrium.

EVOLUTION RATE CALCULATIONS

The evolution rate calculations were based on a system weight balance. The system consisted of a fuel tank and an evacuated chamber called the reservoir. See sketch below.

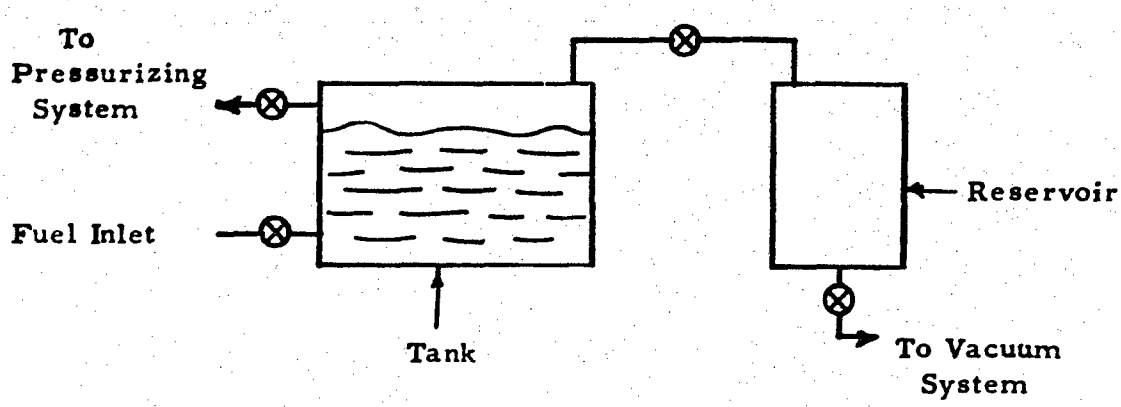

Note, from the above sketch, that when the vacuum system valve and pressurizing system valves have been closed any gas or vapor that leaves the tank must enter the reservoir. Expressed mathematically

$$\Delta n_r = \frac{\Delta P_r V_r}{Z_r R T_r} = \frac{\Delta P_v V_v}{Z_v R T_v} + \Delta n_e \qquad (1)$$

For the purpose of these calculations, Z_r is assumed to equal 1.0 at pressures below atmospheric. This is approximately true for both the fuel vapors and the pressurizing gases used in this study. For this reason Z_r has been omitted in all calculations.

If evolution did not take place the quantity of pressurizing gas and fuel vapor leaving the tank would be a direct function of the pressure change in the fuel tank.

$$\Delta n_v = \frac{\Delta P_v V_v}{Z_v R T_v} \qquad (2)$$

A computation of the quantity of gas due to evolution may be made when: 1) the quantity of gas that comes out of the fuel tank due to pressure change (excluding that due to evolution) and, 2) that quantity of gas entering the reservoir due to both evolution and vapor-space loss is known.

$$\Delta n_e = \Delta n_r - \Delta n_v \qquad (3)$$

$$\Delta n_e = \frac{\Delta P_r V_r}{Z_x R T_r} - \frac{\Delta P_v V_v}{Z_v R T_v} \qquad (4)$$

At the reservoir pressures used, i.e., 0 - 10 psia, $Z_r \cong 1.0$

$$\Delta n_e = \frac{1}{R}\left[\frac{\Delta P_r V_r}{T_r} - \frac{\Delta P_v V_v}{Z_v T_v}\right] \qquad (5)$$

The use of a linear change rate, i.e., $\frac{\Delta P}{t} = K$ gives the evolution rate for the total fuel charged.

$$\frac{\Delta n_e}{t} = \frac{1}{Rt}\left[\frac{\Delta P_r V_r}{T_r} - \frac{P_v V_v}{Z_v T_v}\right] \tag{6}$$

The weight of fuel charged can be determined, when the volume of fuel charged and its density at the charge temperature are known.

$$W = \rho \cdot V_i \tag{7}$$

The evolution rate, to be of most use, should be based on a unit quantity of fuel. Therefore the evolution rate per unit weight of fuel can be expressed as follows:

$$E = \frac{\Delta n_e}{Wt} = \frac{1}{\rho_i V_i Rt}\left[\frac{\Delta P_r V_r}{T_r} - \frac{\Delta P_v V_v}{Z_v T_v}\right] \tag{8}$$

Due to practical difficulties, such as changes in density of the liquid fuel due to temperature and pressurizing gas, certain corrections are required. In the cases of air and nitrogen, the effect of the pressurizing gas on liquid density is negligible. In the case of ethane the effect is greater and the correction required is of appreciable magnitude.

The fuel tank ullage was kept small, i.e., small vapor-liquid-ratio, during all tests to maximize the effect of gas evolution. Therefore small temperature changes, although causing small changes in fuel volume, caused relatively large changes in ullage volume. Using Bureau of Standards reference data* for the volumetric expansion coefficient, a

* Cragoe, C.S. Bureau of Standards Misc. Publication No. 97. 1929.

calculation of the change in liquid-fuel-volume for a temperature change can be made. This calculation provides a means for computing the change in ullage volume.

$$V_{\Delta L} = V_i \alpha (T_L - T_i) \tag{9}$$

$$V_L = V_i + V_{\Delta L} = V_i \left[1 + \alpha (T_L - T_i)\right] \tag{10}$$

$$V_v = V_s - V_L = V_s - V_i \left[1 + \alpha (T_L - T_i)\right] \tag{11}$$

Substituting this correction back into Equation (8)

$$E = \frac{1}{\rho_i V_i Rt} \left[\frac{\Delta P_r V_r}{T_r} - \frac{\Delta P_v \left(V_s - V_i \left[1 + \alpha (T_L - T_i)\right] \right)}{Z_v T_v} \right] \tag{12}$$

Equation (12) was used for computing the evolution rates of air* in Fuel B (RJ-1). An additional correction for vapor pressure is required in the case of Fuel A (JP-4). The correction factor for Fuel A is developed later.

* The term air as used here denotes the mixture of oxygen and nitrogen leaving the tank and entering the reservoir. Due to the somewhat selective solubility of the fuels, i.e., oxygen being more soluble than nitrogen, the actual gas evolved from the liquid will be somewhat oxygen enriched when compared to the gas in equilibrium in the vapor space. The deviations are small however, and for most purposes negligible.

* Cragoe, C. S. Bureau of Standards Misc. Publication No. 97. 1929.

Due to the very high solubility of ethane in petroleum fuels, the liquid fuel densities deviate considerably with pressurizing-gas pressure-level. The density-temperature effect is also amplified. This latter problem is due to the fact that the solubility of ethane, in petroleum fuels, increases quite rapidly when temperatures decrease from ambient. Figures 31 and 32 show the density variation, due to pressurizing-gas pressure at various temperature levels, when equilibrium conditions are maintained.

A calculation of the liquid and ullage volumes at any pressure level can be made using this data and interpolating as required. This is done using the weight of fuel charged, from Equation (7), which remains constant; and, the basic definition of density, i.e., $\rho = \frac{W}{V}$ at any condition.

$$W = \rho_i V_i = \rho_L V_L \tag{13}$$

$$V_L = \frac{\rho_i V_i}{\rho_L} \tag{14}$$

$$V_v = V_s - V_L = V_s - V_i \frac{\rho_i}{\rho_L} \tag{15}$$

Since the ρ_L value is at run-temperature condition, further temperature correction (i.e., expansion coefficient correction) is not required.

In actual practice equilibrium conditions are not obtained during a test run except at the initial starting point, and prior to a decrease in pressure. The deviation from equilibrium is a function of many variables. A few of these variables are; rate of pressure change, surface area, viscosity and nucleation sites. To accurately obtain the dynamic densities required for a rigorous calculation, quite elaborate equipment

would be required. As correction for deviation from equilibrium is just one of the correction factors, useful only on the ethane pressurizing system, it was felt that approximations were in order. The approximation consists of using the arithmetic mean density from Figure 31 and/or Figure 32 when both the initial and final equilibrium pressures are known. (Where the final pressure is that pressure which the system finally attains after a pressure change). The arithmetic mean was used for its simplicity and the fact that in the pressure increments used, the density deviations are nearly a linear function.

$$V_v = V_s - V_i \left(\frac{\rho_i}{\frac{\rho_{L,1} + \rho_{L,2}}{2}} \right) \qquad (16)$$

Obviously under conditions of a pressure change at equilibrium, this approximation becomes nearly exact. Under conditions of non-equilibrium the correction error increases to a maximum. This maximum error should not exceed more than an estimated 10 per cent of the change in density nor less than 1 per cent of the average density. The diagram below may clarify this statement.

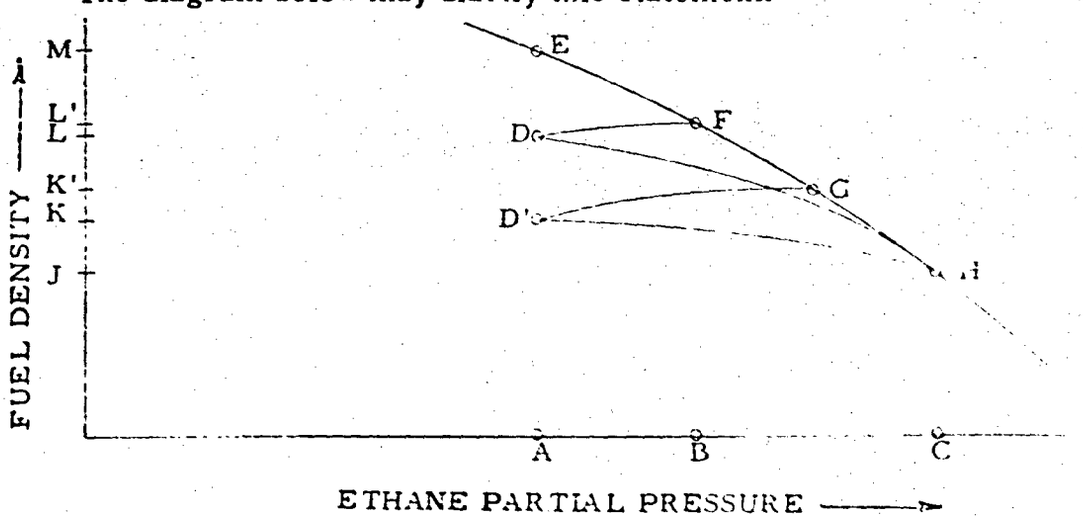

The curve E-H represents a typical density-pressure plot similar to Figures 31 and 32 obtained under equilibrium conditions. Curve D-H and D'-H represent the plots obtained by venting the tank from pressure level "C" to pressure level "A" under non-equilibrium conditions (D'-H being more rapid than D-H). Curve D-F represents the change in density after the vent is shut and equilibrium conditions are obtained. The average density during a test run would be that determined by D or D' and H, representing pressures "A" and "C", and densities J, L or K. As points D or D' are not easily obtained, use is made of points F or G, respectively. In the case of curve D'-H the average density for a pressure change from "C" to "A" can be expressed as follows:

$$\rho_{average} = \frac{\rho_J + \rho_K}{2} = \frac{\rho_{L,1} + \rho_{L,2}}{2} \approx \frac{\rho_J + \rho_{K'}}{2} \approx \frac{\rho_{L,1} + \rho_{L,3}}{2} \qquad (17)$$

The average density for curve D-H can be expressed similarly.

Substituting Equation (16) into Equation (8)

$$E = \frac{1}{\rho_i V_i Rt}\left[\frac{\Delta P_r V_r}{T} - \frac{\Delta P_v\left[V_s - \frac{2 V_i \rho_i}{\rho_{L,1} + \rho_{L,3}}\right]}{Z_v T_v}\right] \qquad (18)$$

In the case of Fuel A (JP-4), a further correction is required due to the vapor pressure of the fuel. Fuel B (RJ-1), having a vapor pressure below 0.1 psia at ambient temperature, was not corrected for this factor.

The presence of appreciable percentages of fuel vapors in the ullage requires some further modification of the basic relationships derived

in Equation (8) to take into account the partial pressure of the fuel. Again rigorous calculations could not be used due to practical limitations; therefore certain approximations were used. Dalton's Law of additive pressure is one of the approximations assumed.

$$P_r = P_f + P_x \tag{19}$$

The fuel-vapor correction would be relatively simple to make if the vapor pressure was not a function of temperature and equilibrium achievement time. The equilibrium deviation is due to the fact that after the tank is vented (as in a climb to altitude at constant guage pressure), time is required for the liquid fuel to exert its full vapor pressure. This is similar to ordinary evolution. The process of transferring molecules from the liquid state to the vapor state is not instantaneous. The process requires a finite time.

The total molal quantities entering the reservoir are approximately defined by

$$\Delta n_r = \Delta n_{v,x} + \Delta n_{v,f} + \Delta n_e \tag{20}$$

$$\Delta n_e = \Delta n_r - \Delta n_{v,f} - \Delta n_{v,x} \tag{21}$$

$$\Delta n_e = \frac{\Delta P_r V_r}{RT_r} - \frac{\Delta p_{v,x} V_v}{Z_v RT_v} - \Delta n_{f,v} \tag{22}$$

When the vapor pressure is zero, $\Delta n_{f,v}$ is zero. If the vapor pressure is finite, $\Delta n_{f,v}$ increases to a limit as a function of time.

Evaluation of $\Delta n_{f,v}$ is involved. Certain simplifying assumptions can be made. The two extreme cases, assuming both to be without gas evolution,

would be the following examples:

Case 1 - Vapor pressure constant during a pressure change (climb). This condition would be closely approximated in a very slow pressure drop.

Case 2 - A relatively long vapor-pressure-equilibrium time causing the fuel-partial-pressure to drop in direct proportion to the pressure decrease. This condition would be approximated in very rapid pressure drops.

In case 1, the ratio of moles of fuel vapor to total moles in the reservoir would equal the ratio of the fuel-vapor-partial-pressure to the total pressure. (Ideal conditions are applicable, inasmuch as the reservoir pressure is subatmospheric). Further the molal ratio would equal the ratio of the vapor pressure to the arithmetic average of the tank pressure before and after a pressure decrease.

$$\frac{\Delta n_{f,r}}{\Delta n_r} = \frac{P_{f,r}}{P_r} = \frac{P_{f,t}}{\frac{P_{t,1} + P_{t,2}}{2}} \tag{23}$$

$$\Delta n_{f,r} = \left[\frac{2\,P_{f.t}}{P_{t,1} + P_{t,2}}\right] \Delta n_r = \Delta n_{f,v} \tag{24}$$

In case 2, the ratio of moles of fuel vapor to total moles in the reservoir is equal to the ratio of the respective pressures. The conditions stated for case 2 are quite similar to those of a tank containing only pressurizing gas and fuel vapor with little, if any, liquid fuel present. Therefore, the quantity of gas leaving the tank is directly proportional to the pressure change. The constituents leave the tank in the same proportions as they

exist in the tank.

$$\frac{\Delta n_{f,r}}{\Delta n_r} = \frac{\Delta p_{f,t}}{\Delta P_t} = \frac{\Delta p_{f,t}}{P_{t,1} - P_{t,2}} \qquad (25)$$

$\Delta p_{f,t}$ represents the partial pressure change of fuel vapor due to the change in total pressure. The smaller the value of the tank pressure, the larger the value of $\Delta p_{f,t}$ for a fixed pressure decrease. The maximum value of $\Delta p_{f,t}$ is equal to the vapor pressure.

For Fuel A (JP-4), the vapor pressure is approximately 1.4 psia at ambient conditions. The maximum pressure increment used was 15 psi and the minimum pressure was 20 psia. Under these conditions, the maximum value of $\Delta p_{f,t}$ can be determined as shown below, assuming case 2 conditions exist.

$$\frac{p_{f,t,1}}{p_{x,t,1}} = \frac{p_{f,t,2}}{p_{x,t,2}} \qquad (26)$$

where

$$p_{f,1} = 1.4 \qquad p_{xt,1} = 35 - 1.4 = 33.6 \text{ psia}$$

$$p_{f,2} = \text{Unknown} \qquad p_{xt,2} = 20 - p_{ft,2}$$

Solving Equation (26) by substitution gives a value of $p_{f,2} = 0.8$

$$\Delta p_{ft} = p_{f,t1} - p_{f,t2} = 1.4 - 0.8 = 0.6 \text{ psi} \qquad (27)$$

This represents the maximum deviation of vapor pressure than can occur in the test system. Since the pressure change is linear, an average vapor pressure can be used satisfactorily.

$$\frac{\Delta n_{f,r}}{\Delta n_r} = \frac{P_{f,r}}{P_r} = \frac{\text{Avg } P_{f,t}}{\frac{P_{t1} - P_{t2}}{2}} \qquad (28)$$

In the example given, the average vapor pressure ($P_{f,t}$) is

$$\frac{1.4 - 0.8}{2} = 1.1 \text{ psia.}$$

Comparing Equation (23) with Equation (28) one can see that the deviation in vapor pressure and thus moles of fuel vapor entering the reservoir might vary by a factor of roughly 25%. In actuality, the variation is much less since neither extreme is realized in practice. Further, since the $\Delta n_{f,r}$ is a small fraction of n_r, it was felt that the variation was within a margin of experimental error. It was therefore arbitrarily assumed that case 1 conditions were fully applicable and the relations derived therefrom were used. Combining Equation (22) and Equation (24), we obtain

$$\Delta n_e = \frac{\Delta P_r V_r}{RT_r} - \frac{p_{v,x} V_v}{Z_v RT_v} - \left[\frac{2p_{f,t}}{P_{t,1} + P_{t,2}}\right] \frac{\Delta P_r V_r}{RT_r} \qquad (29)$$

$$\Delta p_{v,x} = p_{x,1} - p_{x,2} = (P_{t,i} - p_f) - (P_{t,2} - p_f) = \Delta P_t = \Delta P_v \qquad (30)$$

$$\Delta n_e = \frac{\Delta P_r V_r}{RT_r} - \frac{\Delta P_v V_v}{Z_v RT_v} - \left[\frac{2p_{f,t}}{P_{t,1} - P_{t,2}}\right] \frac{\Delta P_r V_r}{RT_r} \qquad (31)$$

Combining Equation (16), bringing in the time and weight factors results in the overall relationship

$$E = \frac{\Delta n_e}{Wt} = \frac{1}{\rho_i V_i RT}\left[\frac{\Delta P_r V_r}{T_r}\left[1 - \left[\frac{2p_{ft}}{P_{t,1} + P_{t,2}}\right]\right] - \frac{\Delta P_v\left[V_s - \frac{2V_i \rho_i}{\rho_{L1} + \rho_{L3}}\right]}{Z_v T_v}\right] \quad (32)$$

The compressibility factor (Z_v) is the mean compressibility of the vapor mixture. Z_v was assumed to be equal to the compressibility of the pressurizing gas as, in the regions where it becomes appreciable, the diluting effect of the fuel vapor is negligible.

CONCLUSION:

For ethane, the relationship shown in Equation (32) was used. Equation (12) was used for the air and nitrogen in Fuel B. The air, nitrogen-Fuel A system required a further modification of Equation (32). The expansion coefficient α was used in place of densities.

$$E = \frac{\Delta n_e}{Wt} = \frac{1}{\rho_i V_i RT}\left[\frac{\Delta P_r V_r}{T_r}\left[1 - \frac{2p_f}{P_{t,1} + P_{t,2}}\right] - \frac{\Delta P_v\left(V_s - V_i\left[1 + \alpha(T_L - T_i)\right]\right)}{Z_v T_v}\right] \quad (33)$$

The equilibrium rate of the evolution curve was derived using the Ostwald Coefficients obtained in Phase 3 of this program.

$$O_c = \frac{V}{V_L} = \frac{V}{\frac{W}{\rho_L}} \tag{34}$$

$$V = O_c \frac{W}{\rho_L} \tag{35}$$

$$\Delta n_c = \frac{\Delta P\ V}{Z_v RT} = \frac{\Delta P\ O_c\ W}{Z_v RT \rho_L} \tag{36}$$

$$\frac{\Delta n_c}{t\ W} = \frac{\Delta P}{t} \frac{O_c}{Z_v RT \rho_L} \tag{37}$$

DISCUSSION

Experimental studies were performed. The apparatus used to make the studies is shown in Figures 26 through 29. All runs were made at ambient temperatures (50°F to 90°F). Agitation was accomplished by the rocking mechanism whose speed could be varied by changing a pulley ratio. The agitation amplitude was held constant at approximately $\frac{1}{2}$ inch as measured at the edge of the tank oven. A detailed description of the equipment and the procedure used is given in the paragraphs entitled "Test Equipment and Procedure". Details of the method used for determining evolution rate are given in the calculations. Figures 33 through 44 illustrate the experimental results.

The following general statements can be made about the air-fuel system:

1. Evolution rate is a linear function of pressure-change-rate.
2. Increased agitation increases the rate of evolution.
3. The effect of air-pressure-level on evolution rate does not appear to be appreciable, at least to 60 psi.
4. Evolution rate is a function of equilibrium solubility, i.e., the greater the solubility the greater the evolution rate.
5. Deviation from equilibrium increases as the rate-of-pressure-change increases.

The nitrogen-fuel system was not investigated very thoroughly. It is expected that the generalized statements made concerning the air-fuel system are applicable to the nitrogen-fuel system.

The ethane-fuel system differs from the air-fuel system in one respect the ethane pressure-level greatly effects the evolution rate. This may be due, in part, to the deviation from ideality of ethane. Another factor in the ethane-fuel system that may affect the evolution rate is the rather extreme change of viscosity and presumably, surface tension with solubility; i.e., with partial pressure.

A comparison of the air-JP-4 and the ethane-JP-4 fuel-systems, at low rates of pressure change, shows that the evolution rate of air is approximately $\frac{1}{4}$ that of ethane. The solubility of air is, however, 1/20 that of ethane under the same conditions. This infers, of course, that air can be removed from the fuel much more readily than ethane.

The effect of agitation on the fuel systems was fairly well defined except for the case of zero agitation. Figure 39 shows the extreme variation of test results. It is believed that the large deviations are due to our inability to obtain equilibrium under conditions of zero agitation.

Although all runs were made at ambient temperature, the temperature varied approximately 5°F to 10°F during a test. Weather variations during the test period covered the temperature range of 50°F to 90°F, averaging roughly 70°F. These temperature variations are one cause of minor deviations noted on the data plots. The effect of temperature on evolution rate is quite appreciable in the ethane-fuel system due to the large effect of temperature on ethane solubility and thus, fuel viscosity and surface tension.

The air-fuel system results obtained in this test are not in agreement with those of Schweitzer and Szebehely. This is believed due, in part, to the difference in agitation severity and the vapor-liquid-ratio used. Schweitzer and Szebehely used a shake-table type agitator with a 1-inch stroke and a vapor-liquid-ratio of 4:1. Work done on the program reported herein was accomplished with a rocking agitator with a $\frac{1}{2}$-inch maximum stroke and a vapor-liquid-ratio of approximately 1:10 Further information is given in Appendix I of this Part, on the work of Schweitzer et. al. The equations of Appendix I were derived by Staff Members of the Stanford Research Institute as part of a sub-contract under the literature survey portion of this program

The ethane-fuel system is also not in agreement with the results predicted by Schweitzer et al In this case an additional factor adds to the discrepancy; ethane does not follow Henry's Law as is required in the calculations of Schweitzer and Zebehely This factor shows up in the effect of pressure level on evolution rate

APPENDIX I DISSOLUTION AND EVOLUTION OF GASES IN LIQUIDS

(Developed by Physical Chemistry Staff of
Stanford Research Institute)

The following equations are based on the work of Schweitzer, et al., * who found that the rate of evolution or dissolution of a gas from various hydrocarbon fractions was proportional to the degree of supersaturation:

$$\text{Assume } \frac{dv}{dt} = -k\,(v - v_e) \qquad (1)$$

where K= pseudo first order rate constant, which is a function of the direction of the process (except very close to equilibrium), temperature, nature of the gas and of the liquid, rate of agitation, etc., but not of the pressure.

* Schweitzer, P. H. and Szebehely, V. G. Gas Evolution in Liquids and Cavitation. Journal of Applied Physics. Volume 21. December, 1950. pp. 1218 - 1224.

v = volume of gas dissolved (measured at NTP) per volume of liquid, at time t.

v_e = volume of gas dissolved per volume of liquid that would be in equilibrium with the pressure p at time t.

Also assume that the dissolved gas is sufficiently dilute so that Henry's law is obeyed:

$$v_e = hp \tag{2}$$

Case I. Closed system, constant temperature. At t = o, $v = v_o$ and $p = p_g$ (not in equil. with v_o).

The material balance is given by

$$pV_g + vV_l = p_f V_g + v_f V_l$$

$$p - p_f = r(v_f - v) \tag{3}$$

where p_f = final equil. pressure at $t = \infty$

v_f = final equil. volume / volume in the liquid

v_g = total volume of gas phase

V_l = total volume of liquid phase

r = volume of liquid / volume of gas

Substituting (2) and (3) into (1) (and noting $v_f = hp_f$)

$$\frac{dp}{dt} = k(1 + rh)(p_f - p) \tag{4}$$

Integrating (4) between $p = p_g$, $t - o$ and $p = p$ and $t = t$:

$$\frac{p_f - p}{p_f - p_g} = e^{-k(1 + rh)t} \tag{5}$$

If the equation is desired in terms of p_o, the pressure in equil. with the initial volume/ volume, v_o, by material balance and Henry's law:

$$p_f - p_g = rh(p_o - p_f) \tag{6}$$

Substituting (6) into (5)

$$\frac{p_f - p}{p_o - p_f} = hr\, e^{-k(1 + rh)t} \tag{5a}$$

Case II. Open system, constant temperature, linear time rate of change of v_e, equil. at $t = o$ ($v_e = v_o$).

$$v_e = v_o + \alpha t \tag{7}$$

(if, for example, there is a linear rate of pressure decrease of z atmos/sec, $\alpha = -hz$)

Substituting (7) into (1),

$$\frac{dv}{dt} = -kv + kv_o + k\alpha t \qquad (8)$$

Equation (8) is a linear equation of 1st order with constant coefficients whose solution is

$$v = Ce^{-kt} + \alpha t - \frac{1}{k^2}(k\alpha - k^2 V_o)$$

$$= Ce^{-kt} + \alpha t - \frac{\alpha}{k} + v_o$$

At $t = o$, $v = v_o$, $\therefore C = \frac{\alpha}{k}$ and

$$v - v_o = \alpha t + \frac{\alpha}{k}(e^{-kt} - 1) \qquad (9)$$

Noting that $v_o - v_e = -\alpha t$ (eq. (7)), equation (9) can be put in the somewhat more useful form:

$$\frac{v_o - v}{v_o - v_e} = 1 - \frac{1}{kt}(1 - e^{-kt}) \qquad (9a)$$

The quantity $(v_o - v) / (v_o - v_e)$ is the ratio of the gas actually evolved (or absorbed) to that which would be evolved at time t had equilibrium obtained. Equation (9) can also be written in terms of pressure:

$$p_e - p = \frac{r}{k}(1 - e^{-kt}) \qquad (9b)$$

If one is interested in, or forced to measure, the total loss of gas from an "open" system (e. g., the loss from a tank partially filled with gasoline and equipped with a vent) the equation must be recast slightly. Denoting the gas lost (measured at NTP) by G, a material balance gives

$$\frac{dG}{dt} + V_l \frac{dv}{dt} = -V_g \frac{dp}{dt}$$

$$\frac{dG}{dt} = -V_l \frac{dv}{dt} - V_g \frac{dp}{dt}$$

Substituting from equation (8) and noting $\alpha = -hz$ and recalling $\frac{dp}{dt} = -z$,

$$\frac{dG}{dt} = kV_l (v - v_o - \alpha t) - \frac{\alpha V_g}{h}$$

$$\frac{dG}{dt} = \alpha V_l (e^{-kt} - 1) - \frac{\alpha V_g}{h}$$

Integrating

$$G = \frac{-\alpha V_l e^{-kt}}{k} - V_l t - \frac{V_g \alpha t}{h} + C$$

At $t = o$, $G = o$, $\therefore$ $C = \frac{\alpha V_l}{k}$

so $G = \frac{\alpha V_l}{k} (1 - e^{-kt}) - \frac{(V_g + V_l)}{h} \alpha t$ (10)

In a somewhat more convenient form:

$$\frac{G}{G_e} = 1 - \frac{V_l h}{V_g + V_l h} : \frac{1}{kt} (1 - e^{-kt}) \quad (10a)$$

where G_e is the total loss of gas if equilibrium had obtained.

SYMBOLS

E	=	Evolution rate
p	=	Partial pressure
P	=	Pressure
R	=	Gas constant
t	=	Time
T	=	Temperature
V	=	Volume
W	=	Weight
Z	=	Compressibility
α	=	Liquid expansion factor
Δ	=	Change
ρ	=	Density

SUBSCRIPTS AND SUPERSCRIPTS

e	=	Pressurizing gas evolving from liquid fuel
f	=	Fuel vapor
i	=	Initial liquid
L	=	Liquid fuel
r	=	Reservoir
s	=	System less reservoir
t	=	Tank
v	=	Tank vapor space
x	=	Pressurizing gas
Δ	=	Change
1	=	Condition 1
2	=	Condition 2
3	=	Condition 3

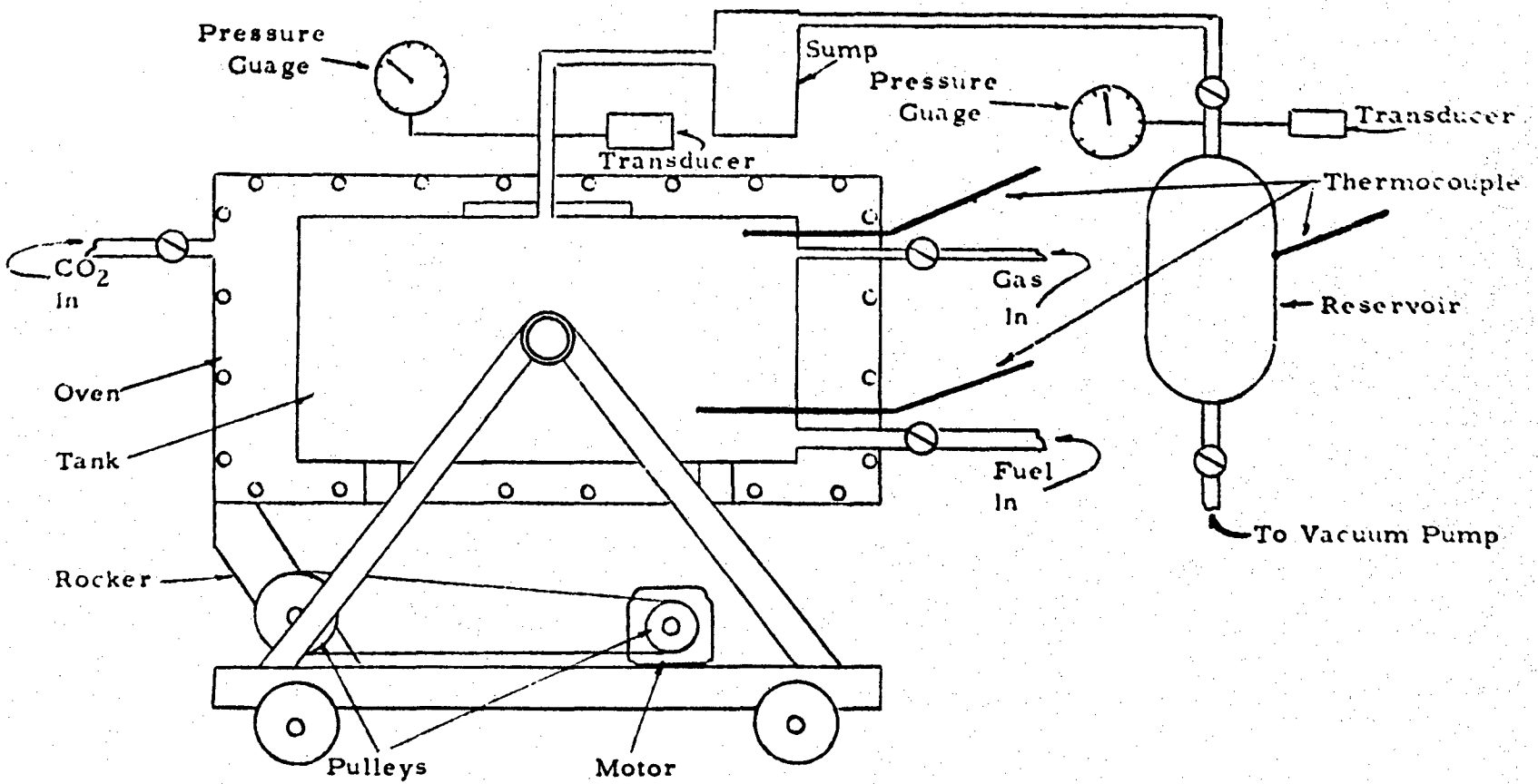

Figure 26 - Schematic of Test Tank and Accessories

Figure 27 - Photograph of Test Fuel Tank

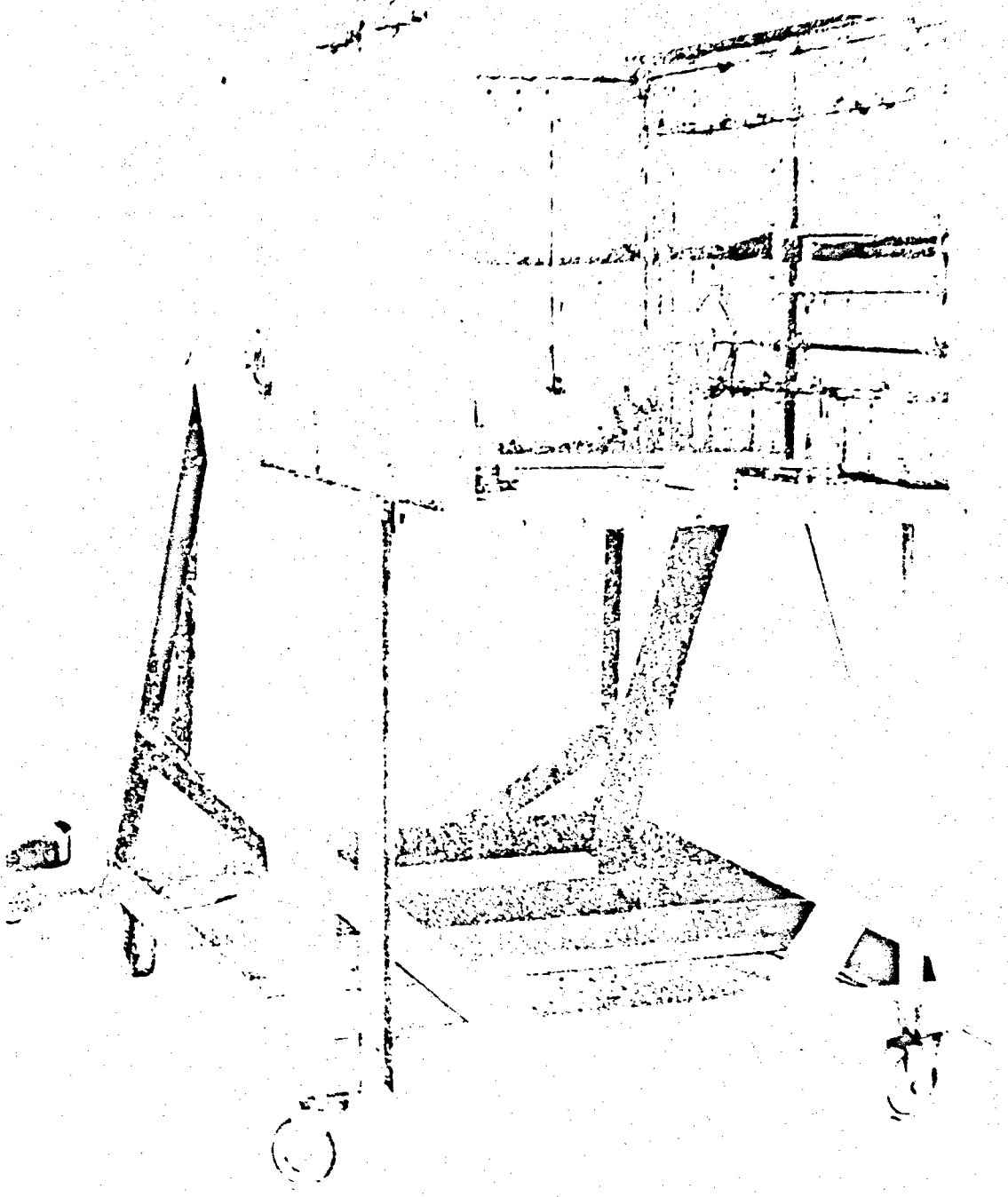

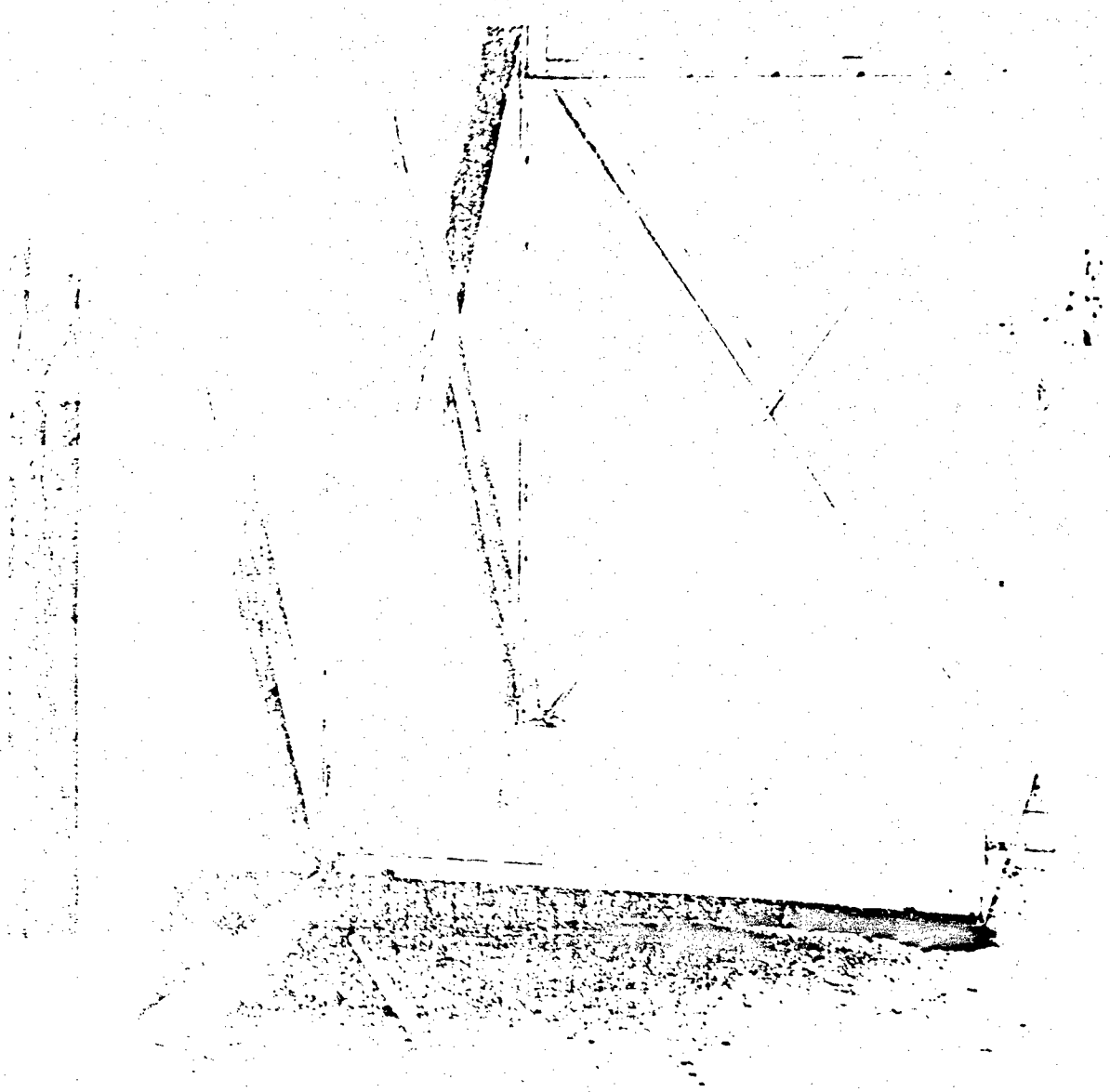

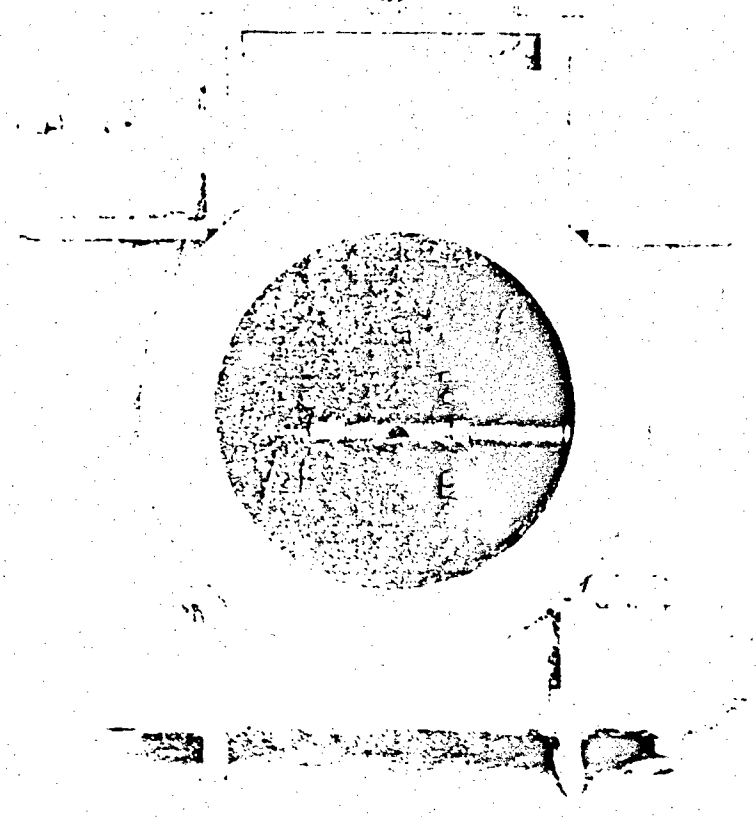

Figure [illegible] with Propeller-Type

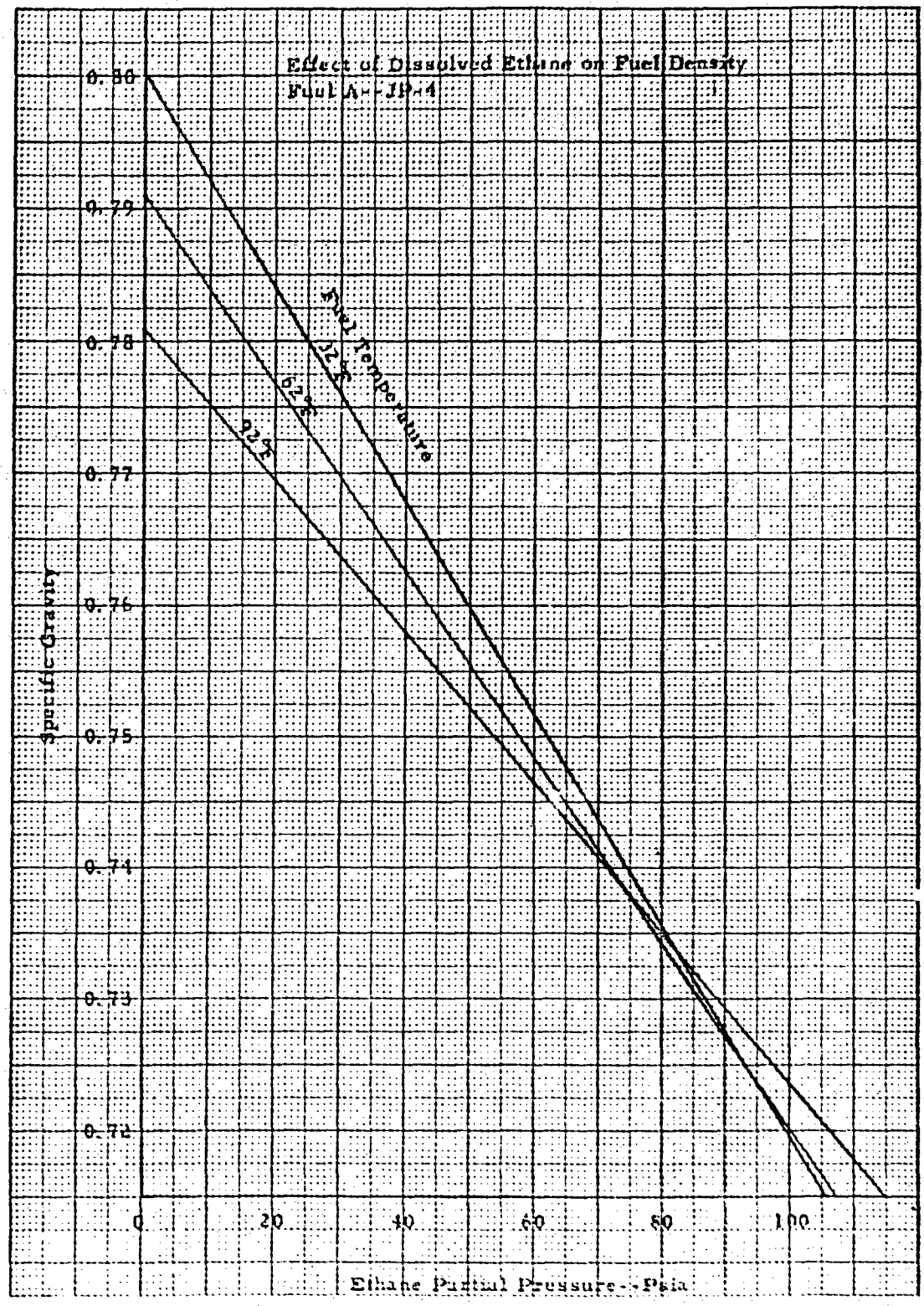

Figure 31 - Effect of Dissolved Ethane on Fuel Density, Fuel A - JP-4.

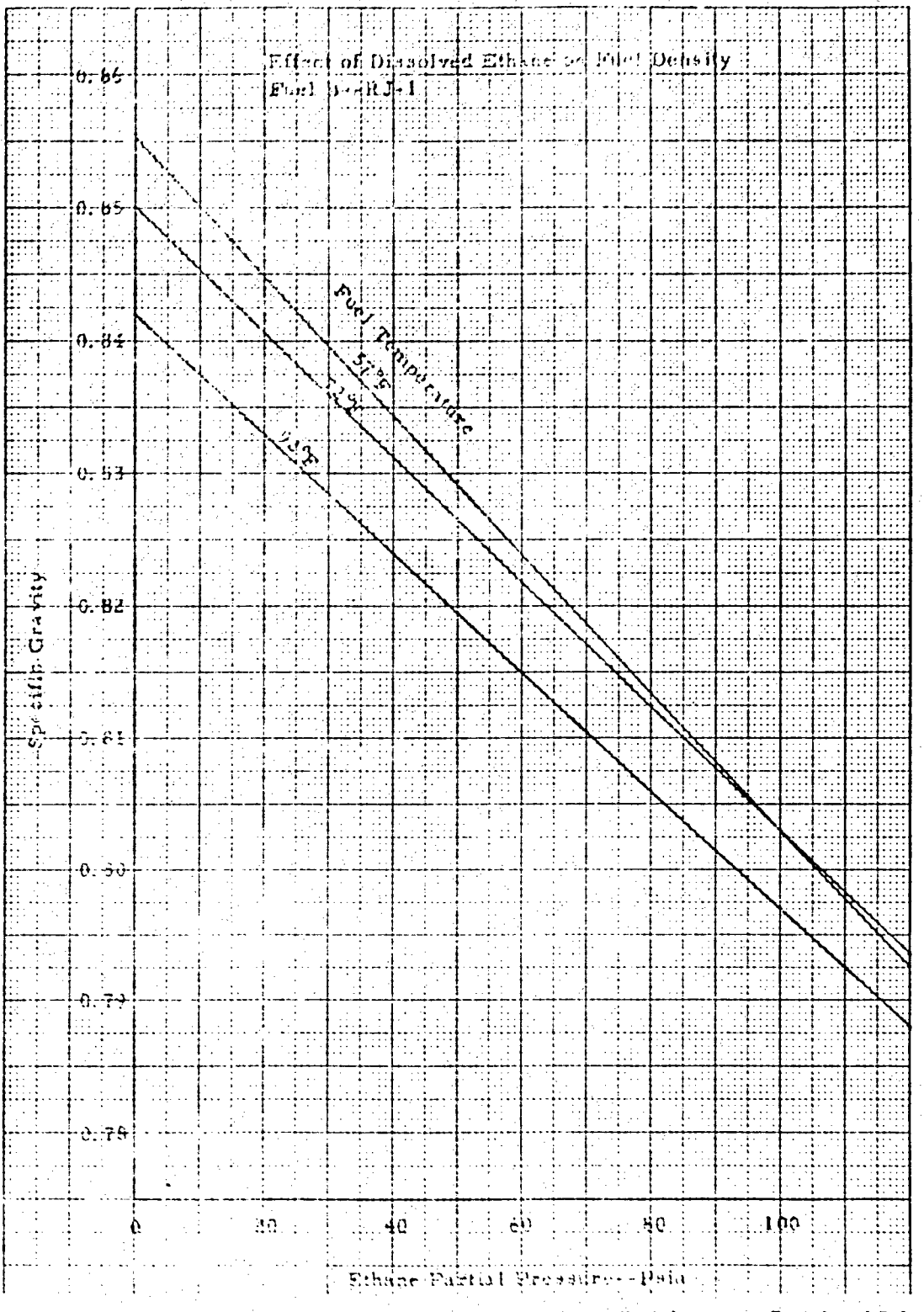

Figure 3. - Effect of Dissolved Ethane on Fuel Density, Fuel b - RJ-1.

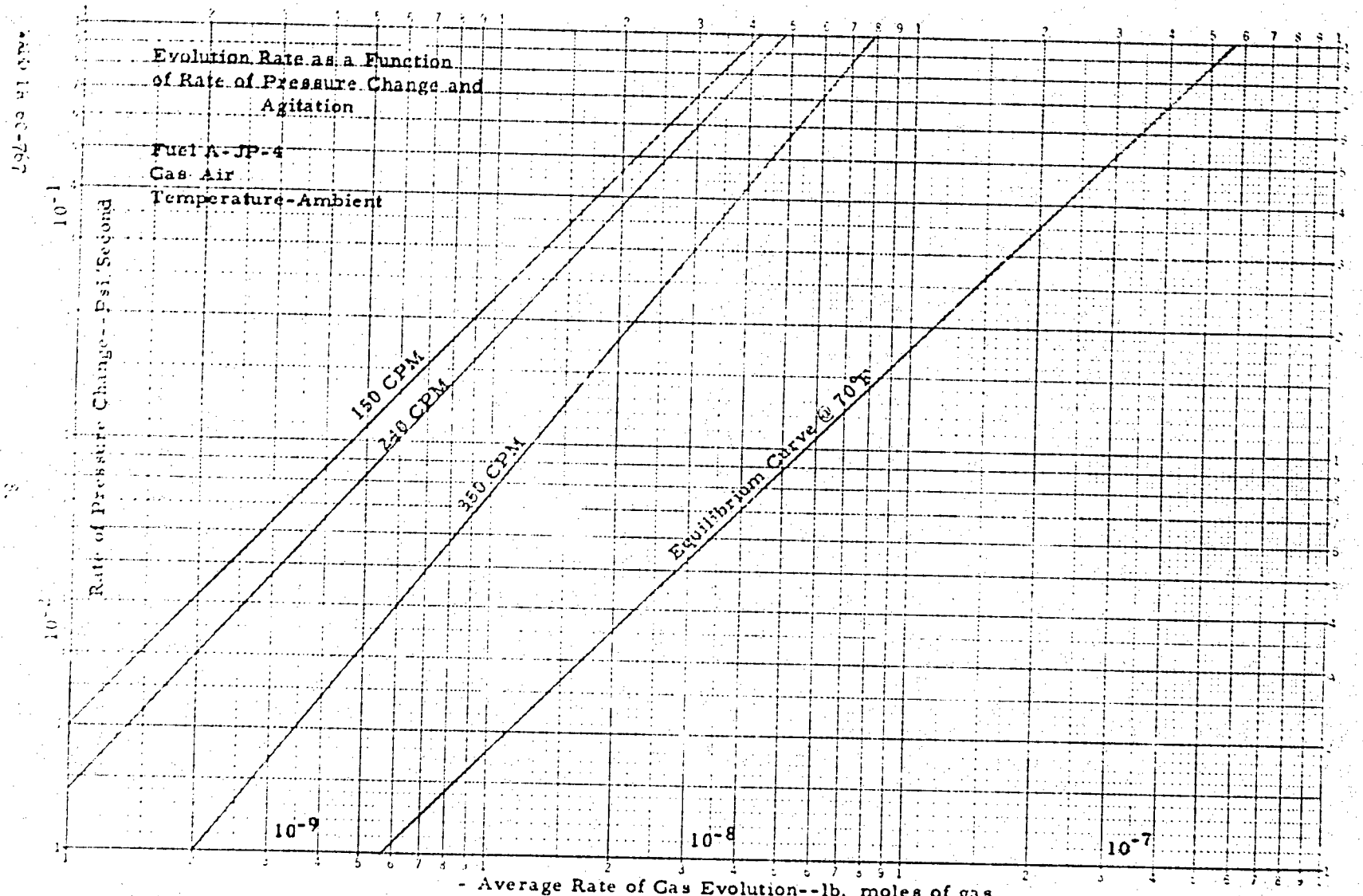

Figure 33 - Air - JP-4 Evolution Rate

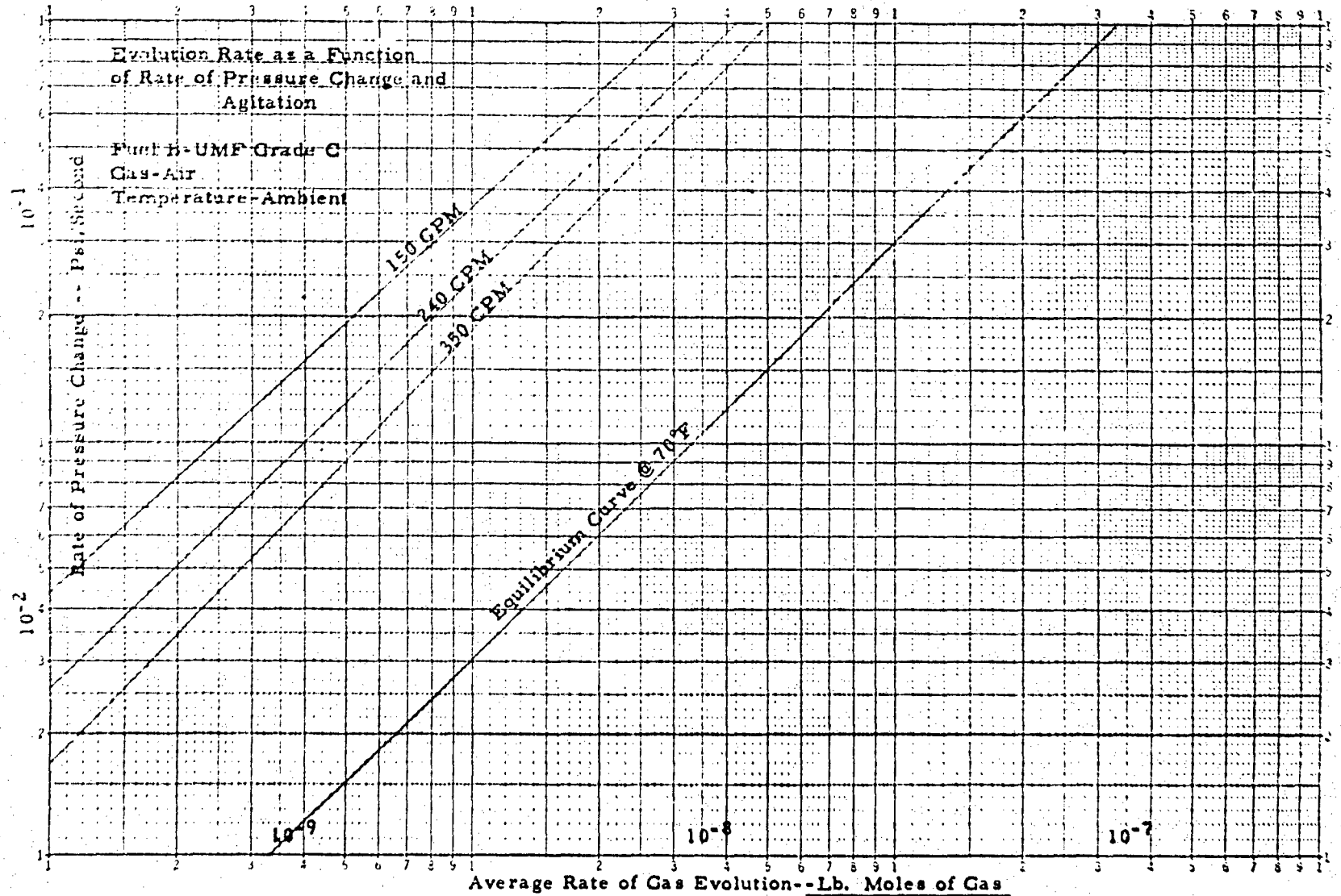

Figure 34 - Air - RJ-1 Evolution Rate

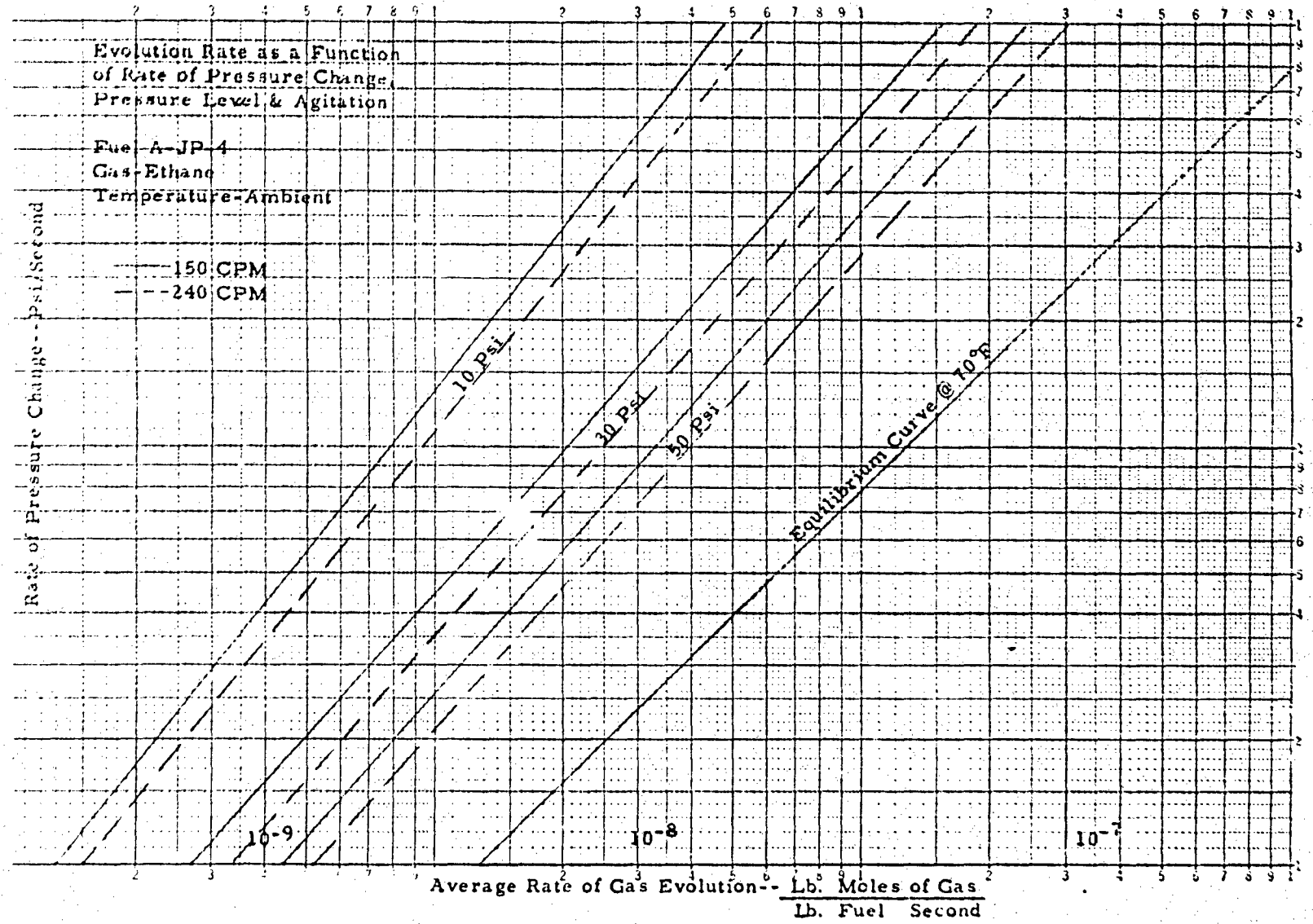

Figure 35 - Ethane - JP-4 Evolution Rate

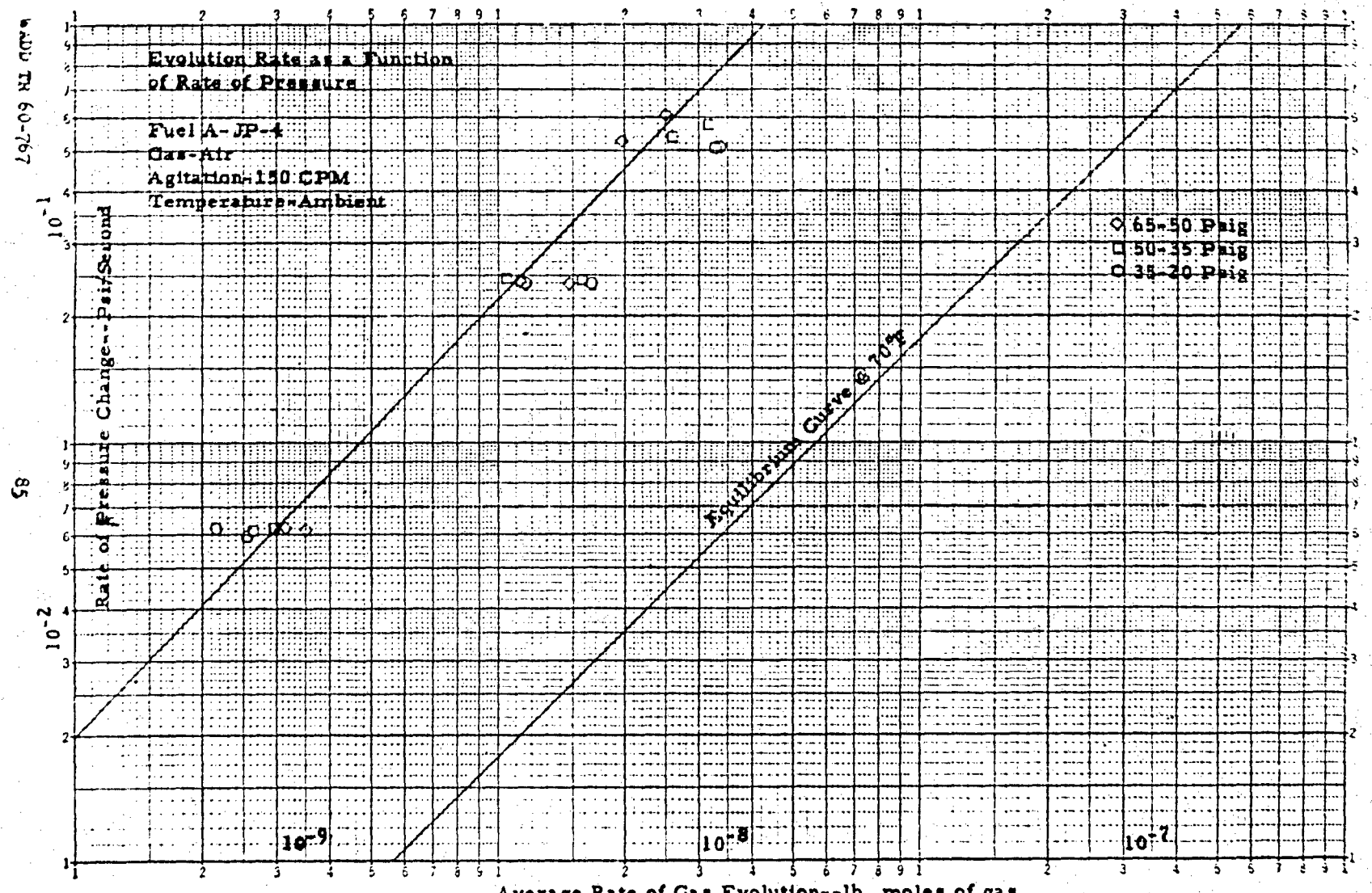

Figure 36 - Air - JP-4 Evolution Rate (150 CPM)

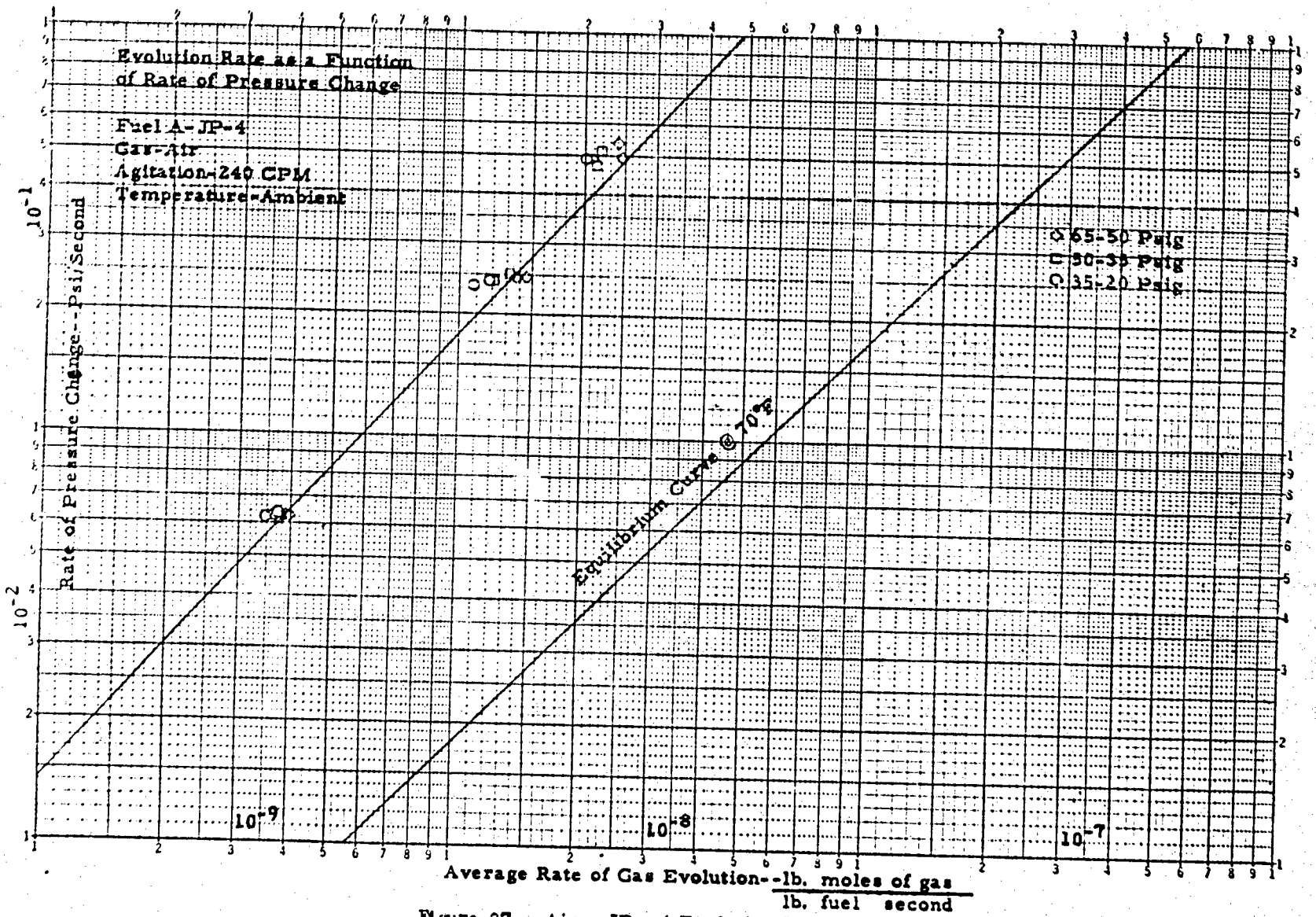

Figure 37 - Air - JP - 4 Evolution Rate (240 CPM)

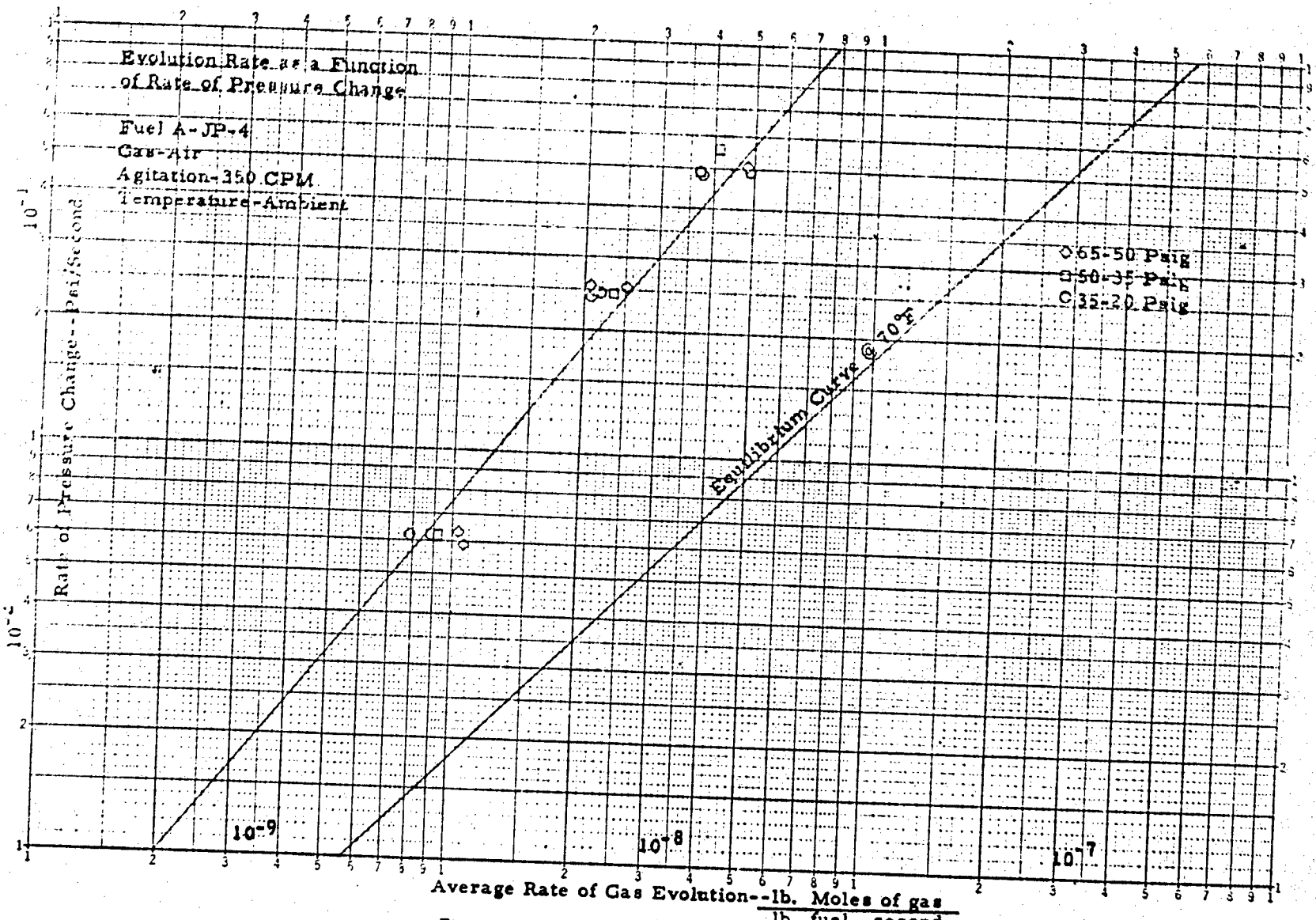

Figure 38 - Air - JP-4 Evolution Rate (350 CPM)

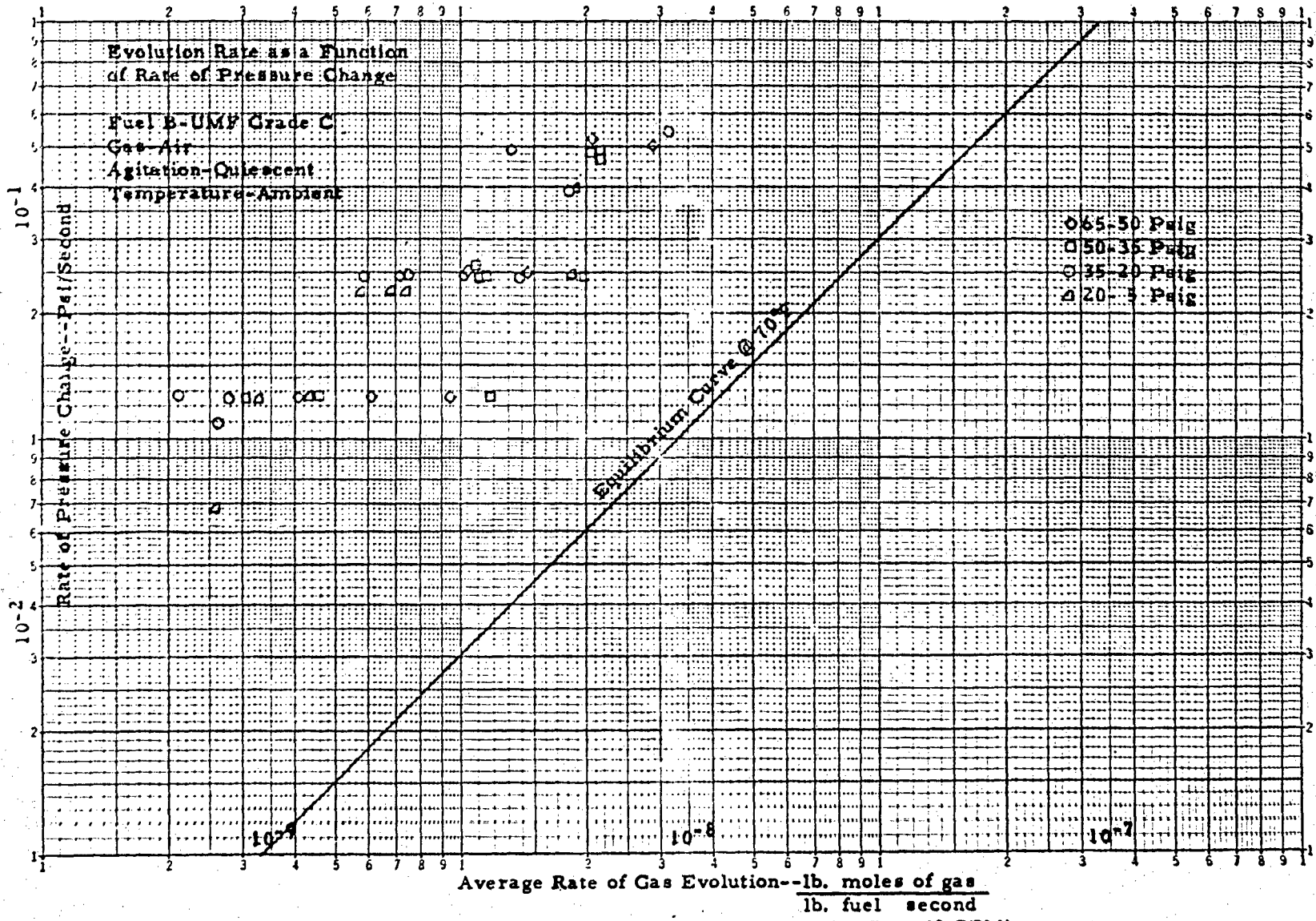

Figure 39 - Air - RJ-1 Evolution Rate (0 CPM)

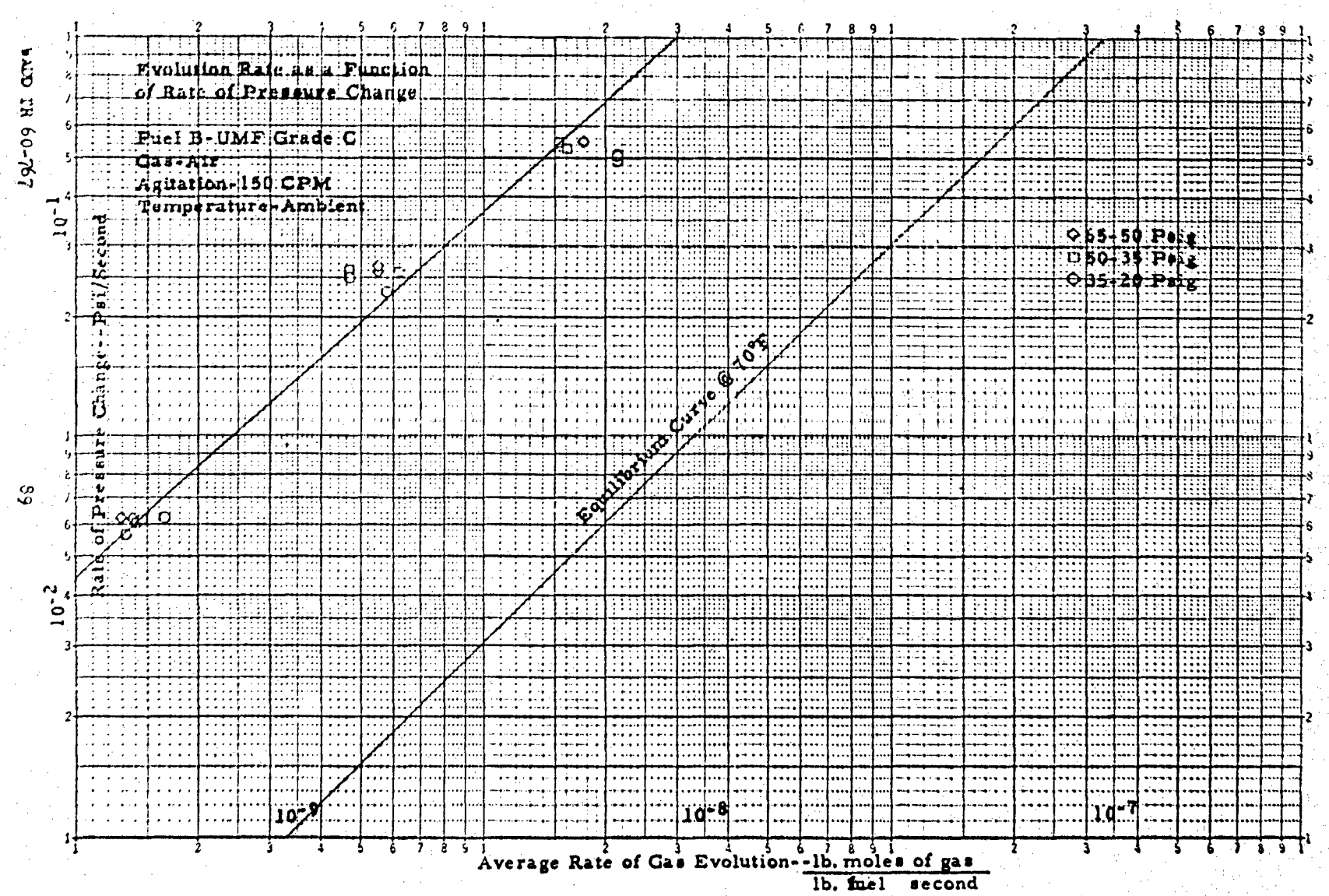

Figure 40 - Air - RJ-1 Evolution Rate (150 CPM)

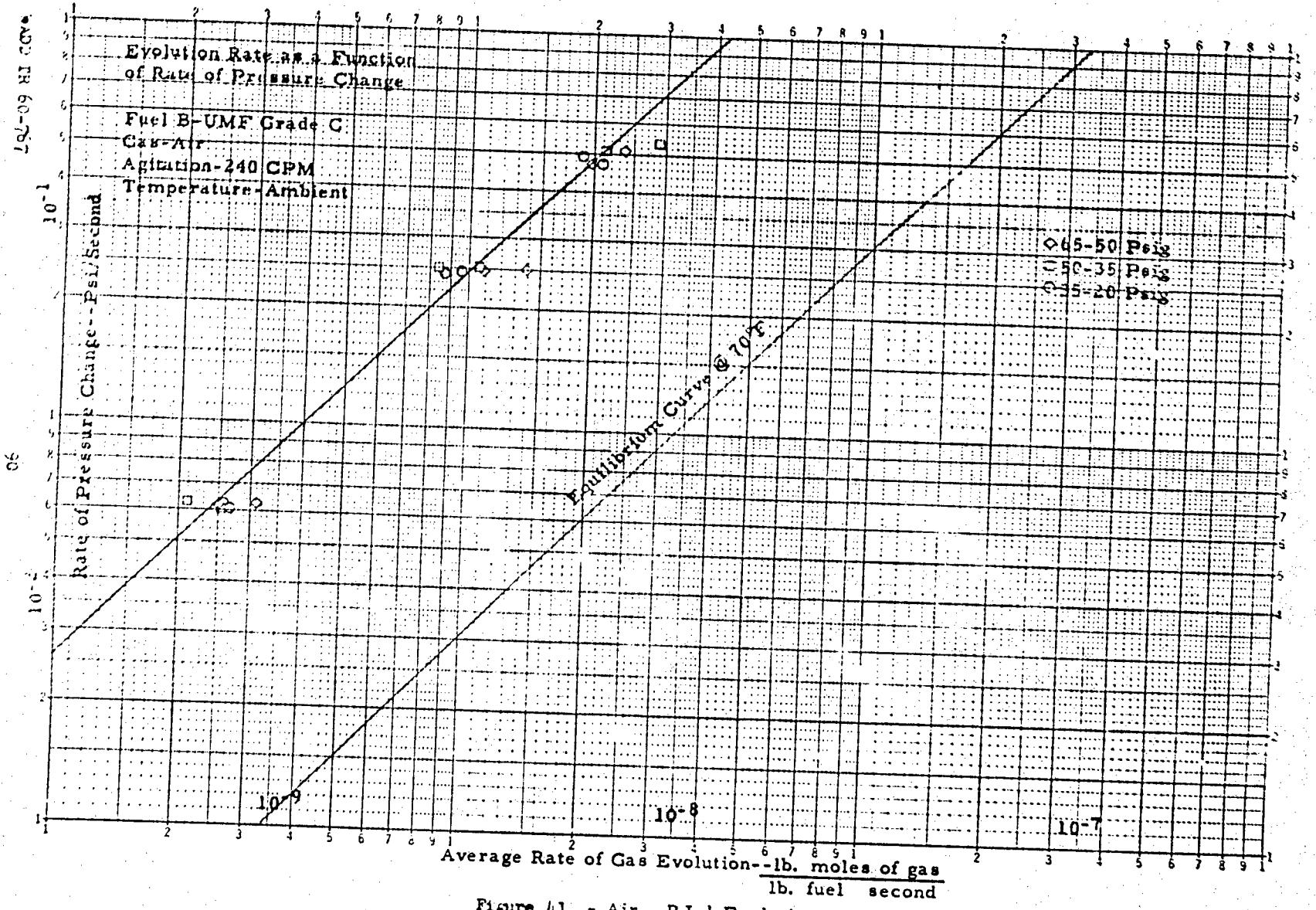

Figure 41 - Air - RJ-1 Evolution Rate (240 CPM)

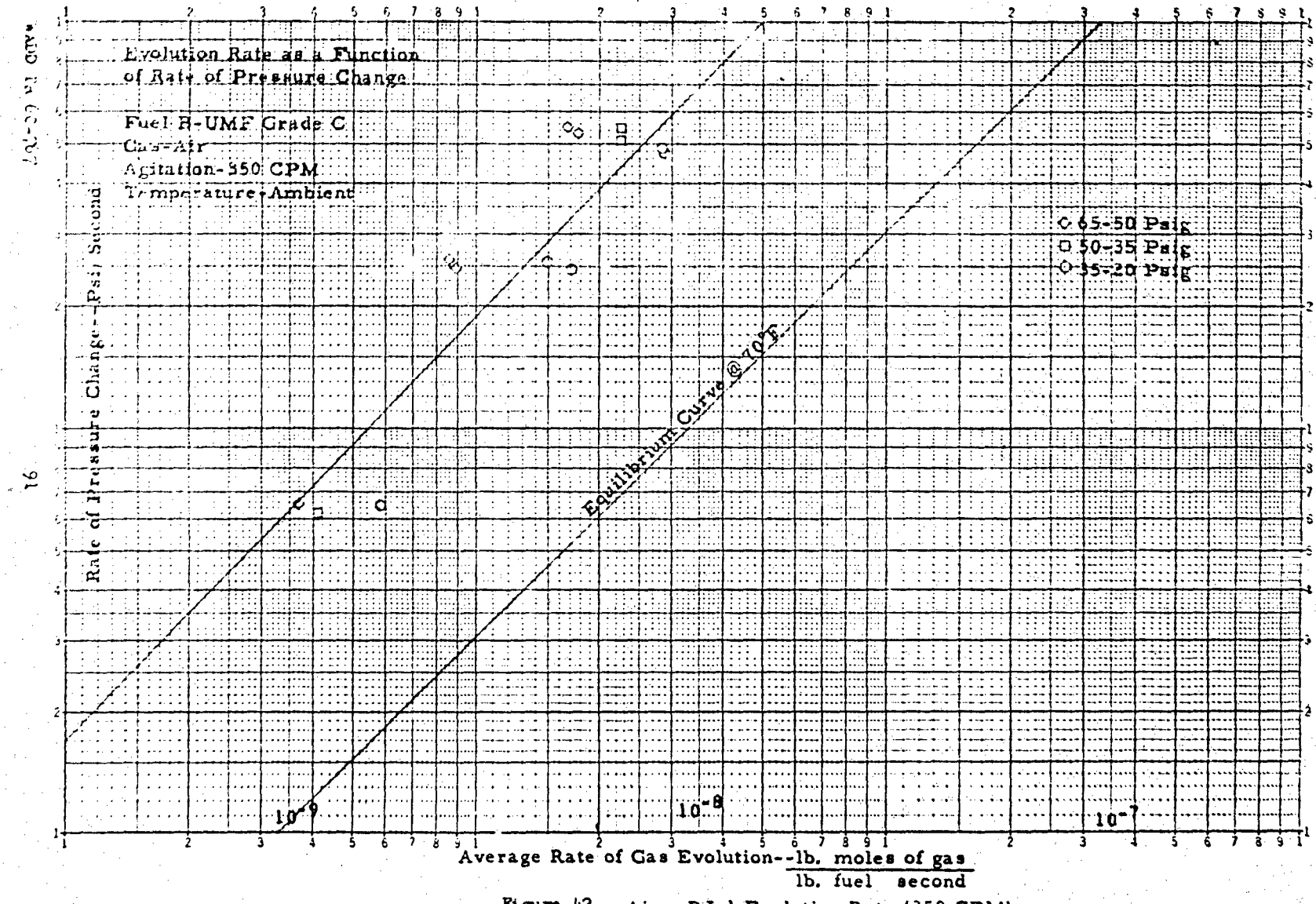

Figure 42 - Air - RJ-1 Evolution Rate (350 CPM)

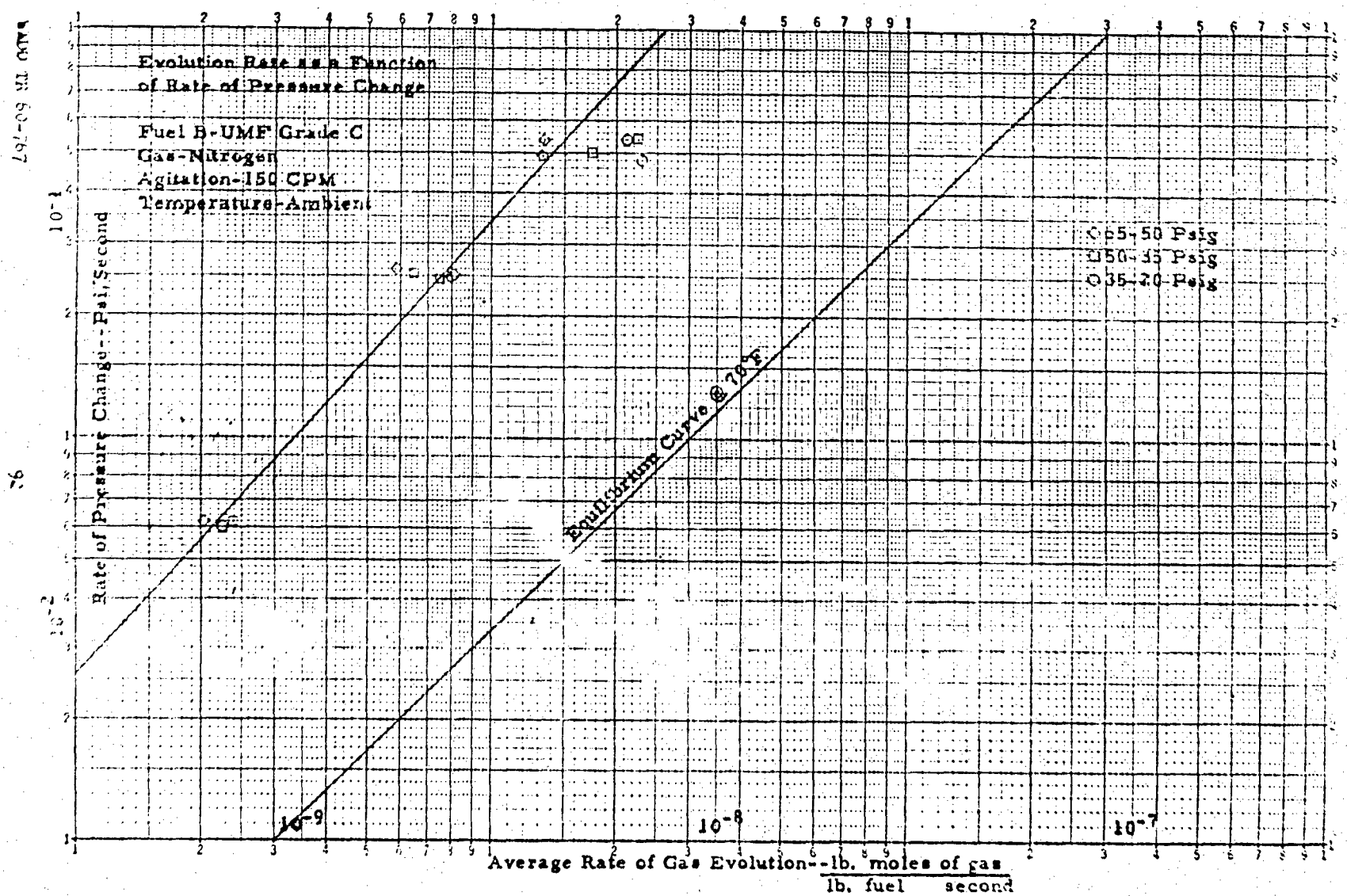

Figure 43 - Air - RJ- 1 Evolution Rate (150 CPM)

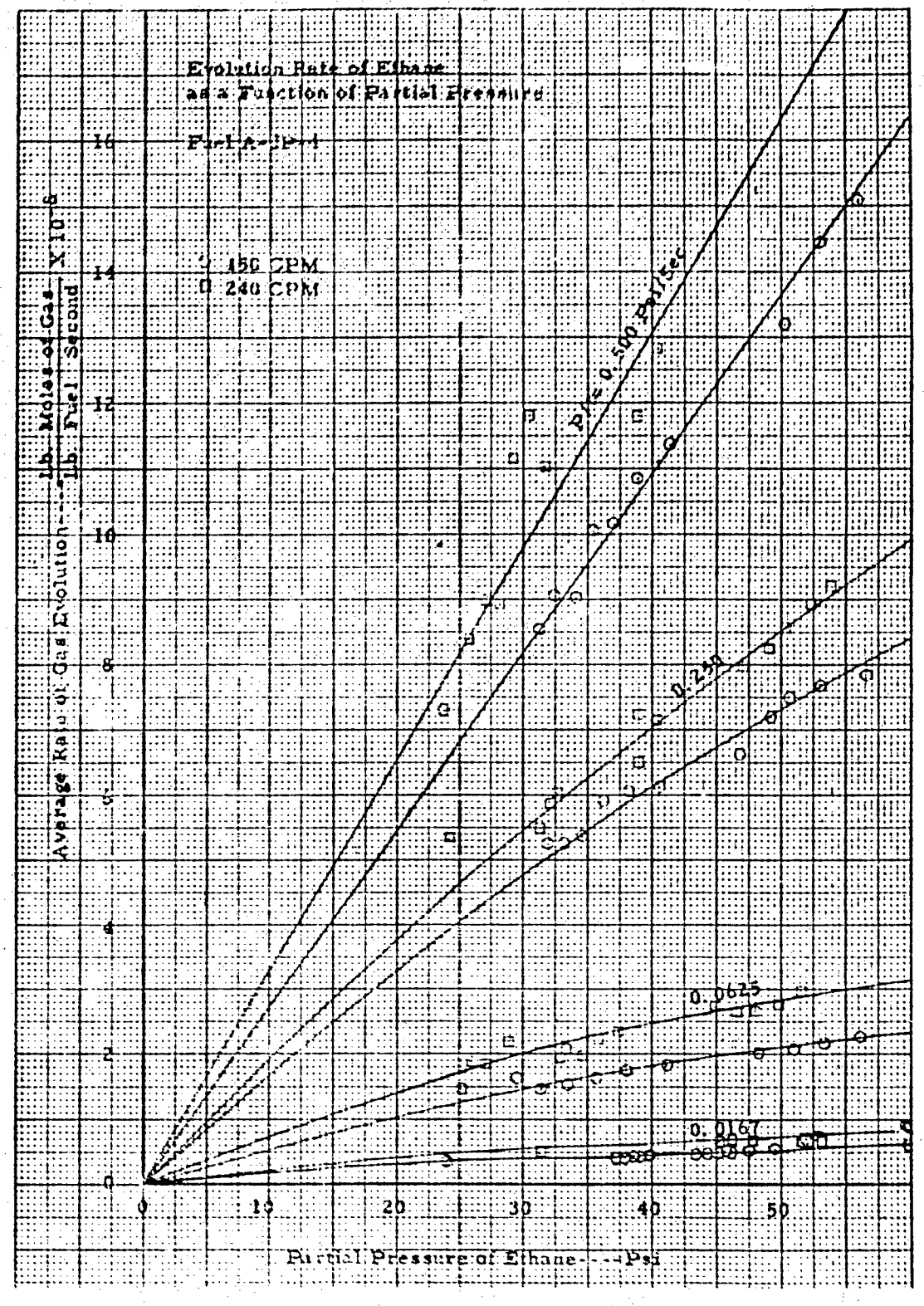

Figure 84 - Ethane - JP-4 Evolution Rate

PART III

VAPORIZATION CYCLE AND THERMODYNAMIC PROPERTIES OF JP-4, RJ-1 AND A SPECIAL FUEL DESIGNATED JP-6-H

INTRODUCTION

This report was first issued in January, 1958 as one of a series of Interim Reports. The interim Reports were submitted to Wright Air Development Center by Thompson Products, Inc. We st Coast Laboratory in partial fulfillment of research program No. AF 33(616)3729.

The material reported here covers the vaporization cycle and thermodynamic properties of JP-4, RJ-1 and a special fuel designated JP-6-H. This data represents results of completed studies.

OBJECTIVE

Studies were made under this part of the program for two basic reasons:

1) The determination of vaporization characteristics of a JP-4, a special JP-6, and an RJ-1* fuel as a function of pressure level. If possible, the pressure range of 0 to 200 psia was to be covered. It was also desired to determine the specific gravity and molecular weight of these fuels as a function of per cent vaporized, and the variation of these physical properties with pressure level.

2) The determination of enthalpy, entropy, specific heat, and heat of vaporization of the three fuels listed, as a function of temperature and pressure. As much of this information as possible was to be presented in the form of enthalpy-entropy diagrams.

* Formerly designated Shell UMF, Grade C

SUMMARY

Objectives 1 and 2 were studied. A brief summary of the results achieved and the determinations made is given in the following paragraphs.

Objective 1

The experimental vaporization work was accomplished using equipment (See Figure 45) designed to obtain a minimum of refluxing such as would be experienced in aircraft fuel tanks in which fuel was being vaporized. Results are shown in Figures 46 through 54. These figures include calculated equilibrium vaporization curves and ASTM distillation curves for comparison with the minimum reflux vaporization data.

Objective 2

Experimental specific heat results are shown in Figures 55 through 57. As expected, the liquid specific heat follows the C = A + BT type relation where: C represents specific heat, A and B are constants, and T represents temperature.

The enthalpy, entropy and heats of vaporization of each of three fuels studied, were computed using empirical correlations plus experimental distillation and density data. Enthalpy - temperature plots in the 0° to 900°F range with pressure as a parameter are shown in Figures 58 through 60 Temperature - entropy plots in the same temperature range with enthalpy and pressure parameters are shown in Figures 61 through 63.

METHODS, EQUIPMENT AND PROCEDURES

Minimum reflux vaporizations of the three test fuels were accomplished in the test cell shown in Figure 45. The fuel vaporized was contained in the inner tube. A heating medium (Ondina oil) was circulated through the annular space between the tubes. This method of heating was chosen in order to maintain the inner tube close to an isothermal condition. Temperature stabilization prevented condensation of vaporized constituents and kept refluxing to a minimum. The only area where refluxing was possible was in the exit tube. A capillary tube of minimum length was used to minimize the effects of this refluxing.

Pressure was manually controlled by a valve in the exit line and was monitored by means of a pressure transducer. The temperature was monitored using thermocouples. Condensation of the vaporized products was accomplished by means of a wet ice bath. Constant evaporation rates were not maintained since this factor does not affect the separation efficiency of the test apparatus, providing the evaporation rate is not sufficiently rapid to cause liquid entrainment. Several tests were conducted to verify separation efficiency.

Fractions were collected in ten per-cent-by-volume increments at each of the pressure levels. The initial and final temperatures were noted. The density of the collected fractions was measured using a calibrated pyncnometer and a precision analytical balance.

Molecular weight determinations were made for each of the fractions. Freeze-point depression methods, with benzene as a solvent, were used to make these determinations.

A Comparison Calorimeter, shown schematically in Figure 64 was used to determine the liquid specific heat of the three test fuels. For detailed information concerning the use of this calorimeter see Reference No. 1. In addition to the physical analyses and ASTM distillations, vapor pressure vs temperature, and density vs temperature tests were made on the fuels. Specific volume techniques and the Specific Volume Apparatus shown in Figure 65 were used to make the density vs temperature determinations.

The Specific Volume Apparatus, slightly modified, was used to measure vapor pressures. A vacuum pump and the liquid nitrogen condenser in the Specific Volume Apparatus were used to de-aerate the fuels. After fuel de-aeration, the vapor pressure was measured at various points in the 50°F to 500°F temperature range by means of a pressure transducer.

ENTROPY AND ENTHALPY CALCULATIONS

The Entropy and Enthalpy charts presented in Figure 58 through Figure 63 were calculated in the following manner:

From the ASTM plots of the fuels tested, the equilibrium vaporization curves were obtained (method of Edmister and Pollock, see Reference 2). The information obtained was extrapolated to low pressures. Liquid enthalpies were computed using basic thermodynamic relationships and Cragoe's empirical relation for specific heat (Reference 3).

$$dH = C_p\,dT \tag{1}$$

$$H_t = H_o + \int_{T_1}^{T^2} C_p\,dT \tag{2}$$

$$C_L = \frac{0.388 + 0.00045T}{\rho^{0.5}} \tag{3}$$

Assuming a datum temperature of 0°F i.e., $H^\circ = O$ at 0°F, substituting (3) and integrating gives

$$H = \frac{0.388T + 0.000255T^2}{\rho^{0.5}} \tag{4}$$

Evaluation of Equation (4) at various temperature levels results in enthalpy values. These values when plotted, result in points from which the saturated liquid line of an enthalpy temperature chart may be drawn. To obtain the saturated vapor line and complete the phase envelope, heats of vaporization must be determined.

Heat of vaporization is defined as the enthalpy difference between the saturated vapor and saturated liquid at constant temperature. For the fuels studied here, this constant temperature is assumed to be the mean average boiling point. Correlations such as those shown in Appendix A (Part V, Supplement V of this Report) were used to obtain the heats of vaporization at one atmosphere and at the mean average boiling point. Heats of vaporization at other temperatures were obtained using the correlation of Watson(see Reference 4).

$$\frac{\lambda}{\lambda_k} = \left[\frac{(T_c - T)}{(T_c - T_m)}\right]^{0.38} \qquad (5)$$

The $\frac{\lambda}{\lambda_k}$ function is the ratio of the heat of vaporization at the desired temperature to the heat of vaporization at the mean average boiling point. The addition of the heat of vaporization to the enthalpy of the saturated liquid at the mean temperature, results in the enthalpy of the saturated vapor.

$$H_{sv} = H_L + H_v \qquad (6)$$

A similar procedure is used to calculate the per cent vaporized lines. Since the enthalpy is normally plotted on a weight basis and the per cent vaporized on the equilibrium vaporization curve on a volume basis, suitable corrections must be made. To make the corrections for Fuel A, density measurements from experimental minimum-reflux vaporizations were used. Knowing the mean temperature of the fuel at different percentages of vaporization and the enthalpy envelope, allows the evaluation of enthalpy change for each of the percentages vaporized. In this statement the mean temperature is presumed to be the arithmetic average boiling point of the fraction, i.e.,

$$T_{\text{mean } 0\text{-}20} = \frac{T_{20} + T_0}{2} \quad T_{\text{mean } 20\text{-}40} = \frac{T_{40} + T_{20}}{2}, \text{ etc.}$$

In the case of narrow boiling range fuels, such as fuels B and C, these corrections are negligible.

At the mean temperature, the heat of vaporization is obtained for the one-atmosphere curve using the enthalpy differential between the saturated vapor and saturated liquid line. If the enthalpy of the twenty per cent fraction is being computed, twenty per cent of the enthalpy differential is added to the liquid enthalpy at the end point temperature; at forty per cent, forty per cent of the differential is added, etc. At another pressure level the assumption is made that the ratio of the enthalpy increments, for any fraction, will change as the ratio of the total enthalpies change.

$$\frac{H_v \text{ @ } 14.7}{H_v \text{ @ } p} = \frac{\Delta H_{20\text{-}40} \text{ @ } 14.7}{\Delta H_{20\text{-}40} \text{ @ } p}$$

If the region being investigated is not near critical conditions this is a reasonable assumption. The enthalpy of the saturated vapor is equal to: 1) the summation of the liquid enthalpy (at the initial boiling point), and 2) the enthalpy of vaporization of all increments.

$$H_{sv} = H_L + \Delta H_{0-20} + \Delta H_{20-40} + \Delta H_{40-60} + \Delta H_{60-80} + \Delta H_{80-100} \quad (7)$$

To evaluate the specific heat at constant pressure of the vapors in the superheat region, the residual method of Deming and Shupe(References 5 and 6), plus generalized compressibility and specific heat charts, were used.

$$\alpha = \frac{RT}{P} - V \quad (8)$$

$$\left(\frac{\partial V}{\partial T}\right)_P = \frac{R}{P} - \left(\frac{\partial \alpha}{\partial T}\right)_P \quad (9)$$

$$\left(\frac{\partial^2 V}{\partial T^2}\right)_P = - \left(\frac{\partial^2 \alpha}{\partial T^2}\right)_P \quad (10)$$

$$C_p = C_p^\circ - \frac{T}{J} \int_{P^\circ}^{P} \left(\frac{\partial^2 V}{\partial T^2}\right)_P dP \quad (11)$$

$$Z = \frac{PV}{RT} \quad (12)$$

$$V = \frac{ZRT}{P} \quad (13)$$

$$\alpha = \frac{RT}{P} - \frac{ZRT}{P} = \frac{RT}{P}(1-Z) \qquad (14)$$

The second differential $\left(\frac{\partial^2 V}{\partial T^2}\right)_P$ was evaluated from Equation (14) by double graphical differentiation at various pressure levels. Graphical integration of the results and substitution into Equation (11) gives the correction to the specific heat due to pressure.

As before, the enthalpy change due to increasing temperature is the integral of the specific heat equation. In the case of the vapors, to simplify calculations, use of the mean specific heat was made.

$$\Delta H = C_{p\ mean}(\Delta T) \qquad (15)$$

The mean specific heat was taken as the arithmetic average over a small temperature increment. The ΔH value computed then was added to the saturated vapor enthalpy and the enthalpy-temperature diagram was completed.

Entropy computations were based also on a datum of 0°F. The thermodynamic relationships used were :

$$dS = \frac{C_p\, dT}{T} \qquad (16)$$

$$dS = \frac{dH}{T} \qquad (17)$$

To compute the saturated liquid line on the temperature-entropy chart, the Cragoe equation was substituted in Equation (16). The equation was then integrated, resulting in

$$S = \frac{1}{\rho^{0.5}} \left[0.181 \, (\ln T_2 - \ln 460) + 0.00045 (T_2 - 460) \right] \quad (18)$$

This equation represents the saturated liquid line.

The temperature-entropy charts presented, (see Figures 61 through 63 were derived from Equations (16) and (17) using the values of change-in-enthalpy presented in the temperature-enthalpy charts. See Figures 58 through 60.

In the superheat region each temperature, substituted in Equation (16), was the arithmetic average which closely approximates the mean over the small increments taken.

Critical constants were determined using correlations contained in Part V, Supplement V. Data in the vicinity of the critical region were obtained by extrapolation.

DISCUSSION

A study of the vaporization cycle and thermodynamic properties of three test fuels, a JP-4, a special JP-6-H and an RJ-1* was completed. The research study results are contained in the data presented in this report and concludes the investigation.

The RJ-1 fuel tested is in effect a Shell UMF Grade C and conforms to specification MIL-F-25558. Both the JP-4 and the RJ-1 test fuels appeared to be representative samples. The JP-6-H test fuel meets specification MIL-F-25656. This fuel is considered special because of the very narrow boiling range. Typical JP-6 fuel boils from 280°F to 530°F. This JP-6-H boiled from 328°F to 405°F. The physical properties of the test fuels are discussed in the following paragraphs.

* Formerly designated Shell UMF Grade C.

Test Fuel A (JP-4) and Test Fuel B(RJ-1) were purchased from the Shell Oil Company. Test Fuel C (JP-6-H) was provided by Wright Air Development Center. The ASTM distillation plot of the JP-4 fuel shows a rather steep rise in the initial ten-per-cent-distilled range.

Figures 66 through 68 show the variation of specific gravity with temperature. For fuels A, and C the decrease of density with increasing temperature is nearly linear until approximately 300°F.

Fuel B shows a linear change of density over the entire test temperature range (0°F to 500°F).

The liquid specific heat plots, shown in Figures 55 through 57 follow the normal trend for hydrocarbon fuels. Fuel A follows the equation $C = 0.472 + 0.0005T$; Fuel B follows the equation $C = 0.420 + 0.00044T$; and Fuel C follows the equation $C = 0.468 + 0.00049T$.

Each of the fuels demonstrates the normal petroleum-vapor-pressure characteristics, i.e., plotting vapor pressure versus temperature on a Cox chart results in a straight line. See Figures 69, 70 and 71.

Minimum reflux distillation data at 14.7 psia (see Figures 46-48 when compared with ASTM distillation data (Figures 72-74 shows the effect of reflux on the vapor product. Minimum reflux distillations have a considerably higher initial boiling point and a somewhat lower end point than ASTM distillations. This is due to the effect of reflux. In aircraft flying at speeds sufficient to cause boiling in the fuel tanks due to aerodynamic heating, the conditions in the tanks will closely follow those of a minimum reflux distillation. This statement is predicated on the assumption that the tank is held at a constant pressure.

Figures 49 through 54 show the variation of density and molecular weight as a function of the fuel fraction vaporized for minimum reflux distillations. The fuel fraction vaporized is plotted as volume per cent. The variation between volume and weight per cent is negligible when the distillation range is 200°F or less. The plots of molecular weight and density flatten out with increasing pressure, the extreme occurring at the critical pressure.

The equilibrium vaporization curves have been included for additional information. See Figures 75 through 77. These curves show the vaporization conditions in a tank where pressure has suddenly been lowered without the loss of fuel vapor from the system.

The vapor specific heat data shown in Figures 78 through 80 were computed from generalized Pressure-Volume-Temperature (P-V-T) data and vapor specific heat correlations at one-atmosphere, using the residual method of Deming and Shupe. See Reference 5. It was assumed that deviations due to pressure below 14.7 psia were insignificant. Therefore, the specific heat at 14.7 psia was used for C_p° in the calculations.

The temperature-enthalpy and temperature-entropy diagrams (Figures 58 through 63) were computed from ASTM distillation data and numerous correlations. The calculations involved are described in this Supplement in paragraphs entitled 'Entropy and Enthalpy Calculations'. These plots are most applicable to a closed fuel system from which liquid fuel only is supplied to the engine and where the fuel tank vapors are not vented. In the case of a wide cut distillate where the tank is vented or vapors are supplied to the engine, the usefulness of the charts is limited. The degree of limitation depends upon the extent of vapor removal from the fuel tank. A number of enthalpy-temperature and entropy-temperature curves can exist for the same initial fuel. The manner in which the fuel is vaporized will determine the curve. It is pointed out that changes in fuel composition due to distillation vary with pressure level. (See Figures 49 through 54). Therefore for ultimate use, three dimensional charts (with the change in composition of the hydrocarbons added) should be constructed for specific applications. In lieu of a three dimensional chart, a series of charts covering successive fuel residues is required to define enthalpy and entropy changes.

CONCLUSION

Although the information shown on the various plots included in this report is valid only for the three fuels tested, certain generalizations can be made. In the case of Fuel A, a representative JP-4 fuel, use of the data for estimation purposes in the design of systems and equipment should be satisfactory. In the case of Fuel B, the deviation between fuels of this type being minor, use of the data for most cases should be well within normal engineering tolerances. However, the data for Fuel C should be treated with caution as it is not a typical JP-6. Fuel C is classified as a 'heart cut', i.e., a narrow boiling range fuel.

REFERENCES

1. Spear, Norman H. Measuring Specific Heat of Liquid at High Temperature. Analytical Chemistry. June 1952. pp 939-941.

2. Edmister, Wayne C. and Pollock, D. H. Phase Relations for Petroleum Fractions. Chemical Engineering Progress. Vol. 44, No. 12. December, 1948. pp 905-926.

3. Cragoe, C. S. Bureau of Standards Misc. Publication No. 97. 1929.

4. Watson, K. M. Industrial and Engineering Chemistry. Vol. 35. 1943. p 398.

5. Deming, W. E. and Shupe, L. E. Physical Reviews. Vol. 37. 1931. pp 638-654. Vol. 38. 1931. pp 2245-2264. Vol. 40. 1932. pp 848-859.

6. Dodge, B. F. Chemical Engineering Thermodynamics. First Edition. McGraw Hill Book Company, Inc., New York and London, 1944.

SYMBOLS

C	=	Specific Heat BTU/lb °F
H	=	Enthalpy - BTU/lb
J	=	Mechanical equivalent of heat
K	=	Characterization factor
MW	=	Molecular Weight
P	=	Pressure - psia
Q	=	Heat of Combustion BTU/lb
R	=	Gas constant - 10.73 psia, ft^3/°R, lb-mole
S	=	Entropy - BTU/lb °F.
T	=	Temperature - °F or °R
V	=	Volume - ft^3
Z	=	Compressibility factor

α = Volume residual

Δ = Increment

λ = Heat of vaporization - BTU/lb*

ρ = Density at 60°F

SUBSCRIPTS AND SUPERSCRIPTS

c = Critical

k = Normal mean average temperature

L = Saturated liquid

m = Mean

p = Constant pressure

r = Reduced conditions

sv = Saturated vapor

t = Total

v = Vaporization

0 to 20, 20 to 40, etc. = 0-20%, 20-40% Fractions

1 = Initial condition

2 = Final condition

* H_v Also used to indicate heat of vaporization.

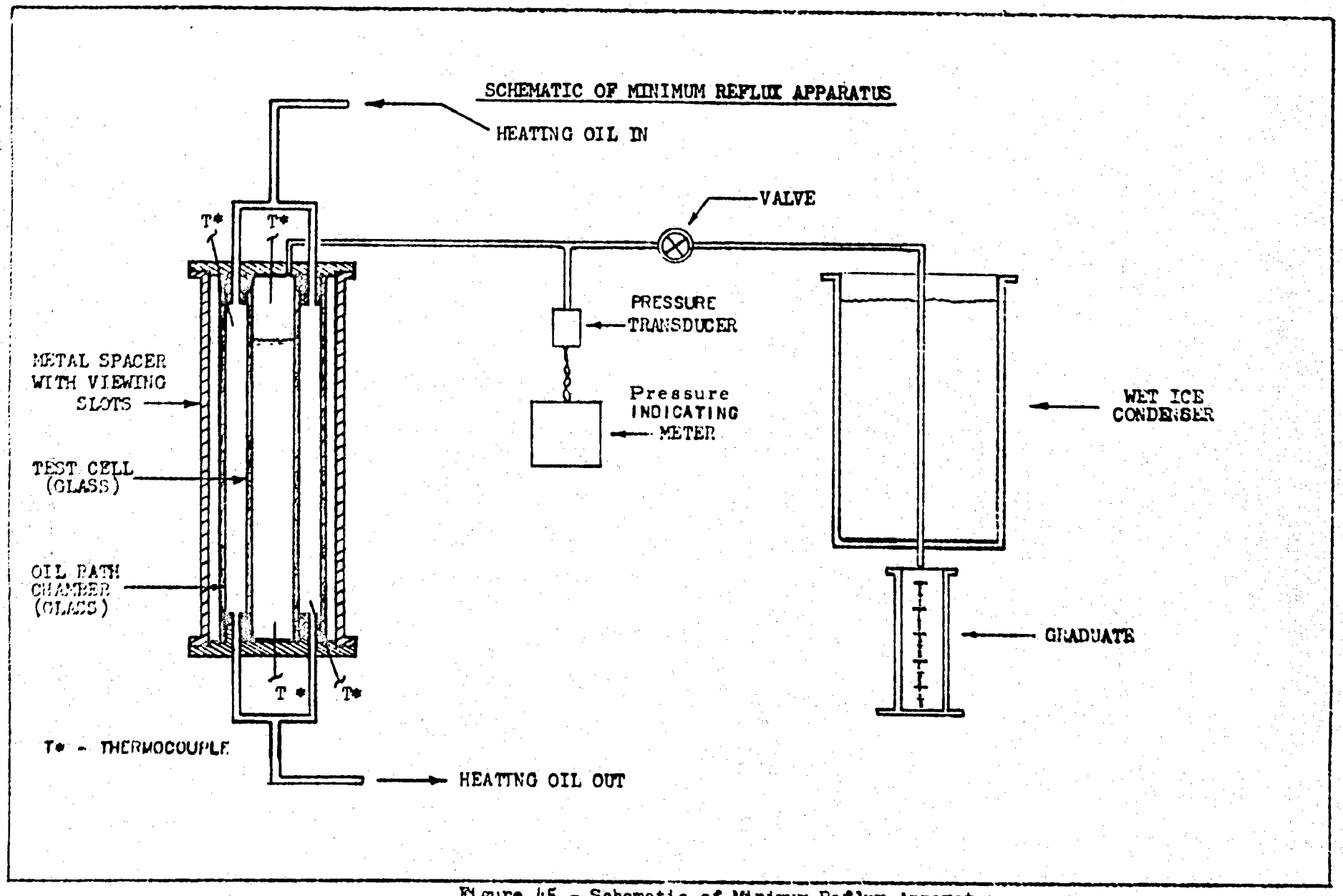

Figure 45 - Schematic of Minimum Reflux Apparatus

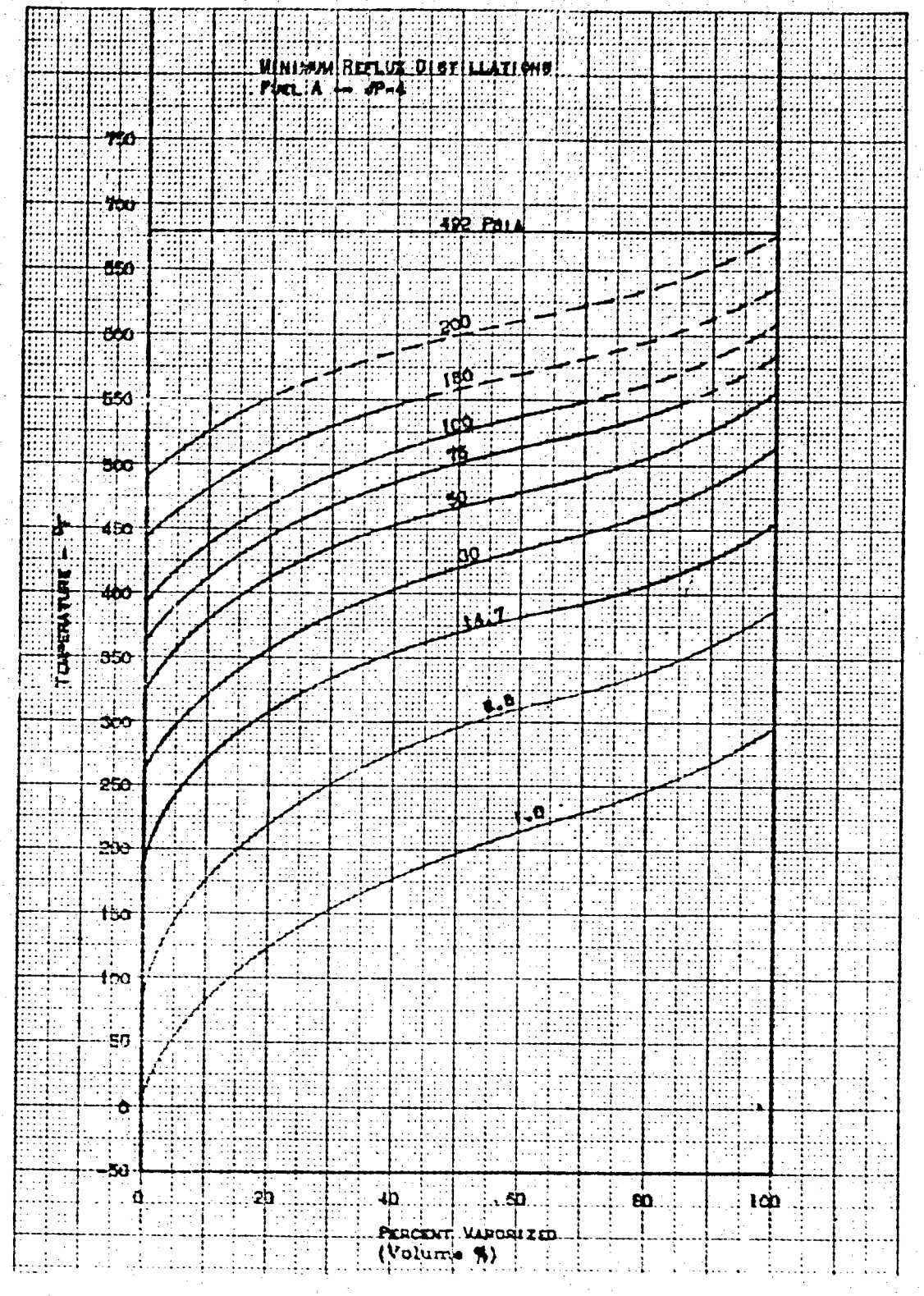

Figure 45 - Minimum Reflux Distillation, Fuel A, JP-4

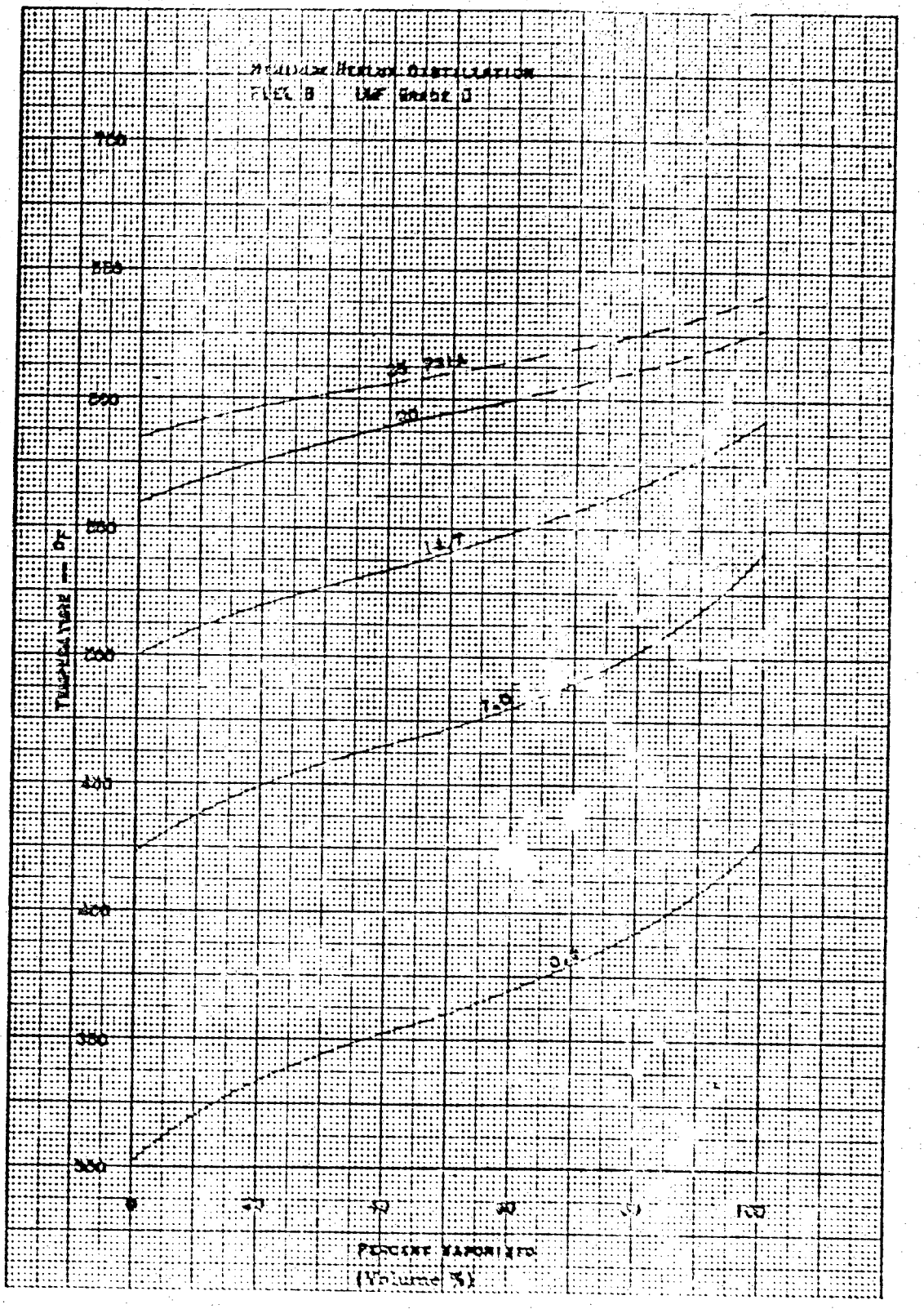

Figure 47 - Minimum Reflux Distillation, Fuel B, RJ-1

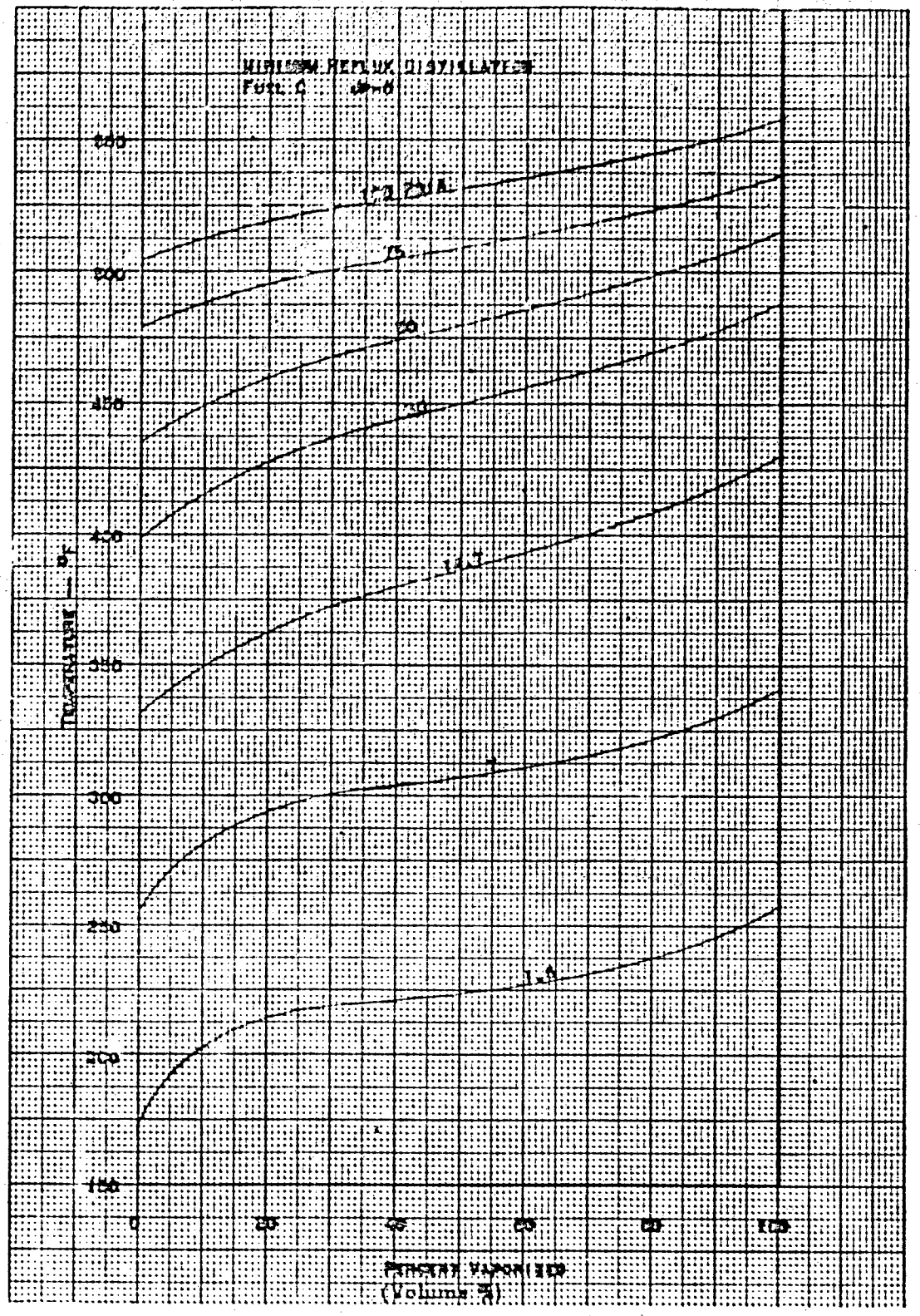

Figure 48 - Minimum Reflux Distillation, Fuel C, JP-6

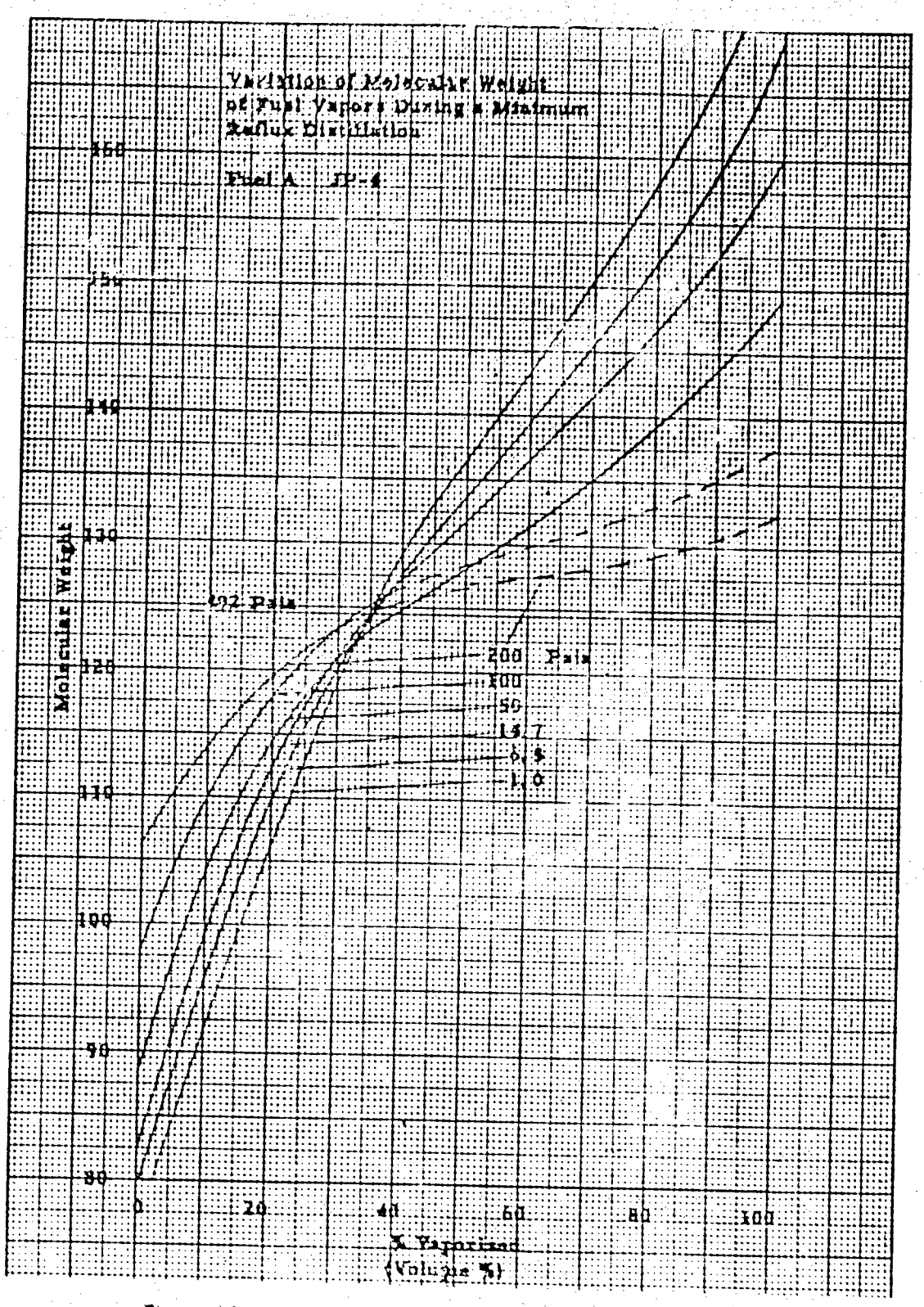

Figure 49 - Molecular Weight of Fuel Vapors, Fuel A, JP-4

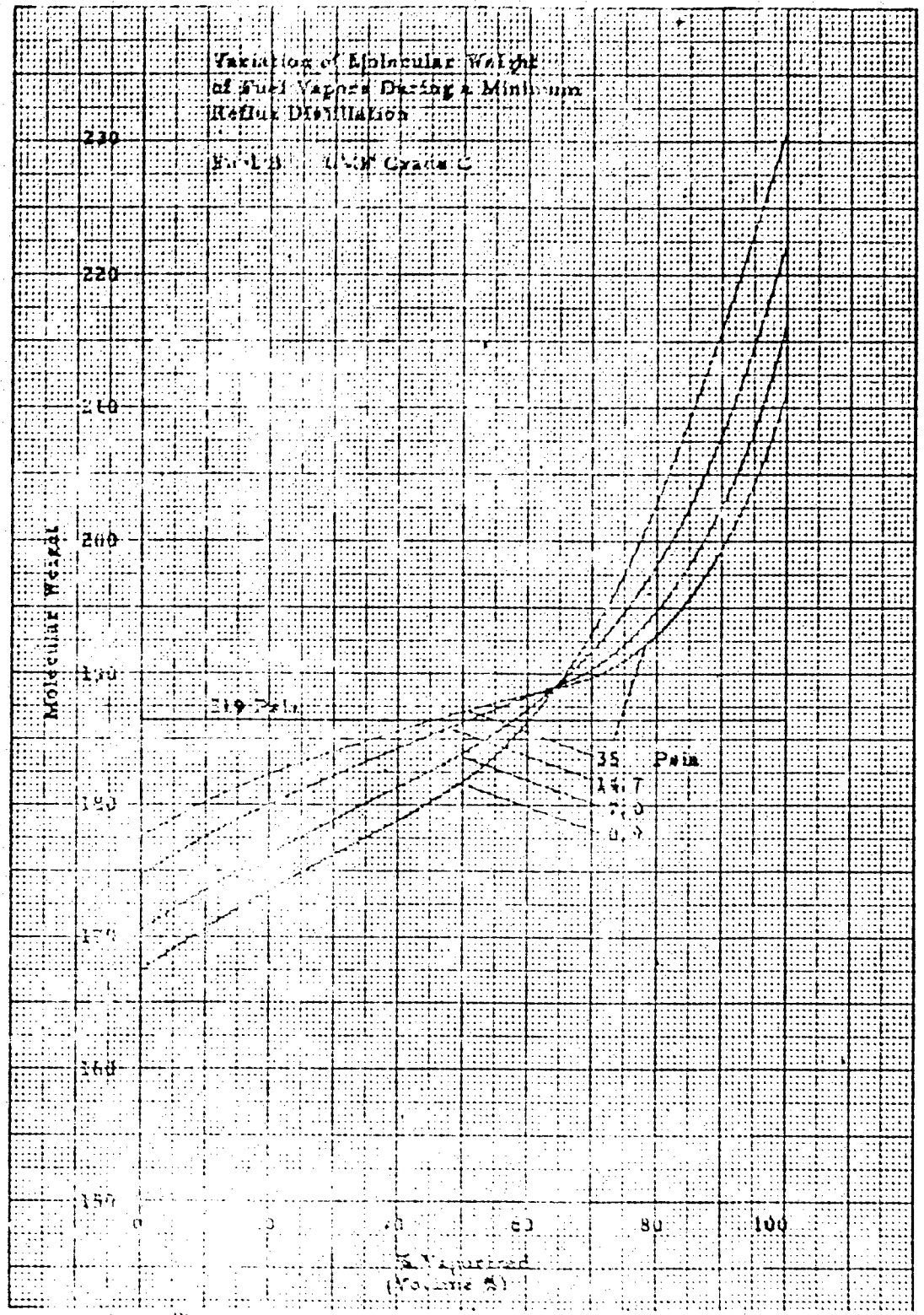

Figure 50 - Molecular Weight of Fuel Vapors, Fuel B, RJ-1

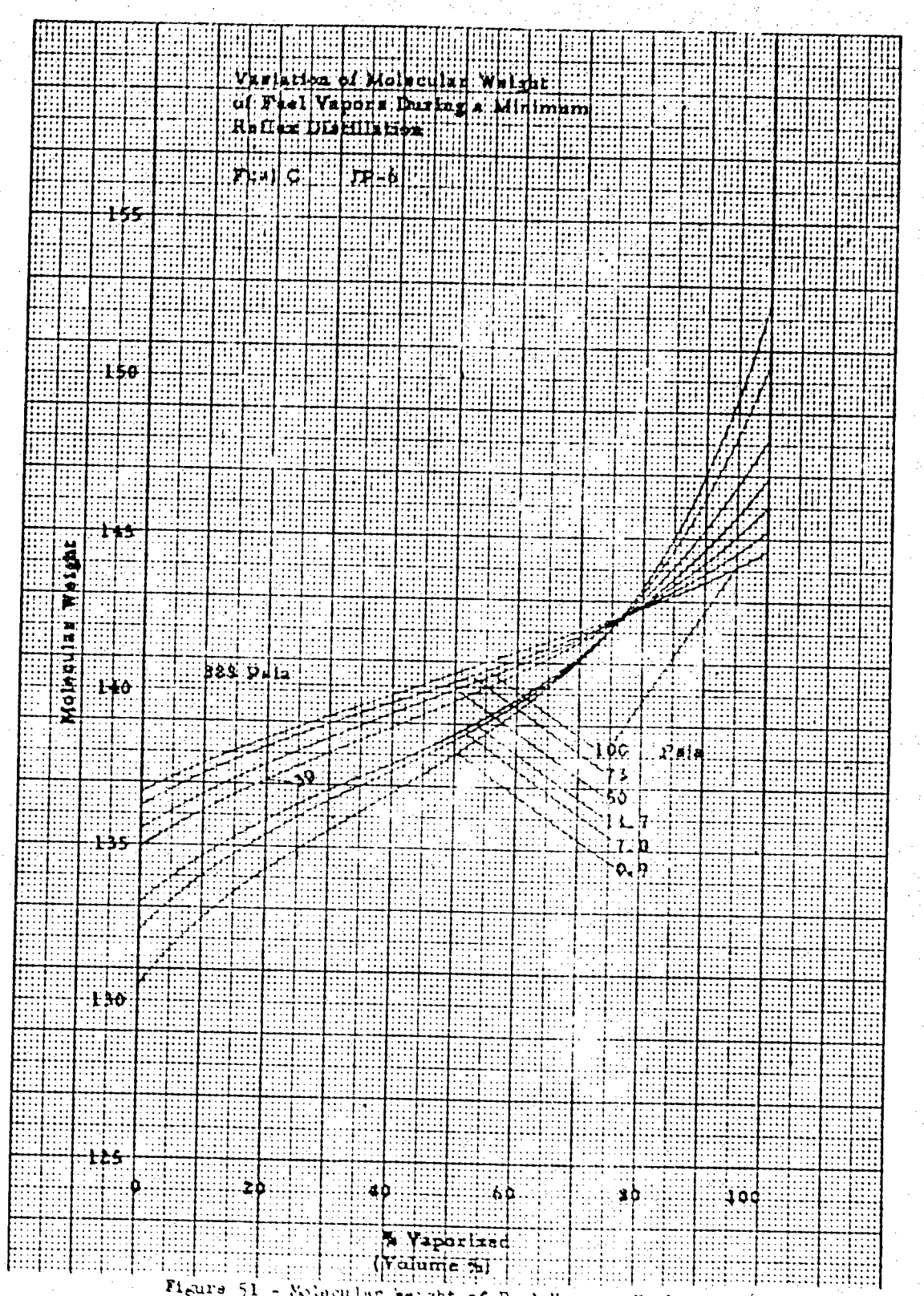

Figure 51 - Molecular Weight of Fuel Vapors, Fuel C, JP-6-H

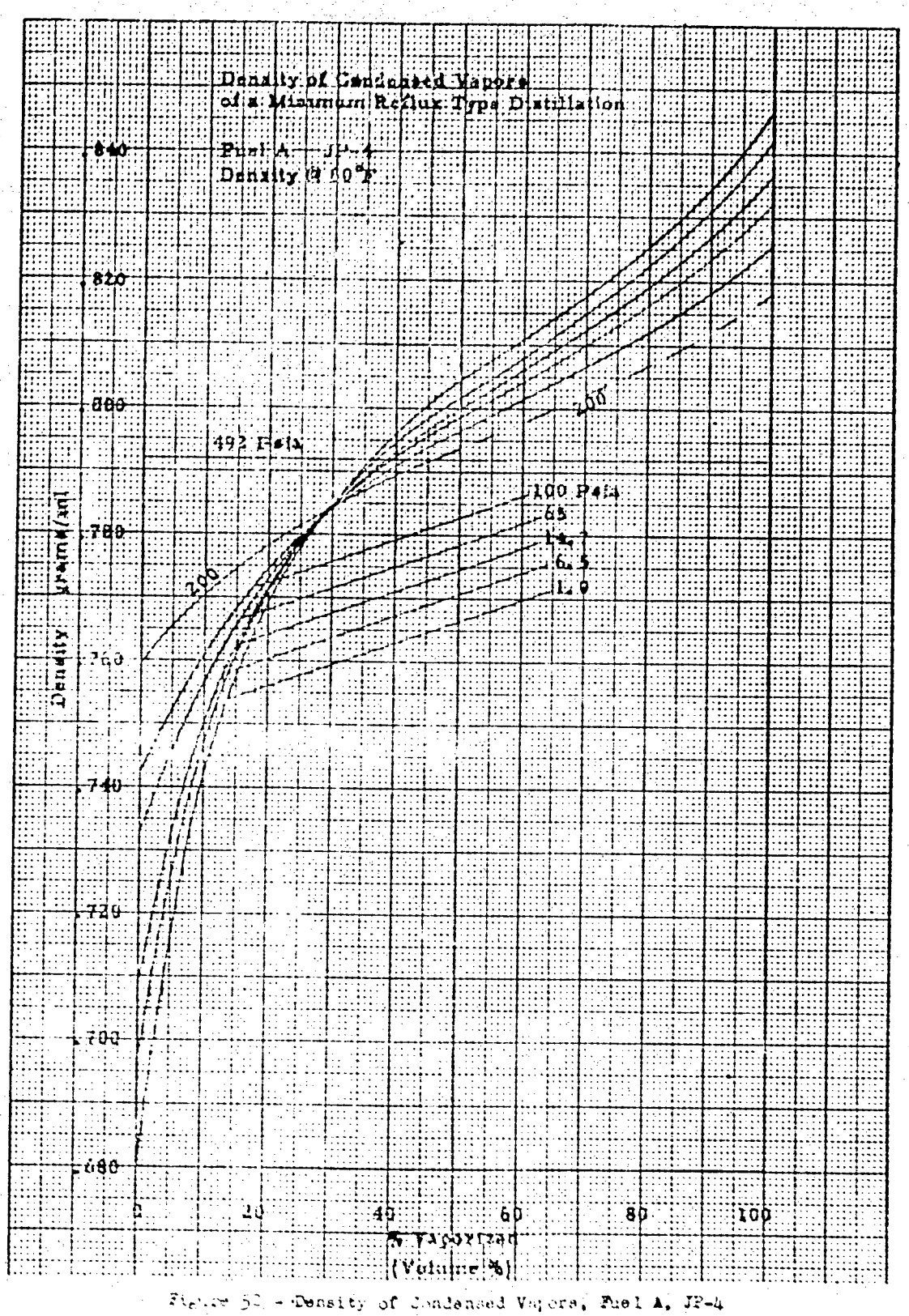

Figure 52 - Density of Condensed Vapors, Fuel A, JP-4

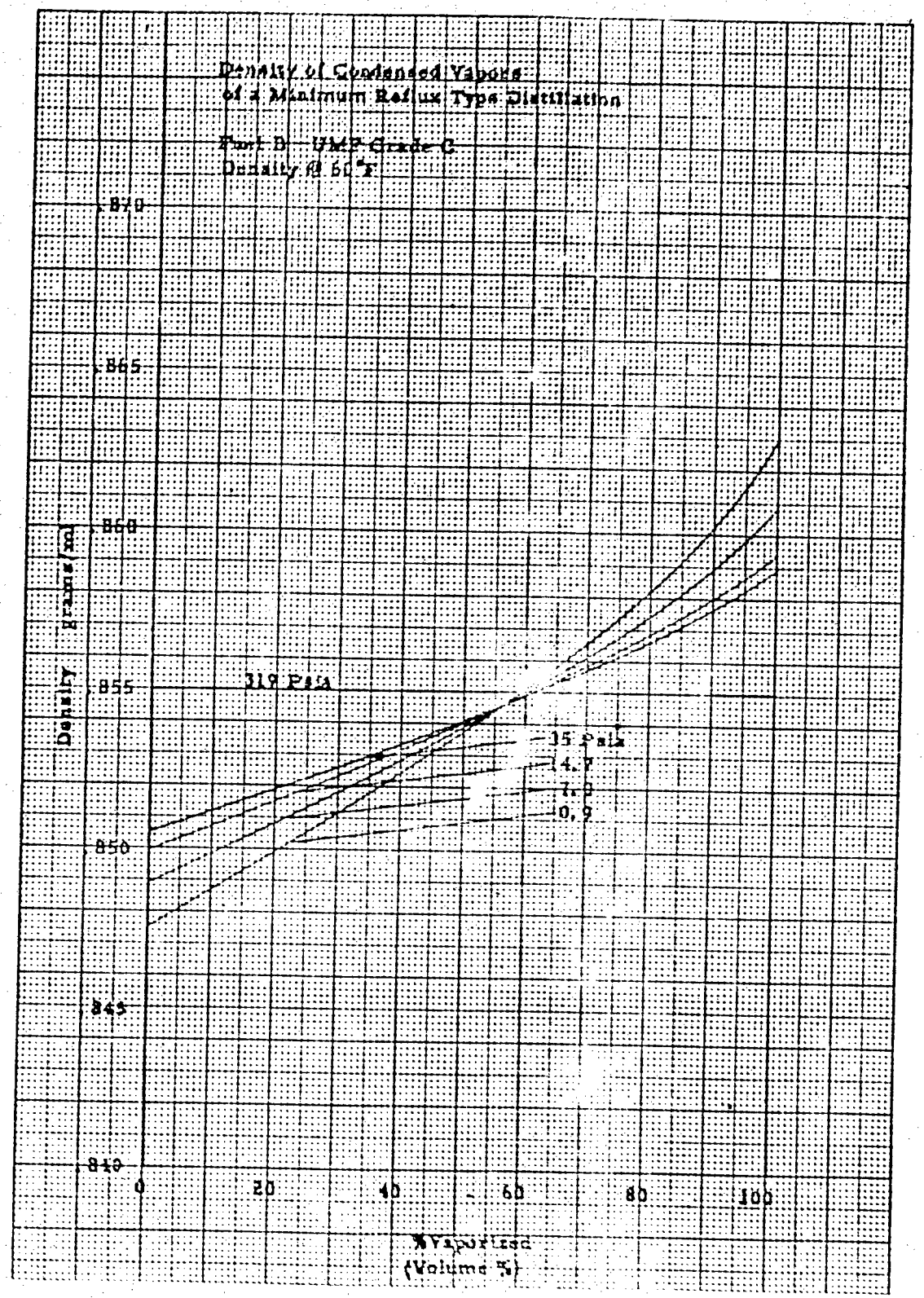

Figure 53 - Density of Condensed Vapors Fuel B, RJ-1

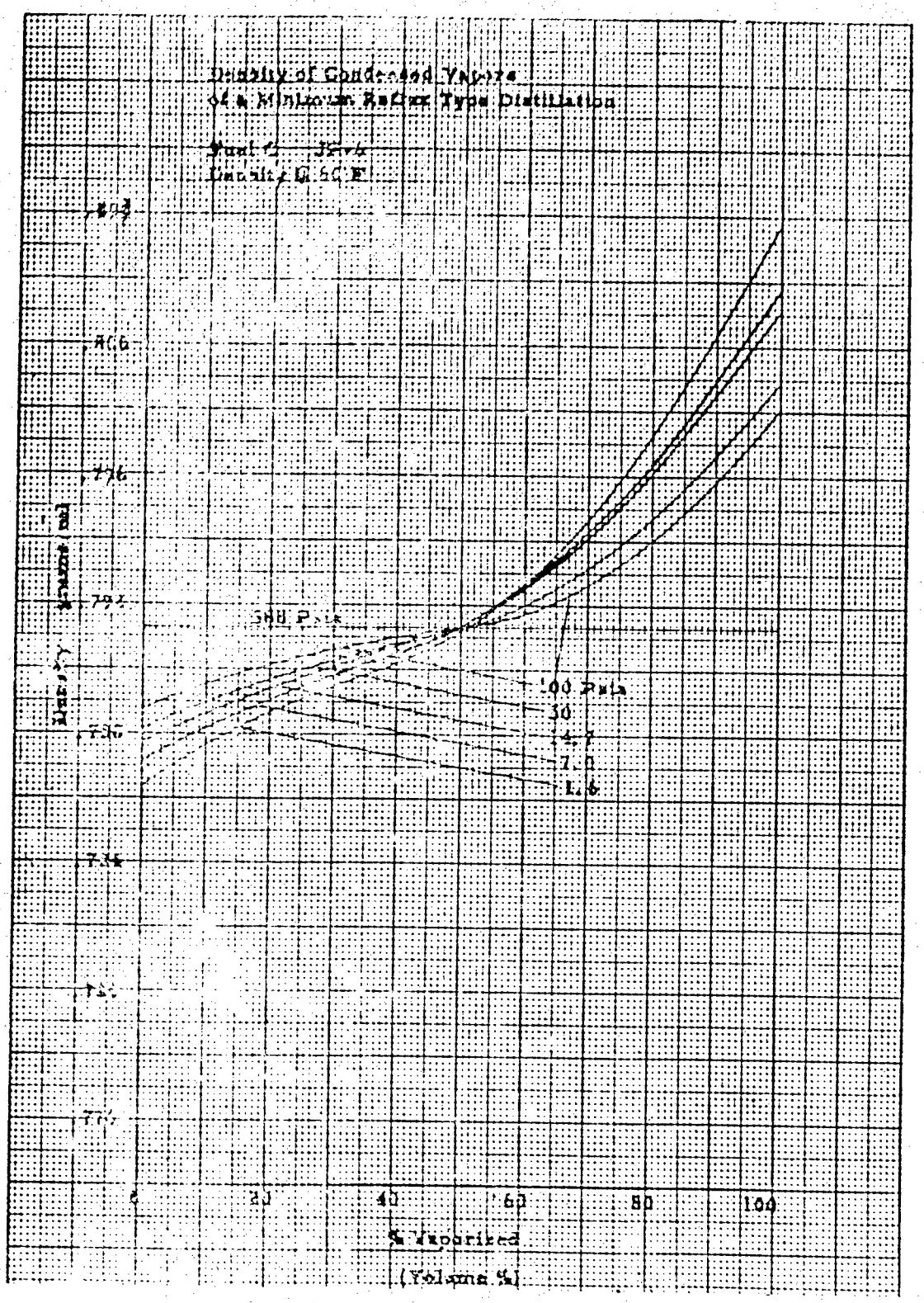

Figure 34 - Density of Condensed Vapors, Fuel C, JP-6-H

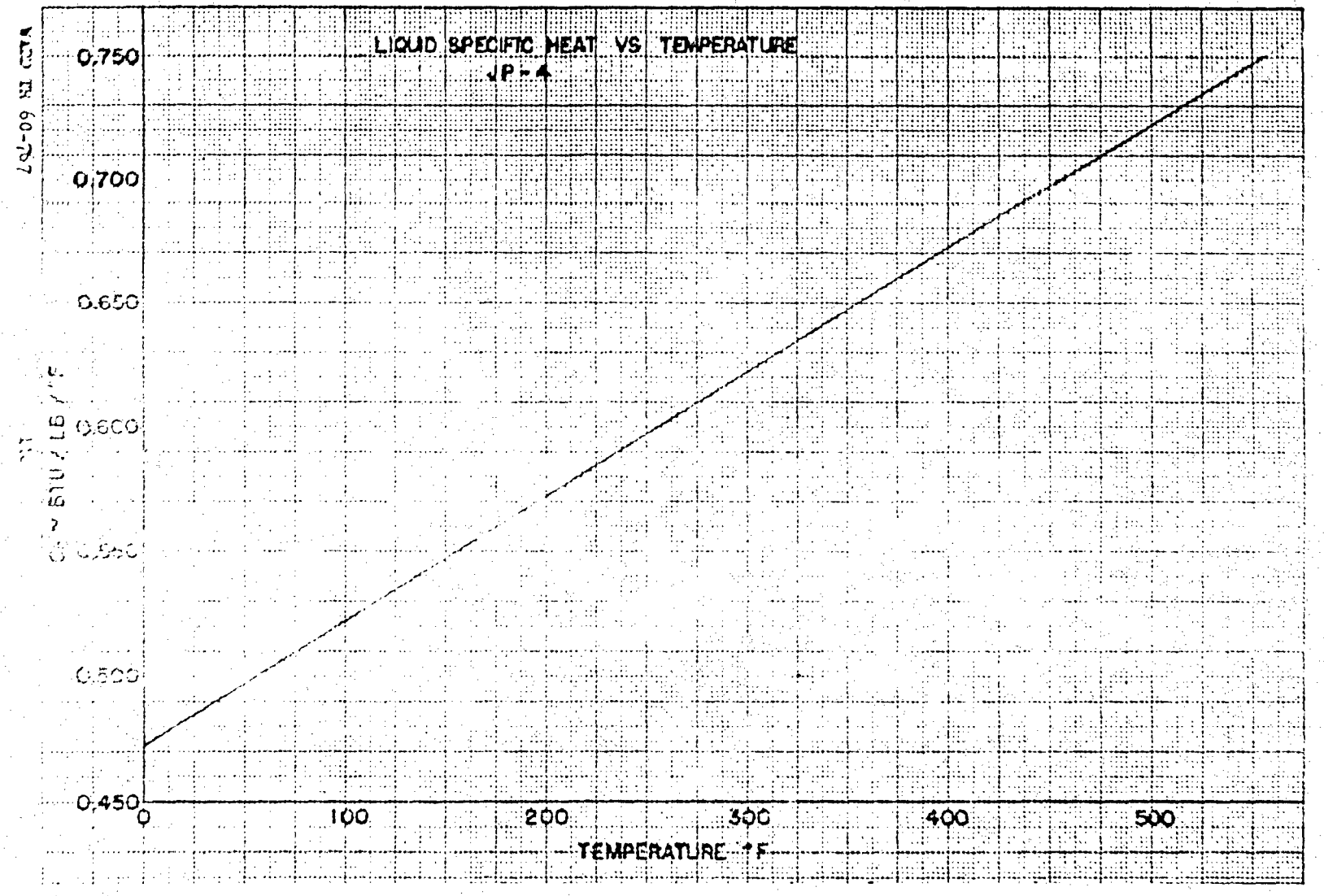

Figure 55 - Liquid Specific Heat, Fuel A, JP-4

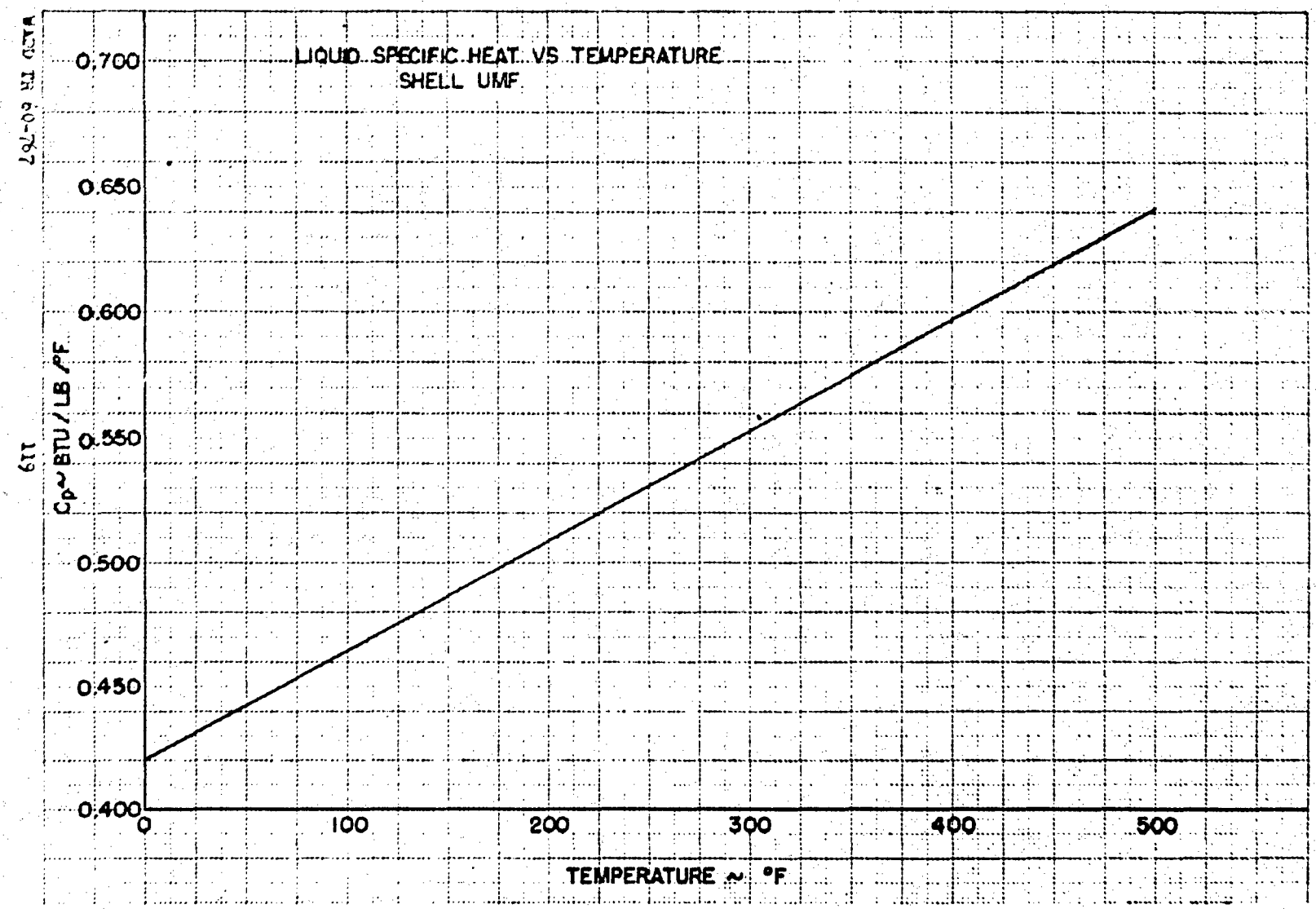

Figure 56 - Liquid Specific Heat, Fuel B, RJ-1

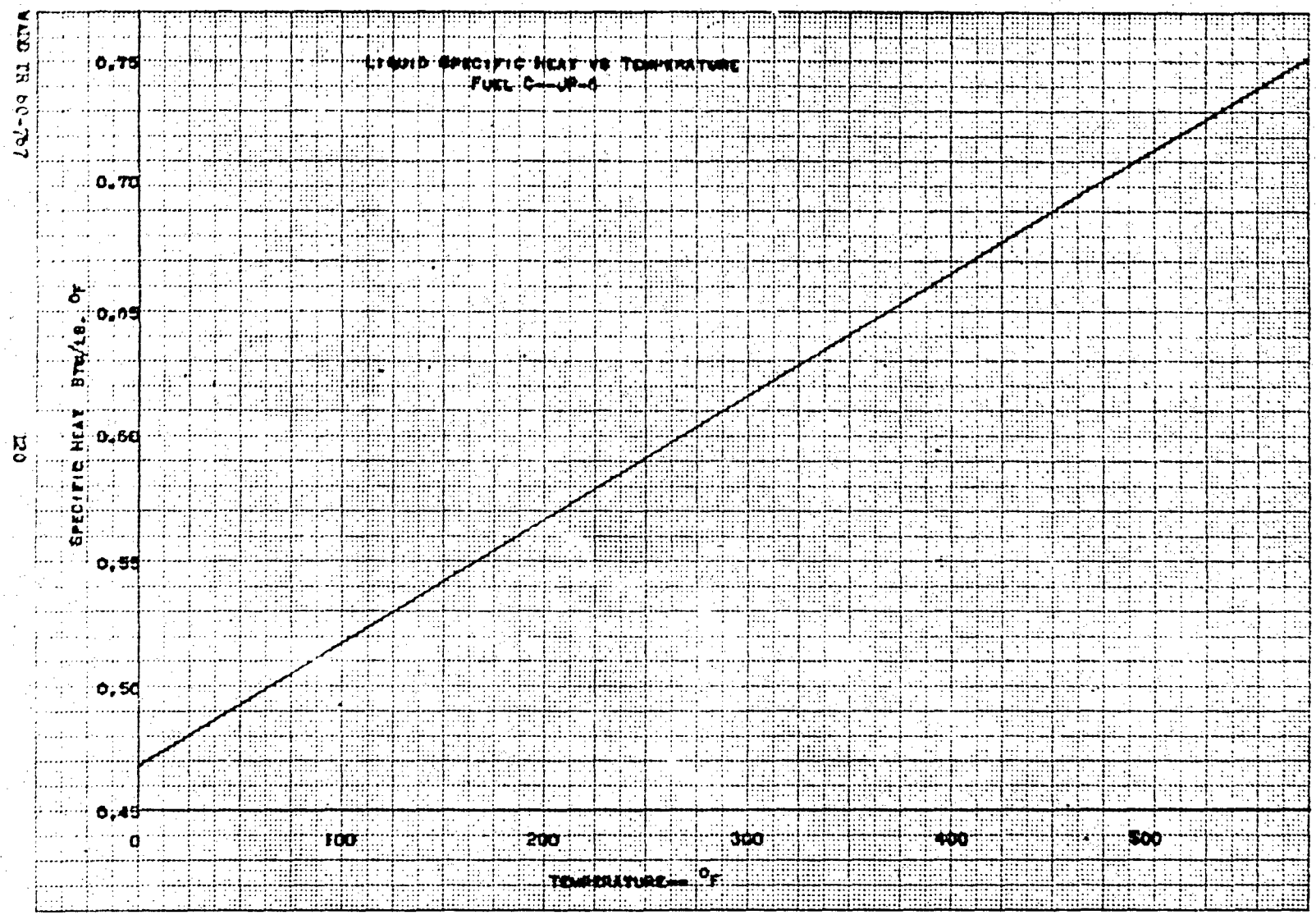

Figure 57 - Liquid Specific Heat, Fuel C, JP-6-H.

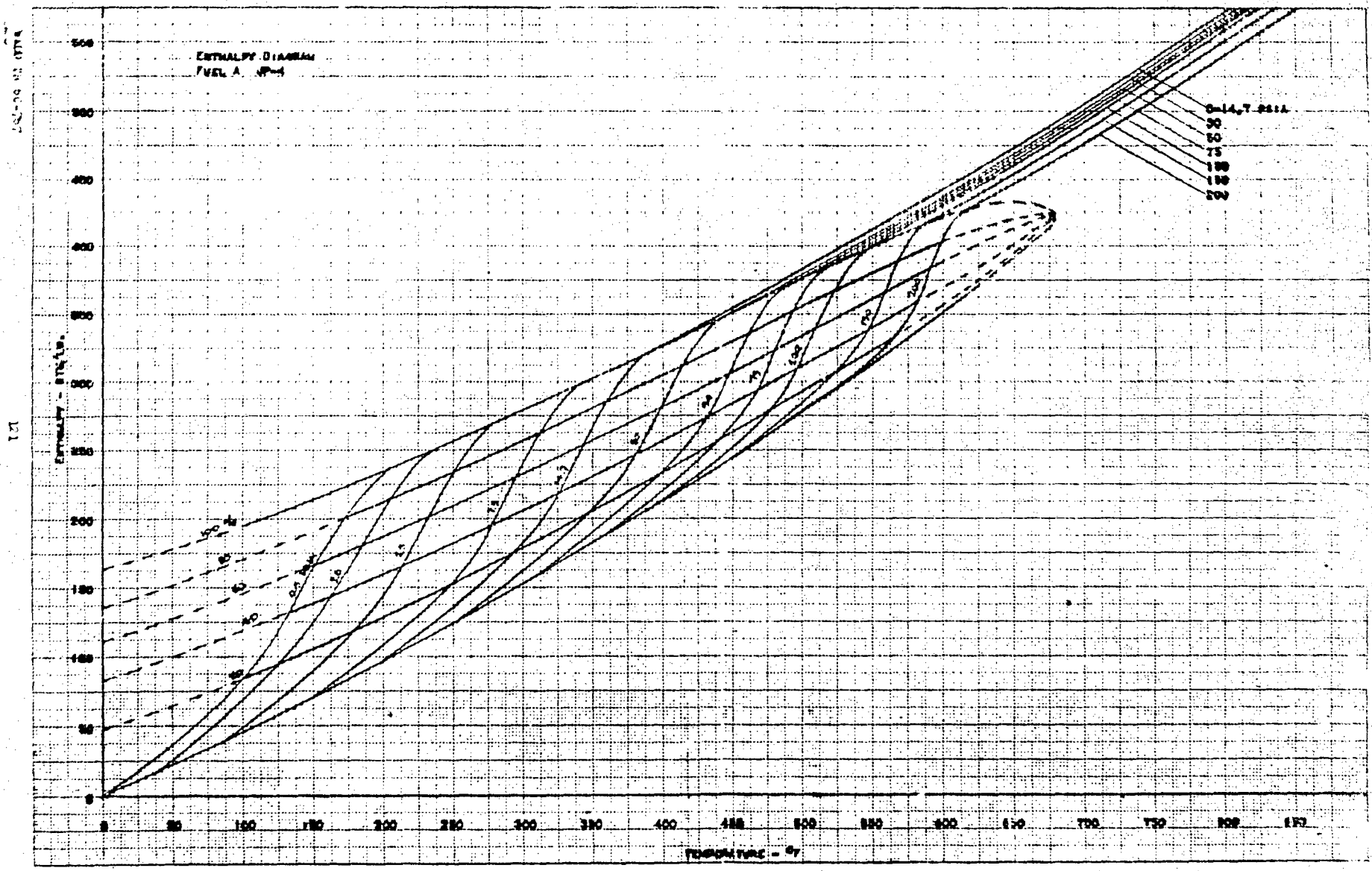

Figure 58 - Enthalpy Diagram, Fuel A, JP-4.

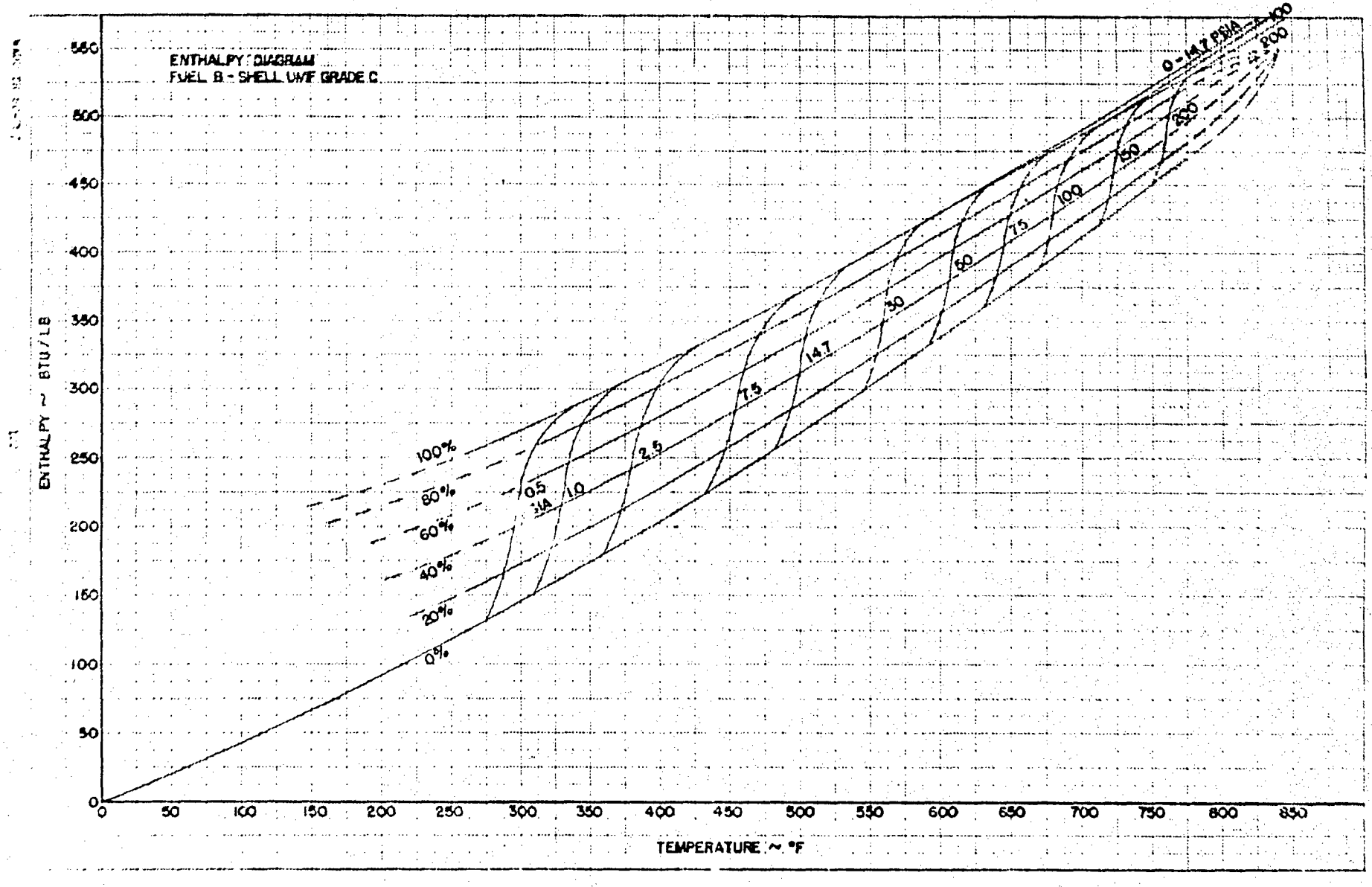

Figure 59 - Enthalpy Diagram, Fuel B, RJ-1

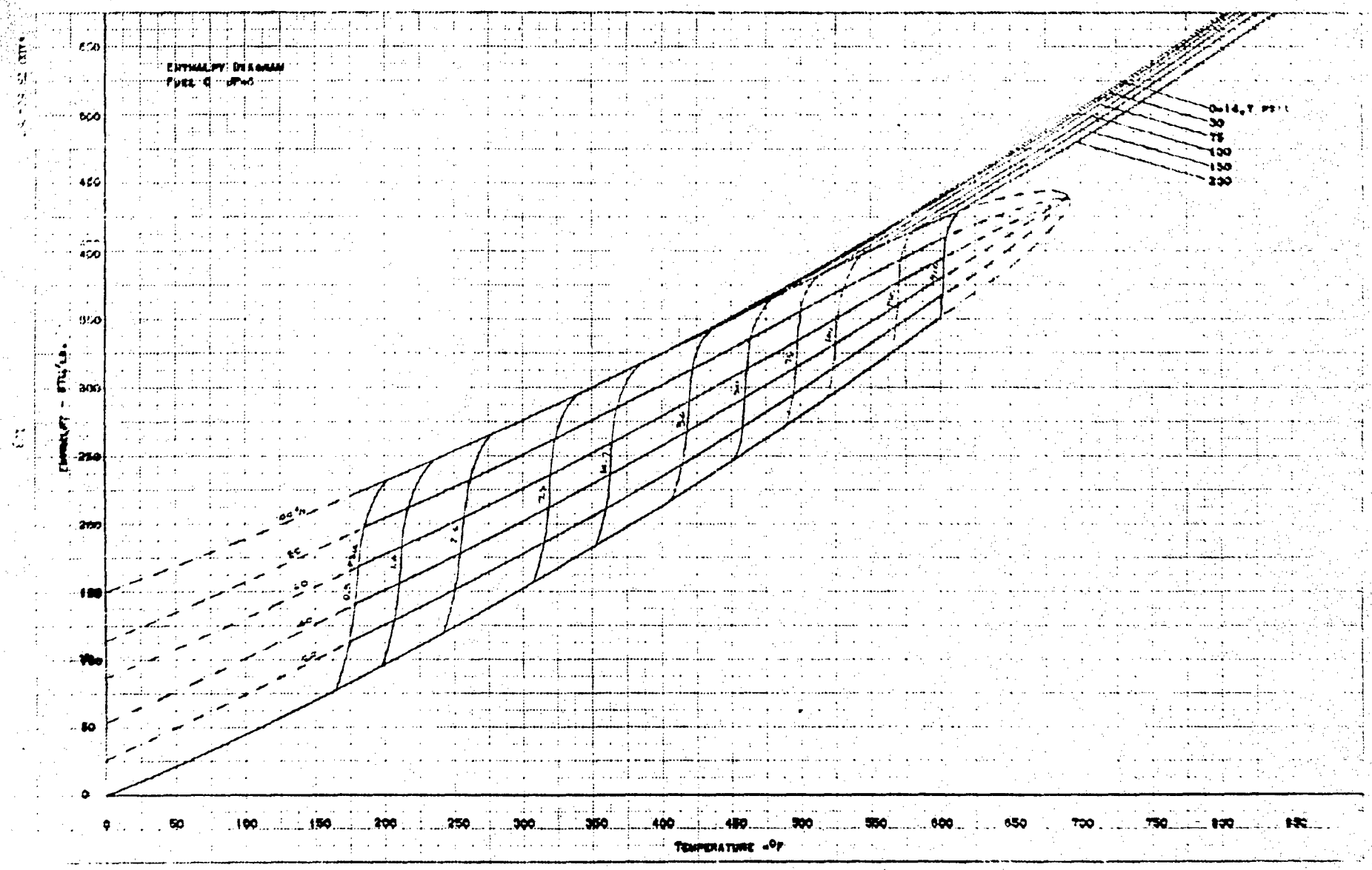

Figure 60 - Enthalpy Diagram, Fuel C, JP-6,-H.

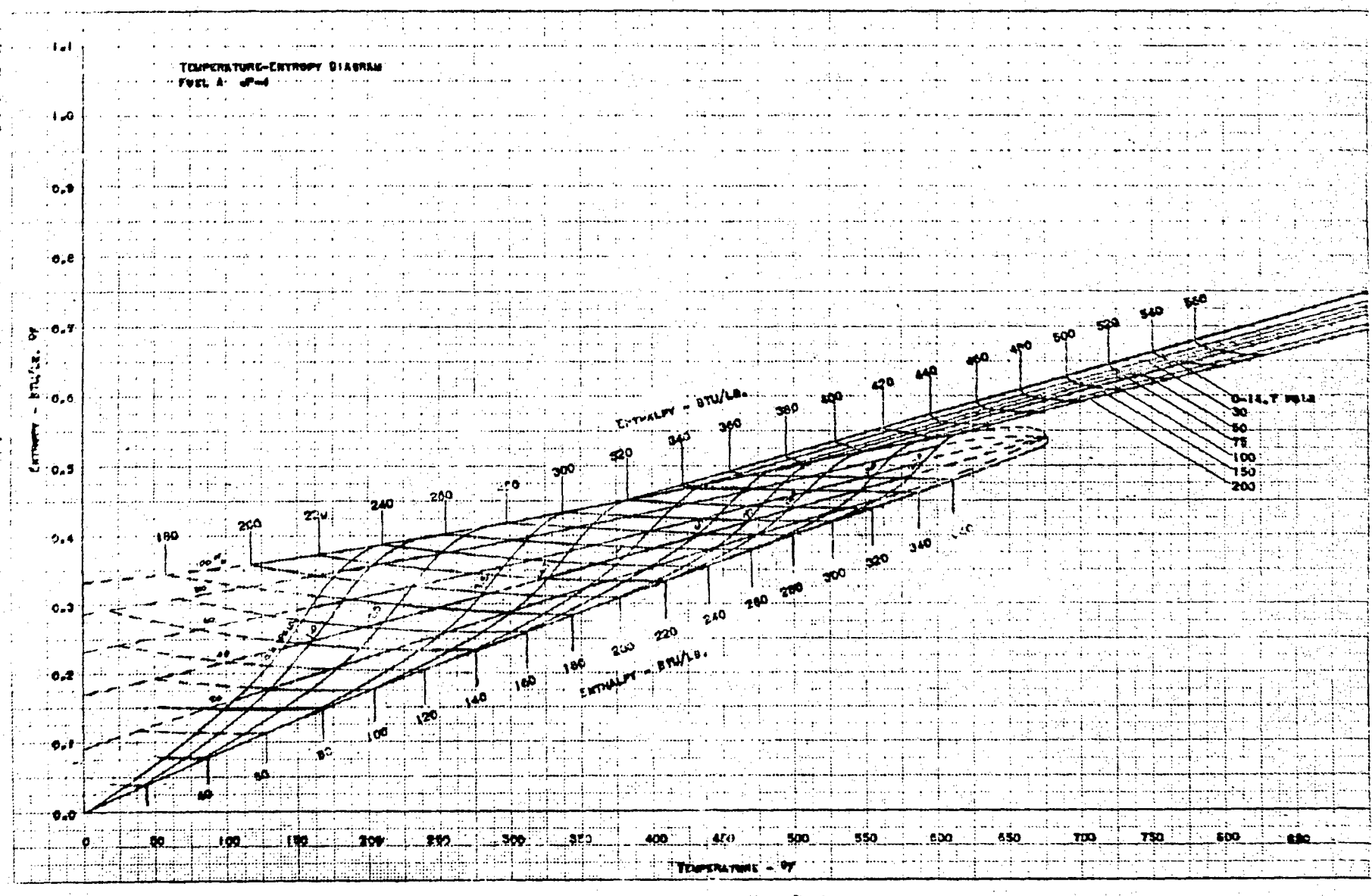

Figure 61 - Temperature Entropy Diagram, Fuel A, JP-4.

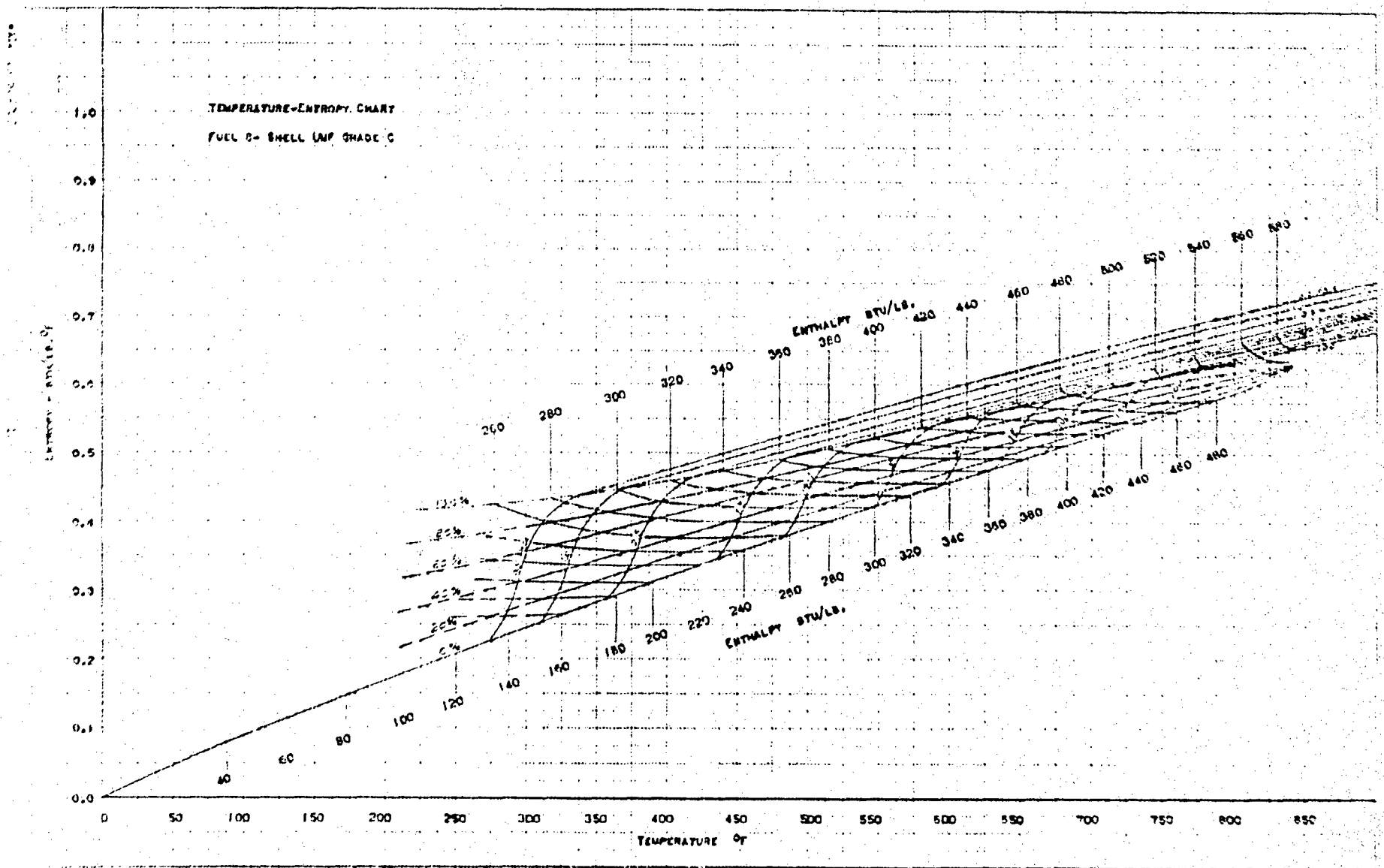

Figure 6. - Temperature Entropy Diagram, Fuel B, RJ-1.

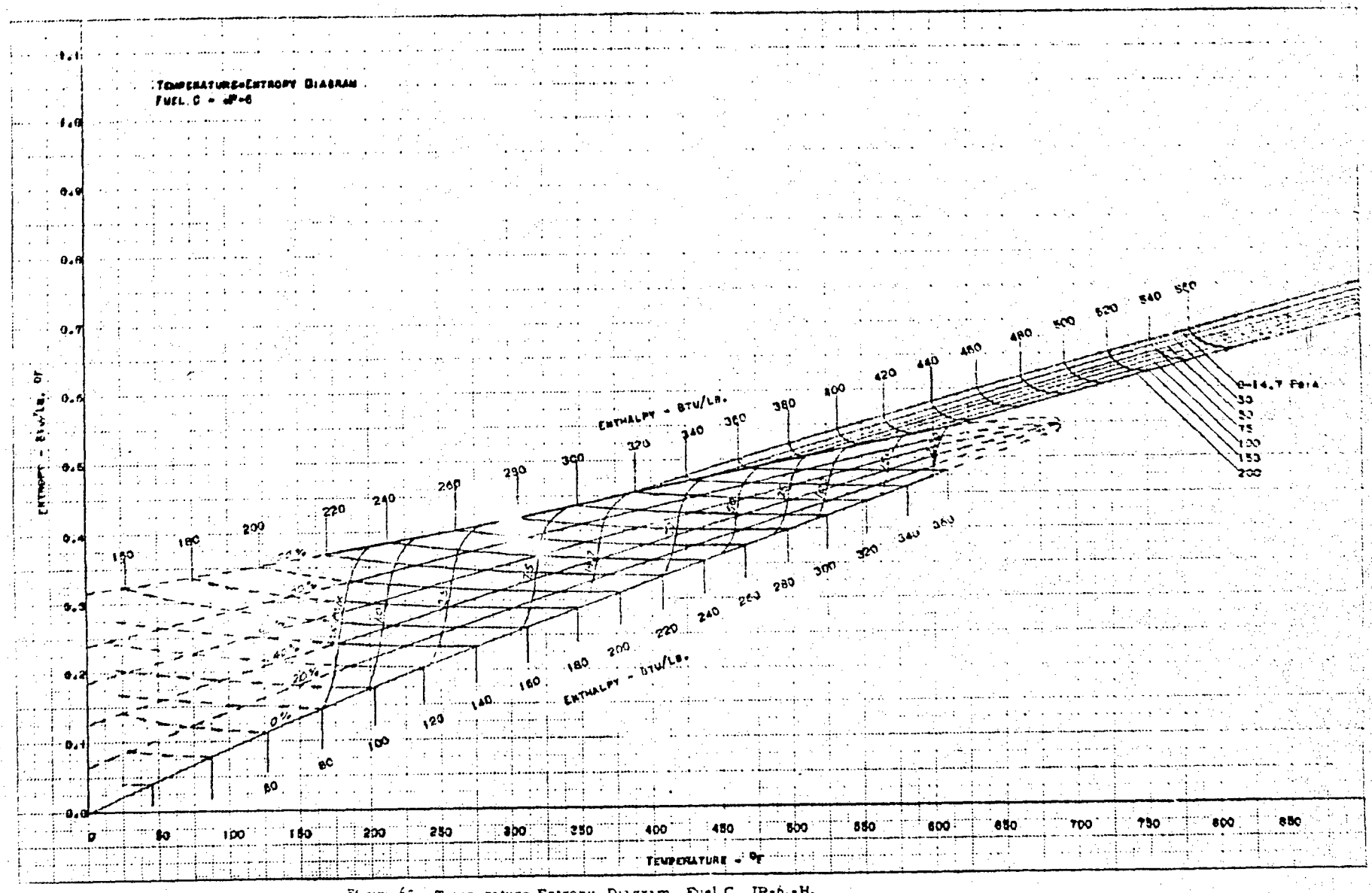

Figure 63 - Temperature Entropy Diagram, Fuel C, JP-6.-H.

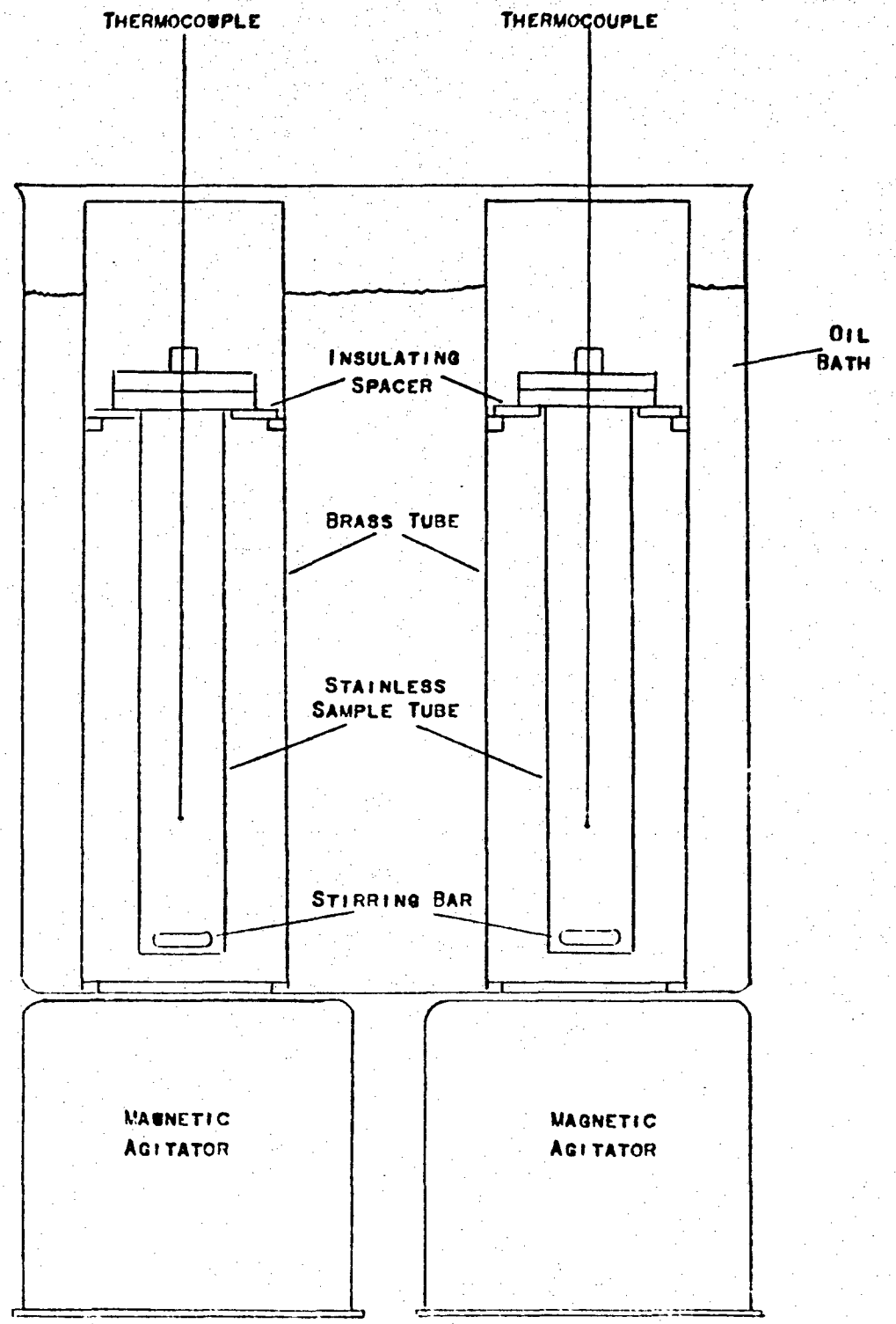

Figure 64 - Schematic of Comparison Calorimeter

NOTE: BATH HEATER AND AGITATOR NOT SHOWN

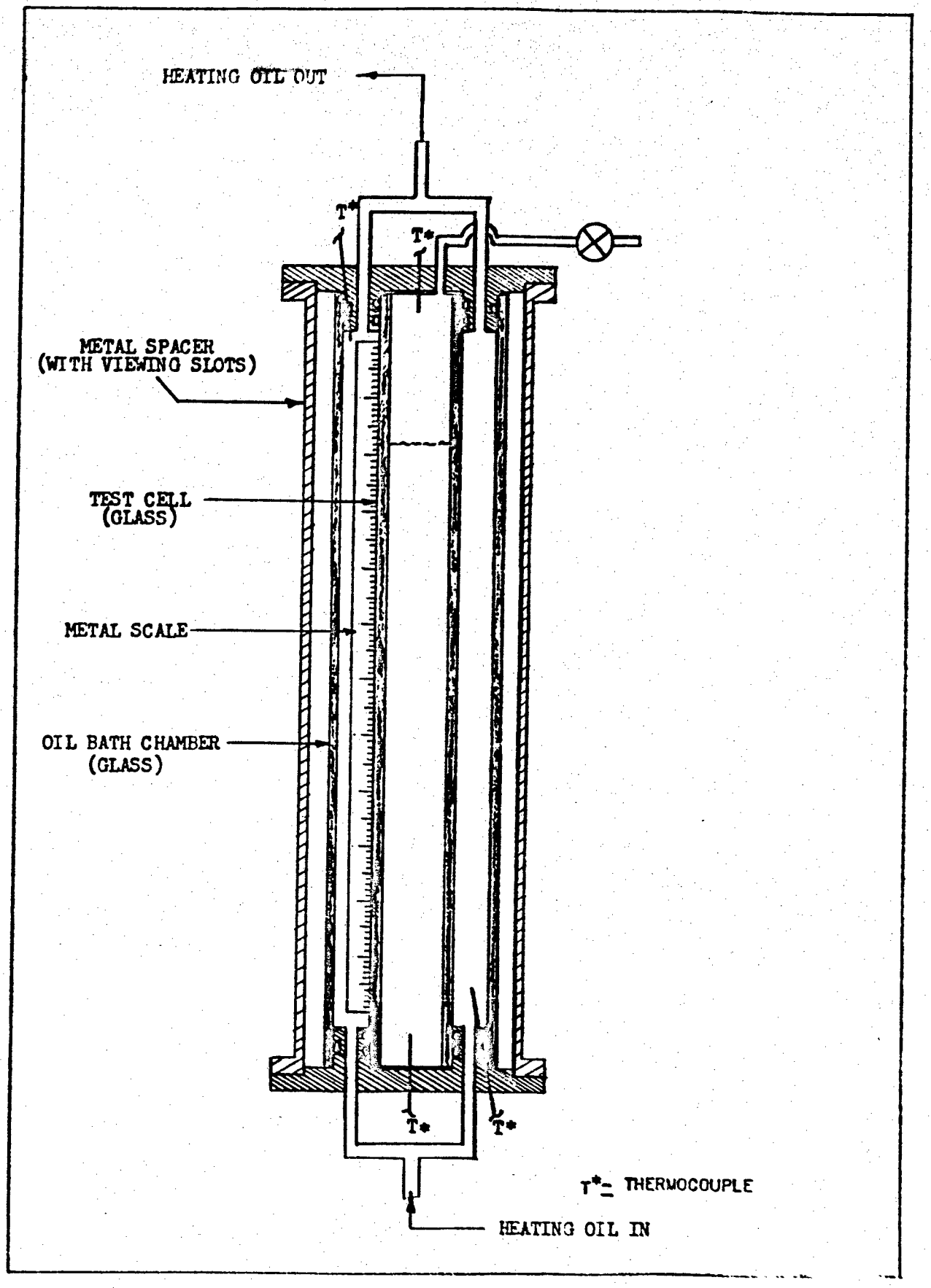

Figure 65 - Specific Volume Apparatus

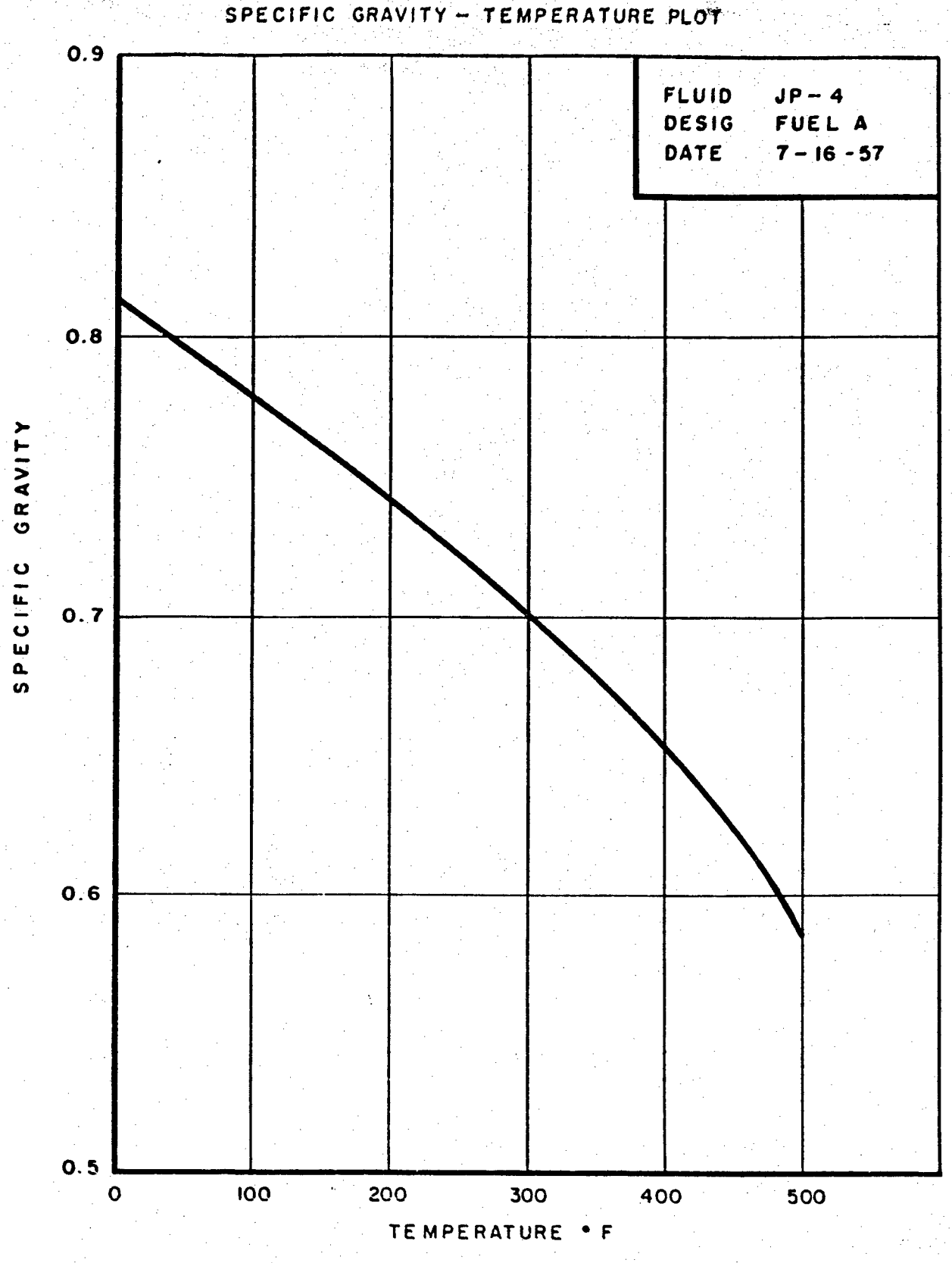

FIGURE 66. SPECIFIC GRAVITY - FUEL A, JP-4

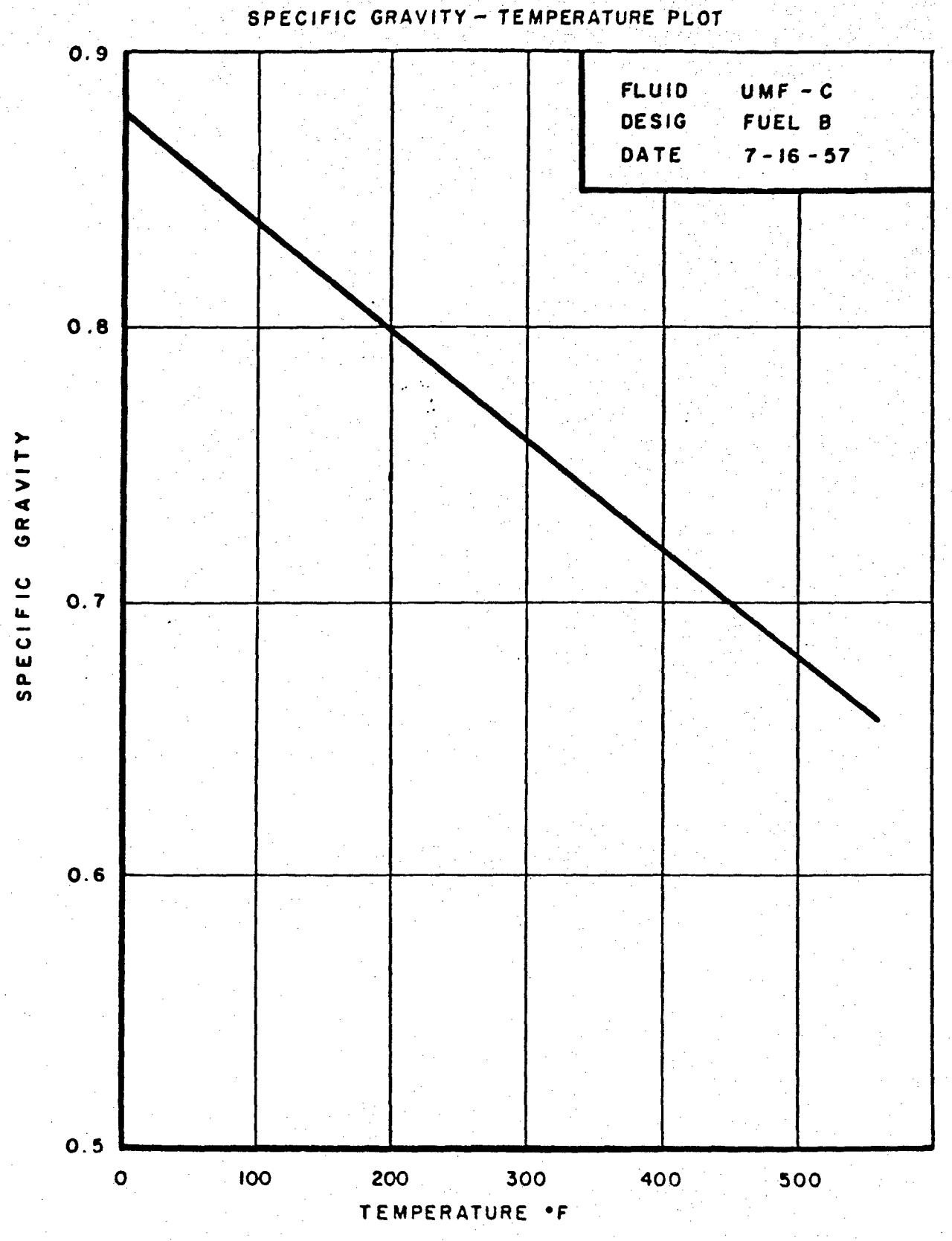

FIGURE 67. SPECIFIC GRAVITY - TEMPERATURE PLOT, FUEL B, RJ-1

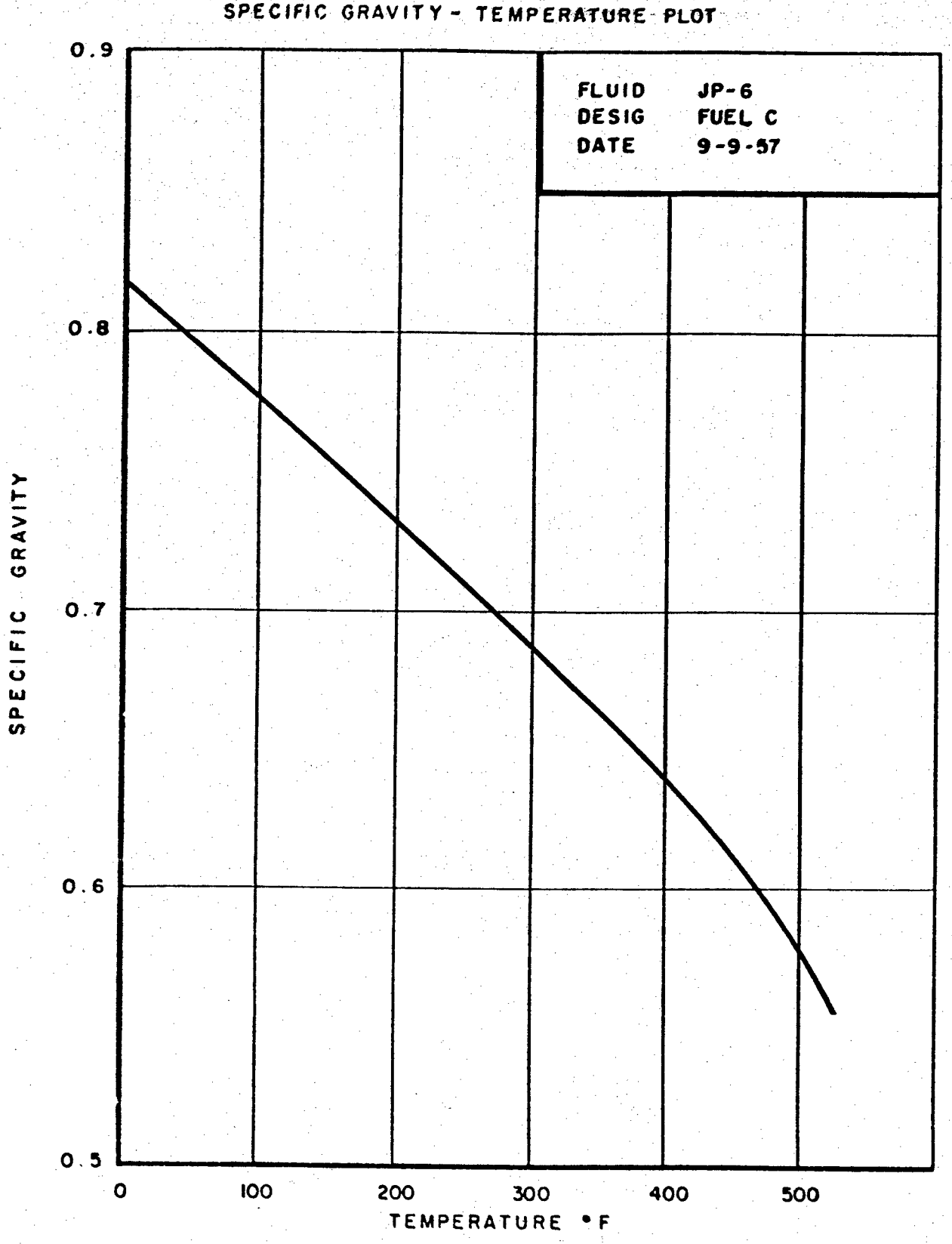

FIGURE 68. SPECIFIC GRAVITY, FUEL C, JP-6-H

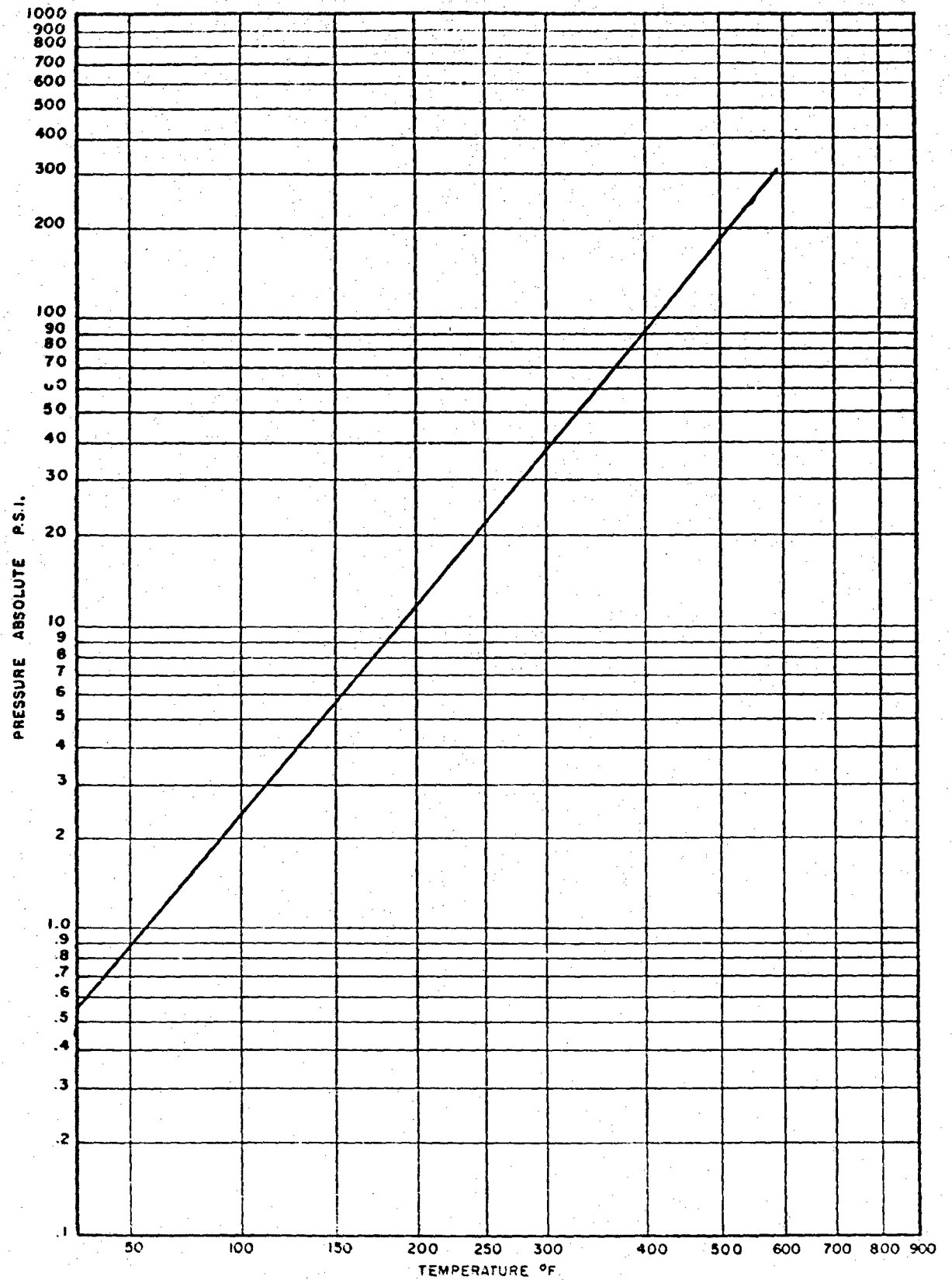

Figure 69 – JP-4 Vapor Pressure Plot, Fuel A.

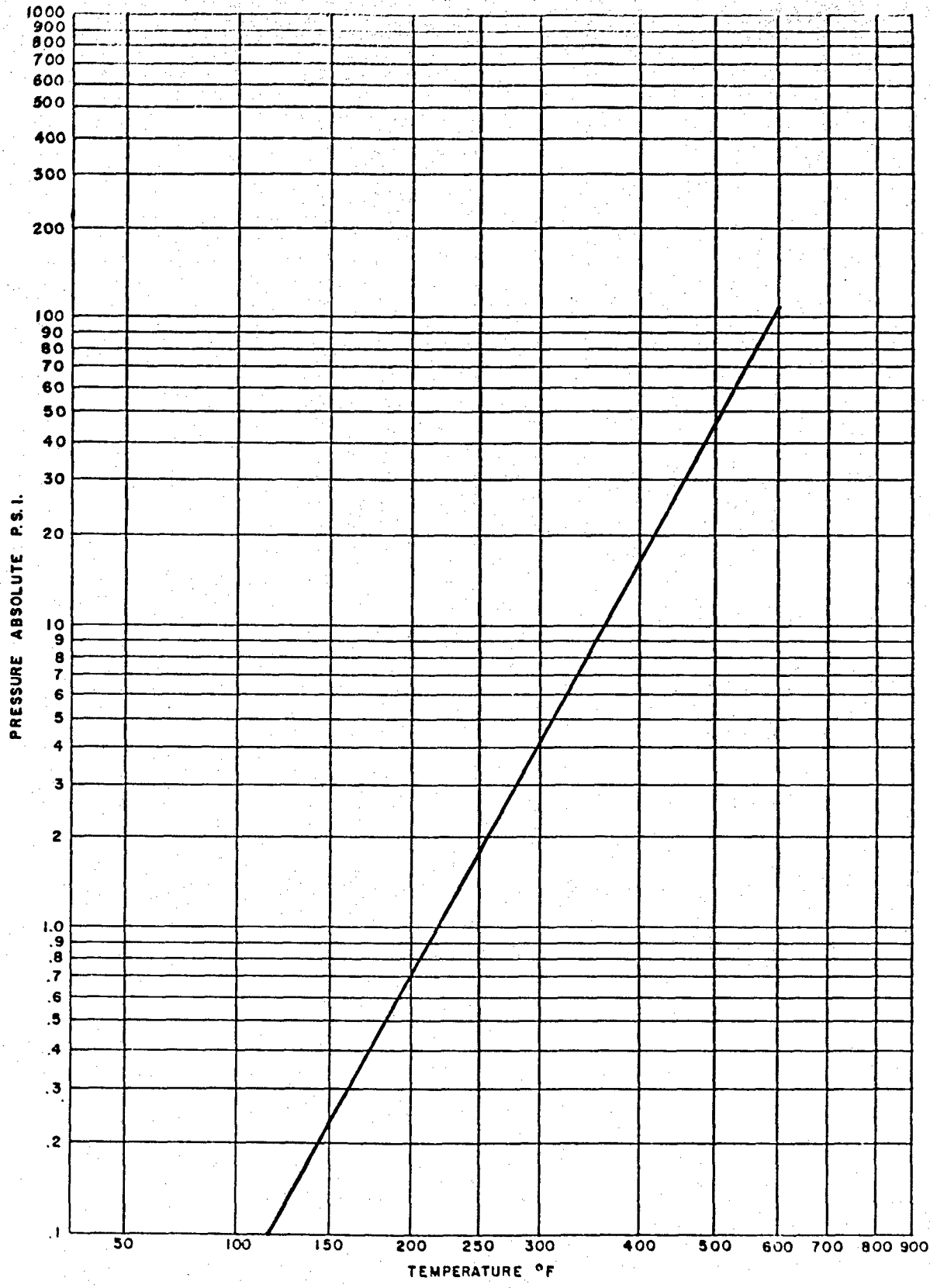

Figure 70 - RJ-1 Vapor Pressure Plot, Fuel B.

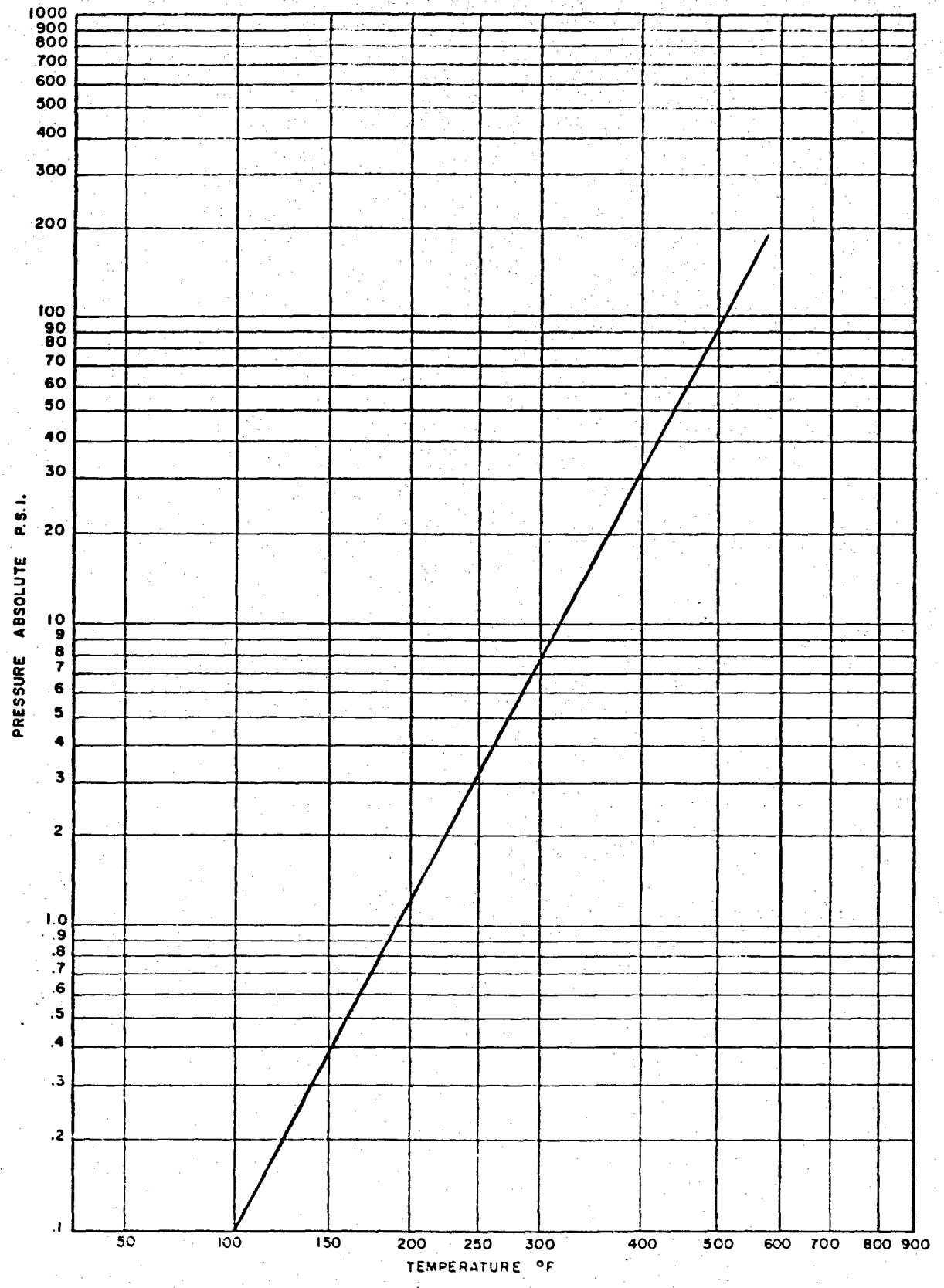

Figure 71 - JP-6 Vapor Pressure Plot, Fuel C.

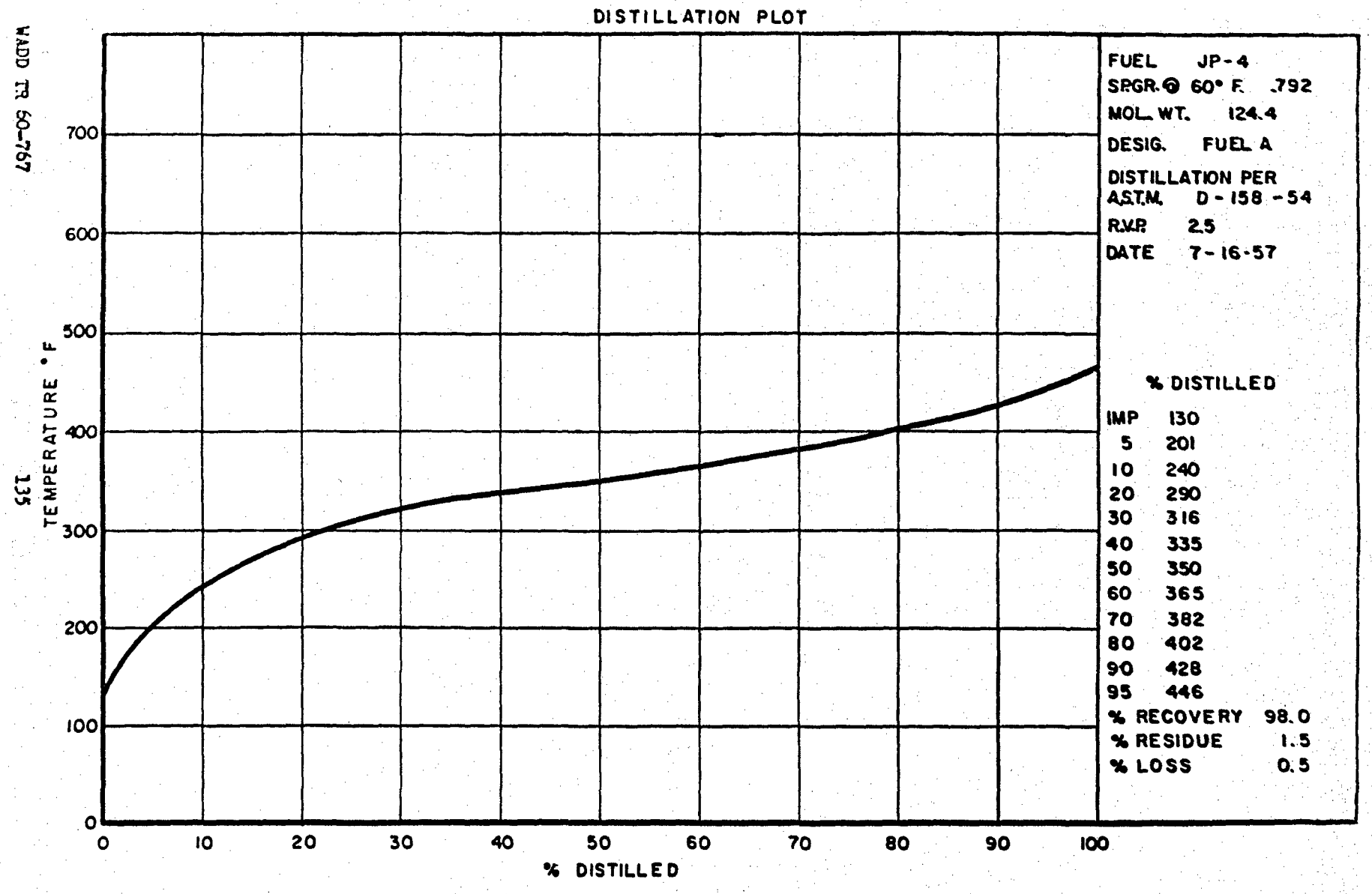

FIGURE 72. DISTILLATION PLOT, FUEL A, JP-4

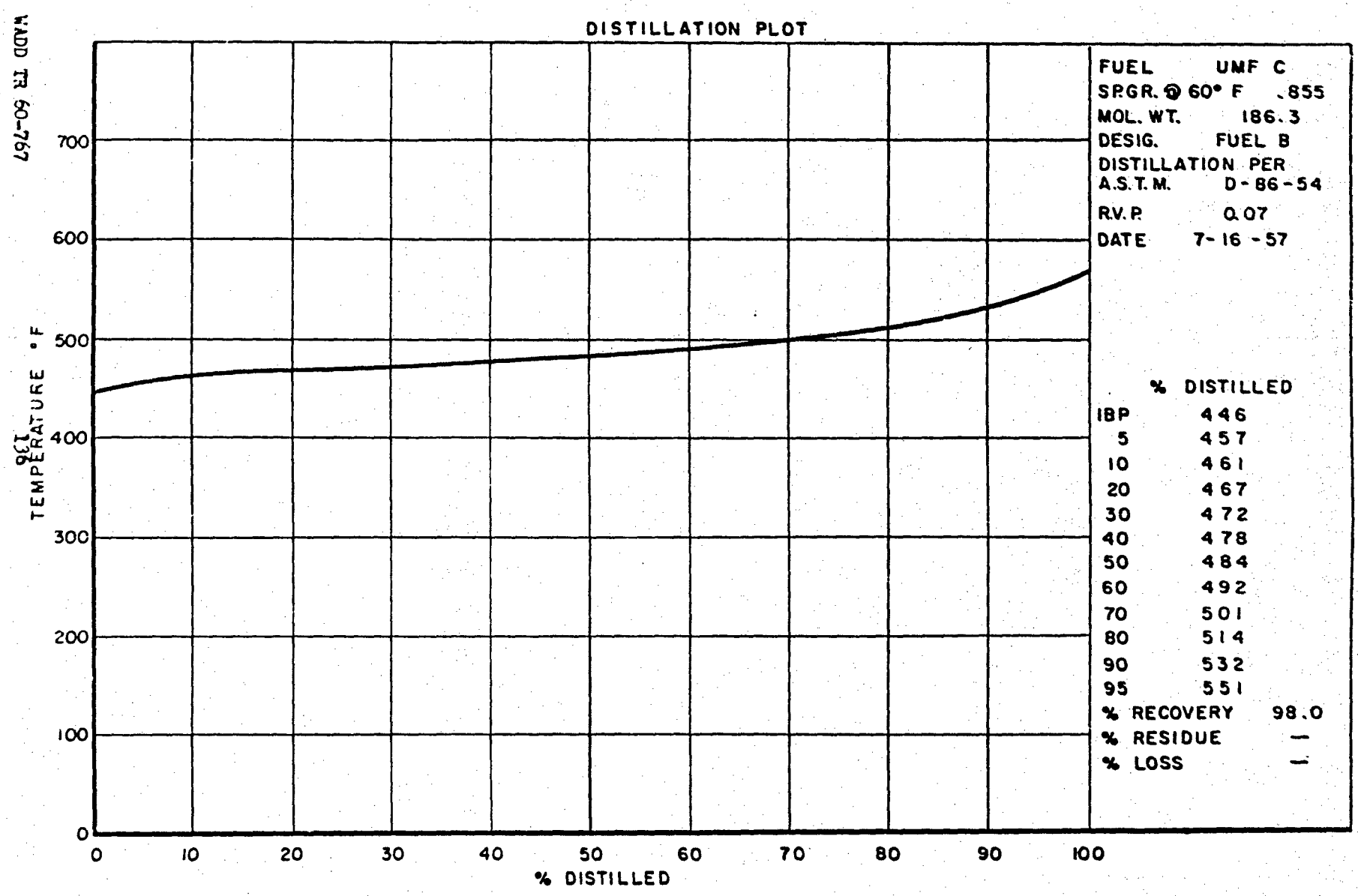

FIGURE 73. DISTILLATION PLOT, FUEL B, RJ-1

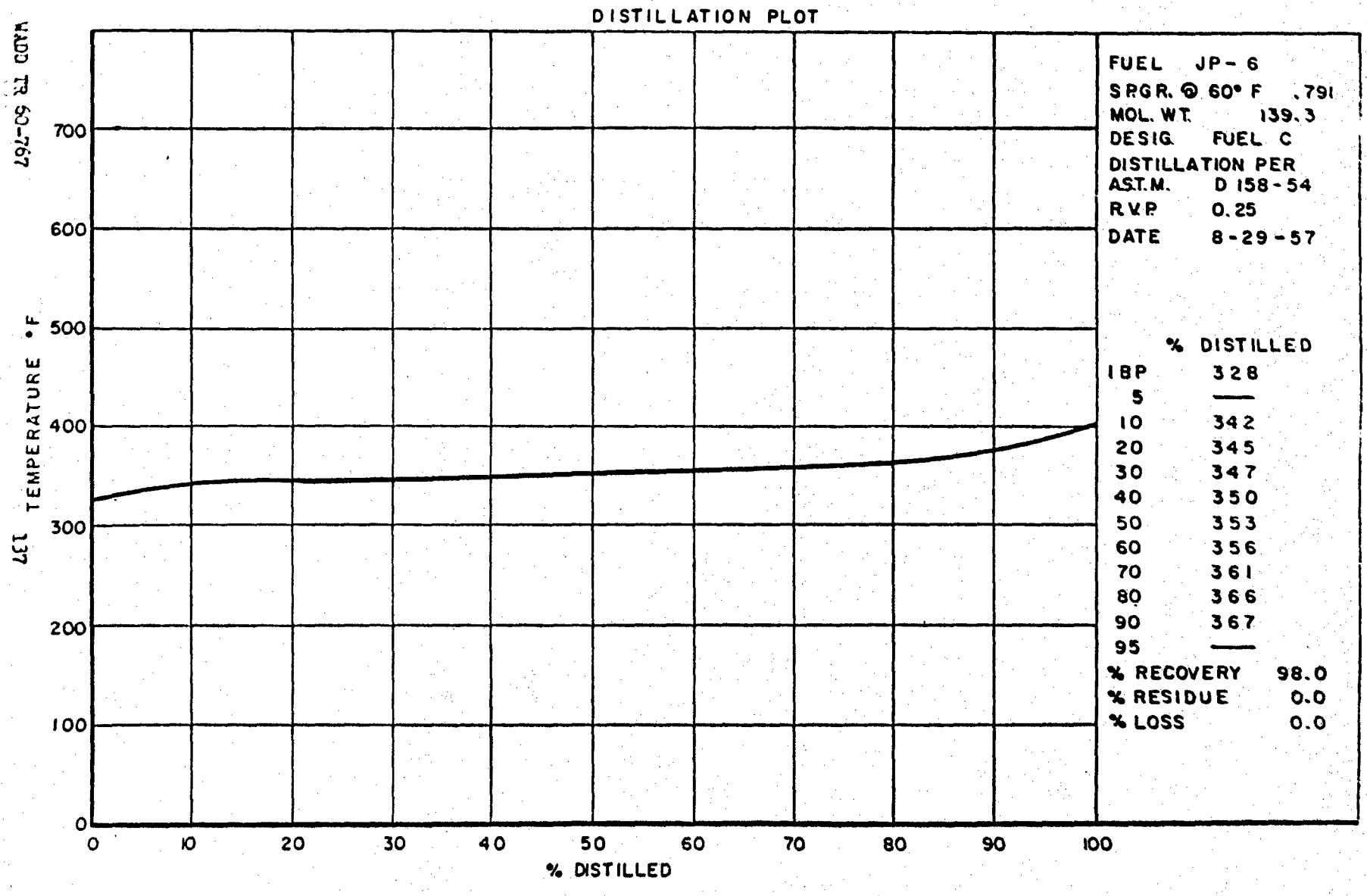

FIGURE 74. DISTILLATION PLOT, FUEL C, JP-6-H

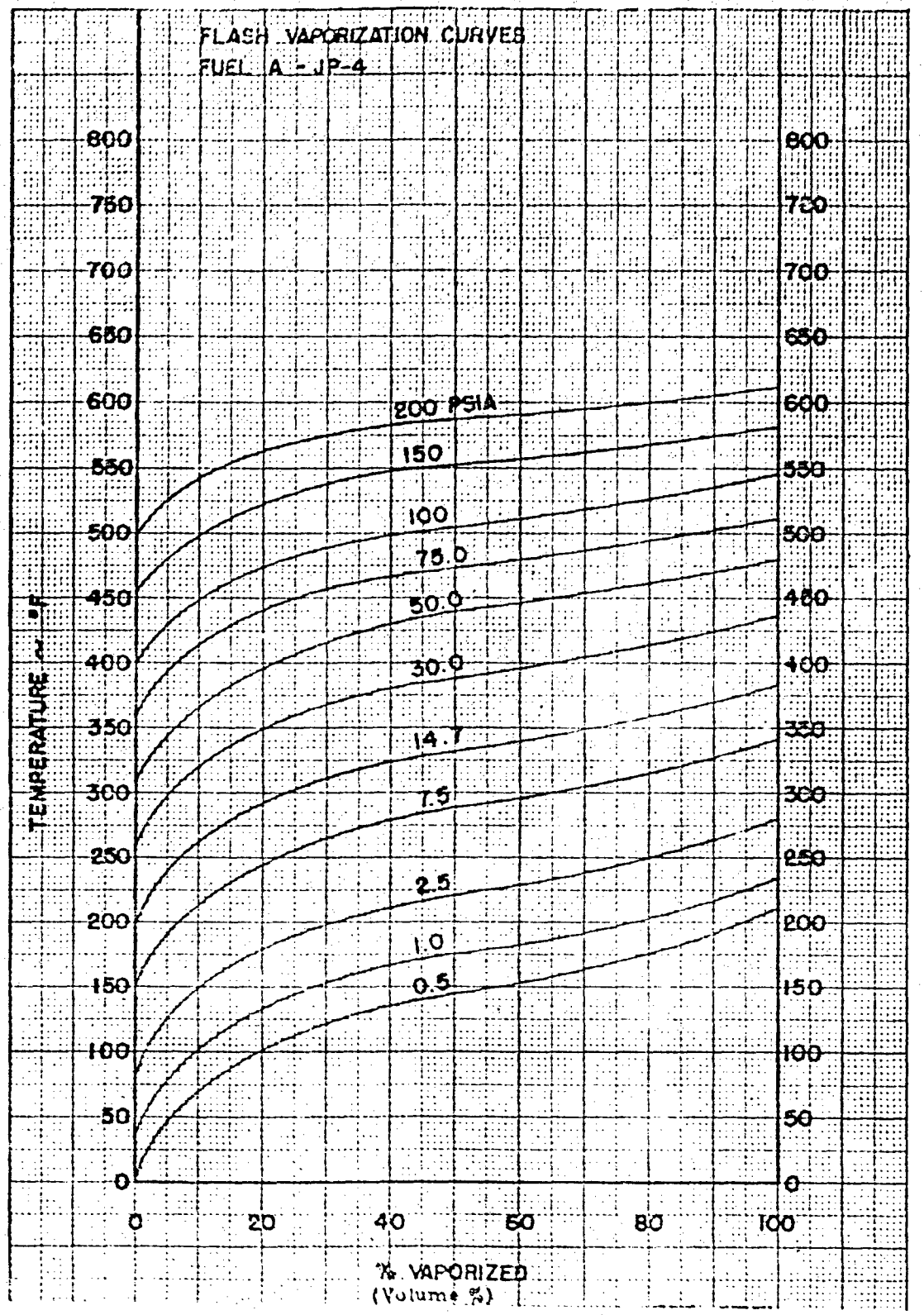

Figure 5 - Flash Vaporizations Curves, Fuel A, JP-4

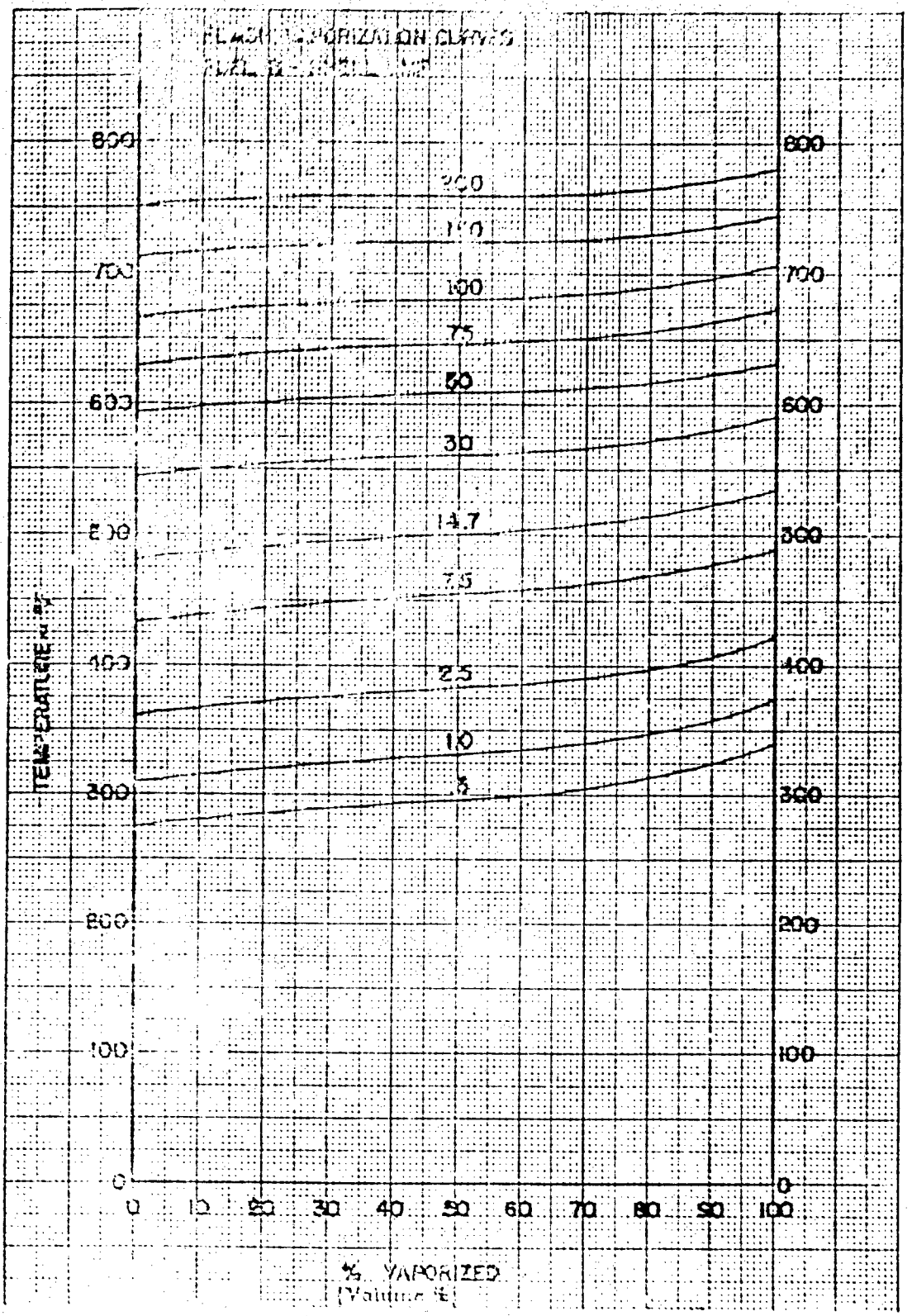

Figure 2. - Flash Vaporization Curves, Fuel B, RJ-1.

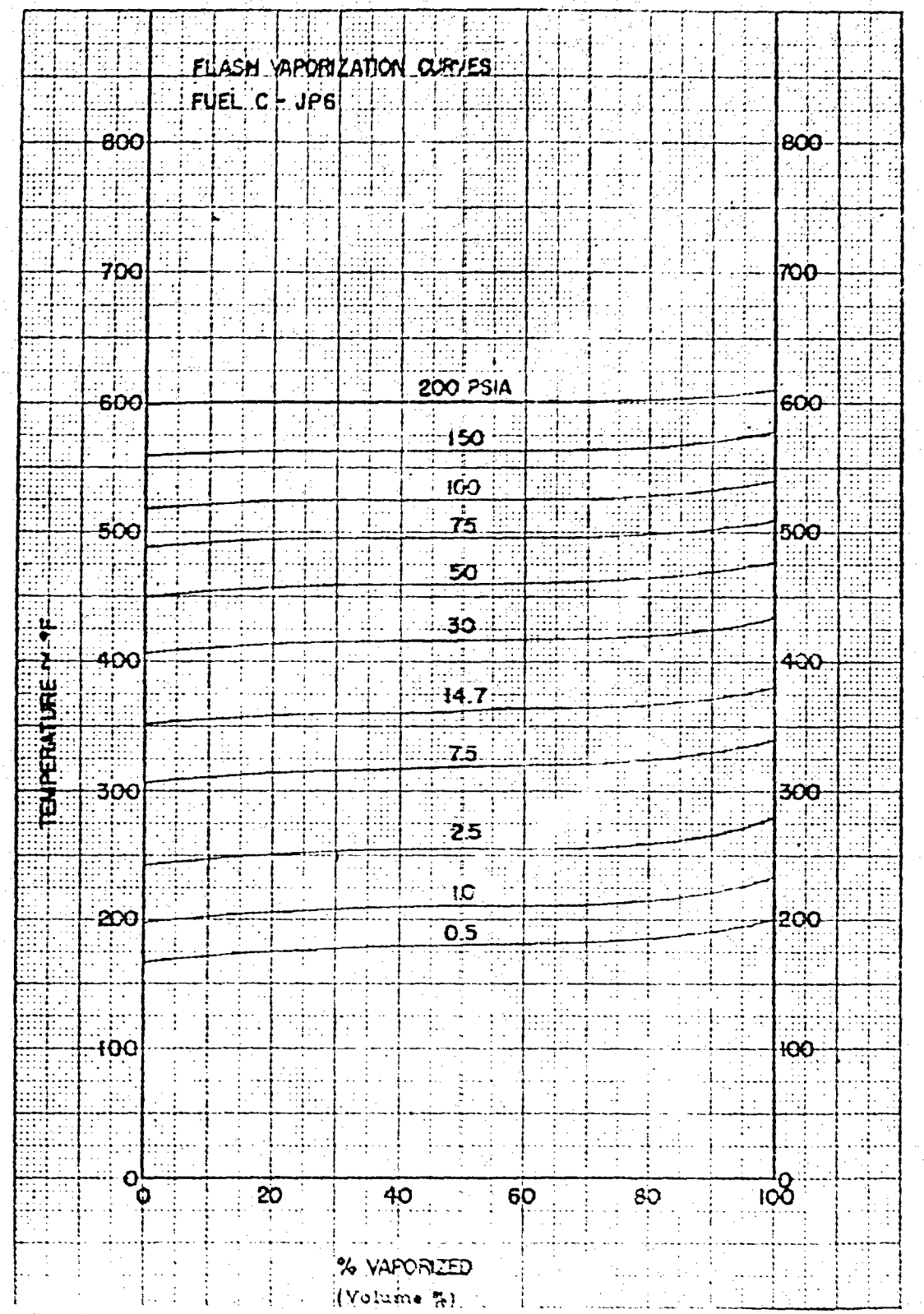

Figure 77 - Flash Vaporization Curves, Fuel C, JP-6.-H.

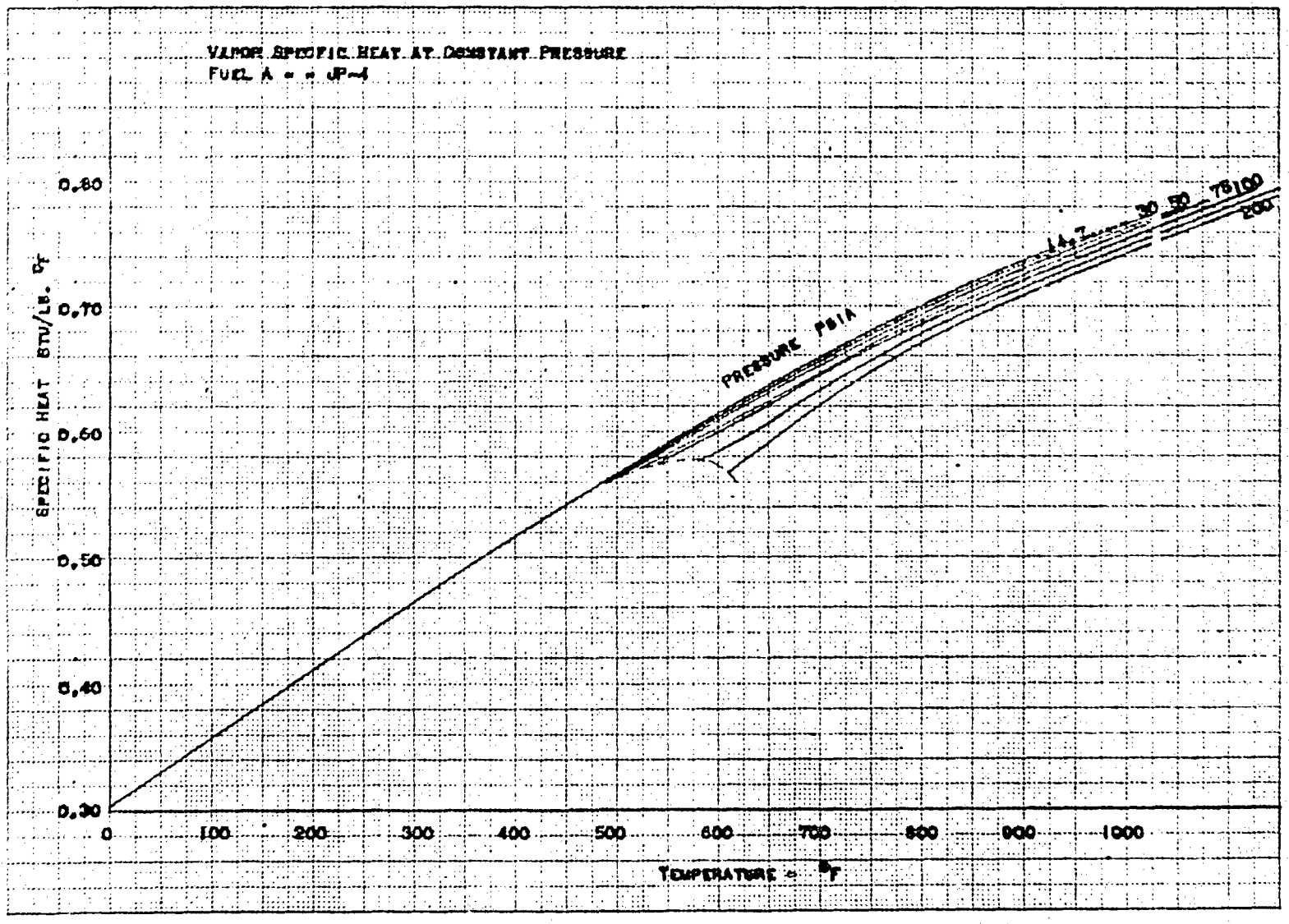

Figure 78 - Vapor Specific Heat at Constant Pressure, Fuel A, JP-4.

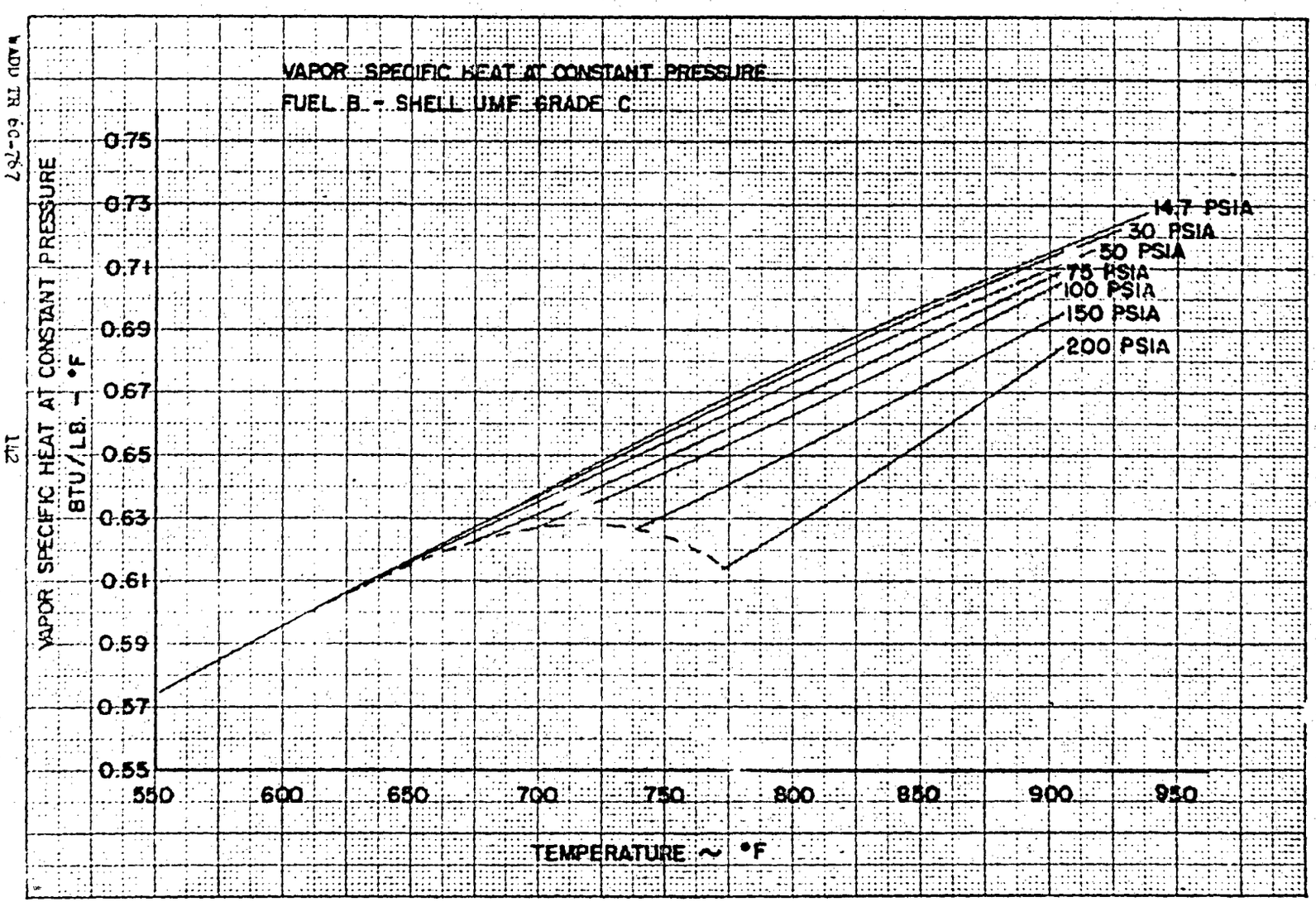

Figure 79 - Vapor Specific Heat at Constant Pressure, Fuel B, RJ-1.

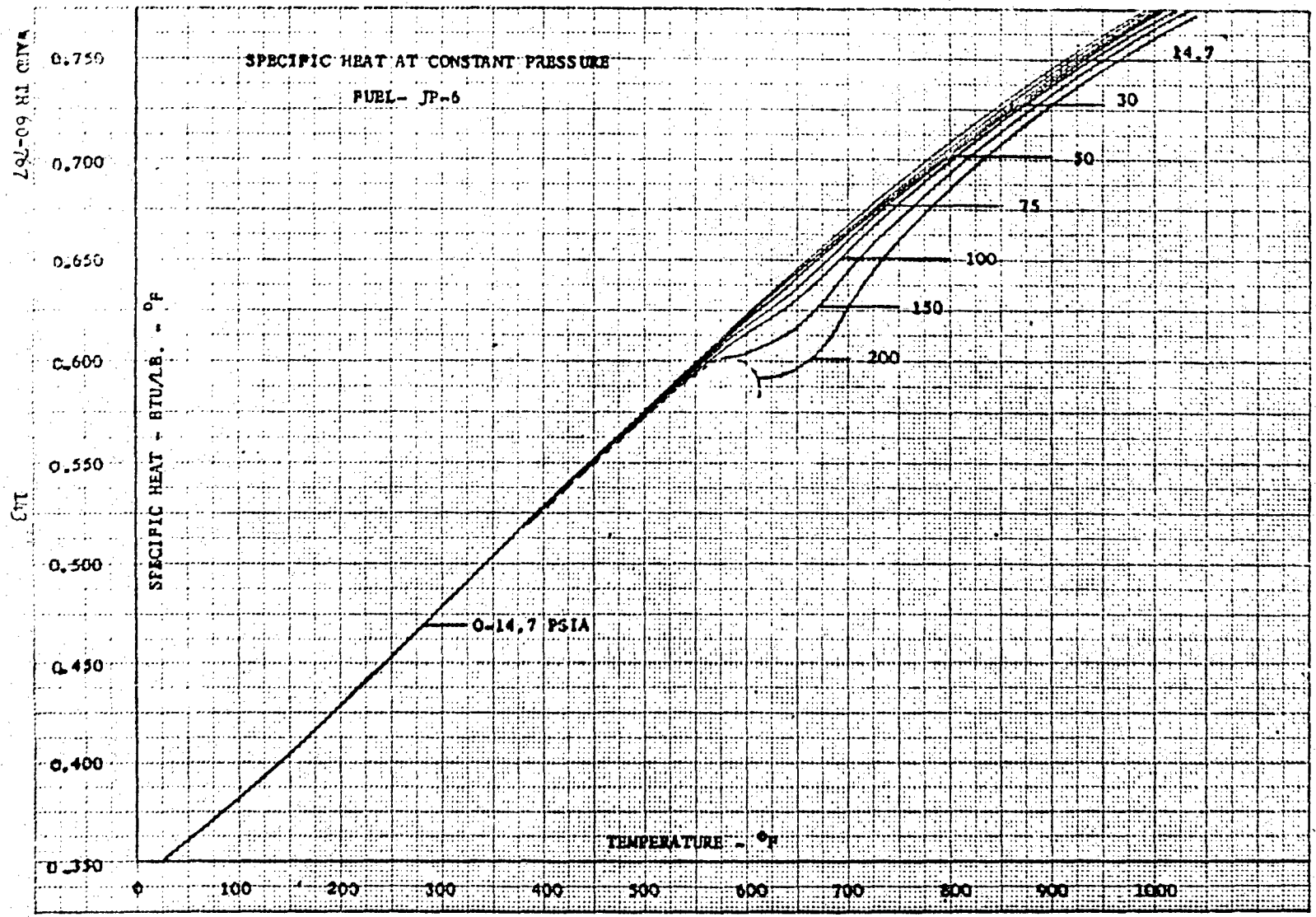

Figure 80 - Vapor Specific Heat at Constant Pressure, Fuel C, JP-6-H.

PART IV

VAPORIZATION CYCLE AND THERMODYNAMIC PROPERTIES OF DECALIN

INTRODUCTION

A report, Ing. Er. 232, a study of the thermodynamic properties of decalin was fourth in a series of Interim Reports. Each of the Interim Reports was offered in partial fulfillment of a research contract conducted under United States Air Force Contract AF 33(616)3729.

The results contained in Part IV of this report Ing. Er. 234, are concerned with the completed study of the thermodynamic properties of decalin.

OBJECTIVE

The purpose of this phase of the program was to determine the thermodynamic properties of commercial decalin. Emphasis was placed on the preparation of enthalpy-temperature and entropy-temperature diagrams. In addition to the thermodynamic properties such as specific heat, vapor pressure, and ASTM distillation; the effect of pressure on the applicable properties was to be determined.

SUMMARY

Decalin, or more precisely, decahydronapthalene, is a hydrocarbon. Decalin possesses many characteristics which make it excellent for use as an aircraft fuel, at elevated temperatures. It has a relatively high boiling point and should be thermally stable to temperatures approaching 800°F. The commercially available product consists, in the main, of a mixture of the cis and trans isomers along with a small quantity of impurities. The boiling range is approximately 30°F as determined by an ASTM distillation. (This represents a liquid temperature range of approximately 10°F.)

Some information is available in the literature References 1 through 7. Where feasible, this information was used to corroborate and complement experimental work done by the West Coast Laboratory of Thompson Products, Inc.

The thermodynamic charts presented in this report were derived in the manner described in Supplement III of this report, with a few minor modifications.

DISCUSSION

The test fuel, commercial decalin, was supplied by Wright Air Development Center (WADC). Figure 81 shows the distillation plot of the fuel as determined by ASTM method D-158-54. It should be realized that in the ASTM method, vapor temperatures are measured. This being the case, superheating of the vapors occurs quite easily, giving rise to the comparatively wide variation in boiling range. Although a distillation range of 32°F is shown on Figure 81 the boiling range using liquid temperatures as the criterion, shows a range of approximately 10°F.

The effect of temperature on specific gravity is shown in Figure 82. Up to approximately 400°F, the density decrease is linear with increasing temperature.

A plot of specific heat is shown in Figure 83. This plot is typical of the hydrocarbons and can be described mathematically by the expression $C_p = 0.351 + 6.2 \times 10^{-4} T$ where T is °F and C_p is BTU/lb°F.

Flash vaporization curves, See Figure 84 were determined using the method of Edmister and Pollock (Reference 9). It is readily evident that for all practical purposes, the test fuel can be considered pure.

Figure 85 is a vapor pressure plot. It should be noted that it also represents the bubble point curve on an Equilibrium Flash Vaporization (E. F. V.) plot.

The variation of vapor specific heat with temperature and pressure is illustrated in Figure 86. The calculations were made using the method described in Supplement III of this report with the exception that C_p° or the specific heat at one-atmosphere was evaluated from the enthalpy-temperature diagram shown in Figure 87. (See the Calculations of this Supplement for additional information).

The thermodynamic charts, Figures 87 and 88 were determined by methods described in detail in Part III of this report. These methods are abridged in the calculation section of Part IV.

Minimum reflux distillations were not performed on decalin due to the narrow boiling range. The E. F. V. plot shown in Figure 85 reflects quite closely what would occur during a minimum reflux distillation of a fuel with a narrow boiling range, such as decalin.

For the same reason i.e., narrow boiling range, the variation of condensed vapor density and molecular weight as functions of per cent distilled and pressure were not experimentally evaluated. The maximum variations in molecular weight would in all probability be ± 1% which is roughly the limit of our present test equipment.. Condensed vapor density would also show a maximum variation of ± 1%.

Figure 89 shows the heat of vaporization. The apparatus shown schematically in Figure 90 was used to determine the value at one atmosphere. The relationship of K. M. Watson (Reference 8) was used to evaluate the heat of vaporization over the range shown.

CALCULATIONS

The mathematics involved in the determination of the thermodynamic properties of decalin are summarized as follows:

$$dH = C_p dT \tag{1}$$

$$H_t = H_o + \int_{T^\circ}^{T^1} C_{p.L}\, dT + \Delta H_v + \int_{T^1}^{T^2} C_{p.g}\, dT \tag{2}$$

$$C_{p.g} = C^\circ_{p.g} - \frac{T}{J} \int_{P^\circ}^{P} \left(\frac{\partial^2 V}{\partial T^2} \right)_P dP \tag{3}$$

$$dS = \frac{C_p\, dT}{T} \tag{4}$$

$$S_t = S_o + \int_{T^\circ}^{T^1} \frac{C_{p.L}\, dT}{T} + \Delta S_v + \int_{T^1}^{T^2} \frac{C_{p.g}\, dT}{T} \qquad (5)$$

If further information is desired, the reader is referred to Part III of this report.

For decalin the $C_{p.L}$ value was determined from the relationship

$$C_p = 0.351 + 6.2 \times 10^{-4} T$$

The value of C_p° was determined by using equation (2) for the enthalpy of the saturated vapor line in the pressure range below 14.7 psia and a $C_{p.g}$ correlation given in Part V of this report.

$$\int_{T^\circ}^{T} C_p^\circ\, dT = H_t - \Delta H_v - H_o - \int_{T^\circ}^{T} C_{p.L}\, dT \qquad (6)$$

All the terms on the right hand side of equation (6) can be determined from the H-T chart. The $C_{p.g}$ value thus determined, in the low temperature, was checked against the uncorrected values given in the correlation. A suitable correction factor then was determined. This method was utilized in place of the UOP K correction factor which is not as suitable in an application concerned with pure compounds.

Heats of vaporization were determined both experimentally and by the use of correlations where data was not available.

REFERENCES

1. Schaafs, W. Sound Velocity and Constitution -- Parts I and II. Zeitschrift für Physikalische Chemie. Volume 194. 1954. pp 28-50.

2. Doldi, S. Physiochemical Properties of Hydronapthalenes. Annales Chemie Applicata. Volume 28. 1938. pp 454-462.

3. Unknown. Vapor Pressure of Cis and Trans Isomers. Journal of Physical Chemistry. Volume 14. 1940. pp 768-773. (USSR)

4. Gardner, G. S. and Brewer, J. E. Vapor Pressure of Commercial High Boiling Organic Solvents. Industrial and Engineering Chemistry. Volume 29. 1937. pp 179-181.

5. Parks, G. S. and Hatton, J. A. The Heat Capacities, Entropies and Free Energies of Cis-and Trans-Decahydronapthalene. Journal of the American Chemical Society. Volume 71. 1949. pp 2773-2775.

6. Seyer, W. F. and Walker, R. D. Physical Chemical Properties of Cis- and Trans-Decahydronapthalene. Journal of the American Chemical Society. Volume 60. 1938. pp 2125-2128.

7. Seyer, W. F. The Heat Capacity of Cis-and Trans-Decahydronapthalene and the Possible Existence of a λ -- Region for the Cis Form at 50.1-50.5°. Journal of the American Chemical Society. Volume 75. 1953. pp 616-621.

8. Watson, K. M. Industrial and Engineering Chemistry. Vol. 35. 1943. p 398.

9. Edmister, W. C. and Pollock, D. H. Phase Relations for Petroleum Fractions. Chemical Engineering Progress. Vol. 44, No. 12. December, 1948. pp 905-926.

SYMBOLS

C = specific heat

H = enthalpy

J = mechanical equivalent of heat

K = characterization factor

P = pressure

S = entropy

T = thermodynamic temperature

V = volume

SUBSCRIPTS AND SUPERSCRIPTS

L = saturated liquid

g = vapor

p = constant pressure

sv = saturated vapor

t = at temperature T

v = vaporization

o = base condition

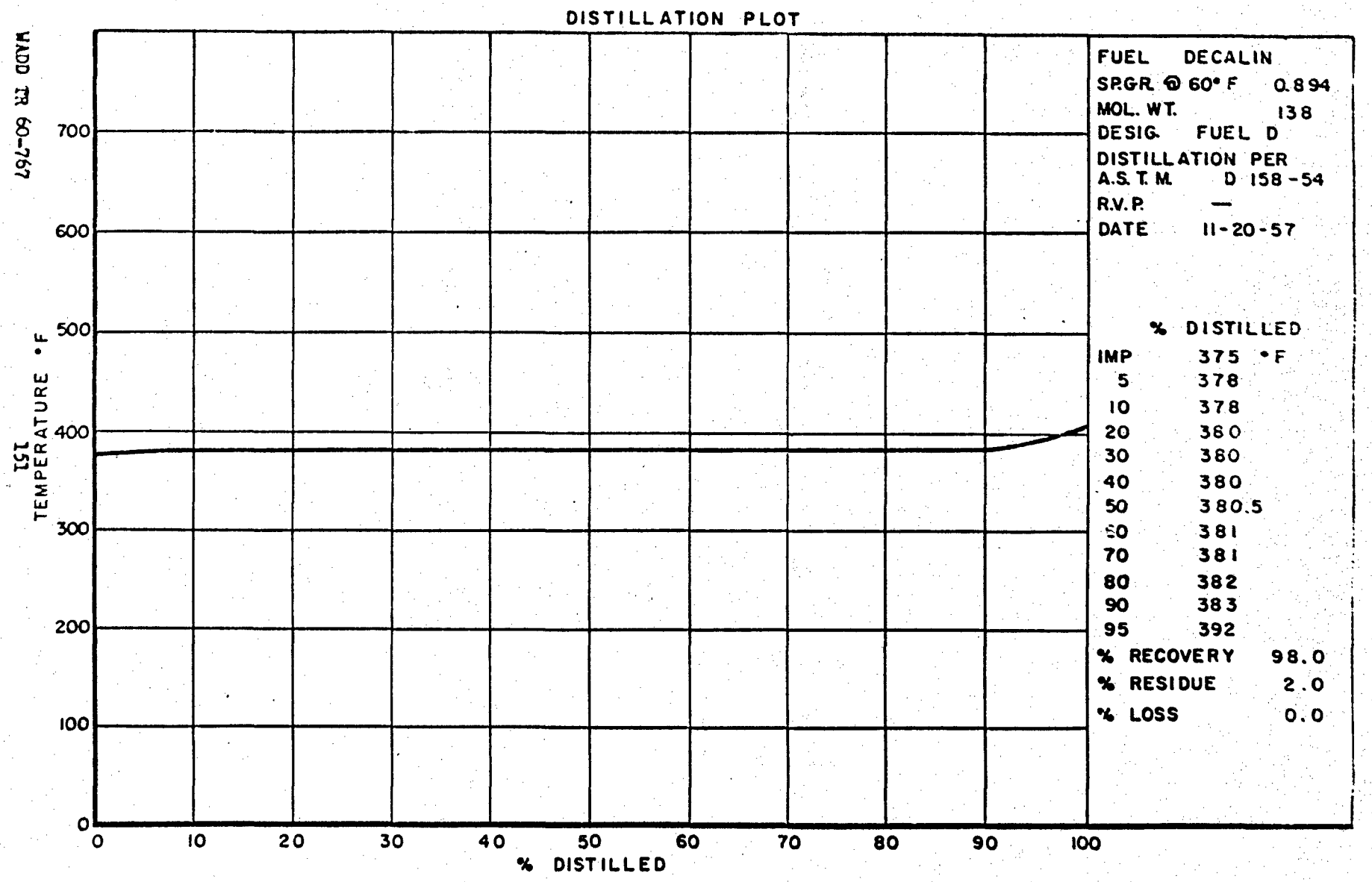

FIGURE 81. ASTM DISTILLATION PLOT

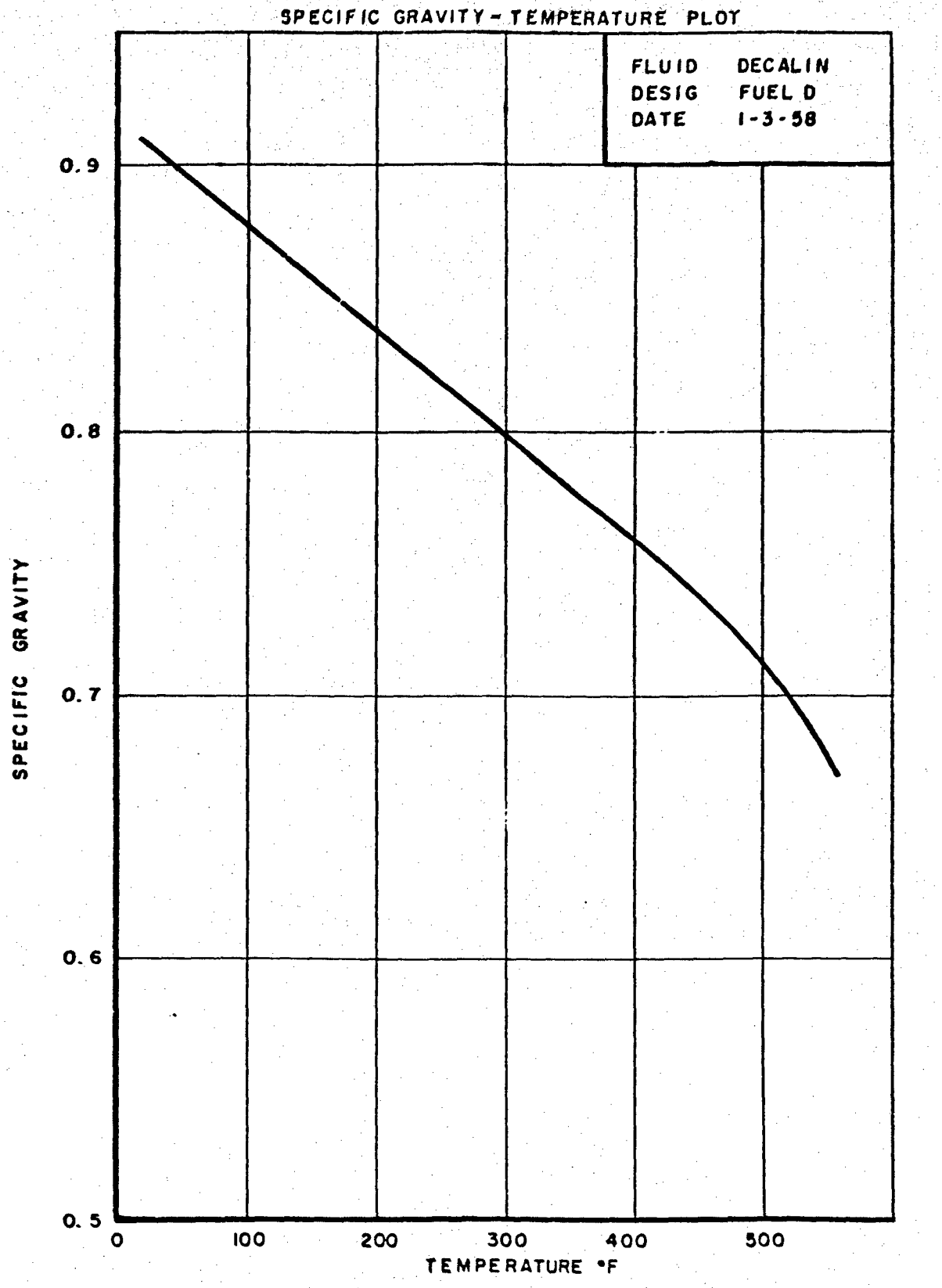

FIGURE 82. VARIATION OF SPECIFIC GRAVITY WITH TEMPERATURE

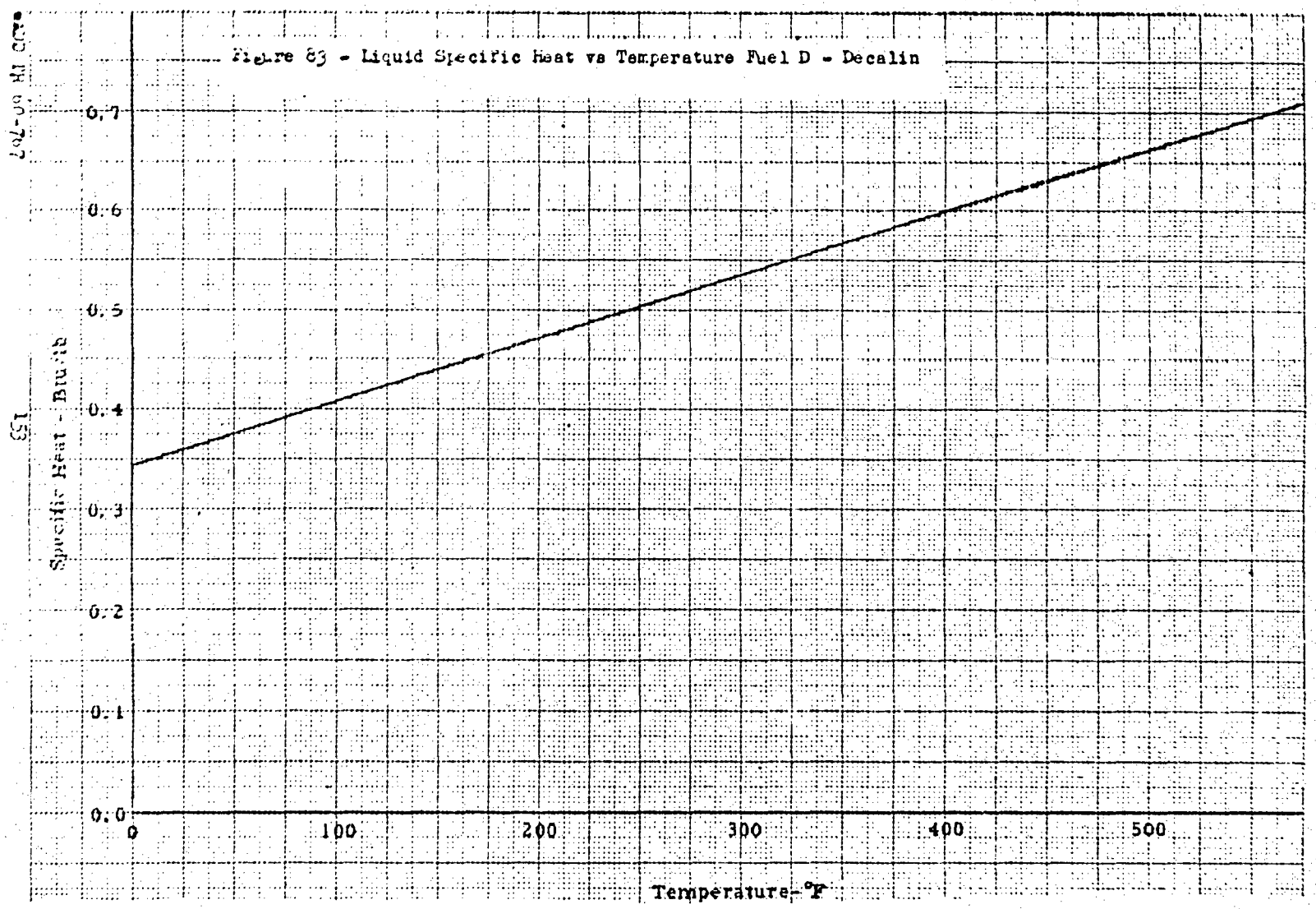
Figure 83 - Liquid Specific Heat vs Temperature Fuel D - Decalin
Specific Heat - Btu/lb
0.7
0.6
0.5
0.4
0.3
0.2
0.1
0.0
0
100
200
300
400
500
Temperature - °F

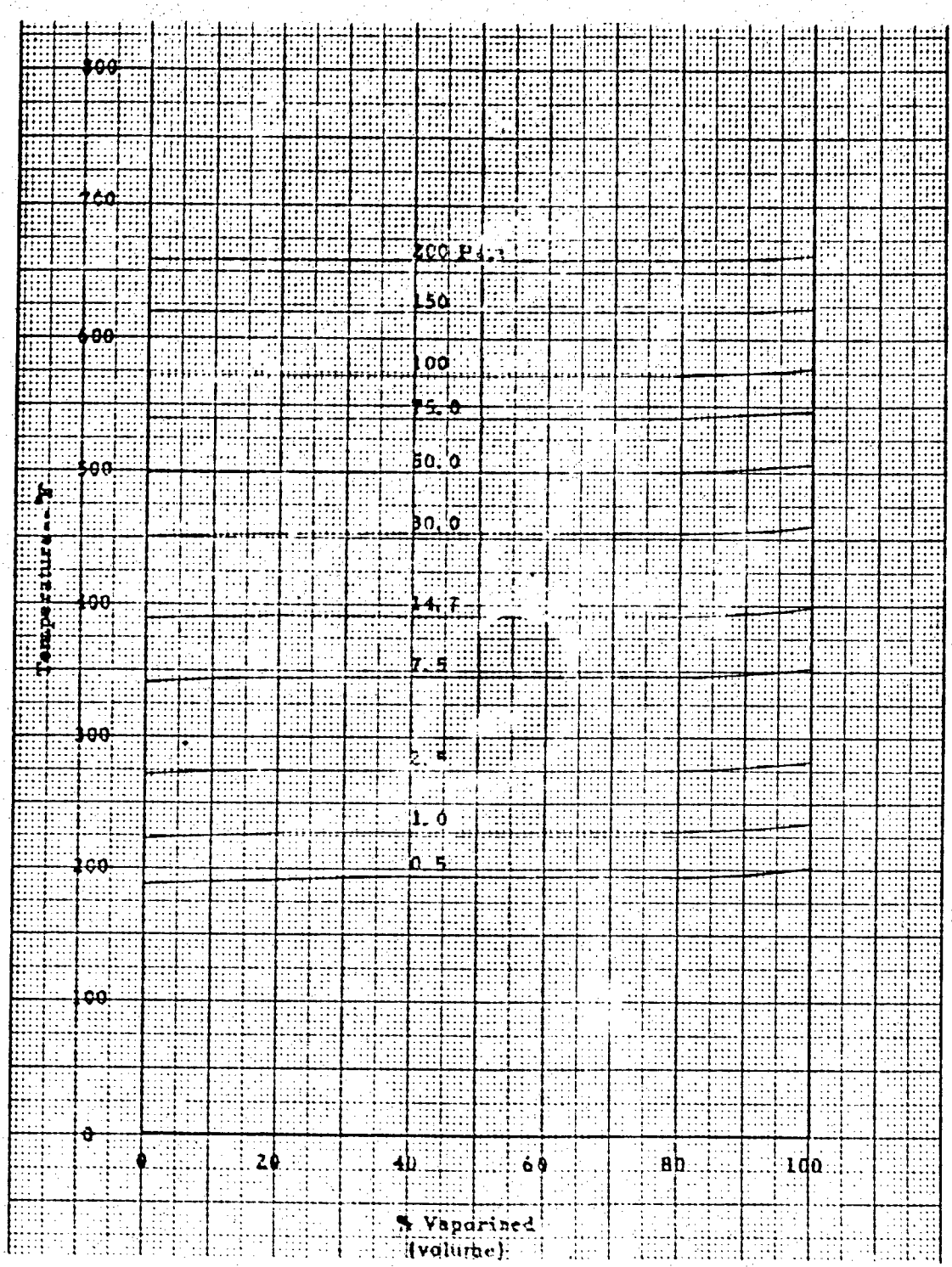

Figure 8. - Flash Vaporization Curves Fuel D - Decalin

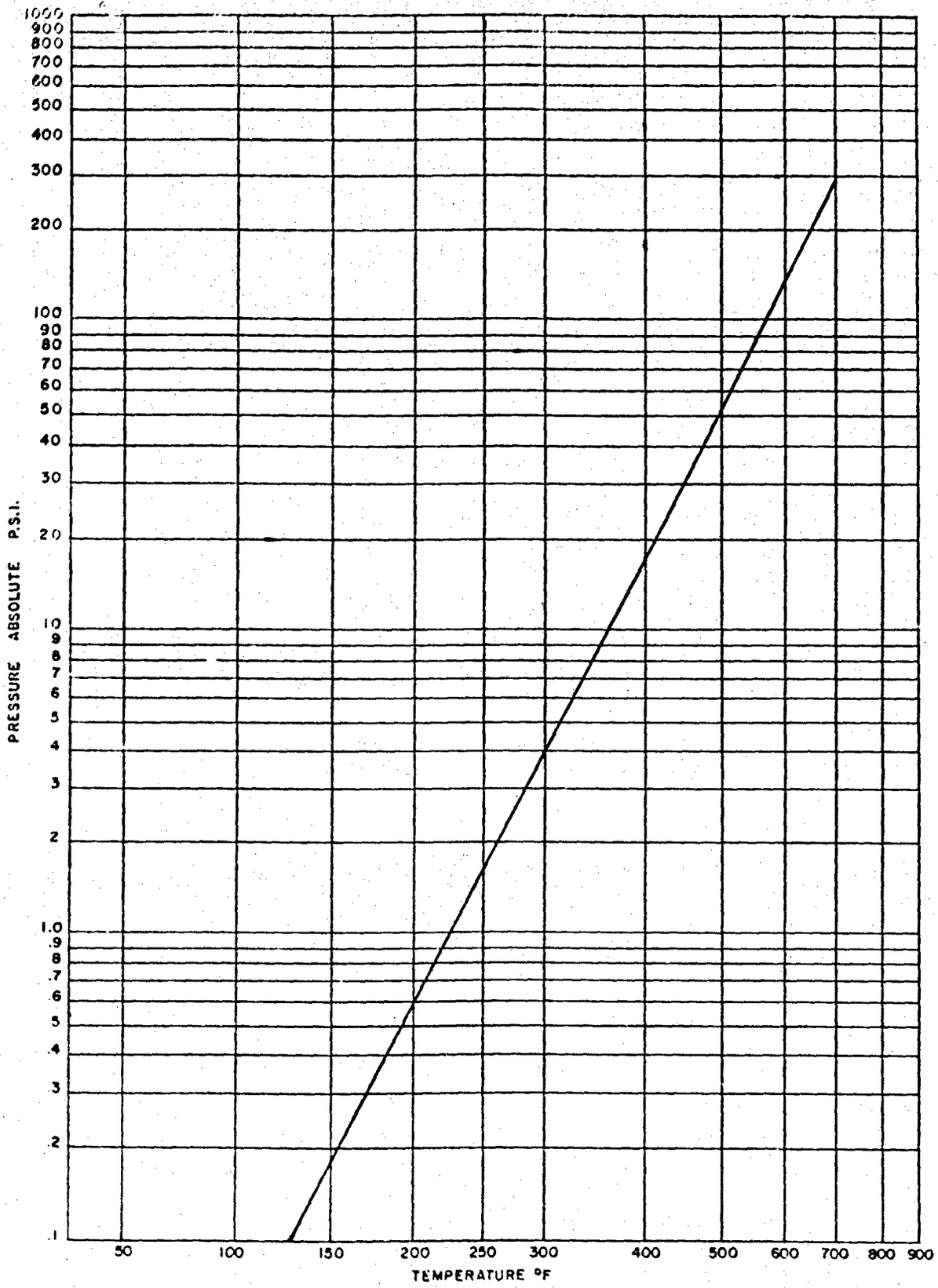

Figure 85 - Decalin Vapor Pressure Plot

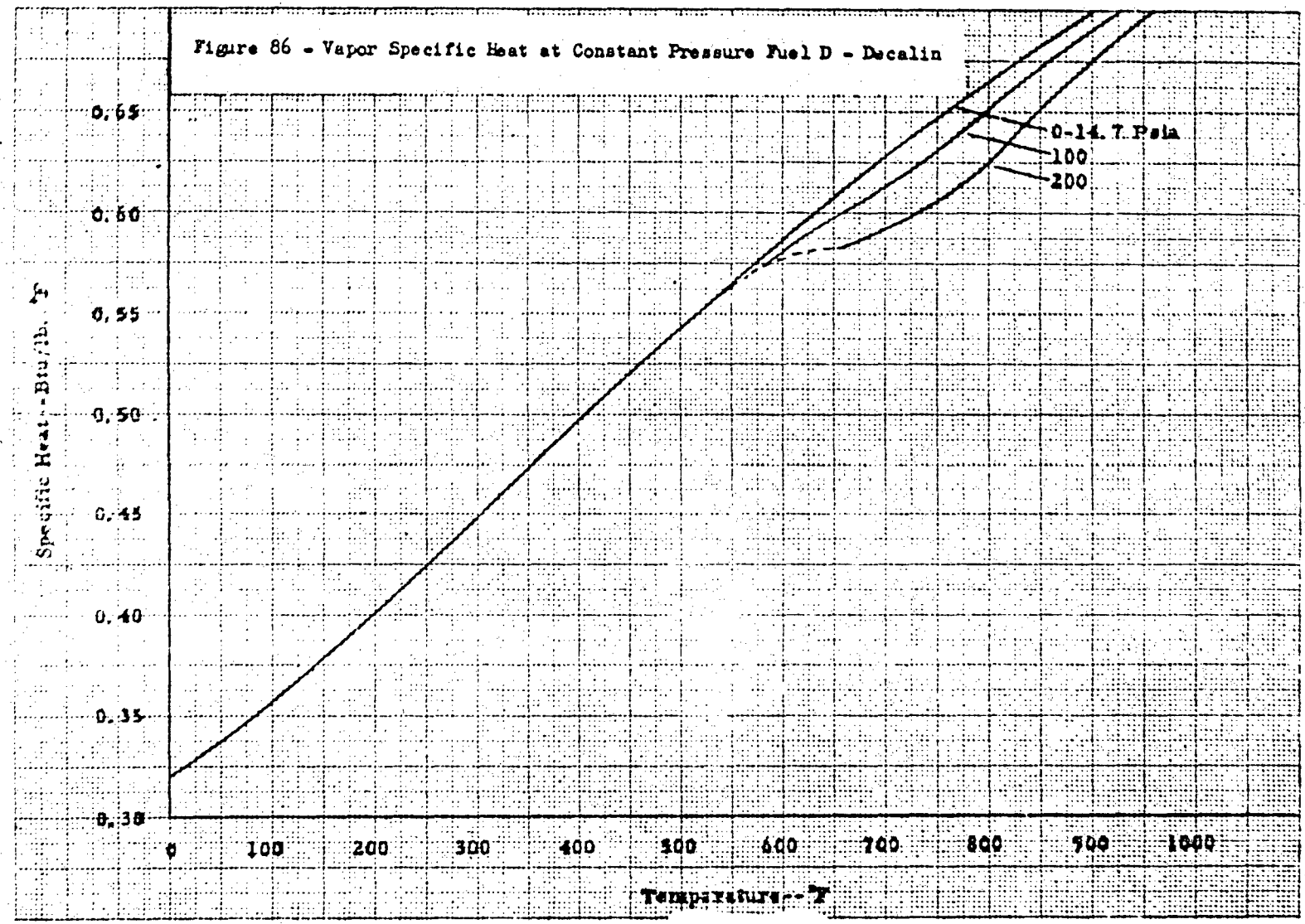
Figure 86 - Vapor Specific Heat at Constant Pressure Fuel D - Decalin
Specific Heat - Btu/lb. °F
0.65
0.60
0.55
0.50
0.45
0.40
0.35
0.30
0
100
200
300
400
500
600
700
800
900
1000
Temperature - °F
0-14.7 Psia
100
200

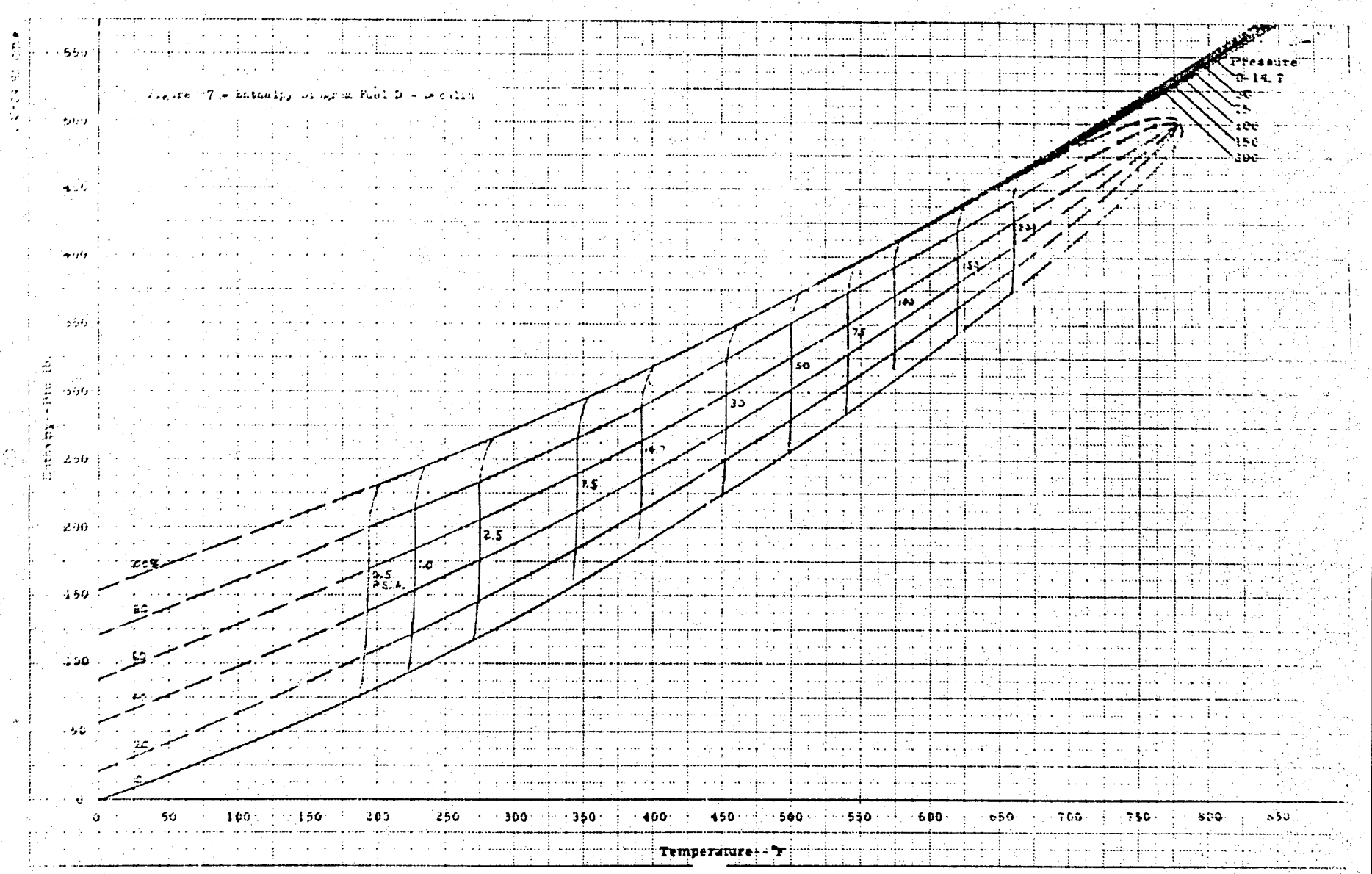
Pressure
0-14.7
25
100
150
200
2.5
50
75
100
150
200
0.5 P.S.I.
1.0
2.5
5.0
14.7
35
50
75
100
150
200
0
50
100
150
200
250
300
350
400
450
500
550
600
650
700
750
800
850
Temperature - °F

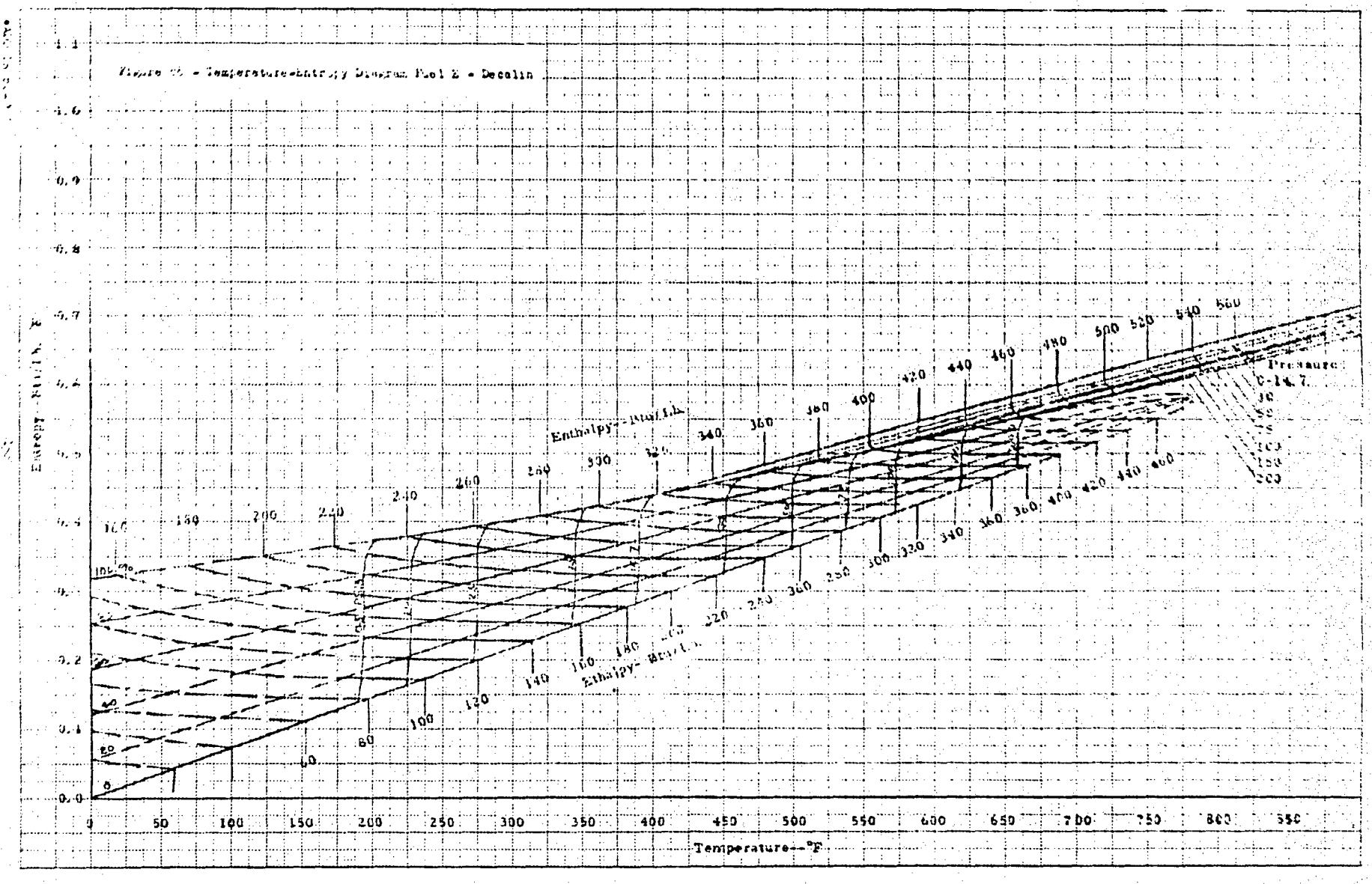
Entropy--Btu/F.P.
Temperature--°F
Enthalpy--Btu/F.P.
Pressure
0-14.7

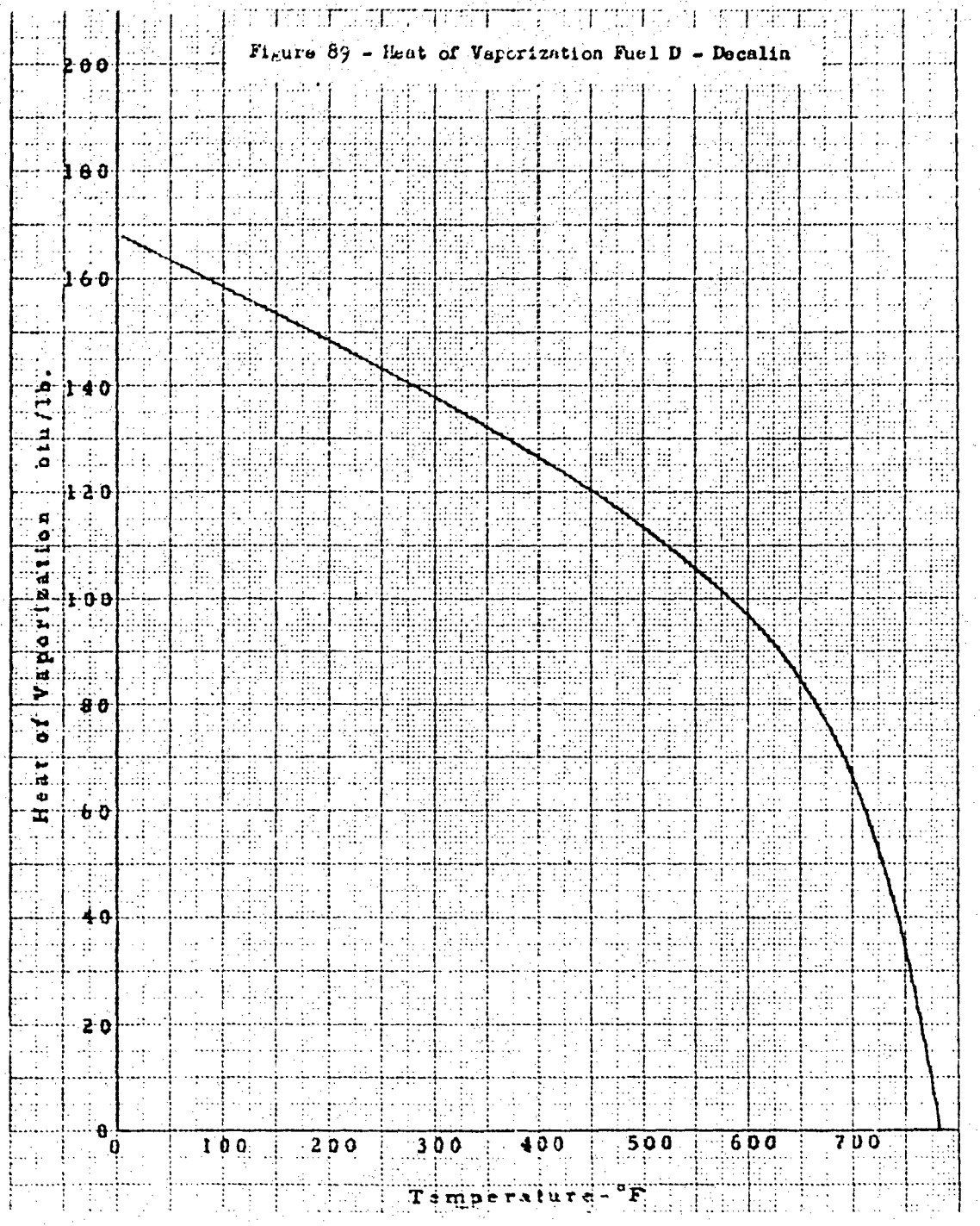

Figure 89 - Heat of Vaporization Fuel D - Decalin

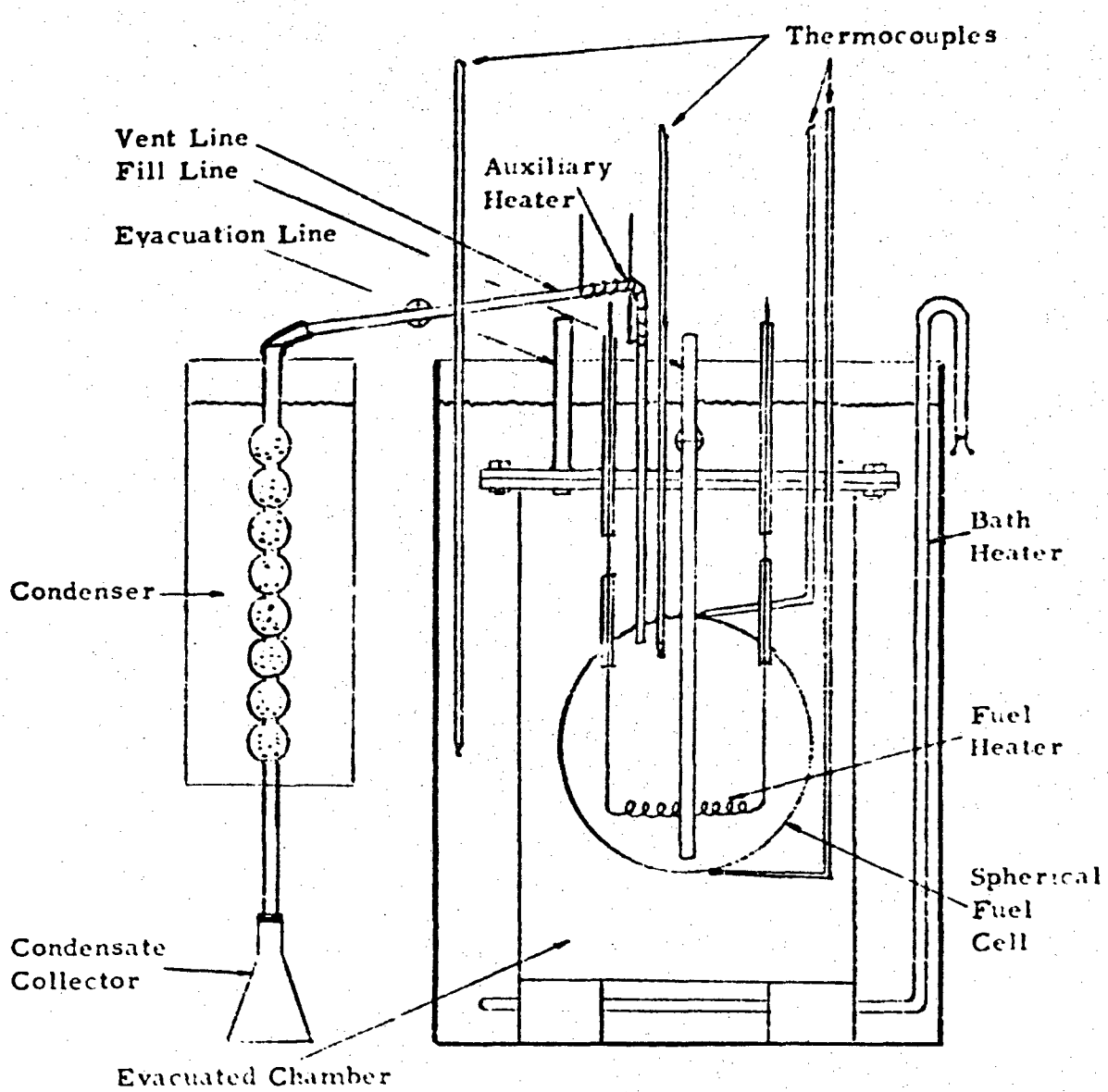

Note: Bath Agitator not shown

Figure 90 - Schematic of Heat of Vaporization Test Apparatus

PART V

GENERALIZED THERMODYNAMIC AND PHYSICAL PROPERTIES OF PETROLEUM TYPE FUELS

INTRODUCTION

There have been numerous articles in the literature describing various physiochemical properties of hydrocarbon fuels. For this information to be of practical use to industry however, it was desirable to have the material condensed and compiled in a form similar to a handbook. The data presented in this Part V fulfills such a function.

Much of the material contained in this report was previously issued as Section II of Engineering Report No. 206 prepared by the West Coast Laboratory of Thompson Products, Inc., Inglewood, Calif. ING. ER. 206 was one of a series of Interim Reports issued under United States Air Force Contract No. AF 33(616)3729. This revised Part V, contains empirically derived correlations necessary to determine generalized thermodynamic and physical properties of petroleum type fuels. The material contained in Part V completes the study of physiochemical properties of selected military fuels.

OBJECTIVE

This generalized study of thermodynamic and physical properties of petroleum type fuels was made for one basic purpose:

1) The determination of the availability of generalized thermodynamic information on hydrocarbon fuels, by means of a literature survey. Any reliable information obtained was to be presented as part of this report.

SUMMARY

All reliable information that could be obtained related to generalized thermodynamic and physical properties of petroleum type fuels is presented in this report. A compilation of charts and nomograms has been included. These charts and nomograms were obtained from an extensive literature survey. They present what is believed to be the most accurate correlations of the physical properties of hydrocarbon fuels available. In some cases, the original charts have been modified slightly to conform to the limitations of the fuel types being investigated.

DISCUSSION OF PHYSICAL DATA

The charts presented in this report are a collection of easily used correlations, covering the physical properties of petroleum-type aircraft fuels. The data, collected from an extensive literature survey, were compared and analyzed. A comparison of this data with available test data then was made. In cases where conflicting information was found, the source which best approximates the average has been presented.

In some instances a number of methods for predicting properties with varying degrees of accuracy are presented. In each case, greater fundamental knowledge of the fuel increases the accuracy of prediction.

All boiling points are referenced to an ASTM distillation.

The characterization factor used is defined as the product of the cube root of the molal average boiling temperature in degrees Rankine and the reciprocal of the specific gravity at 60°F.

$$K = \frac{\sqrt[3]{T_{\text{molal average}}}}{\rho_{60}}$$

The volumetric average boiling point, unless otherwise defined, shall be taken as the arithmetic mean of the 10, 30, 50, 70, and 90 per cent temperatures of an ASTM distillation.

$$\text{VABP} = \frac{T_{10} + T_{30} + T_{50} + T_{70} + T_{90}}{5}$$

DENSITY - GRAVITY RELATIONS

See Figure 91

Using this graph the specific gravity at 60°F can be converted to pounds per gallon, pounds per cubic foot, or degrees API.

VOLUMETRIC EXPANSION COEFFICIENT

See Figure 92

Shown in this chart is the correction factor for the effect of temperature on the liquid expansion of petroleum fractions. In general, the useful range of this chart is between 0°F and 300°F. The chart is also useful in determining volume changes due to temperature as an alternate to the use of density relationships. An example illustrating the use of this correction factor follows:

Problem:

Find the change in volume due to a temperature change of 75°F for 100 ft^3 of fuel which has a 40° API gravity.

Answer:

From chart $\alpha = 4.74 \times 10^{-4}\ ft^3/ft^3\ °F$

Change in Volume $\Delta V = \alpha \times \Delta T \times V_o$

$$\Delta V = 4.74 \times 10^{-4} \times 75 \times 100 = 3.555\ ft^3$$

VARIATION OF VAPOR PRESSURE WITH FUEL TEMPERATURE

See Figure 93

Vapor pressure as a function of volatility factor is presented on this chart. Volatility factor is defined as the sum of the ASTM volumetric average boiling point and the ASTM initial boiling point.

MOLECULAR WEIGHT AS A FUNCTION OF BOILING POINT AND GRAVITY

See Figure 94

The plot shown in this figure presents a means of estimating the average molecular weight of a petroleum fraction. The estimated deviation is plus or minus ten per cent.

GENERALIZED P-V-T RELATIONS
See Figure 95

The usefulness of this plot cannot be overemphasized. Nearly all deviations from ideality can be computed using the compressibility factor indicated. Pseudo-critical temperature and pressure should be used to determine reduced temperature and pressure. Information on pseudo-critical temperature and pressure will be found in paragraphs of this Supplement entitled 'Critical Properties'. Data on reduced conditions greater than those shown in Figure 95 can be obtained from the original source. (See Reference L)

LIQUID ENTHALPY - SPECIFIC HEAT NOMOGRAM
See Figure 96

If two conditions are known(temperature and specific gravity at 60°F), use of this information with the data plotted in Figure 96 will permit determination of the enthalpy (above 0°F), the specific heat, and the gravity of liquid fractions. The maximum error estimated for this plot is plus or minus five per cent.

PROPERTIES OF PETROLEUM FRACTIONS NOMOGRAM
See Figure 97

This nomogram is quite useful as a rapid means of determining the following properties of hydrocarbon fractions:

a. Gravity
b. Carbon/ Hydrogen weight ratio
c. UOP 'K' Characterization factor
d. Aniline point
e. Latent heat of vaporization
f. Molecular weight
g. Mean average boiling point

RELATIONSHIP BETWEEN VARIOUS AVERAGE BOILING POINTS
See Figure 98

A knowledge of the volumetric average boiling temperature is required to use the plot presented in this figure. The plot shows the relationship of the other average temperatures to the volumetric average boiling point.

HYDROGEN CONTENT OF HYDROCARBONS
See Figure 99

This plot presents: 1) a means of estimating the percentage of hydrogen in a hydrocarbon fraction to be used in determining heating properties and, 2) the solution of chemical reaction problems.

APPROXIMATE CHANGE OF SPECIFIC GRAVITY WITH TEMPERATURE
See Figure 100

This plot provides information concerning the variation of specific gravity with temperature in greater detail than the data plotted in Figure 90

CRITICAL PROPERTIES

Numerous correlations have been based on the theory of corresponding states; i. e., at the critical conditions, or proportion thereof, most substances behave in the same manner. For example, the physical properties of one substance at conditions having half the value of the criticals are the same as those of another substance at the corresponding condition (relative to its critical condition).

Reduced Pressure - Ratio of actual pressure to critical pressure (both absolute values)

Reduced Temperature - Ratio of actual temperature to critical temperature (both absolute values)

Mathematically

$$P_r = \frac{P}{P_c}$$

$$T_r = \frac{T}{T_c}$$

In the case of mixtures such as petroleum fractions, use of the actual critical properties shows poor correlation with the theory of corresponding states. To improve the correlation, a pseudo-critical state was conceived which can be related to the true critical conditions. Thus, in the case of petroleum fractions, the reduced conditions are given mathematically as follows:

$$P_r = \frac{P}{P_{pc}}$$ P_{pc} = pseudo critical pressure

$$T_r = \frac{T}{T_{pc}}$$ T_{pc} = pseudo critical temperature

In this Section plots of focal temperatures and pressures are shown. Although these functions have no theoretical basis, they have been derived as an empirical means of determining the equilibrium vaporization characteristics of petroleum fractions. The focal temperature and pressure represent the point on a Cox chart to which the various vaporization percentage lines converge. Knowledge of the equilibrium vaporization characteristics at some pressure plus the focal point, allows the estimation of the equilibrium vaporization characteristics at other pressure levels.

CRITICAL PRESSURE
See Figure 101

In order to determine the critical pressure, a knowledge of the ten-to-ninety per cent slope of the ASTM distillation curve along with the API gravity of the fraction is required. In the example shown on the plot, a fuel having a volume average boiling point of 276°F, a gravity of 60° and a ten-to-ninety per cent slope of 3.0 would have a critical pressure of 496 psia.

PSEUDO-CRITICAL PRESSURE
See Figure 102

This plot is straightforward, requiring a knowledge of only the mean boiling temperature and the API gravity.

FOCAL PRESSURE
See Figure 103

Knowledge of the critical pressure is required for the determination of focal pressure from this plot. The value obtained from the ordinate is the difference between the focal and critical pressures, thus

$$P_f = P_c + (P_f - P_c)$$

CRITICAL TEMPERATURE
See Figure 104

The difference between the critical temperature and the volumetric average boiling point is plotted as a function of gravity and volumetric average boiling point.

PSEUDO-CRITICAL TEMPERATURE
See Figure 105

This plot is straightforward, requiring a knowledge of only the molal average temperature and the API gravity.

FOCAL TEMPERATURE
See Figure 106

Knowledge of the critical temperature is required for the determination of focal temperature from this plot. The value obtained from the ordinate is the difference between the focal temperature and the critical temperature, thus

$$T_f = T_c + (T_f - T_c)$$

LIQUID SPECIFIC HEAT

The values of specific heat given in this Part V are shown in three plots. The difference in the plots is the degree of estimated accuracy. If K factor and API gravity are available, the plot shown in Figure 107 is recommended.

LIQUID SPECIFIC HEAT AS A FUNCTION OF K FACTOR AND GRAVITY AT 60°F.
See Figure 107

The estimated accuracy of this plot is ± two-per-cent for petroleum fractions similar to aviation fuels.

APPROXIMATE LIQUID SPECIFIC HEAT AS A FUNCTION OF GRAVITY.
See Figure 108

This plot is based on a 'rule of thumb' equation

$$C_p = \frac{0.41}{\rho}$$

and is a ± ten-per-cent estimate of specific heat for use in cases where only the density of a fraction at any temperature is known.

LIQUID SPECIFIC HEAT AS A FUNCTION OF GRAVITY AT 60°F
See Figure 109

The accuracy of this plot is estimated at ± five-per-cent for a wide variety of petroleum fractions. The plot is based on Cragoe's equation, Reference 2.

VAPOR SPECIFIC HEAT

There appears to be some differences between various investigators regarding the values of vapor specific heat. The specific heat plots presented herein represent the best average of eight correlations.

VAPOR SPECIFIC HEAT AT ONE-ATMOSPHERE PRESSURE
AS A FUNCTION OF K FACTOR AND GRAVITY AT 60°F
See Figure 110

If the gravity and K factor information is available, this plot should provide data with an accuracy estimate of plus or minus two per cent.

VAPOR SPECIFIC HEAT AT ONE-ATMOSPHERE PRESSURE
AS A FUNCTION OF GRAVITY AT 60°F
See Figure 111

In cases where only gravity is known, this plot can be used with a resulting accuracy approximating plus or minus five per cent.

PRESSURE CORRECTION FOR MOLAR HEAT CAPACITY OF GASES
See Figure 112

The effect of pressure on the specific heat at constant pressure is given on this chart. The correction factor is the difference between the specific heat at a pressure sufficiently low for the gas to act ideally and the specific heat at the pressure in question (with both quantities in molar units). The correction is added to values obtained from Figures 110 or 111 after making the proper unit conversion.

GENERALIZED HEAT CAPACITY DIFFERENCES
See Figure 113

The difference between the specific heat at constant pressure and constant volume is shown on this chart. Here again the quantities are in molar units.

HEAT OF VAPORIZATION

The term heat of vaporization is quite ambiguous when applied to mixtures. The usual definition of heat of vaporization is the heat required to vaporize a unit quantity of liquid at the boiling point. This definition requires some modification for use with a mixture having a range of boiling points rather than a single boiling point. The values given in the plots in this section are the heats of vaporization assuming that the whole material boiled at the mean-average-boiling-point of an ASTM distillation.

In effect, the heat of vaporization, as referenced in this discussion, is the heat required to vaporize a unit quantity at the mean average temperature with varying pressure. The H_v obtained in this manner is less than the heat required to vaporize a unit quantity at one-atmosphere. The difference between these H_v values increases as the boiling range becomes wider.

Heat of vaporization of a fuel as presented here can be viewed also as the difference in enthalpy at constant temperature between the zero and the one-hundred per cent vaporized curves. If the enthalpy envelope is available, the heat of vaporization at constant pressure can be determined by obtaining the difference between the enthalpy at the one-hundred-per-cent-vaporized line (at the end point temperature) and the zero-per-cent-vaporized line (at the initial boiling point).

HEAT OF VAPORIZATION AT ONE-ATMOSPHERE PRESSURE AND MEAN AVERAGE BOILING POINT

See Figure 114

The plot can be used if the mean average boiling point is known and the molecular weight or the API gravity. It is recommended that the correlation be based on experimental molecular weights. See the plot illustrated in Figure 97 for an additional correlation.

LATENT HEAT NEAR THE CRITICAL TEMPERATURE

See Figure 115

At the critical temperature, the latent heat of vaporization is zero. The latent heat of vaporization changes abruptly in a few degrees below the critical (approximately 50 BTU/lb. in 50°F). The plot presented covers only the area near the critical temperature.

In order to use this plot, a knowledge of the critical temperature and characterization factor is required. The family of curves shown on the plot are for critical temperatures of 450, 500, 550, 600, 650, 700, 750, 800, 850, 900, 950, and 1000°F. Interpolation for curves having critical temperatures at the values between the limits of 400°F to 1000°F can be made because the latent heat is zero at the critical temperature. For example:

> The heat of vaporization at 650°F, of a fuel having a K factor of 11.0 and a critical temperature of 675°F, would be 54.5 BTU/lb.

HEAT OF VAPORIZATION CORRECTION DUE TO TEMPERATURE

See Figure 116

This correction is to be applied to the heat of vaporization data obtained from the Nomogram shown in Figure 97 or the Nomogram shown in Figure 114

For example:

> A fuel having a mean average temperature of 400°F, a critical temperature of 720°, and a molecular weight of 150, would have a heat of vaporization of 122.5 BTU/lb. (See the Nomogram shown in Figure 97) If the pressure were increased such that, at the new pressure, the mean average temperature was 500°F, then the latent heat would have to be corrected. From the plot shown in Figure 116

$T_c - T_k = 720 - 400 = 320°F.$ $T_c - T = 720° - 500° = 220°F.$

The heat of vaporization at 500°F is

$$H = \lambda / \lambda_k \times H_v @ 1 \text{ atm}$$

$$H = (0.86) \times (122.5) = 105.35 \text{ BTU/lb.}$$

ENTHALPY

The heat-content property of petroleum fractions is obtained by integrating the specific heat equation over the temperature range desired. Normally the datum is taken as H = 0 at 0°F.

HEAT CONTENT OF PETROLEUM FRACTIONS
See Figure 117

In the plot shown in Figure 117 the enthalpy of the liquid is assumed to be zero at 0°F. A typical example is illustrated in this plot which shows the method for determining corrections due to K factors other than 12.0 and pressures above one-atmosphere.

HEAT OF COMBUSTION

Both gross and net heats of combustion plots are illustrated in the figures applicable to this topic. The difference between the gross and net heat is the heat of vaporization of the water formed due to combustion of the hydrogen present. Only the net heat is of practical significance in normal usage.

GROSS HEATS OF COMBUSTION
See Figure 118

Knowledge of the API gravity and K factor gives the gross heating value.

NET HEATS OF COMBUSTION
See Figure 119

The plot of this figure is similar to the plot shown in Figure 118

VISCOSITY

Both vapor and liquid viscosity correlations are included in the discussion of this topic. Liquid viscosities are given at 100°F and 210°F, the standard temperatures in general use by the petroleum industry. For values at other temperatures, graphical extrapolation or interpolation on the special viscosity chart paper of the Bureau of Standards is recommended.

ABSOLUTE VISCOSITY OF HYDROCARBON VAPORS AT ONE-ATMOSPHERE

See Figure 120

Vapor viscosities in centipoise are shown as a function of molecular weight in this figure.

KINEMATIC VISCOSITY OF HYDROCARBON VAPORS AT ONE-ATMOSPHERE

See Figure 121

In this figure, vapor viscosities in centistokes are chosen as a function of molecular weight.

VISCOSITY OF GASES AT HIGH PRESSURE

See figure 122

The effect of pressure on the visco..ty ratio (i.e., ratio of viscosity at pressures above one-atmosphere to that at one-atmosphere) is shown as a function of reduced pressure in this Figure. In correlations of this type, the pseudo-critical pressure should be used for the determination of reduced pressure.

RELATION OF VISCOSITY AT 100°F TO CHARACTERIZATION FACTOR

See Figure 123

The average boiling point shown by the plot in this Figure is the molal average. Use of this plot is straightforward. Knowledge is required of the API gravity and either the molal average boiling point or the K factor; viscosity can then be determined.

RELATION OF VISCOSITY AT 210°F TO CHARACTERIZATION FACTOR

See Figure 124

The average boiling point, as illustrated in this Figure, is the molal average. The factors applicable to the plot shown in Figure 123 also apply to this plot. Knowledge is required of the API gravity and either the molal average boiling point or the K factor; viscosity can then be determined.

APPENDIX I

The correlations found in this Appendix were compiled and cross checked in part by the empirical relationships outlined in the following paragraphs.

LIQUID SPECIFIC HEAT

1. Watson, Nelson and Murphy. Industrial and Engineering Chemistry. Vol. 25. 1933, p 880.

$$C_p = 0.6811 - 0.308\rho + T\,(0.000815 - 0.000306\rho)\,(0.055K + 0.35)$$

2. Cragoe. Bureau of Standards Misc. Publication No. 97. 1929.

$$C_p = \frac{1}{\rho^{0.5}}\,(0.388 + 0.00045T)$$

3. Fortsch and Whitman. Industrial and Engineering Chemistry. Vol. 18. 1926. p 795.

$$C_p = \frac{(210 - \rho)\,(T + 670)}{2030}$$

4. Shaff. Chemical Processing. March 1955. p 90.

$$C_p = \frac{1}{\rho^{0.5}} + 0.000389T - 0.0229$$

5. Unknown

$$C_p = \frac{0.41}{\rho_x}$$

ρ_x = Specific Gravity at the temperature the specific heat is desired.

6. Watson and Fallon. National Petroleum News, June 7, 1944. p R372.

$$C_p = \left[0.355 + 1280 \times 10^{-6}\,(°API)\right] + \left[503 + 1.17\,(°API)\right] \times 10^{-6} T$$

7. Goldstern. Petroleum Zeitschrift. Vol. 32 No. 36. 1936. p 1.

$$C_p = \frac{0.402 + 0.00045\,(T - 32)}{\rho^{0.5}}$$

8. Mullins. Journal Institute of Petroleum. Vol. 33. 1947. p 44.

$$C_p = 0.0009T - 0.499\rho + 0.856$$

where T is in °Centigrade

9. Gaucher. Industrial and Engineering Chemistry. Vol. 27. 1935. p 57.

$$C_p = \frac{0.623 - 0.0187\,(T)^{\frac{1}{3}}}{\rho^{3/2}} + \frac{0.000355\,(T)}{\rho^{3}} + 0.00045\,(T - 492)$$

where

T is molal average in °R .

10. Gaucher. Industrial and Engineering Chemistry. Vol. 27. 1935. p 57.

$$C_p = 1.323 - 0.2005K + 0.0107K^2 + 0.00045\,(T - 32)$$

SPECIFIC HEAT OF VAPORS

1. Bahlke and Kay. Industrial and Engineering Chemistry. Vol. 21. 1929, p. 942.

$$C_p = \frac{(4.0 - \rho)\,(T + 670)}{6450}$$

2. Bahlke and Kay. Industrial and Engineering Chemistry. Vol. 21. 1929. p 942.

$$C_p = (4.0 - \rho) \times (0.109 + 0.00014T)$$

where T is in °Centigrade.

3. Watson and Fallon. National Petroleum News. 1944. p R372.

$$C_p = (0.0450K - 0.233) + (0.440 + 0.0177K \times 10^{-3}T) - 0.153 \times 10^{-6} T^2$$

4. Cragoe. Bureau of Standards Misc. Publication No. 97. 1929.

$$C_p = \frac{0.388 + 0.00045\ T}{\rho^{\frac{1}{2}}} - \frac{0.09}{\rho}$$

5. Sweigert and Beardsley. Experimental Station Bulletin 2, Georgia School Technological Engineering. 1938.

$$C_p = \frac{8.68 + 0.0889\ (T + 460)}{MW}$$

The kerosene vapors having molecular weights near 170 in the temperature range -60 to 650°F.

6. Watson and Nelson. Industrial and Engineering Chemistry. Vol. 25. 1933. p 880.

$$C_p = \frac{(4.0 - \rho)\ (T + 670)\ (0.12K - 0.41)}{6450}$$

HEAT OF VAPORIZATION

1. Kistiakowsky, Zeitung Physik and Chemische, Vol. 107, 1923, p 65.

$$H_v = \frac{7.58\,T_b + 4.56\,T_b \log T_b}{MW}$$

where

T_b = mean average boiling point.

2. Cragoe, Bureau of Standards Misc. Publication No. 97, 1929.

$$H_v = \frac{1}{\rho}\ (110.9 - 0.09T) \times \frac{5}{9}$$

3. Trouton equation

$$H_v = \frac{20.5\,T}{MW}$$

where

T is the molal average boiling point in Kelvin

4. Clausium Clapeyron equation

$$H_v = \frac{dP}{dT} \times (V_g - V_L) \times T$$

where

$\frac{dP}{dT}$ is the change in vapor pressure with temperature;

$(V_g - V_L)$ is the vapor - liquid volume difference per mole

T is the temperature in absolute units.

5. Goldstern. Petroleum Zeitschrift. Vol. 32, No. 36. 1936. p 1.

$$H_v = \frac{60 - 0.05\,(T-32)}{\rho}$$

HEAT OF COMBUSTION

1. Cogliano and Jessup. Bureau of Standards Report 2348. March 18, 1953.

$$Q \text{ net} = 17,608 + (0.2054\ A \times \rho) - 7.245 \times 10^{-6} (A \times \rho)^2 - 140(\%s)$$

where

A = aniline point °F

%s = per cent sulphur

2. Cogliano and Jessup. Bureau of Standards Report 2348. March 18, 1953.

$$Q \text{ net} = 22,130 + \frac{2,560}{\rho - 1.53}$$

3. Rothberg and Jessup. Industrial and Engineering Chemistry. Vol. 43. 1951. p 981.

$$Q = 17,944.9 + 0.1043 \times (A \times \rho)$$

4. Fein, Nelson and Sherman. Industrial and Engineering Chemistry. Vol. 45. 1953. p 610.

$$Q \text{ net} = 17,145.9 + 0.5195\ (A \times \rho) - 0.69113 \times 10^{-4} (A \times \rho)^2 T$$

$$0.47772 \times 10^{-8} (A \times \rho)^3 - 0.1235 \times 10^{-12} (A \times \rho)^4.$$

5. Fein, Nelson and Sherman. Industrial and Engineering Chemistry. Vol. 43. 1951. p 981

$$Q \text{ net} = 8,505.4 + 846.81K + 114.92\ \rho + 0.121865 - 9.951K\ \rho.$$

CRITICAL PROPERTIES

1. Roess. Journal of the Institute of Petroleum Technology. Vol. 22. 1936. p 665.

$T_{critical} = 202.7 + 1.591a - 6.29 \times 10^{-4} a^2$

where $a = \rho \times$ (T volumetric average + 100)

SYMBOLS

C	=	Specific Heat BTU/lb °F.
H	=	Enthalpy - BTU/lb
J	=	Mechanical equivalent of heat
K	=	Characterization factor
MW	=	Molecular Weight
P	=	Pressure - psia
Q	=	Heat of Combustion BTU/lb
R	=	Gas constant - 10.73 psia, ft^3/°R, lb-mole
S	=	Entropy - BTU/lb °F.
T	=	Temperature - °F or °R
V	=	Volume - ft^3
Z	=	Compressibility factor
α	=	Volume residual

Δ = Increment

λ = Heat of vaporization - BTU/lb*

ρ = Density at 60°F.

SUBSCRIPTS AND SUPERSCRIPTS

c = Critical

k = Normal mean average temperature

L = Saturated liquid

m = Mean

p = Constant pressure

r = Reduced conditions

sv = Saturated vapor

t = Total

v = Vaporization

0 to 20, 20 to 40, etc. = 0-20%, 20-40% Fractions

1 = Initial condition

2 = Final condition

*H_v Also used to indicate heat of vaporization.

REFERENCES

The source of plots illustrated in Part V Figures are listed below.

1. Maxwell, J. B. Data Book on Hydrocarbons, First Edition, D. Van Nostrand Company, Inc., Princeton, New Jersey, March, 1951. pp 21, 41, 72, 73, 148, 174, 175, 177.

2. Cragoe, C. S. Bureau of Standards, Misc. Publication No. 97, Nov. 9, 1929.

3. Barnett, Henry C. and Hibbard, Robert R. Properties of Aircraft Fuels, National Advisory Committee for Aeronautics Technical Note 3276, Lewis Flight Propulsion Laboratory, Cleveland, Ohio. August 1956. p 78.

4. Bureau of Standards Data.

5. Findl, E. and Edwards, H. Vaporization Cycle and Thermodynamic Properties of Jp-4, RJ-1 and JP-6-H. ING. ER 234. Study of Physiochemical Properties of Selected Military Fuels. Thompson Products, Inc. Part V, Supplement V. December 1958.

6. Winn, F. W. Physical Properties by Nomogram. Petroleum Refiner. Feb. 1957. p 157.

7. Watson, K. M. and Nelson, W. L. Industrial and Engineering Chemistry Vol. 25. 1933, p880; Vol. 29, 1937, p 1408.

8. Hougen, O. A. and Watson, K. M. Chemical Process Principles Charts. John Wiley and Sons, Inc., New York, N. Y. April 1956.

9. Nelson, W. L. Oil and Gas Journal, January 27, 1938. p 184.

10. Edmister, W. C. and Pollock, D. H. Chemical Engineering Progress, Vol. 44 No. 12. pp 911, 924, 925.

11. Holcomb and Brown. Industrial and Engineering Chemistry. Vol. 24, 1932, p 210; Vol. 18, 1926, p 795.

12. Edmister, W. C. The Petroleum Engineer. Dec. 1950. p C-16.

13. Edmister, W. C. Petroleum Refiner. Nov. 1948. p C-16.

14. Nelson, W. L. Oil and Gas Journal. July 26, 1947. p 254.

15. Watson, K. M. Industrial and Engineering Chemistry, Vol. 35, 1943, p 398.

16. Fine, R. S., Wilson, H. I. and Sherman, J. Net Heat of Combustion of Petroleum Hydrocarbons. Industrial and Engineering Chemistry, Vol. 45, 1953, p 610.

17. Bell, H. S. American Petroleum Refining. Copyright 1945, Third Edition, D. Van Nostrand Company, Inc. Princeton, New Jersey. pp 54, 55.

18. Rothenberg, A. J., Edwards, H., Woodell, E. W., Volatility Characteristics of Eight Types of Turbine Fuel at Temperatures to 450°F., West Coast Research and Development Laboratory, Report No. ING. ER. 176, Thompson Products, Inc., June 15, 1954.

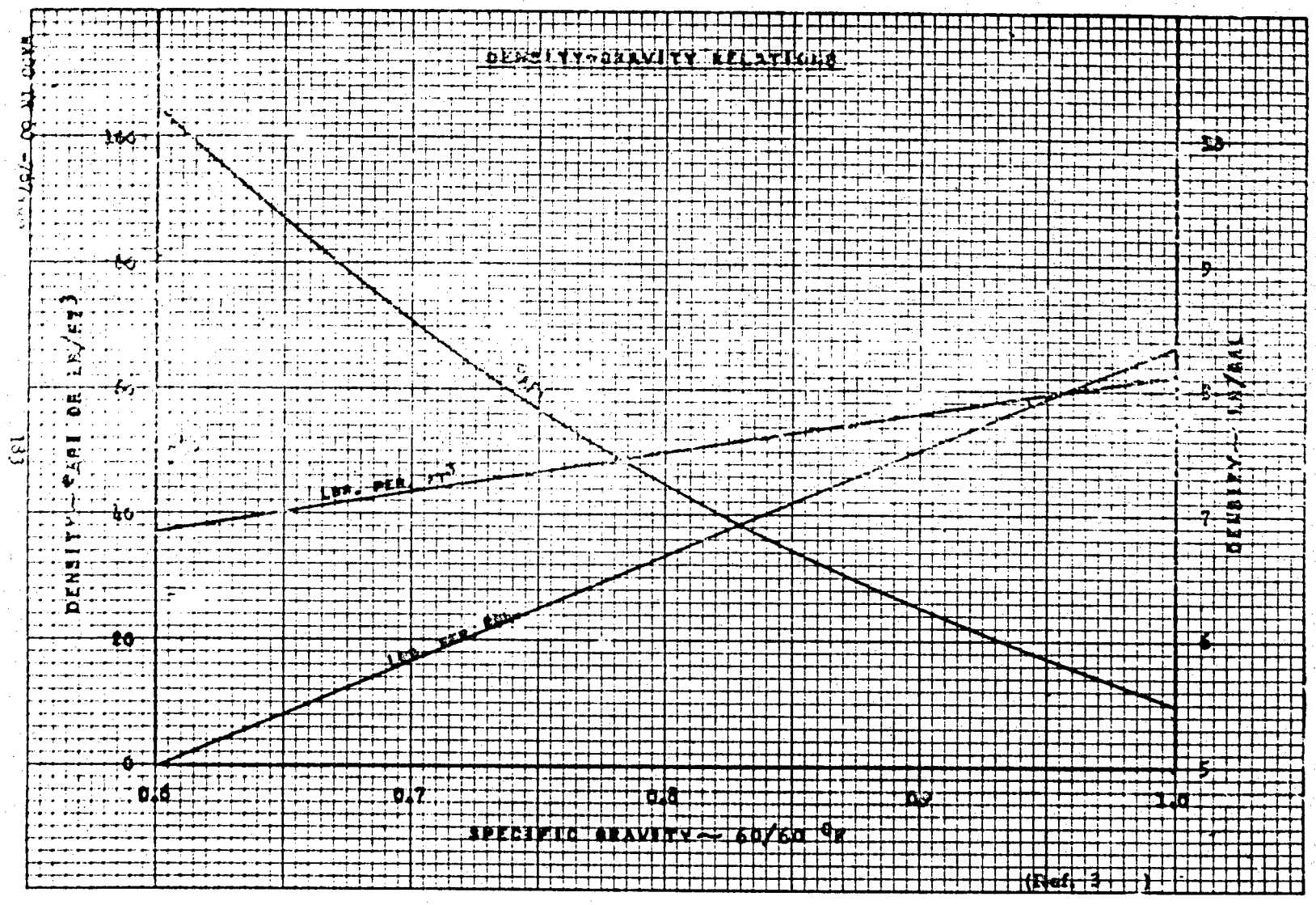

Figure 91 Plot of Density-Gravity Relations.

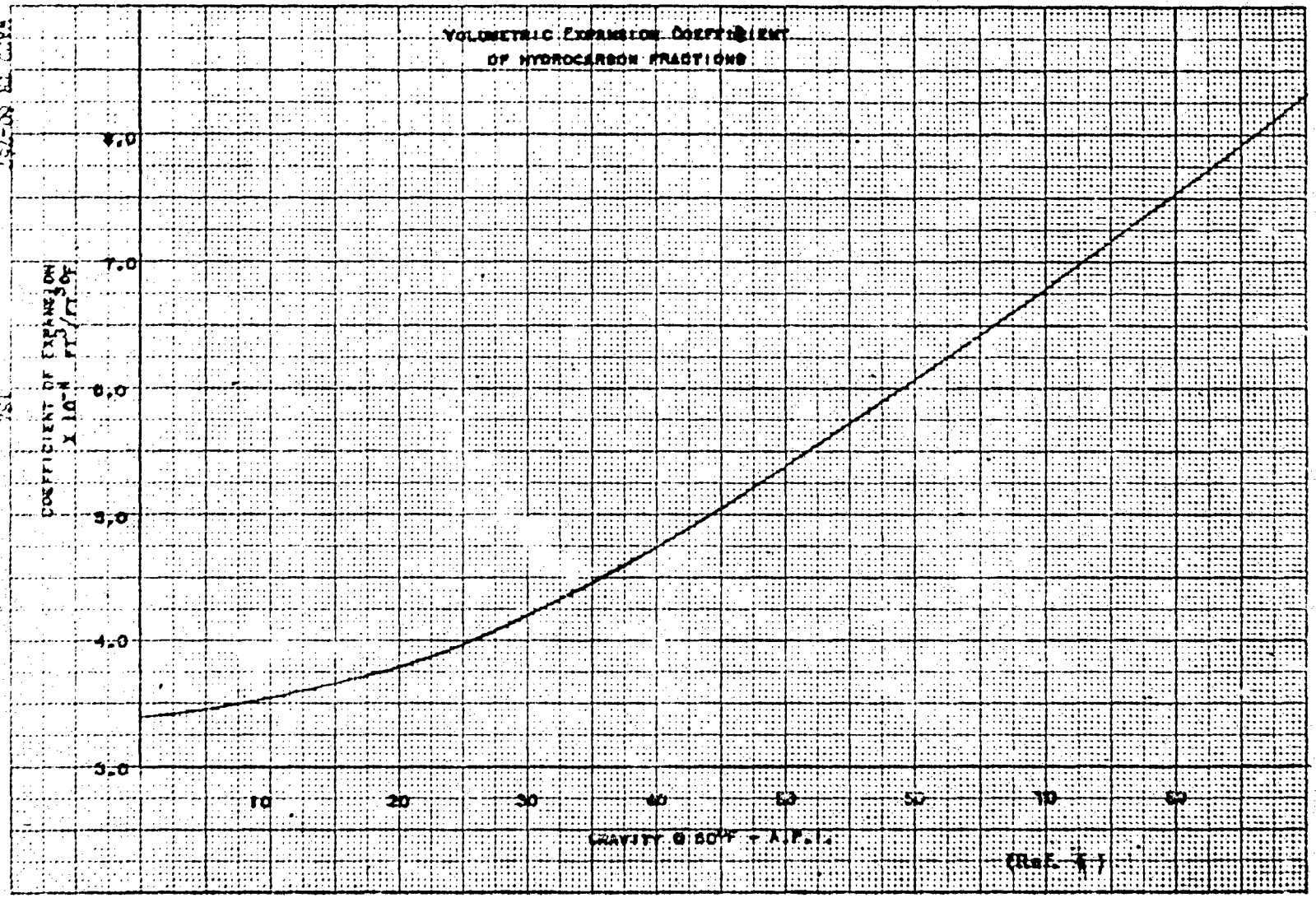

Figure 92 - Plot of Volumetric Expansion Coefficient of Hydrocarbon Fractions.

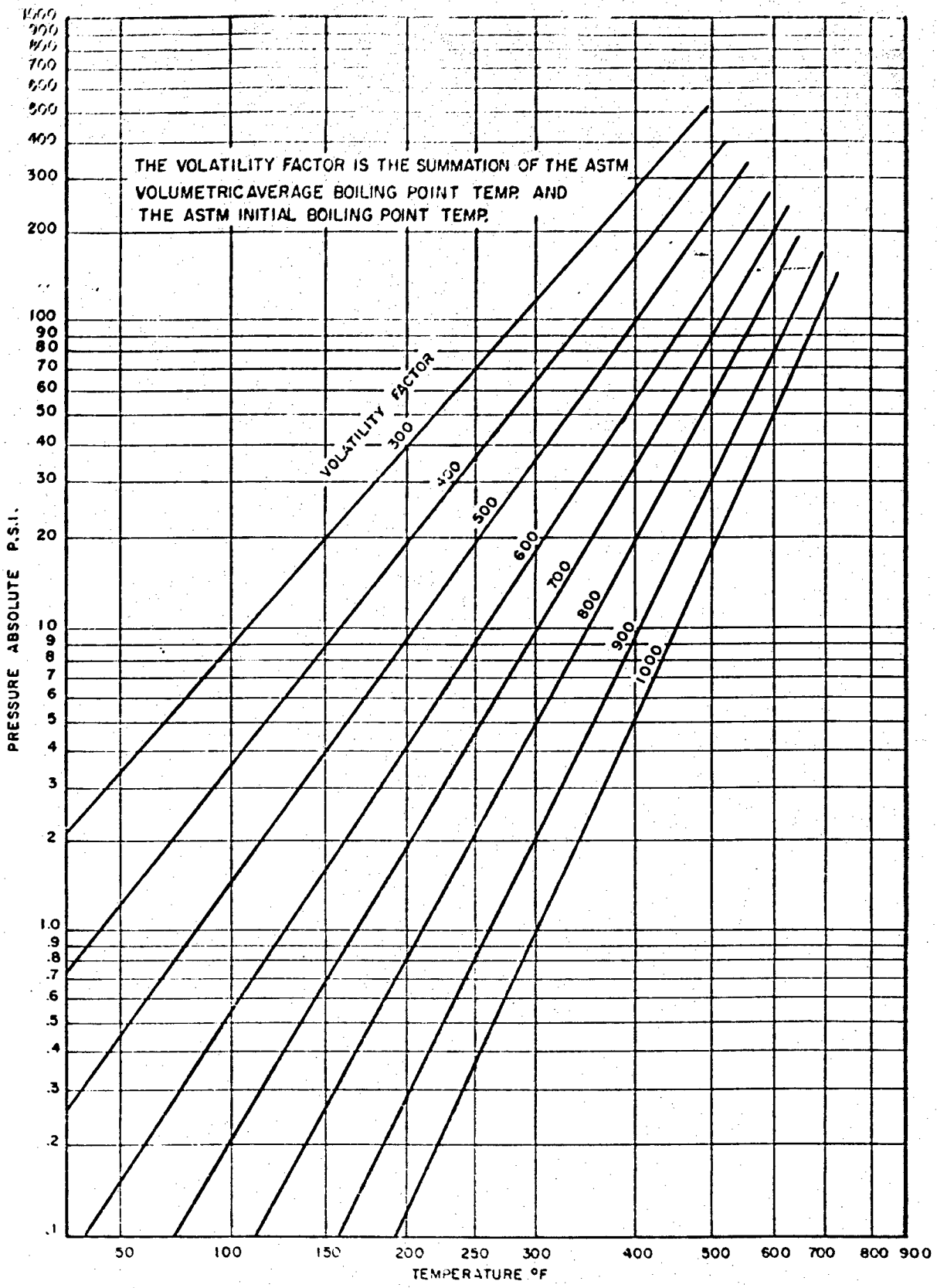

Figure 93 - Variation of Vapor Pressure with Fuel Temperature.

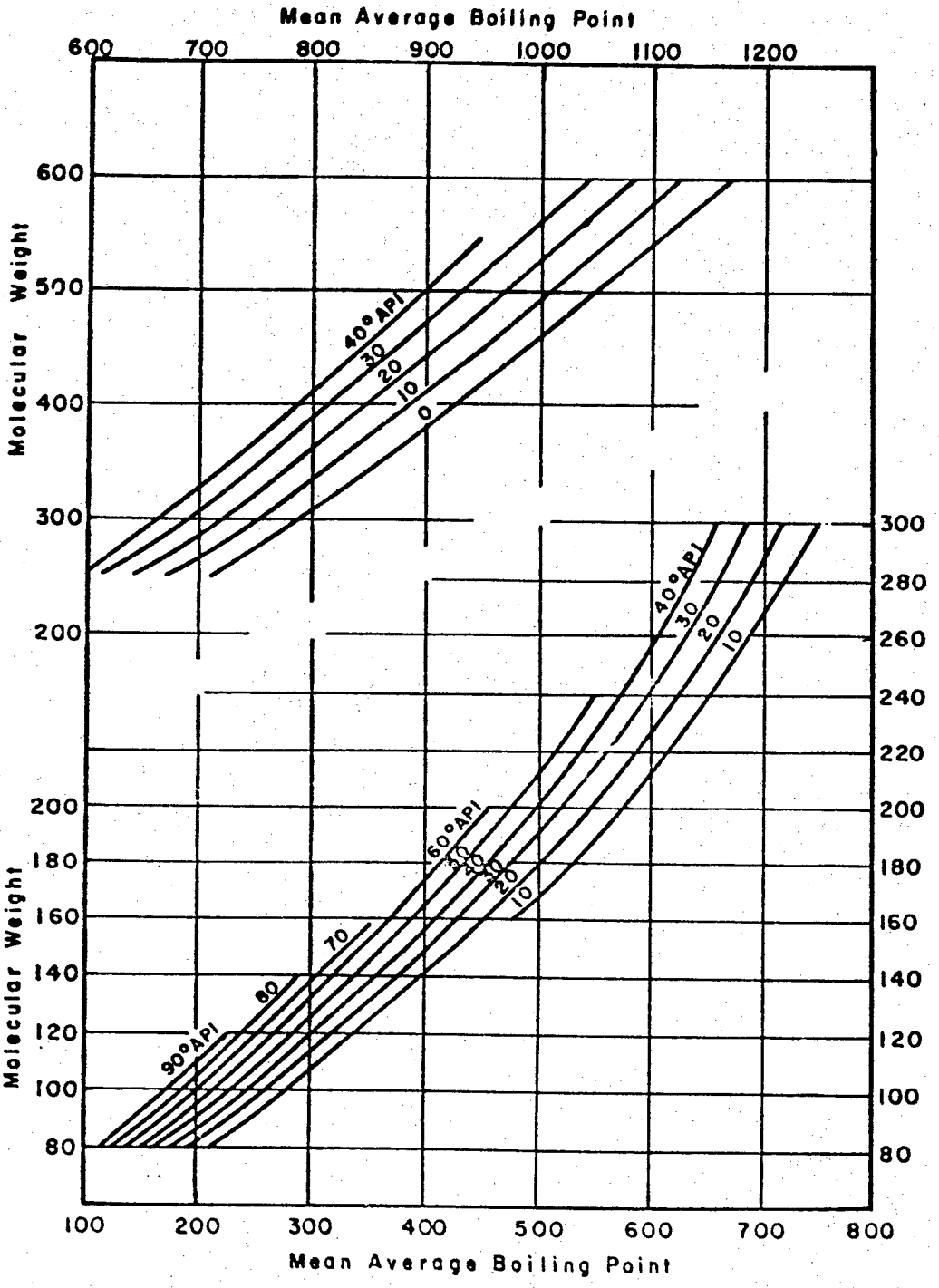

Figure 94 - Plot of Molecular Weight vs Boiling Point and Gravity

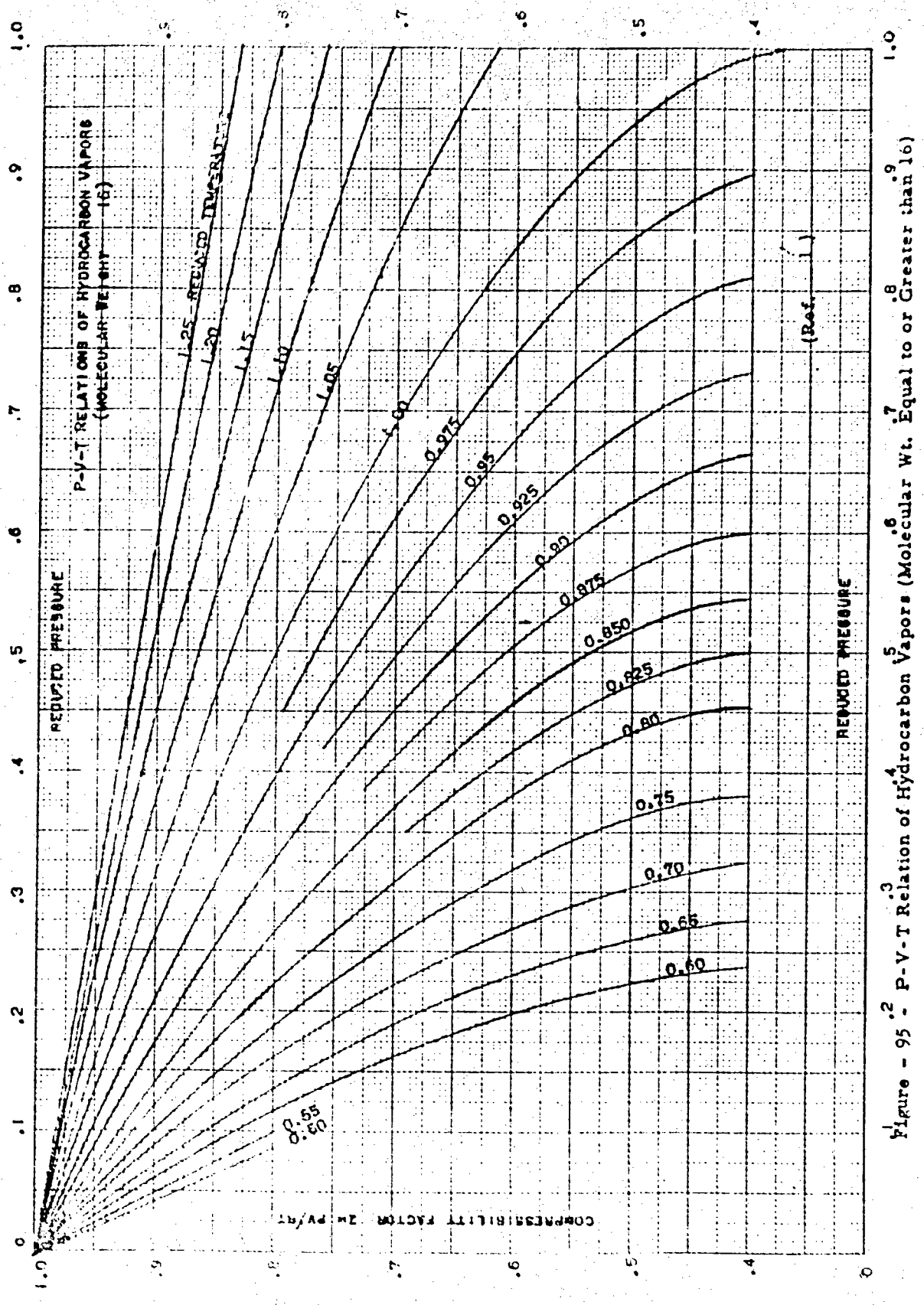

Figure - 95 - P-V-T Relation of Hydrocarbon Vapors (Molecular Wt. Equal to or Greater than 16)

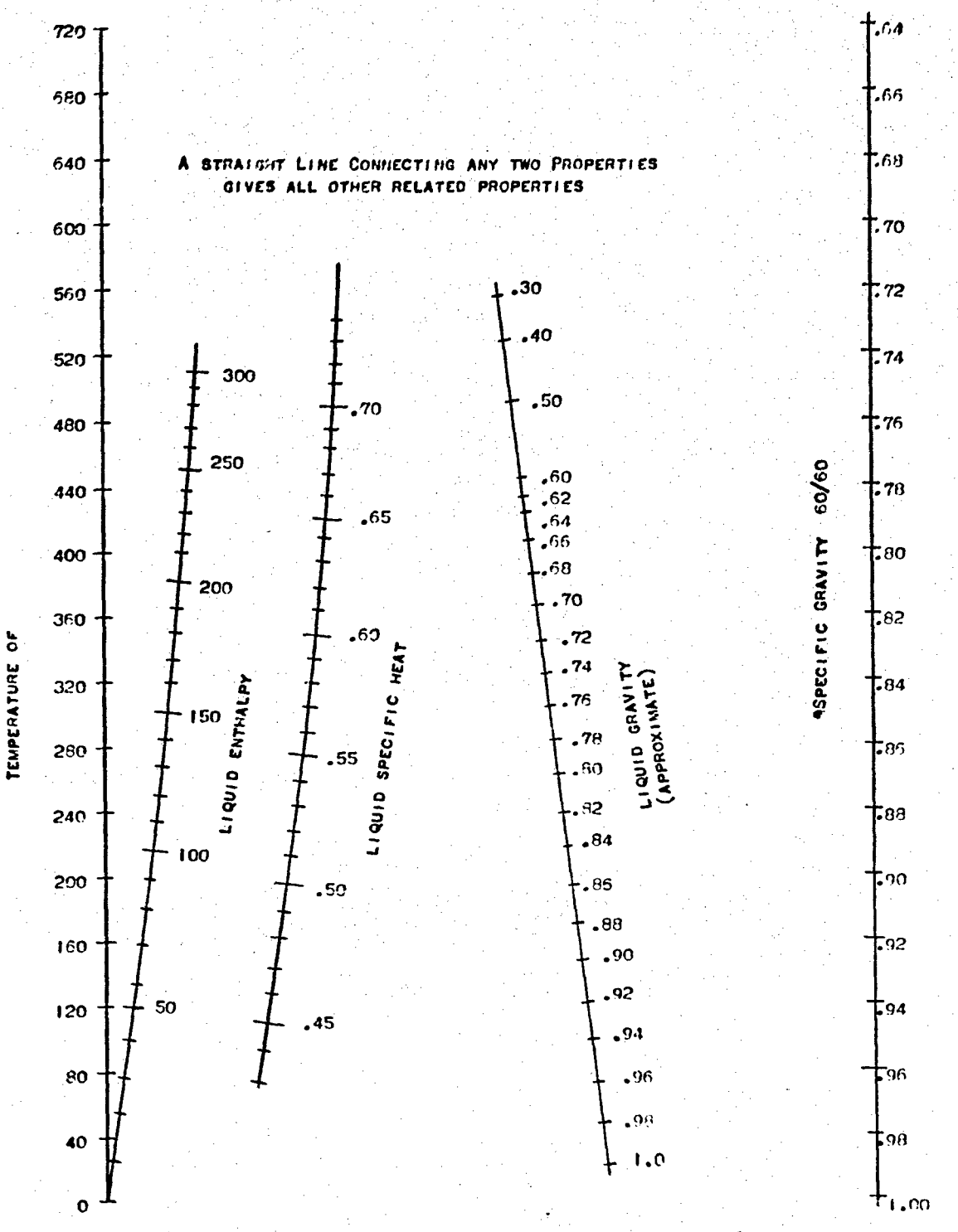

(Ref. 5)

Figure 96 - Properties of Liquid Petroleum Fractions Nomogram.

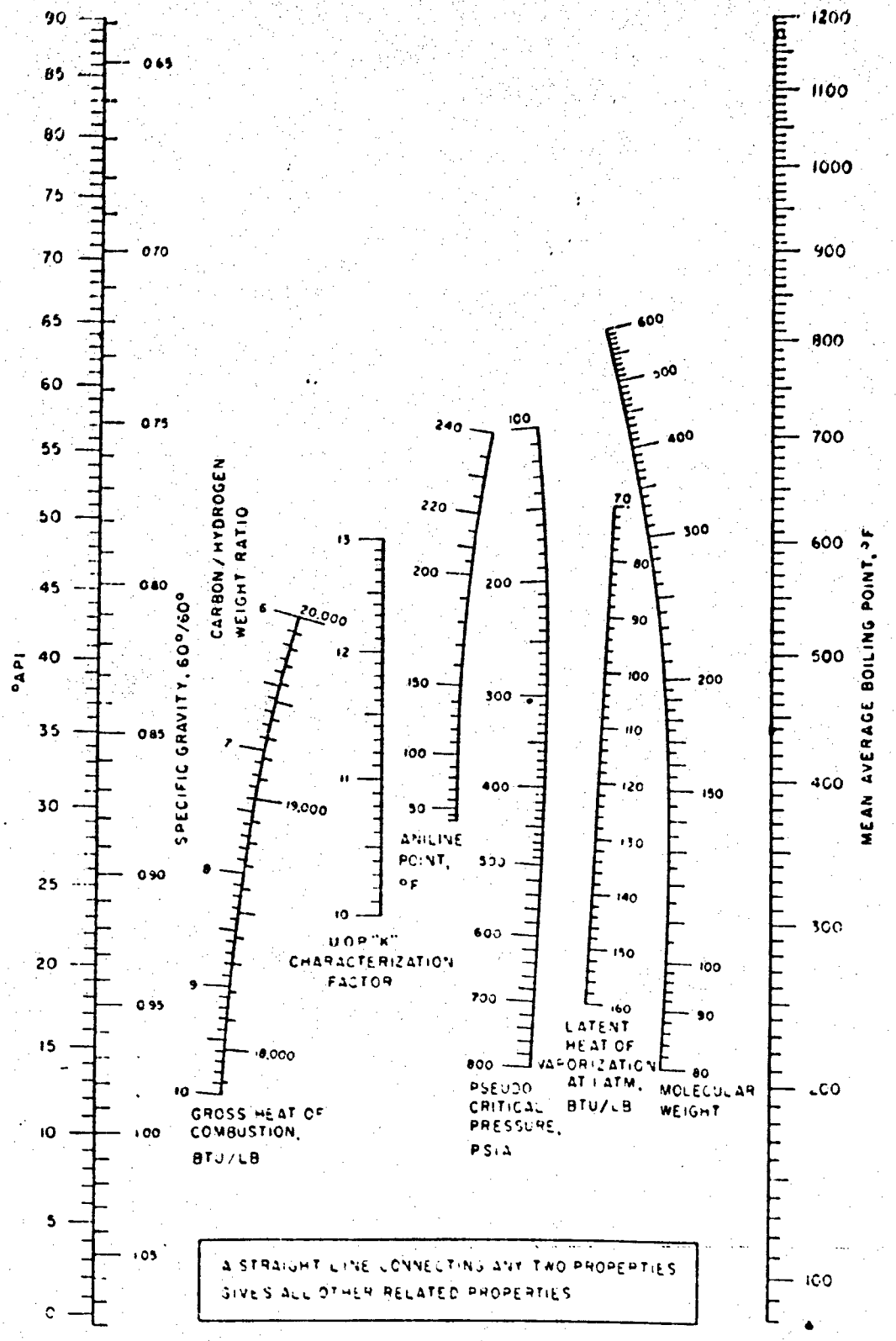

Figure 97 - Properties of Petroleum Fractions Nomogram

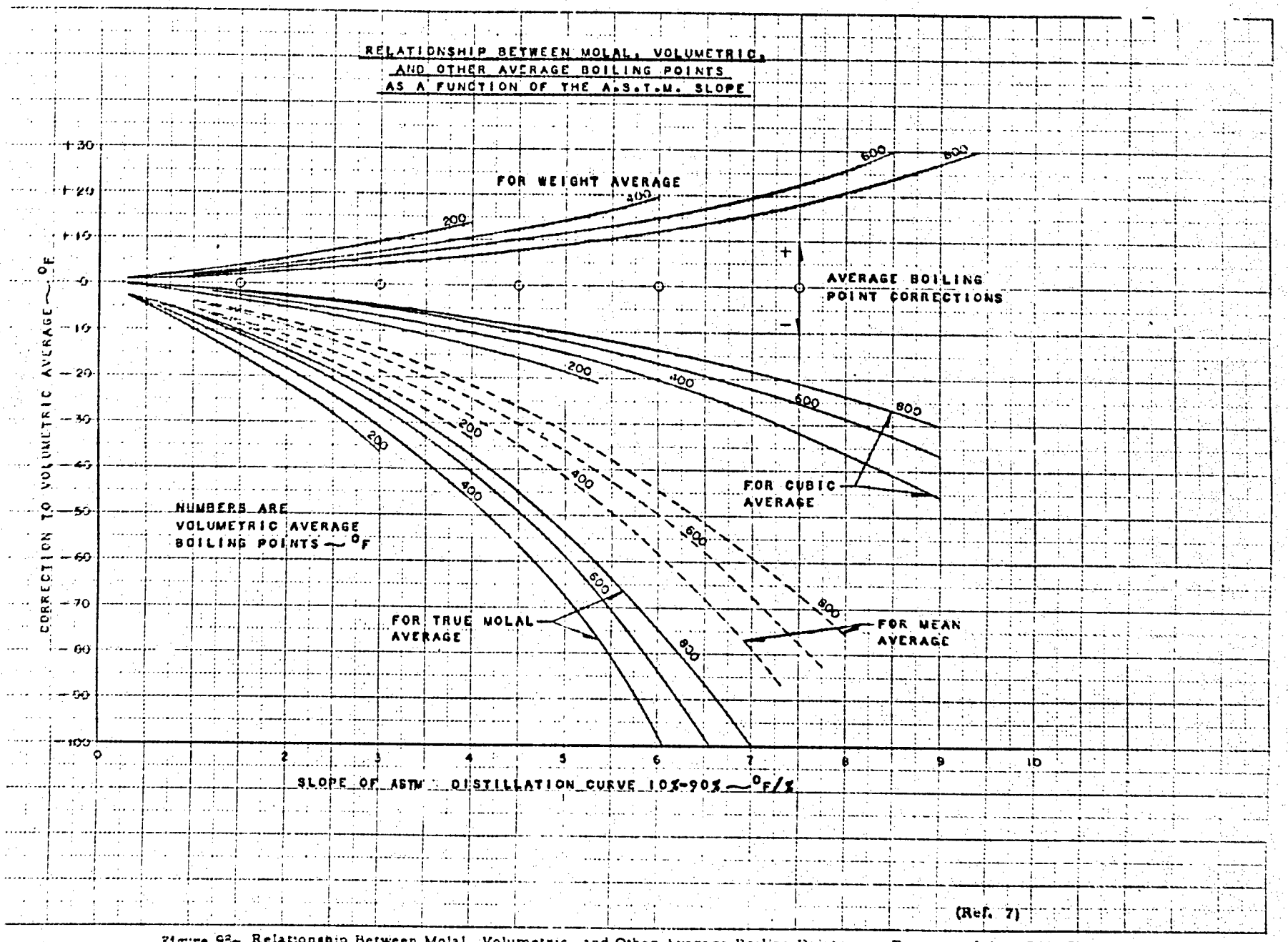

Figure 98. Relationship Between Molal, Volumetric, and Other Average Boiling Points as a Function of the ASTM Slope.

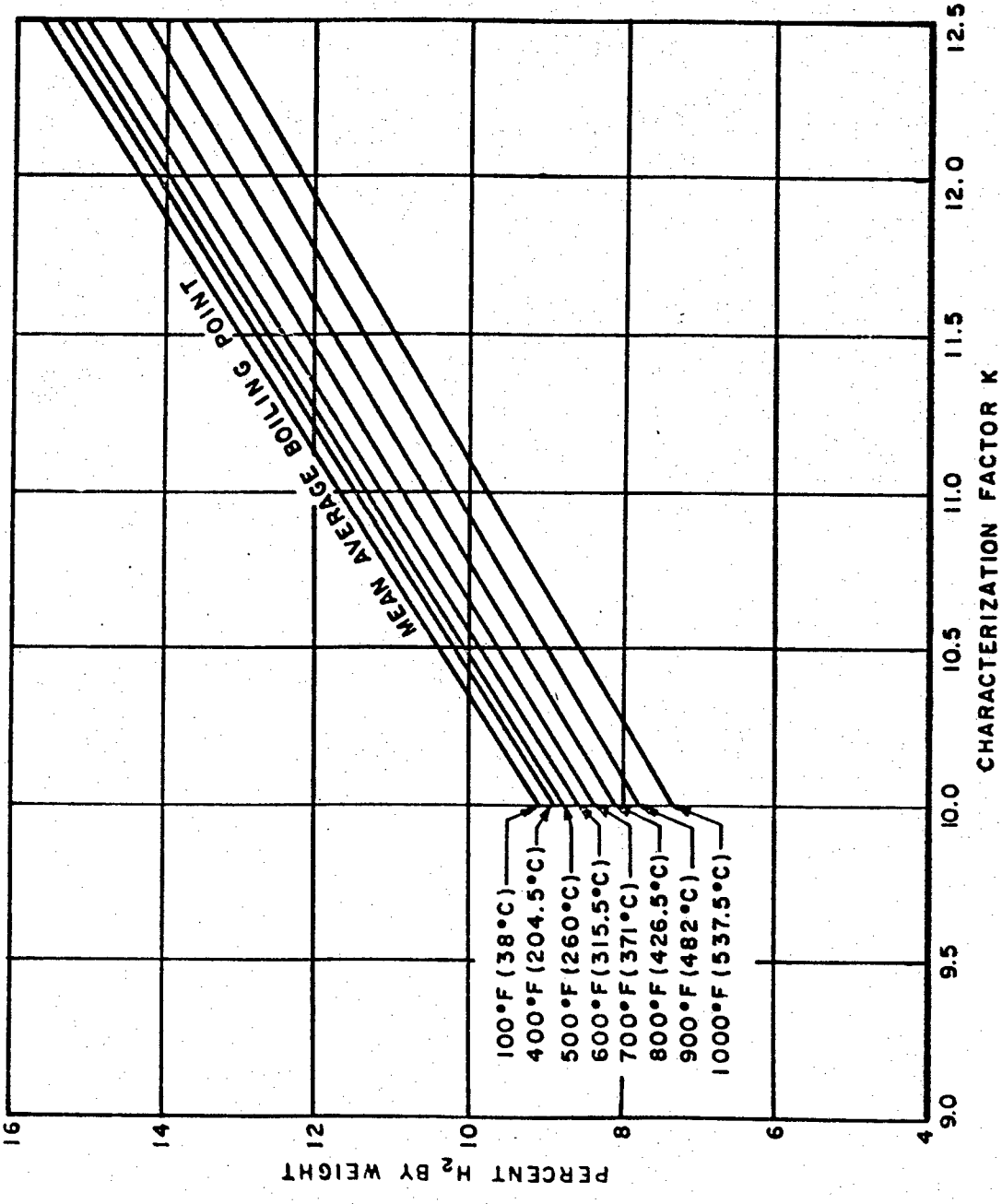

Figure 99 - Hydrogen Content of Hydrocarbons

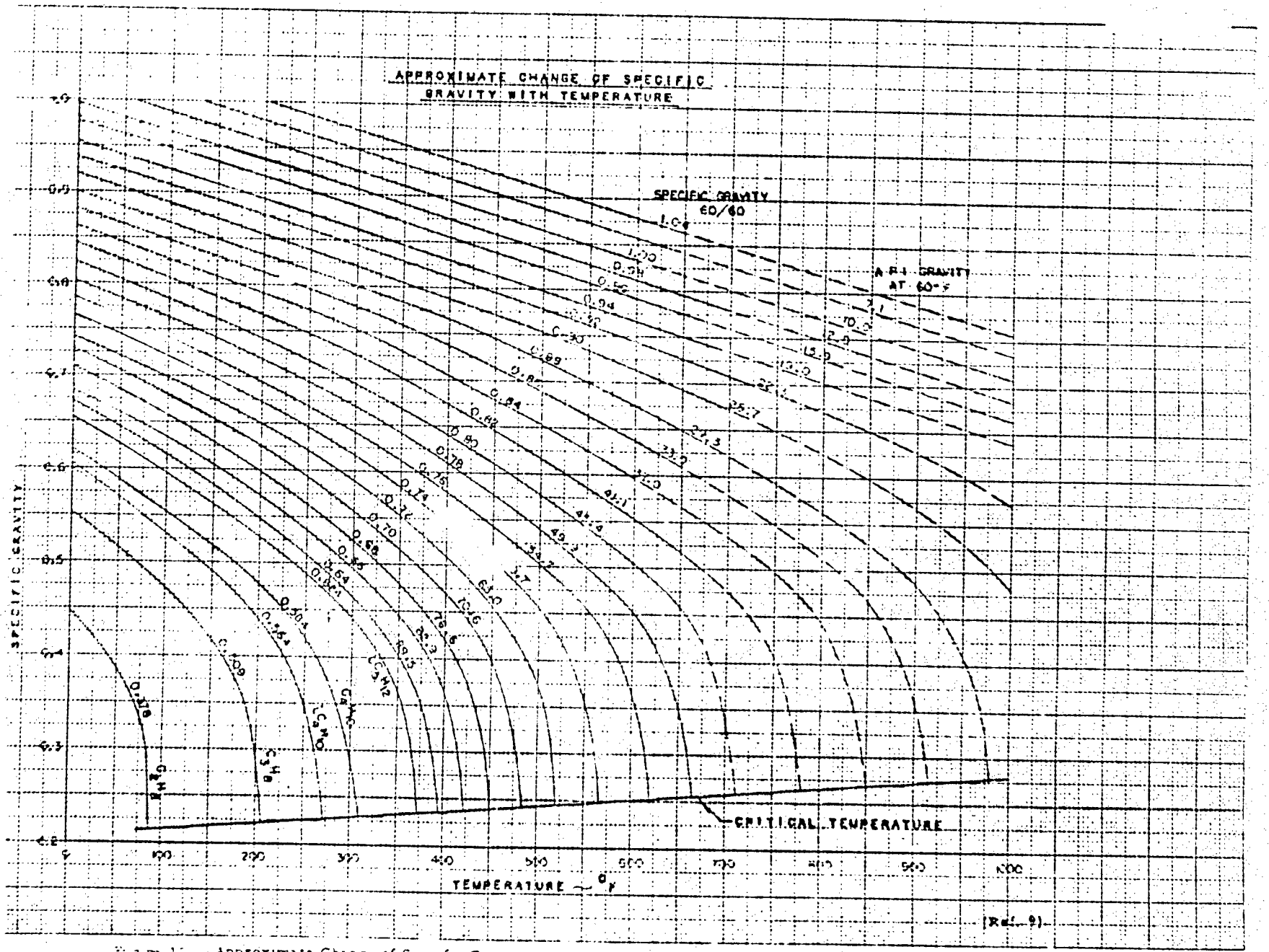

Figure 13. - Approximate Change of Specific Gravity With Temperature.

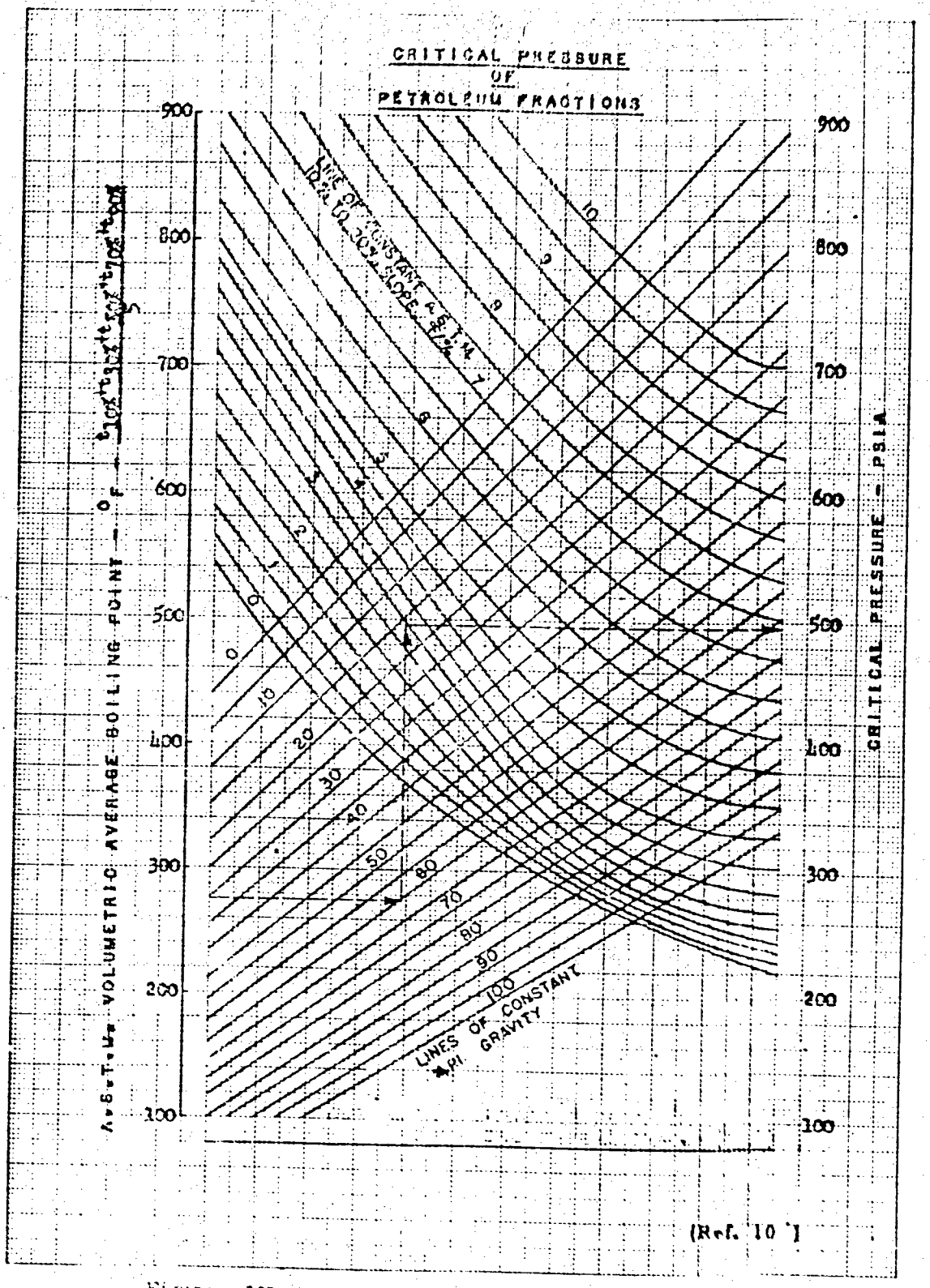

Figure 101 - Critical Pressure of Petroleum Fractions.

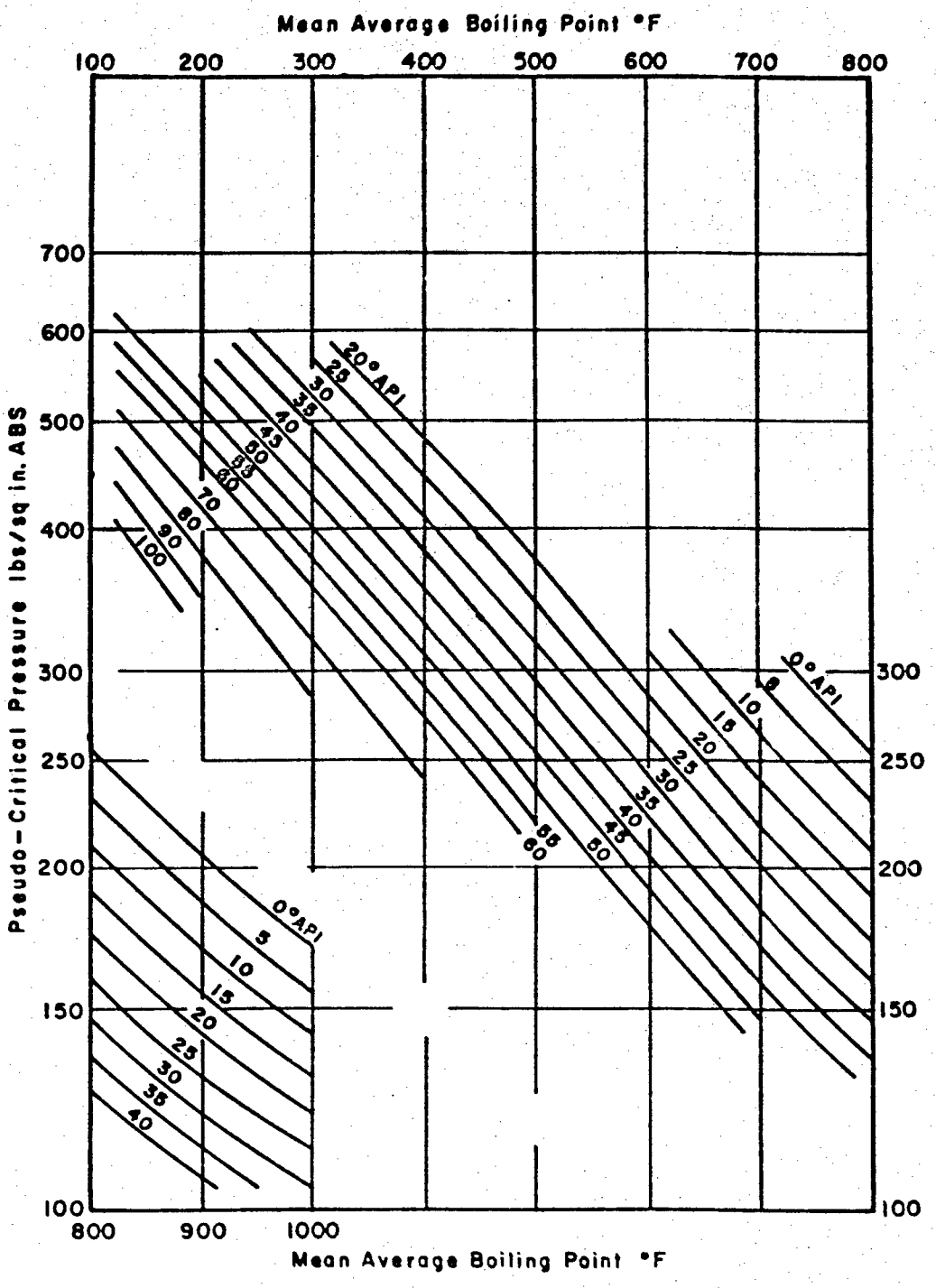

(Ref. 1)

Figure 102 - Pseudo-Critical Pressure of Petroleum Fractions

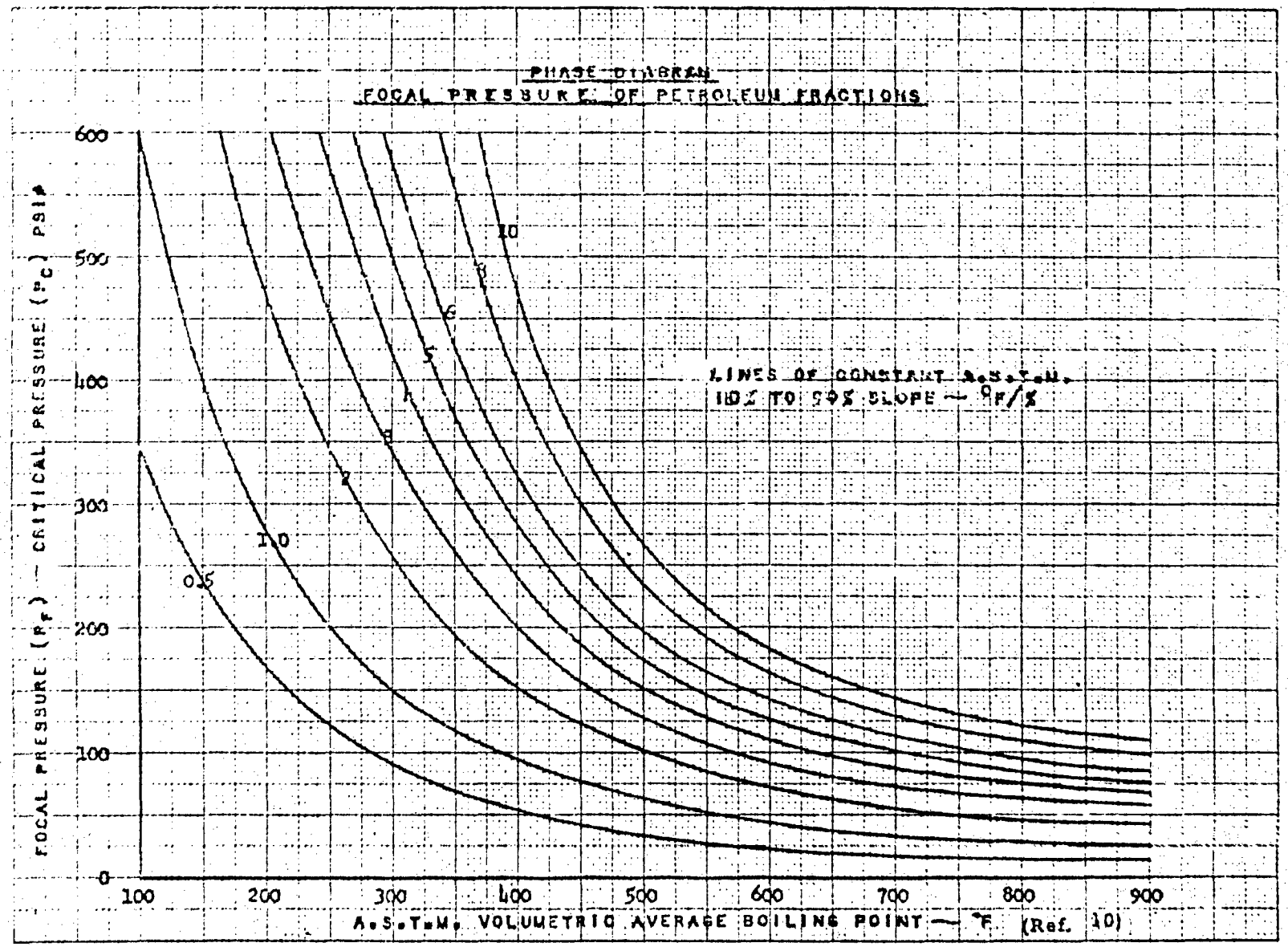

Figure 103 - Focal Pressure of Petroleum Fractions.

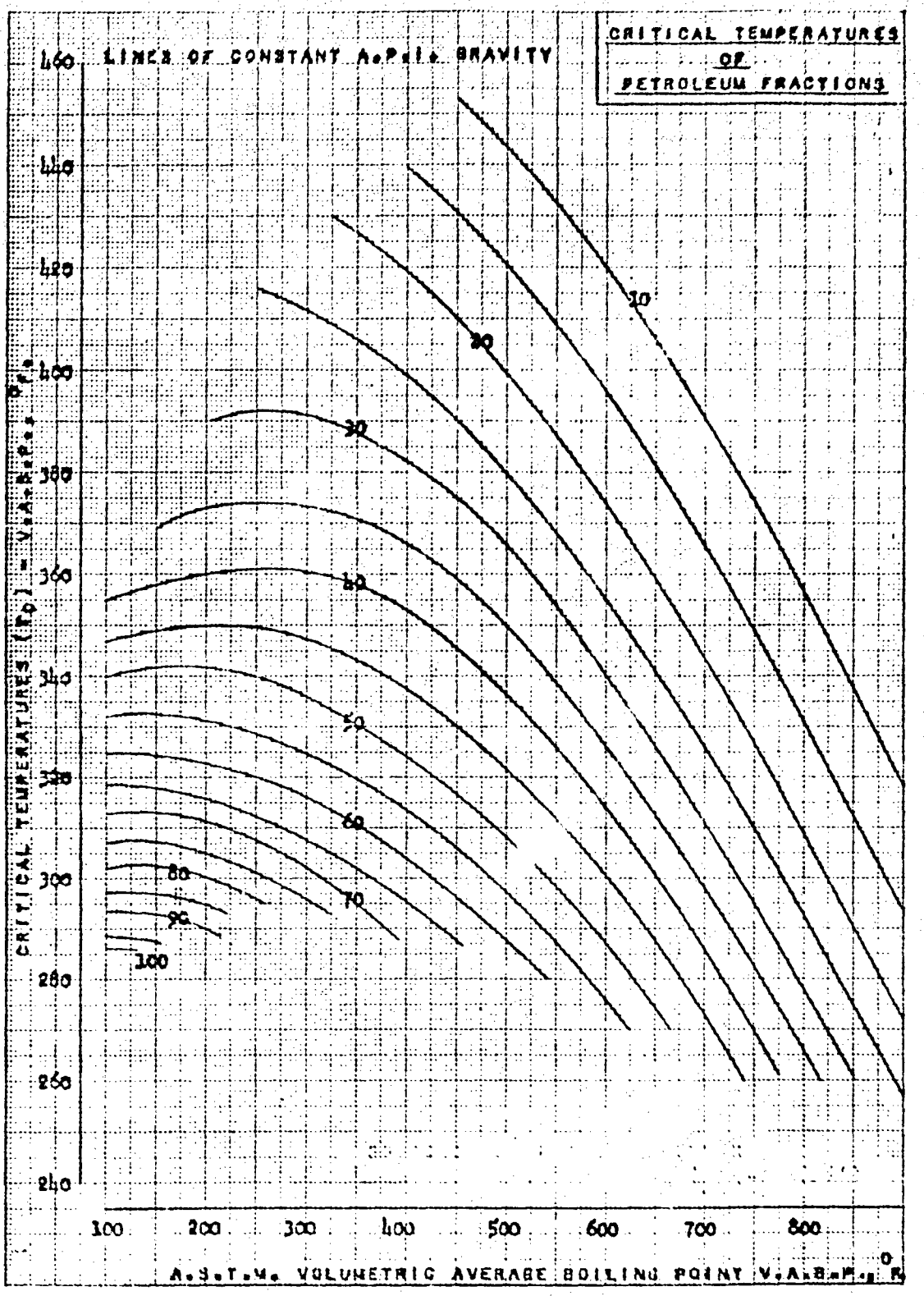

(Ref. 10)

Figure 102 - Critical Temperatures of Petroleum Fractions

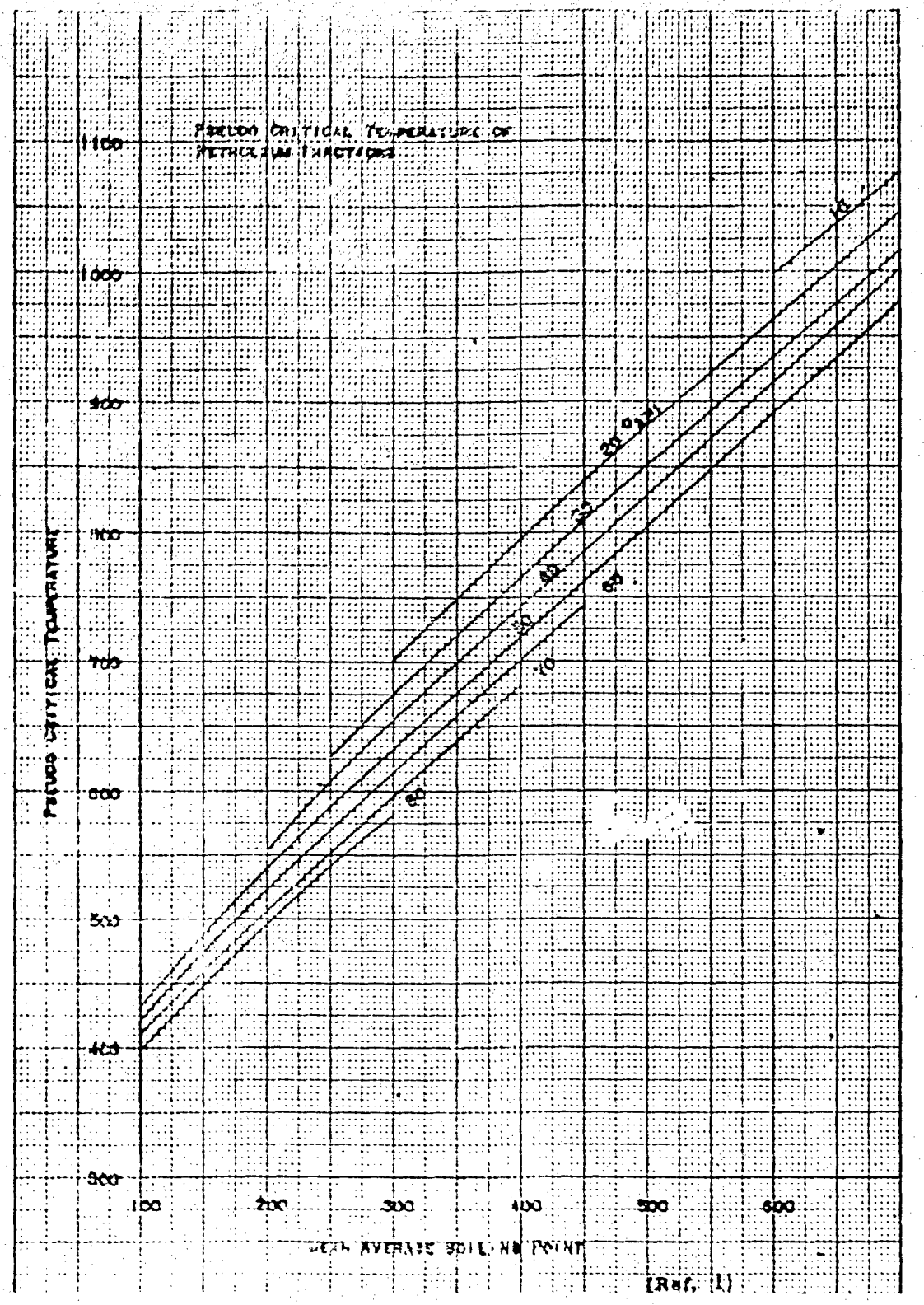

Figure 105 - Pseudo-Critical Temperature of Petroleum Fractions

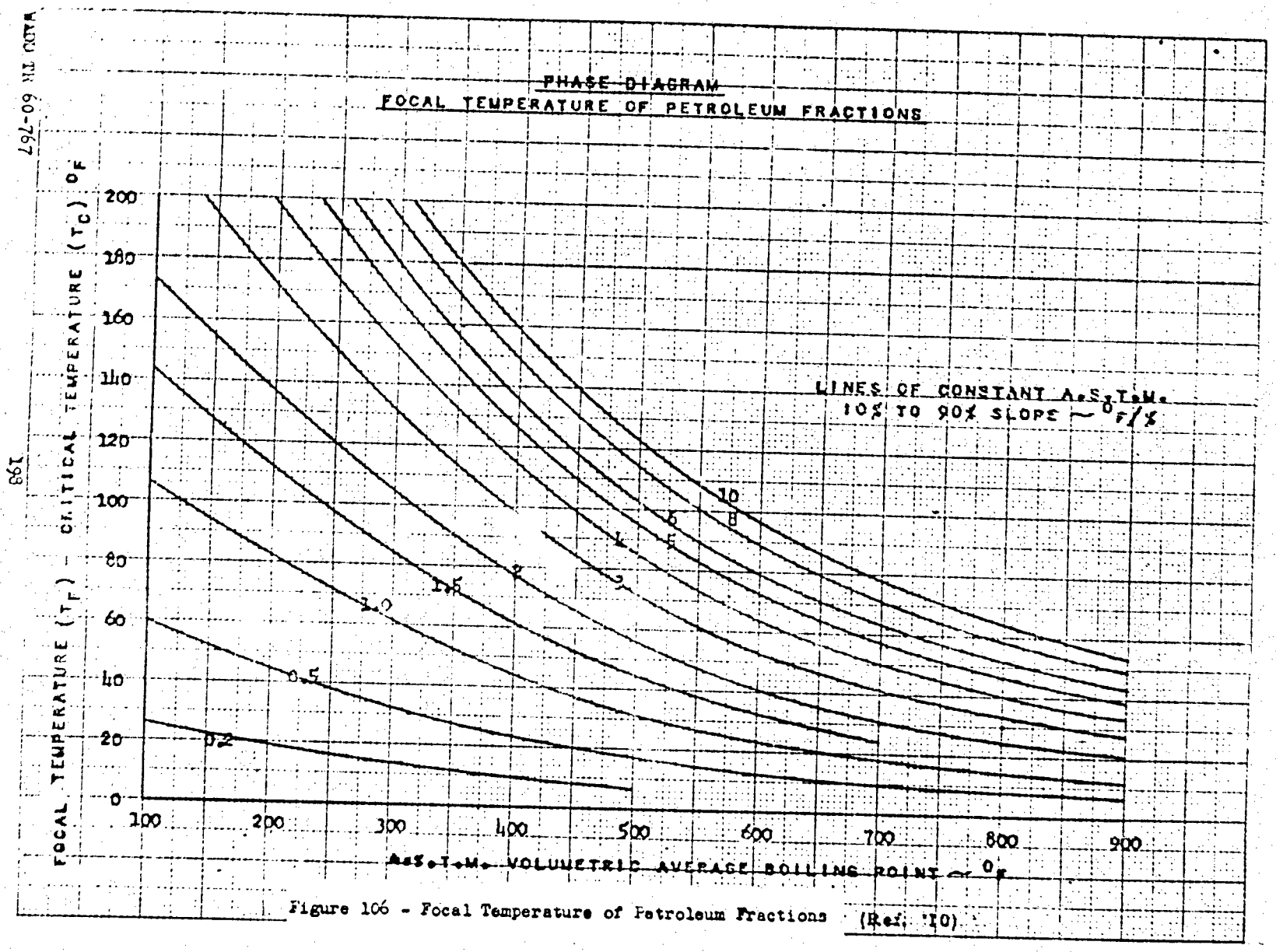

Figure 106 - Focal Temperature of Petroleum Fractions (Ref. '10)

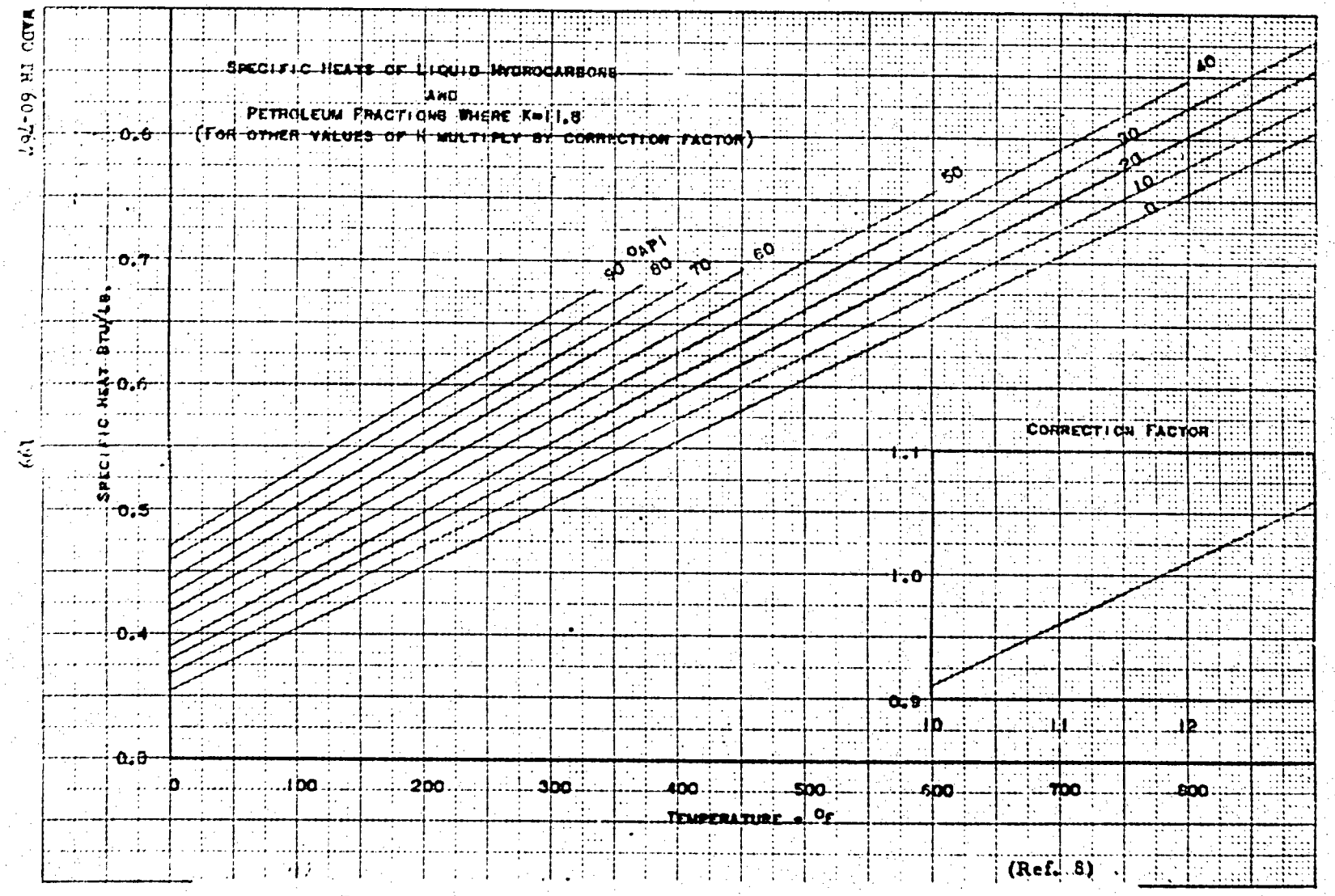

Figure 107 - Specific Heats of Liquid Hydrocarbons and Petroleum Fractions

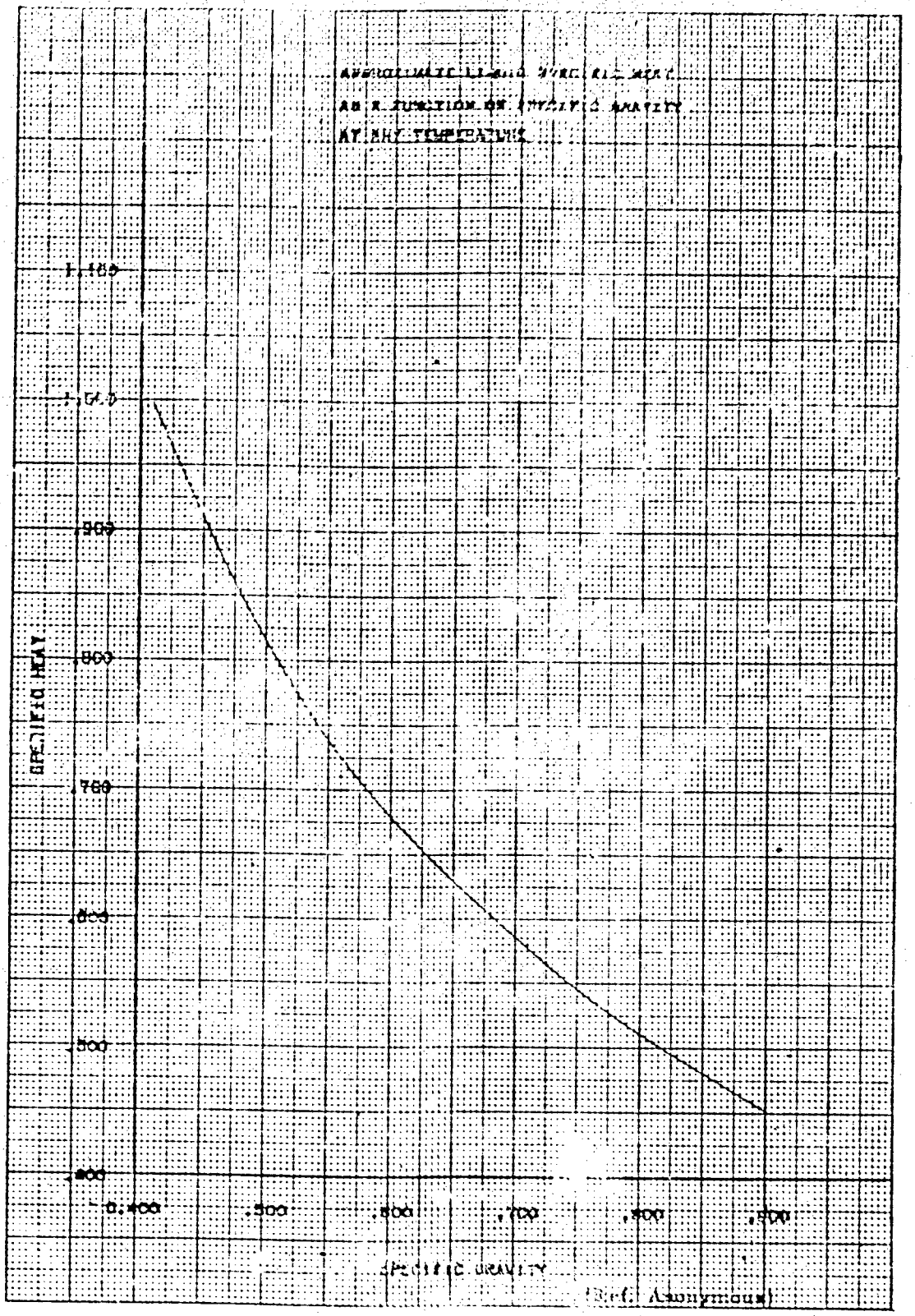

Figure 108 - Approximate Liquid Specific Heat as a Function of Gravity

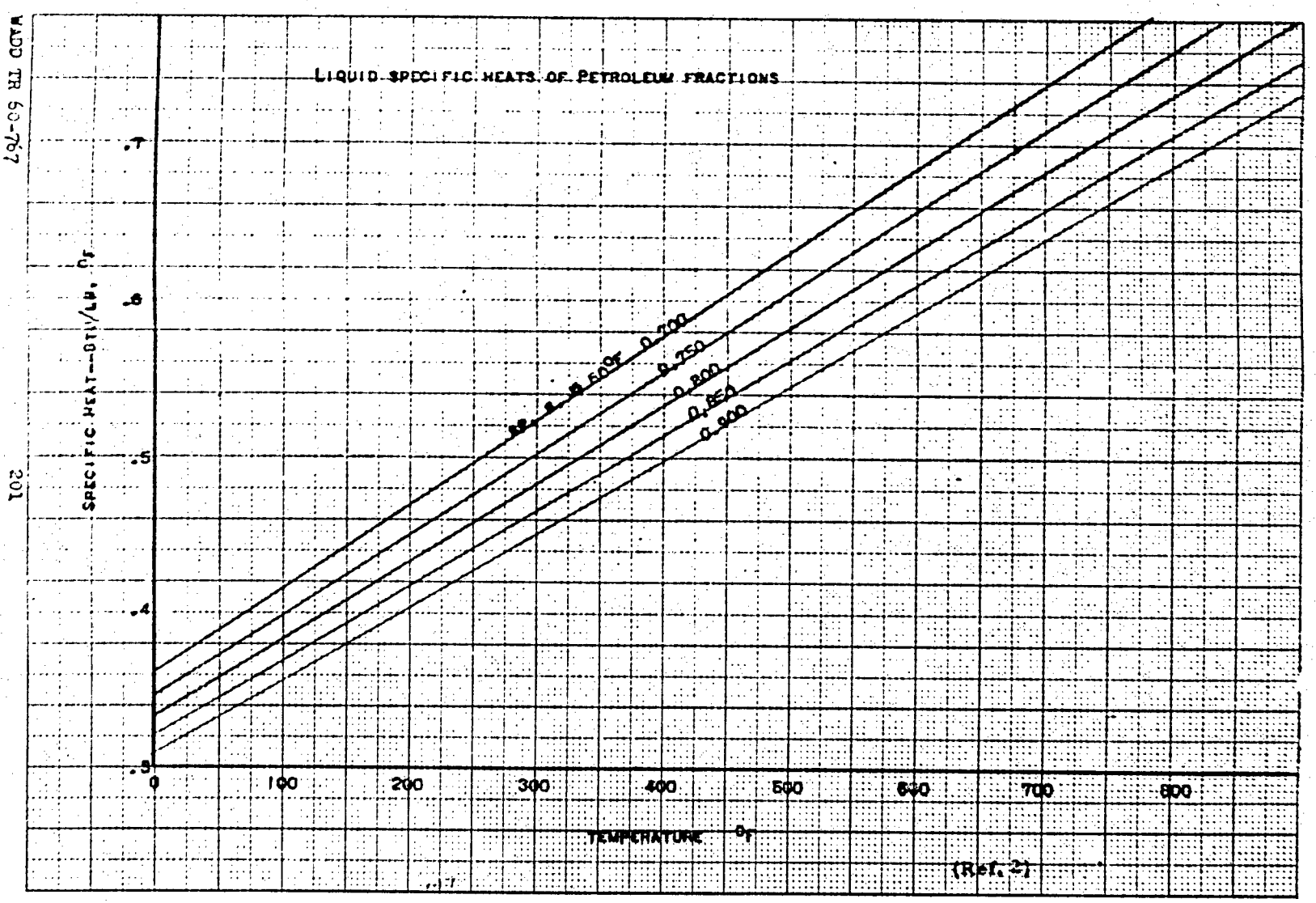

Figure 109 - Liquid Specific Heats of Petroleum Fractions.

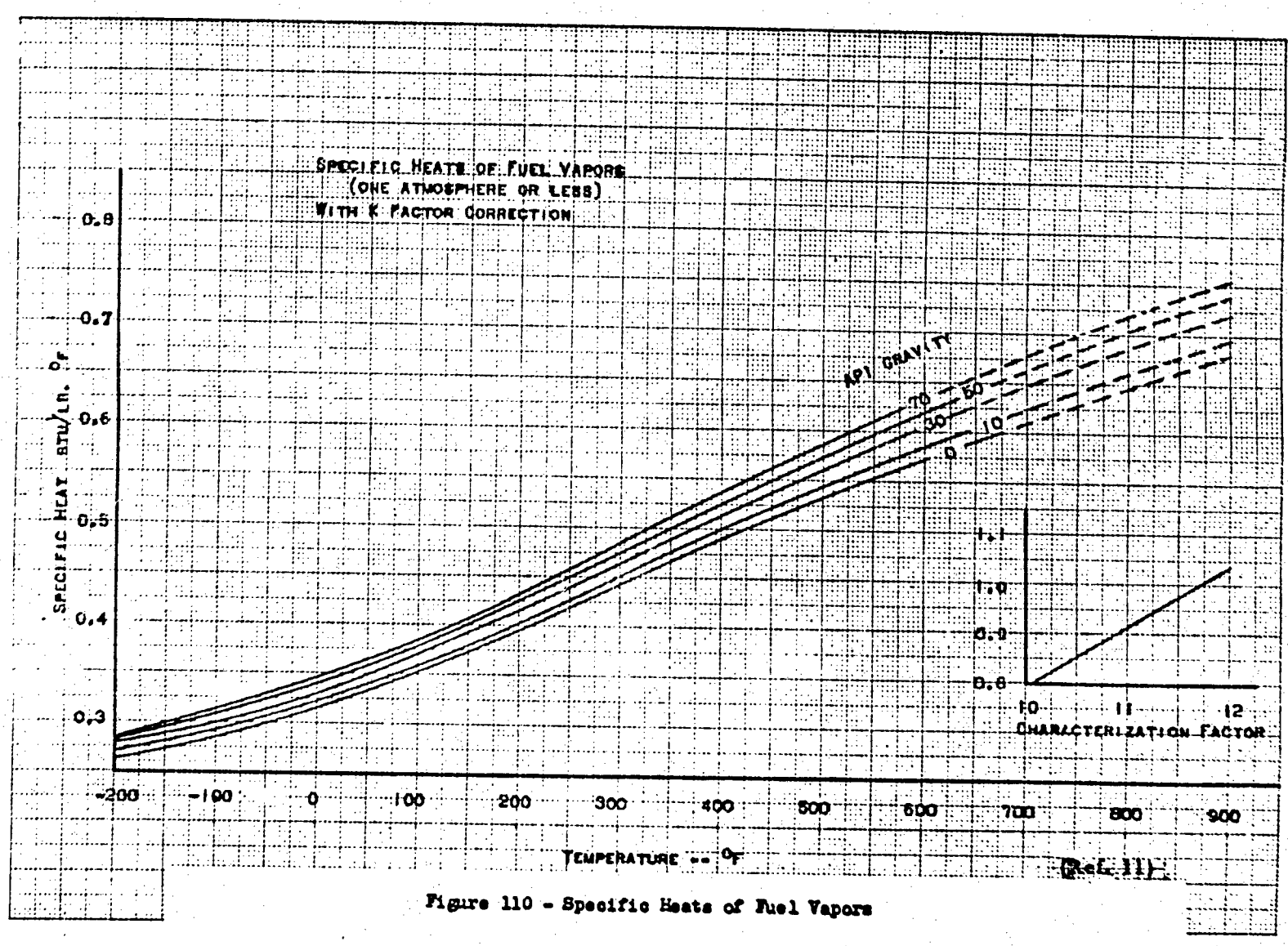

Figure 110 - Specific Heats of Fuel Vapors

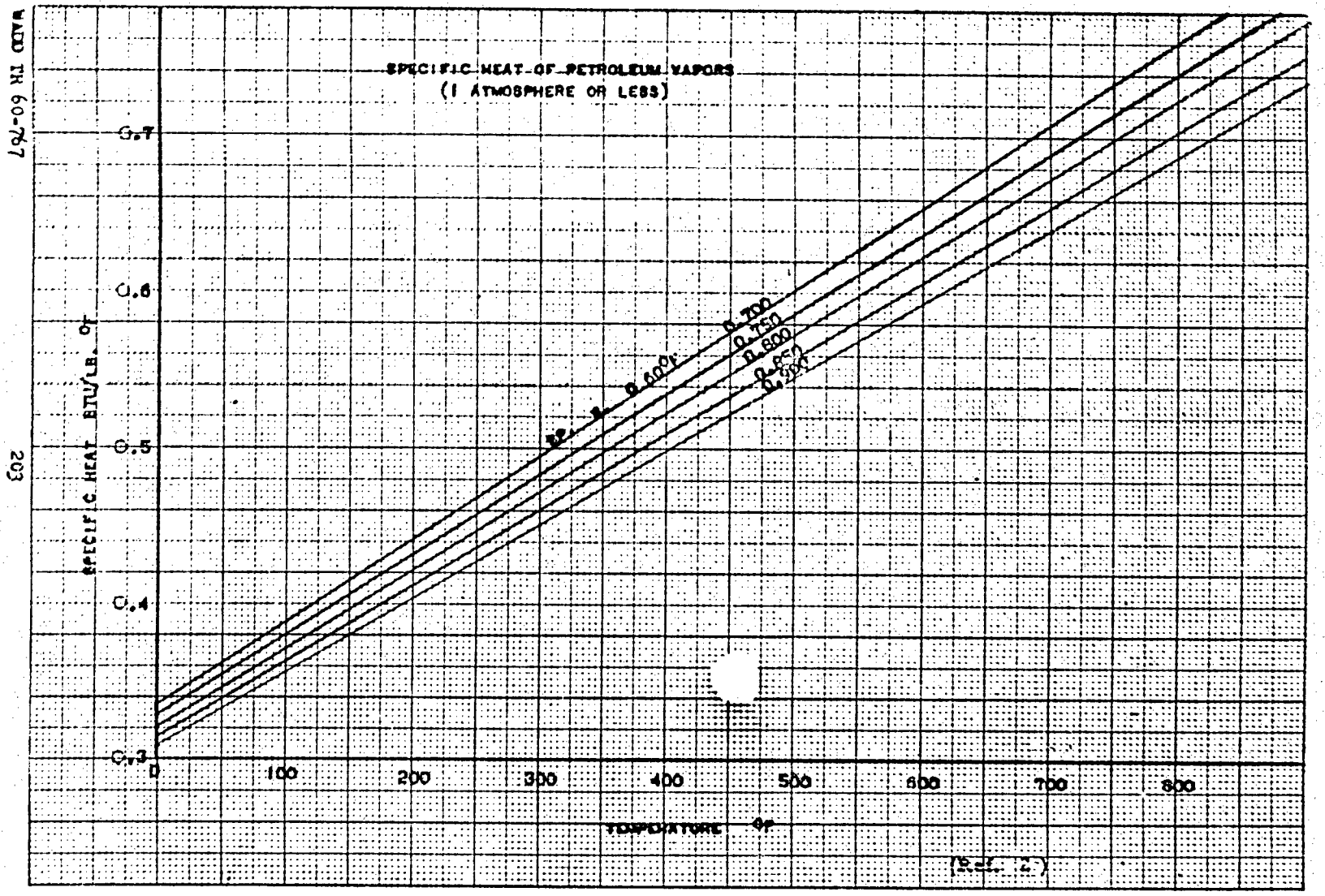

Figure 111 - Specific Heat of Petroleum Vapors.

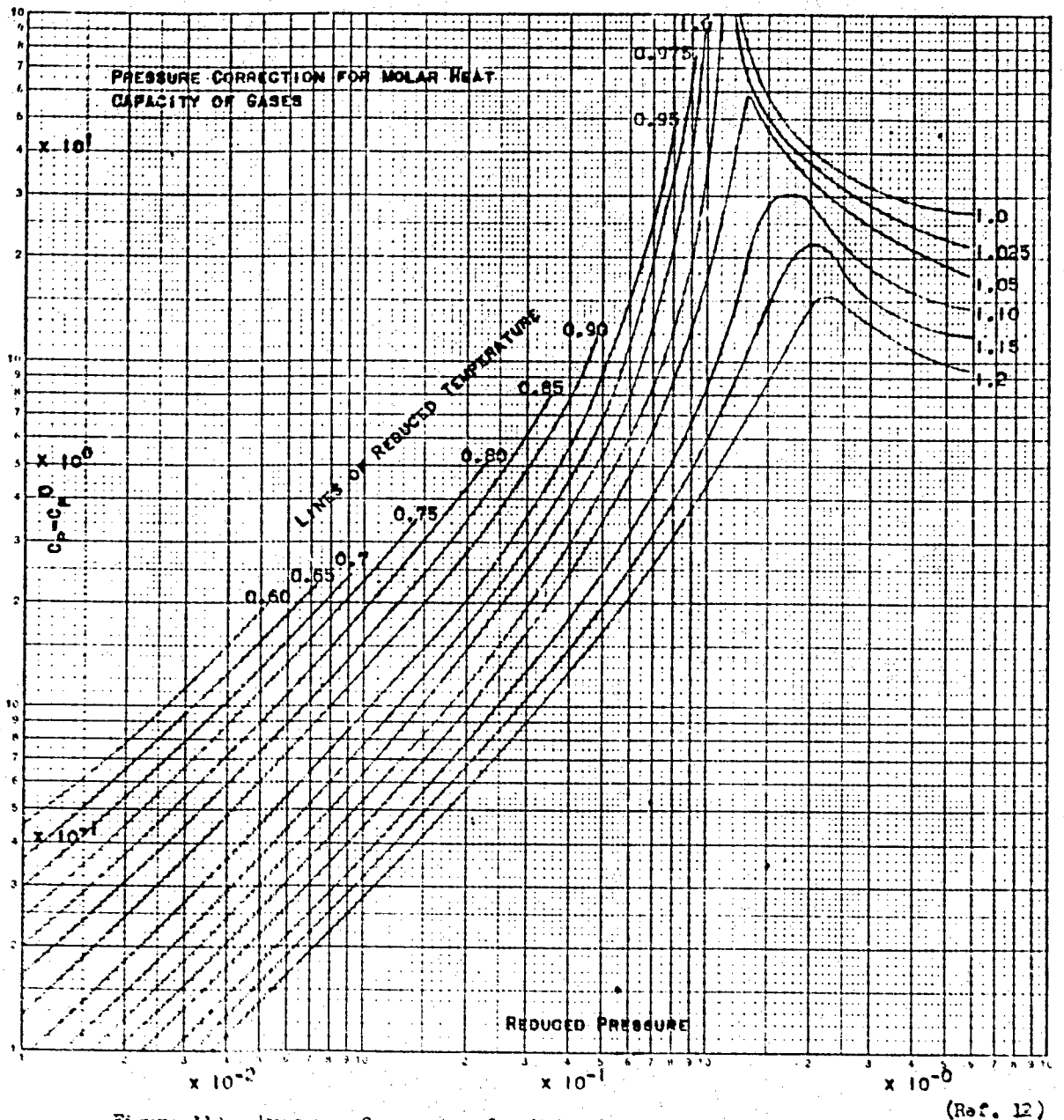

(Ref. 12)

Figure 11.2 - Pressure Correction for Molar Heat Capacity of Gases

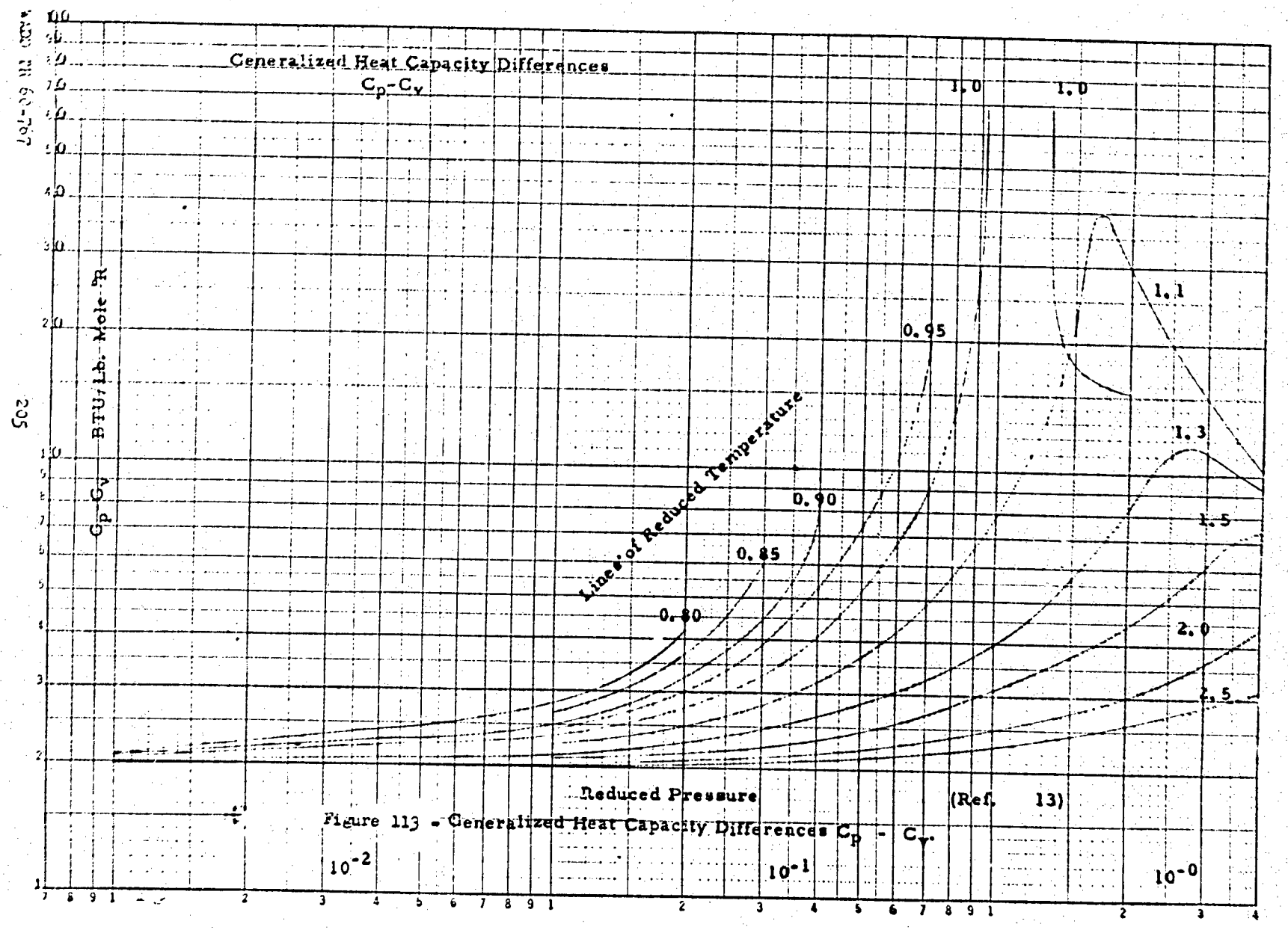

(Ref. 13)

Figure 113 - Generalized Heat Capacity Differences C_p - C_v.

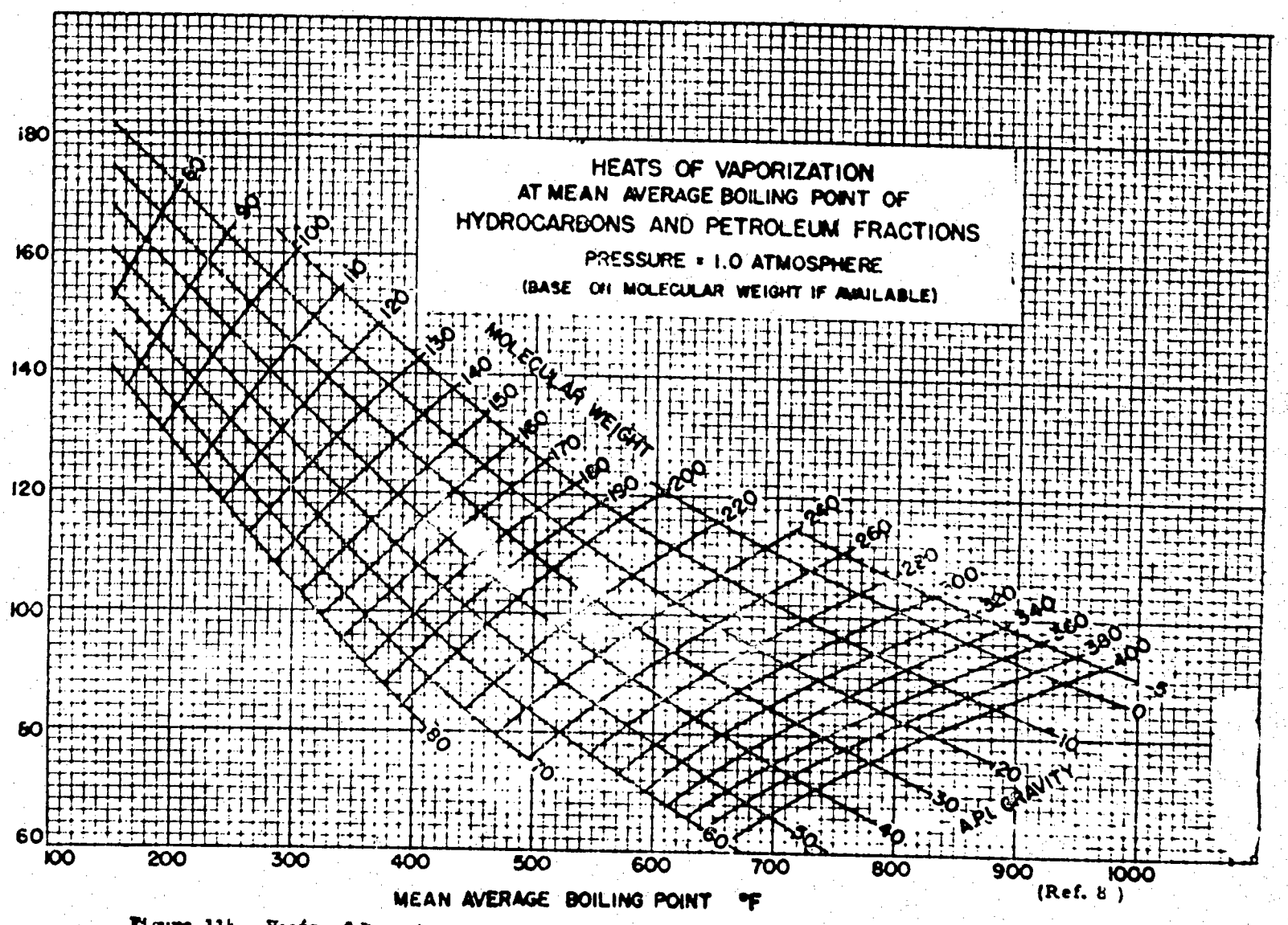

Figure 114 - Heats of Vaporization of Hydrocarbons and Petroleum Fractions.

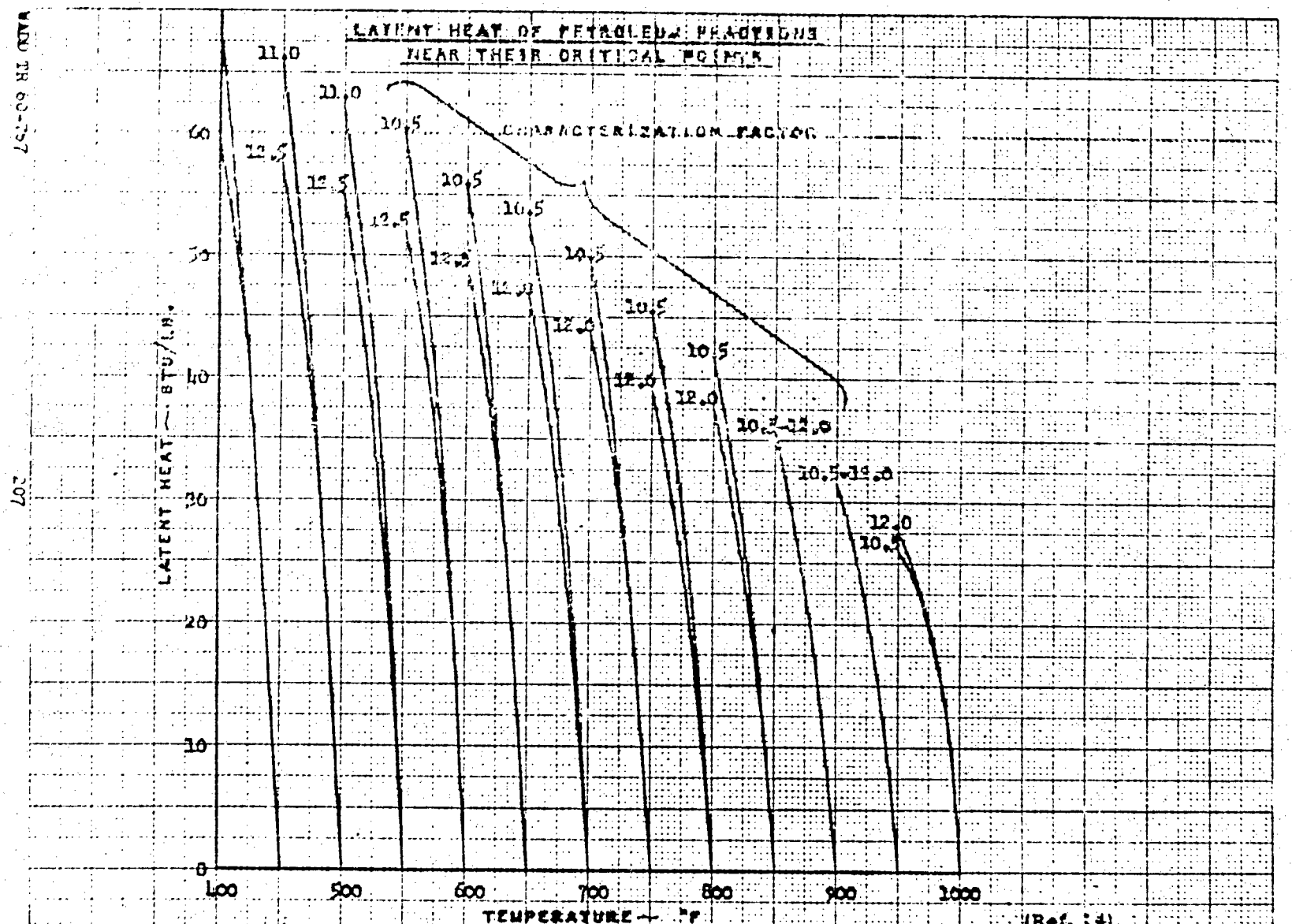

Figure 115 - Latent Heat of Petroleum Fractions Near Their Critical Boiling Points.

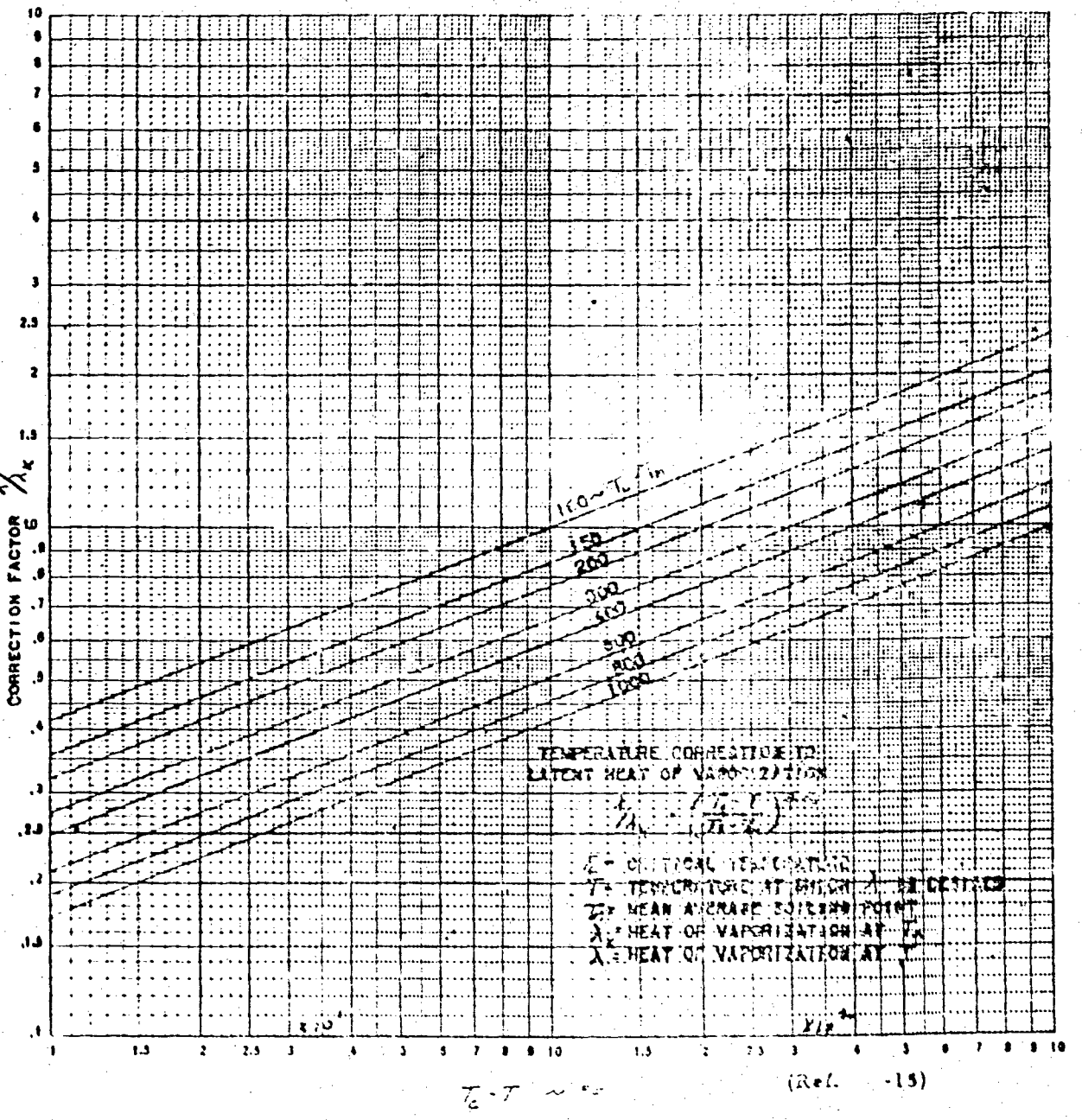

Figure 116 - Temperature Correction to Latent Heat of Vaporization.

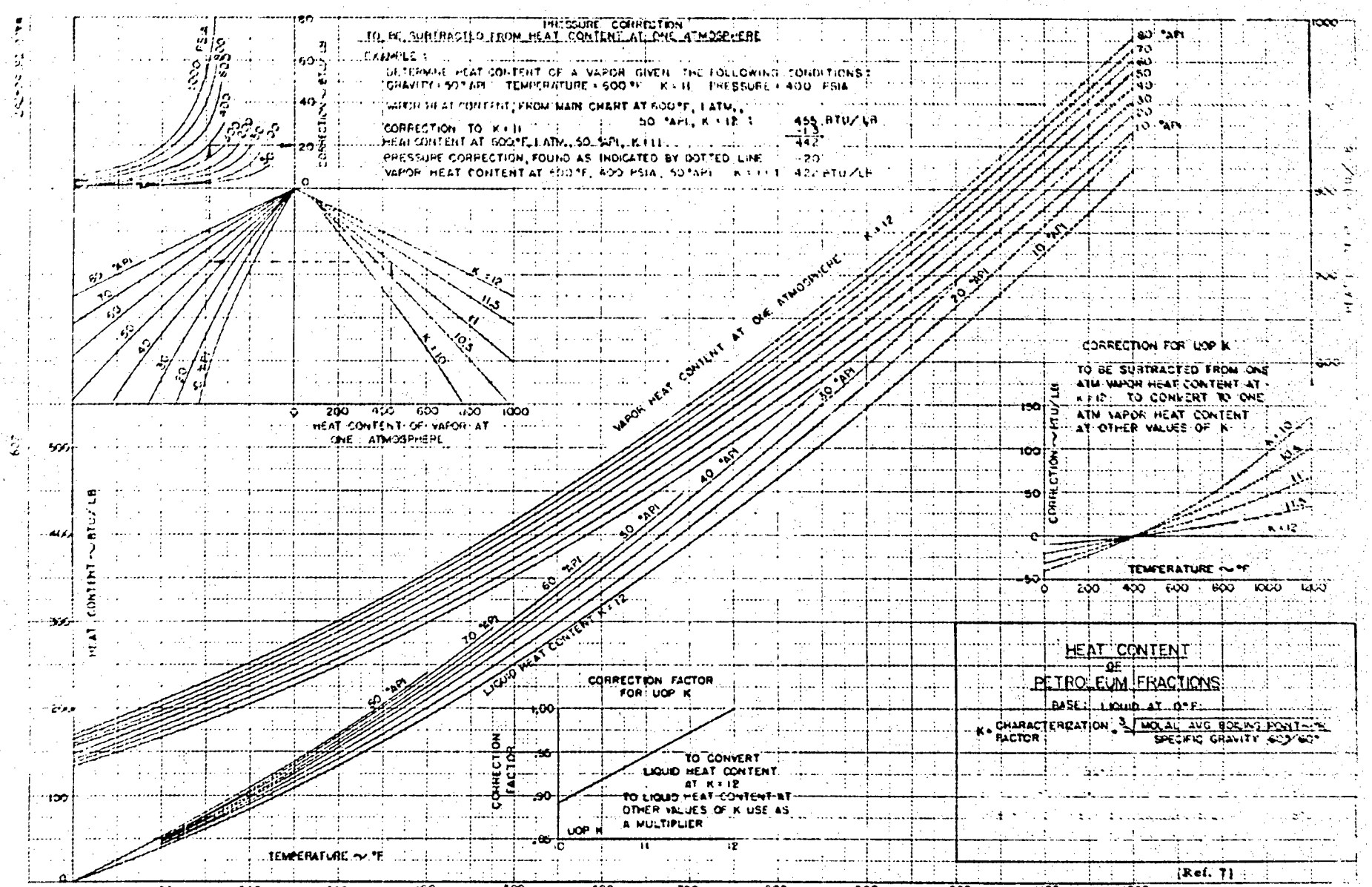

Figure 117 - Heat Content of Petroleum Fractions.

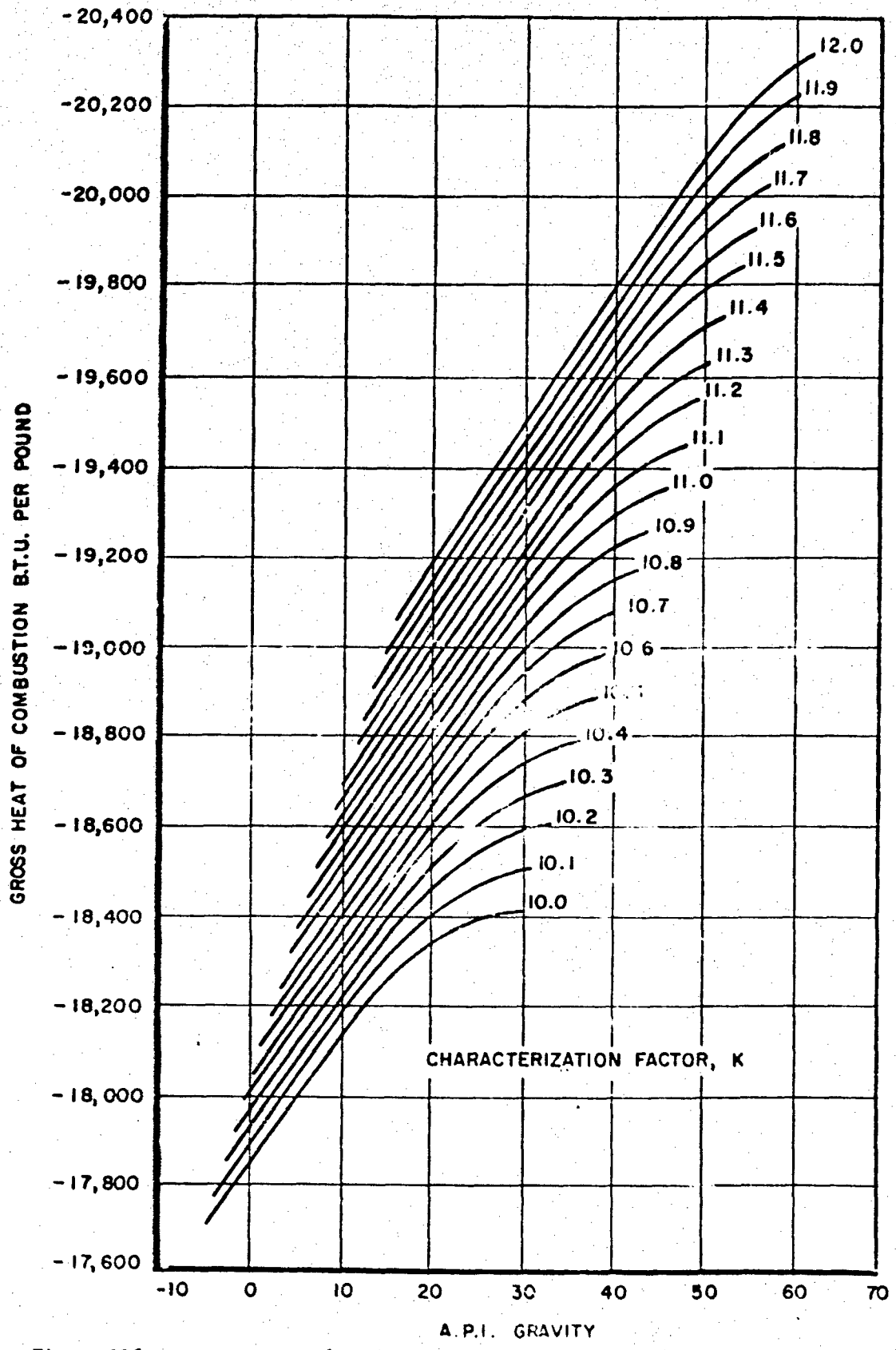

Figure 118 - Gross Heats of Combustion of Liquid Petroleum Hydrocarbons

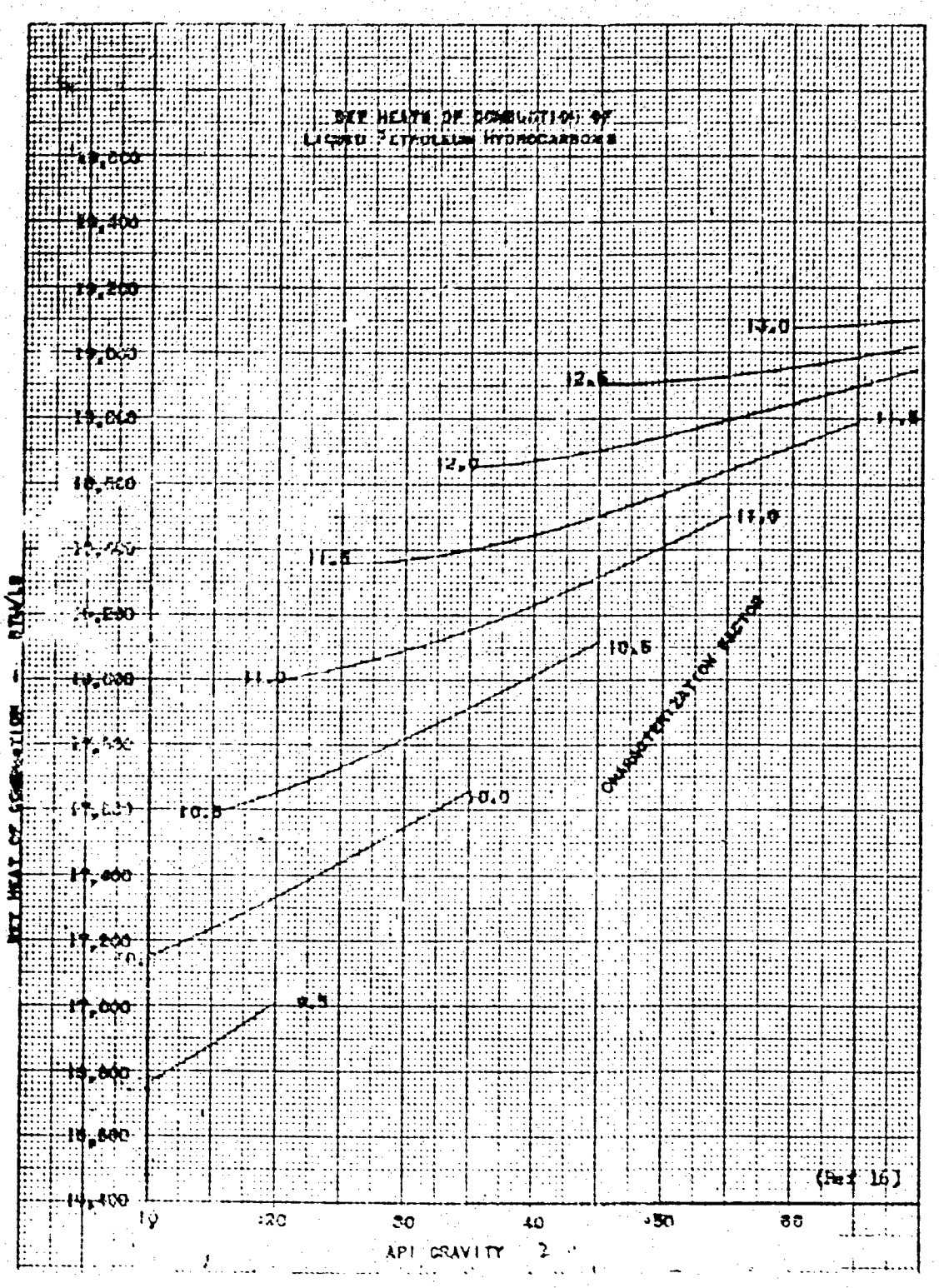

Figure 119 Net Heats Combustion of Liquid Petroleum Hydrocarbons

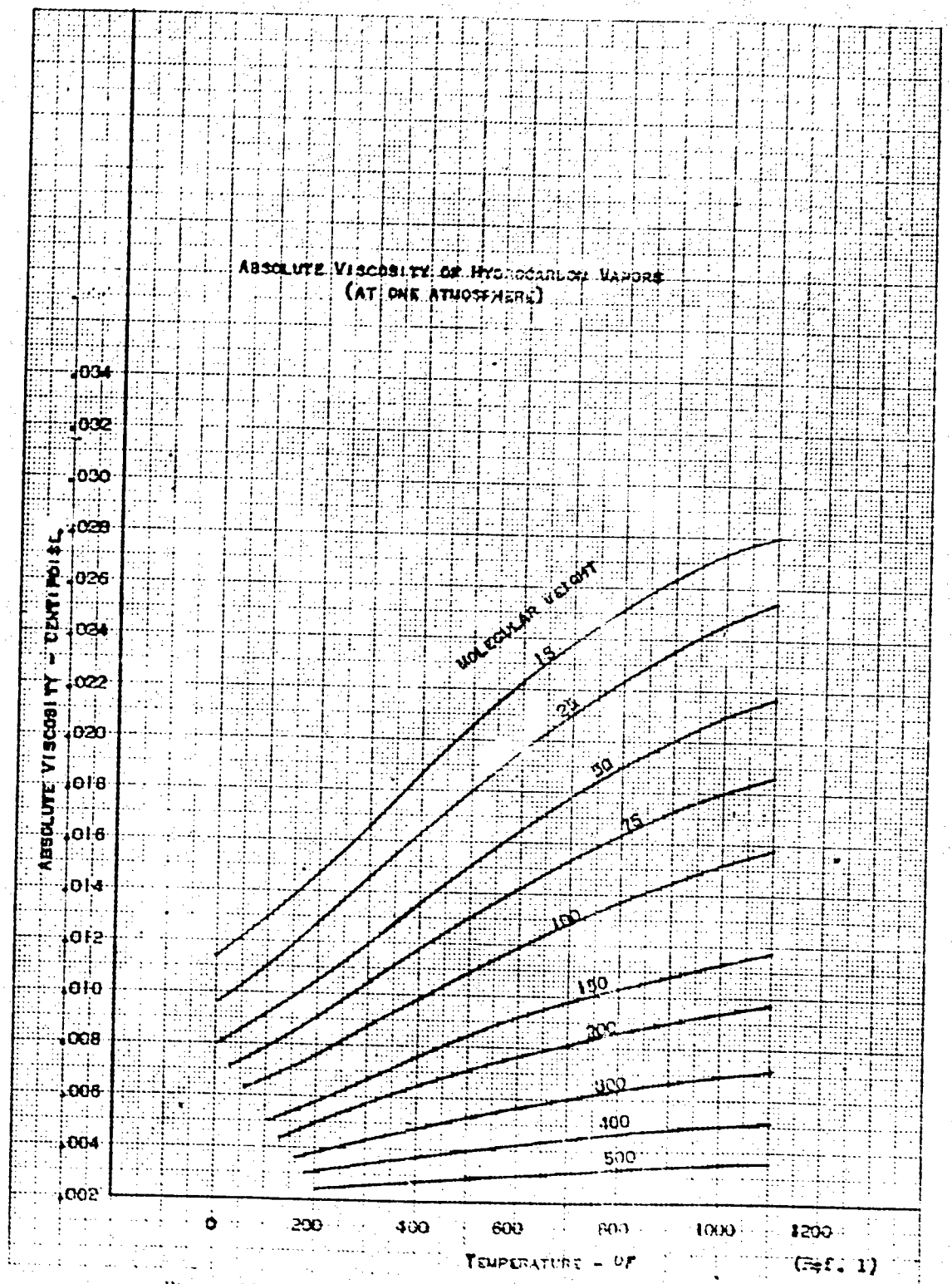

Figure 120 - Absolute Viscosity of Hydrocarbon Vapors

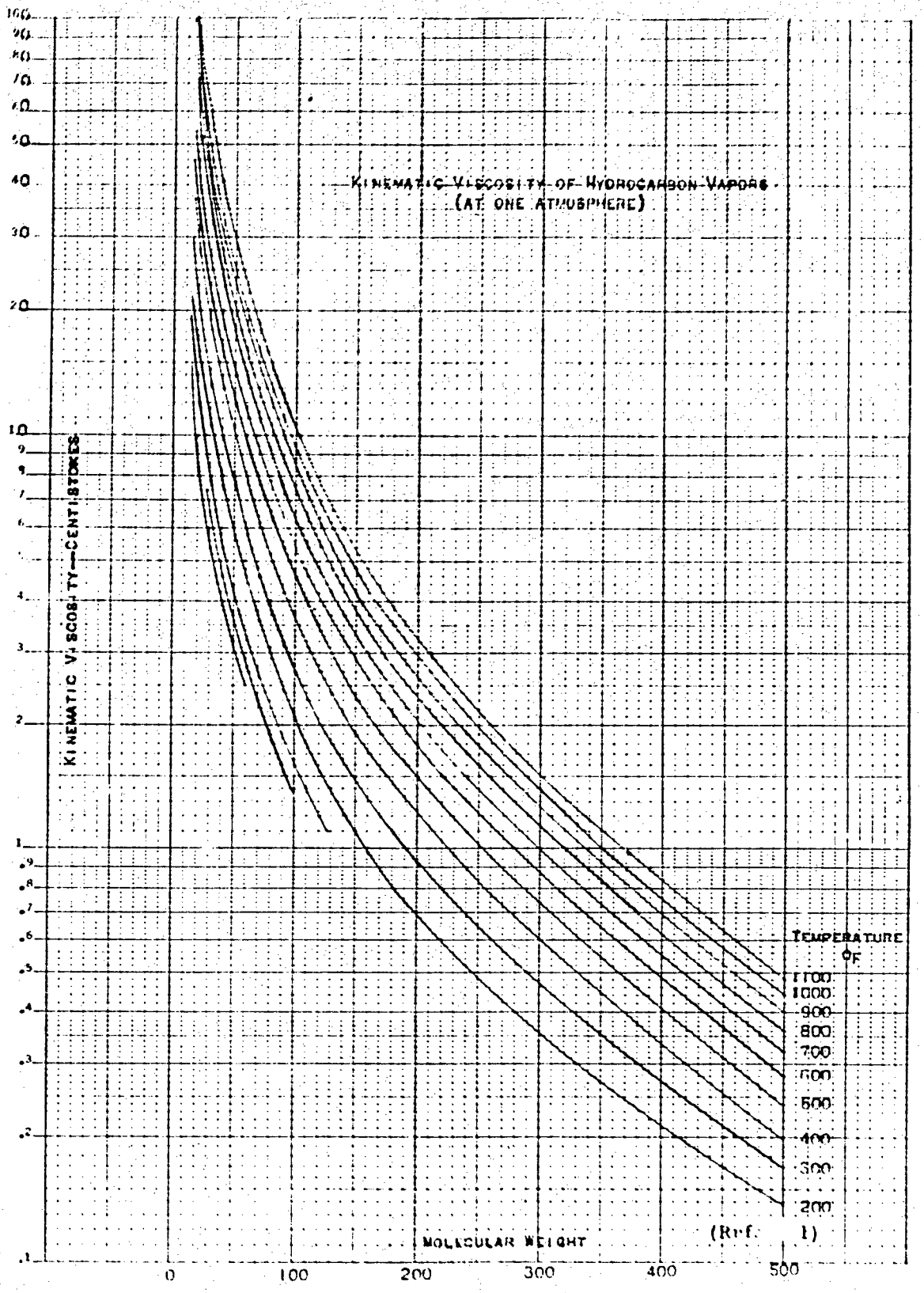

Figure 121 - Kinematic Viscosity of Hydrocarbon Vapors

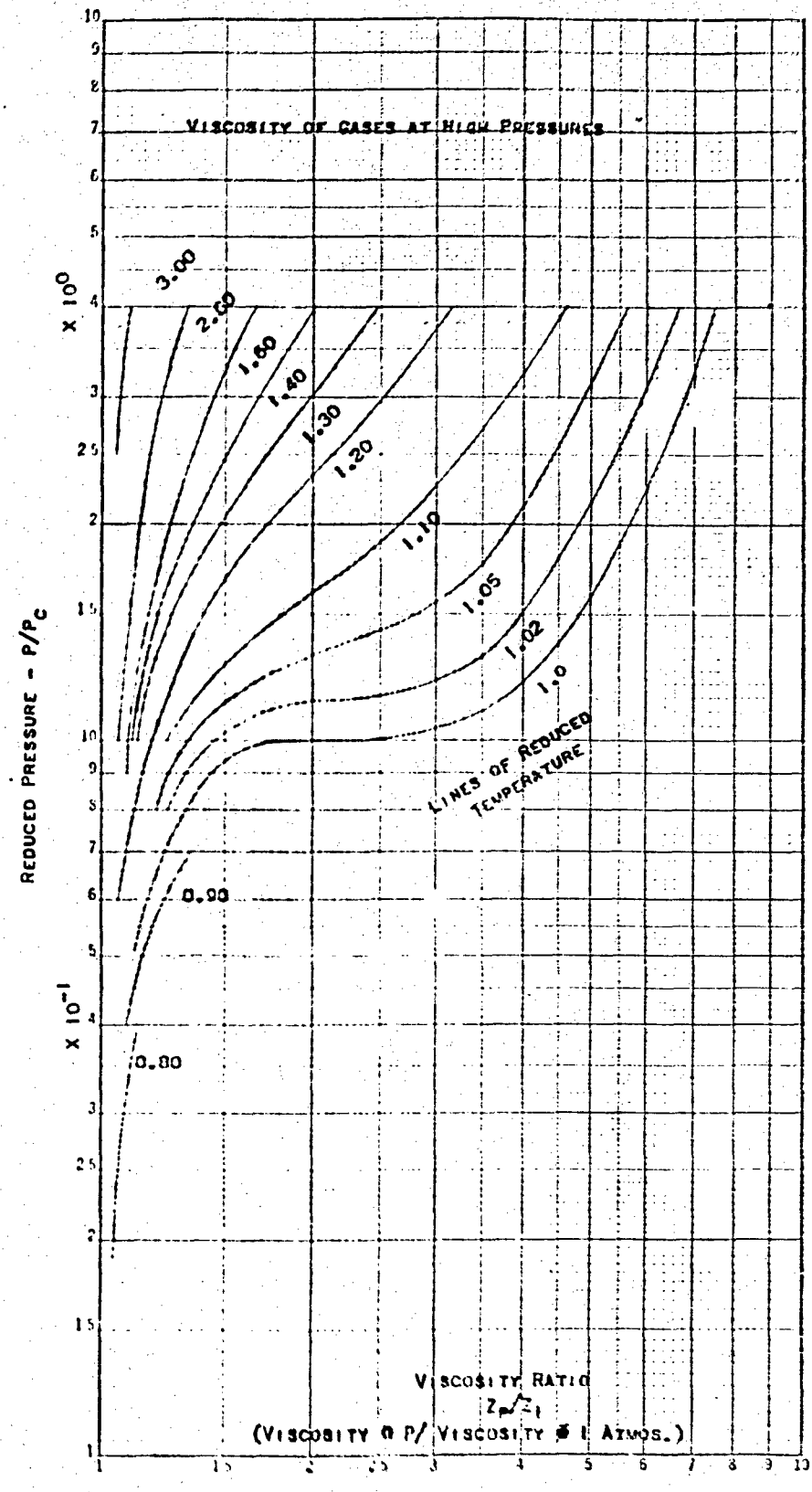

(Ref. 1)

Figure 1.2 - Viscosity of Gases at High Pressure

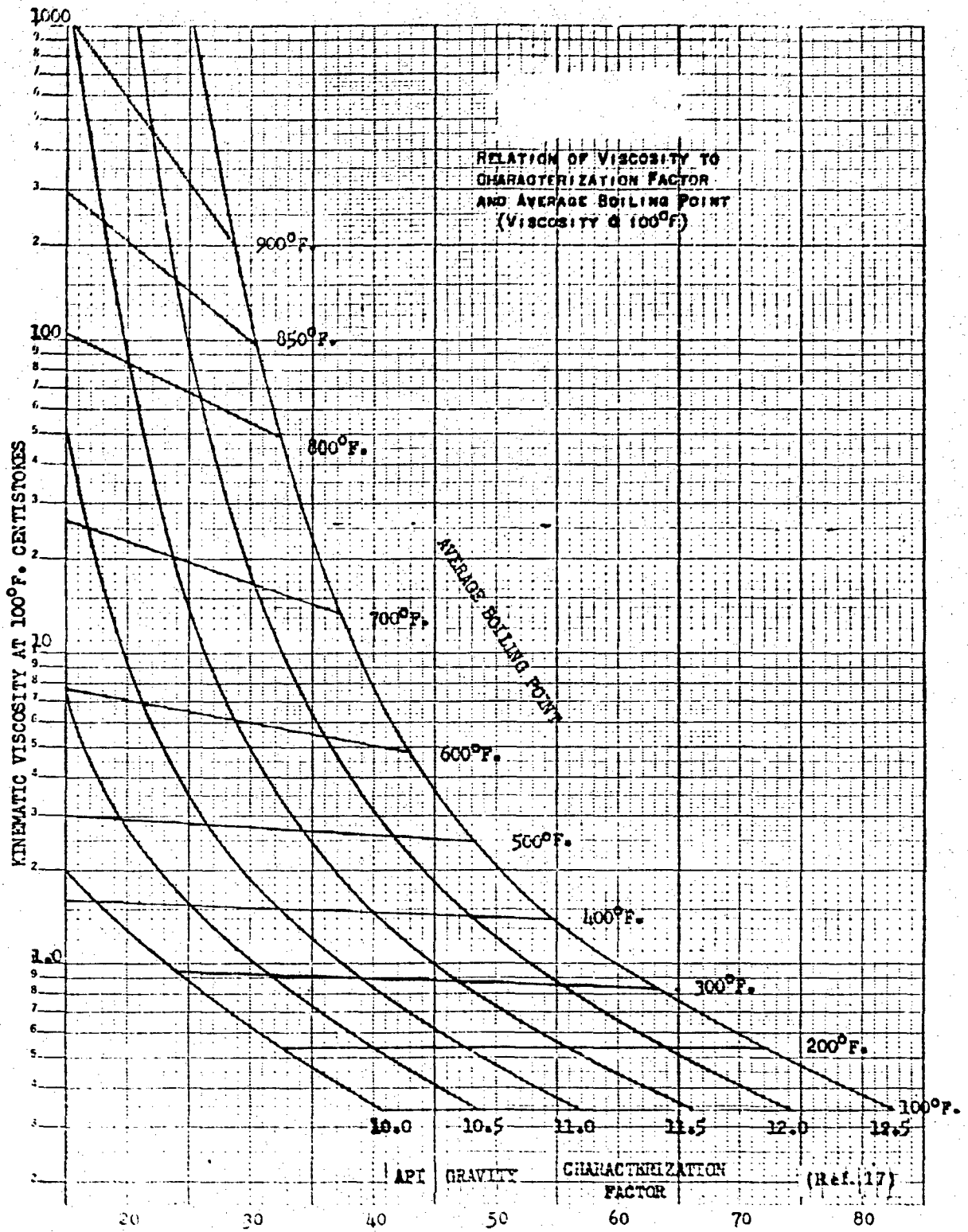

Figure 1.3 - Relation of Viscosity to Characterization Factor and Average Boiling Point (Viscosity at 100°F)

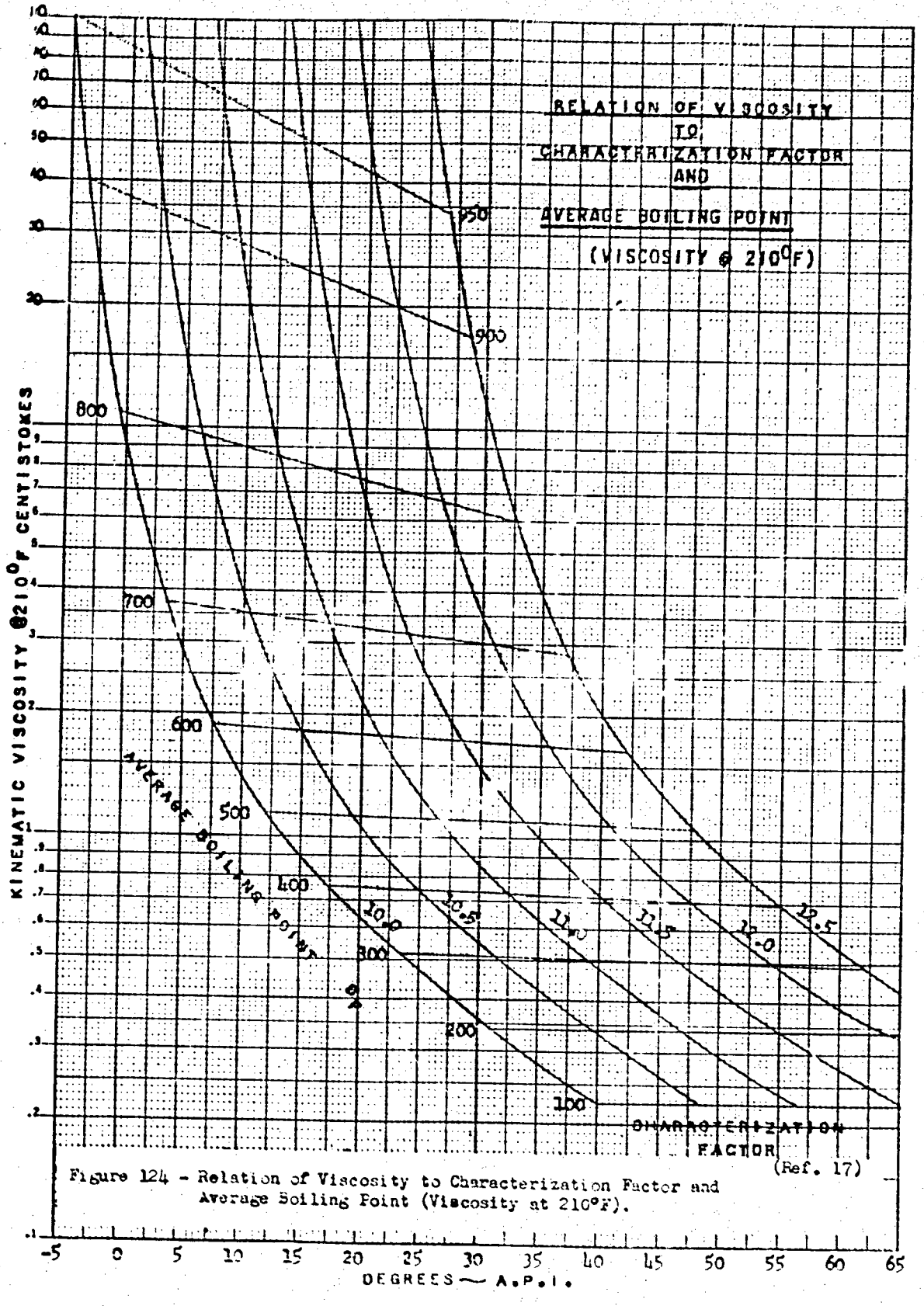

Figure 124 - Relation of Viscosity to Characterization Factor and Average Boiling Point (Viscosity at 210°F). (Ref. 17)

THOMPSON PRODUCTS, INC., Inglewood Laboratory STUDY OF PHYSIOCHEMICAL PROPERTIES OF SELECTED MILITARY FUELS, by E. Findl, H. Brande and H. Edwards, December 1960, 216p. incl. figs. and tables. (Project 3048; Task 30178) (ASD TR 60-767) (Contract AF 33(616)-3729)

Unclassified Report

A study was made of the physical and thermodynamic properties of four aircraft fuels. These were MIL-F-5624C Grade JP-4, MIL-F-25558 Grade RJ-1, MIL-F-25656 Grade JP-6 and Decalin. Properties evaluated included the solubility and evolution rate of air, nitrogen and ethane in fuel and the effects of these gases on density and viscosity. Thermodynamic properties including specific

(over)

UNCLASSIFIED

heats, enthalpy and entropy were determined for each of the four fuels, a determination was made of vaporization characteristics of each fuel and the variations of density on a function of temperature. Included is a literature survey correlation compilation for the determination of physical the thermodynamic properties of petroleum fuels.

UNCLASSIFIED

THOMPSON PRODUCTS, INC., Inglewood Laboratory STUDY OF PHYSIOCHEMICAL PROPERTIES OF SELECTED MILITARY FUELS, by E. Findl, H. Brande and H. Edwards, December 1960, 216p. incl. figs. and tables. (Project 3048; Task 30178) (ASD TR 60-767) (Contract AF 33(616)-3729)

Unclassified Report

A study was made of the physical and thermodynamic properties of four aircraft fuels. These were MIL-F-5624C Grade JP-4, MIL-F-25558 Grade RJ-1, MIL-F-25656 Grade JP-6 and Decalin. Properties evaluated included the solubility and evolution rate of air, nitrogen and ethane in fuel and the effects of these gases on density and viscosity. Thermodynamic properties including specific

(over)

UNCLASSIFIED

heats, enthalpy and entropy were determined for each of the four fuels, a determination was made of vaporization characteristics of each fuel and the variations of density on a function of temperature. Included is a literature survey correlation compilation for the determination of physical the thermodynamic properties of petroleum fuels.

UNCLASSIFIED